2014

Higgs Effects in Neutrino Physics and Heavy Quark Systems

Ahmed Rashed
University of Mississippi

Higgs Effects in Neutrino Physics and Heavy Quark Systems

Ahmed Mohammed Mostafa Rashed

A dissertation submitted in partial fulfillment
of the requirements for the degree of

Doctor of Philosophy
in the Department of Physics and Astronomy

University of Mississippi

May 2014

ABSTRACT

This work presents a study of the effects of multi-Higgs doublets on the properties of neutrino sector and heavy quark systems. The phenomenological implications of multi-Higgs models, which contain multi-Higgs doublets, in the neutrino and quark sector are discussed in this dissertation. The two-Higgs-doublet model (2HDM), in which two Higgs doublets are introduced, is the simplest extension to the scalar sector of the standard model (SM). A new boson state was recently seen in the CMS (Compact Muon Solenoid) and ATLAS (A Toroidal LHC Apparatus) experiments at the LHC (Large Hadron Collider).

We investigate the multi-Higgs models contributions in understanding various phenomena in the neutrino sector. Introducing a model to explain the neutrino oscillation phenomenon within the framework of multi-Higgs doublets is considered. We introduce different flavor symmetries in the lepton sector and study the phenomenological consequences in both the scalar and lepton sectors. The leptonic mixing in the symmetric limit can be, among other structures, the bi-maximal (BM) or the tri-bimaximal (TBM) mixing. We find that a mixing model with 2-3 flavor symmetry can explain the nonzero θ_{13} measurements. In our study, neutrino masses were proposed where its smallness is not due to the seesaw mechanism, i.e. not inversely proportional to some large mass scale. It comes from a one-loop mechanism with dark matter in the loop consisting of singlet Majorana fermions within a model with A_4 flavor symmetry.

A relevant point of interest in the neutrino sector is the study of the nonstandered interactions and its implications to neutrino oscillation. Here, we introduce the nonstandard interaction effects at the detectors of neutrino oscillation experiments and the impact of extracting the neutrino mixing angles is studied. The extractions of the atmospheric mixing angle θ_{23} rely on the standard model cross sections for $\nu_\tau + N \to \tau^- + X$ in ν_τ appearance experiments. Corrections to the cross sections from the charged Higgs and W' contributions modify the measured mixing angle. We include form factor effects in the new physics calculations and find the deviations of the mixing angle.

The quark sector has enriched our knowledge of particle physics. Lots of new theories and discovering new attributes of particles have been done in the quark sector. Therefore, we study the decay channel of the quarkonium $\eta_b \to \tau^+\tau^-$ to search for the existance of an additional Higgs field or a new gauge boson. We estimate the standard model branching ratio for this decay to be $\sim 4 \times 10^{-9}$. We show that considerably larger branching ratios, up to the present experimental limit of $\sim 8\%$, is possible in models with a light pseudoscalar or a light axial vector state. Also, in this dissertation we study the forward-backward asymmetry $A_{\rm FB}$ in the top quark pair production in the $t\bar{t}$ rest frame. In this work we seek for a new gauge boson to accommodating the CDF (Collider Detector at Fermilab) measurement of the $A_{\rm FB}$, which has a deviation from the next-to leading order (NLO) SM prediction. A $u \to t$ transition via a flavor-changing Z' can explain the data. We consider the most general form of the tuZ' interaction, which includes vector-axial vector as well as tensor type couplings, and study how these couplings affect the top forward-backward asymmetry.

DEDICATION

I dedicate this dissertation to my wonderful family. Particularly to my understanding and patient wife who has put up with these many years of research, and to our precious daughters who are the joy of our lives. I would like to thank her for continued support throughout all my endeavors in life, both academic and personal. I must also thank my loving mother who has given me her fullest support. There is no doubt that without her continued support and counsel I could not have done it. Finally, I dedicate this work to my late father.

ACKNOWLEDGMENTS

I would like to thank all of those people who helped make this dissertation possible. First, I wish to thank my advisor Dr. Alakabha Datta for all his guidance, encouragement, support, and patience. His sincere interest in various areas of particle physics has been a great inspiration to me throughout working on this dissertation. Also, I would like to thank my defence committee members Dr. Luca Bombelli, Dr. Robert Kroeger, Dr. Don Summers, and Dr. Ahmed Kishk for their very helpful insights. I also thank Sandip Pakvasa, Nita Sinha, and Yue-Liang Wu for useful comments and discussion. I would like especially to thank my team work colleagues for useful discussions. I want to thank my fellow students that I studied with during the comprehensive exam: Phil Blom, Rasheed Adebisi, and Sumedhe Karunarathne. Particularly, I appreciate Phil Blom for his useful notes.

This work was supported in part by the US-Egypt Joint Board on Scientific and Technological Co-operation award (Project ID: 1855) administered by the US Department of Agriculture, summer grant from the College of Liberal Arts, the Graduate Student Council Research Grant from the University of Mississippi, and in part by the National Science Foundation under Grant No. 1068052.

TABLE OF CONTENTS

LIST OF FIGURES

Figure Number Page

CHAPTER 1
INTRODUCTION

The standard model (SM) of particle physics is a $SU(3) \times SU(2) \times U(1)$ gauge theory which combines the color gauge group $SU(3)$ of the strong interaction with the Glashow-Weinberg-Salam (GWS) model of electroweak theory ($SU(2) \times U(1)$). The standard model recognizes two types of elementary fermions: quarks and leptons. The model distinguishes twelve different fermions: six quarks and six leptons, each with a corresponding anti-particle. Each quark comes in three different color charges, while the remaining fermions (leptons) do not carry color charge. They are arranged in a very tidy symmetrical structure. They are arranged under $SU(2)$ in six left-handed families: three families consist of two quarks forming doublets, and another three consist of two leptons each. Each left-handed fermion has a corresponding right-handed one that does not contribute in the doublets. Quarks and leptons are the building blocks which build up matter, i.e., they are seen as the "elementary particles". In the standard model, gauge bosons are defined as force carriers that mediate the strong, weak, and electromagnetic fundamental interactions. The strong interaction is mediated by massless vector boson so-called gluon, of which there are eight. The weak interaction has two massive charged mediators ($W^{\pm}$) and one neutral (Z^0). The electromagnetic interaction couples to all charged quarks and leptons via the photon. Lastly, the Higgs boson is the only scalar particle that exists in the SM. In 2012 a previously unknown boson was discovered at the Large Hadron Collider (LHC); its properties are still being studied to confirm whether or not it is the Higgs boson.

Quarks are peculiar as they posses electric charges which are fractions of that for the electron. A phenomenon called color confinement results in quarks being perpetually bound to one another, forming color-neutral composite particles called hadrons. There are two types of hadrons, the Baryon which is a system of three quarks (e.g. the proton) or Mesons, a two quark system containing a quark - antiquark pair (e.g. the pion or pi-meson). For

leptons, electron, muon and tau (which are referred to as different flavors of the lepton), there is a corresponding neutrino associated with it. Leptons do not participate in the strong interaction and are generally not seen within the nucleus. The discovery of neutrino mass via flavor oscillations is a clear sign of physics beyond the standard model (BSM). Originally, the evidence of this phenomenon was of astrophysical origin but now it has been convincingly confirmed by terrestrial experiments.

Despite the spectacular achievements in the last ten years or so, a lot of open questions are still seeking for answers to complete our understanding of the neutrino sector. In the following, we mention some of them:

- What is the sign of the mass squared difference $\Delta m^2_{31} (\equiv m^2_3 - m^2_1)$ or the character of the neutrino mass hierarchy?
- What is the mass scale of the neutrinos? Why are neutrino masses so small?
- Why is the pattern of the neutrino mixing so different from that of the quarks? Is there any connection between quarks and leptons?
- Are the neutrinos Dirac or Majorana particles?
- Is $\sin^2 2\theta_{23}$, where θ_{23} is the atmospheric mixing angle, exactly maximal $(= 1)$? If $\sin^2 2\theta_{23} \neq 1$, what is its octant?
- How many neutrino species are there? Do sterile neutrinos exist? Are three-flavor oscillations enough?

non-zero value for θ_{13} has been observed by MINOS and T2K experiments [1, 2, 3] would increase the possibility of observing CP-violation in the lepton sector. Non-zero θ_{13} also brings in the possibility of large Earth matter effects [4] for GeV energy accelerator neutrinos travelling over long distances. Matter effect on neutrino oscillations depends on the $\text{sgn}(\Delta m^2_{31})$.It is opposite for neutrinos and anti-neutrinos. For a given $\text{sgn}(\Delta m^2_{31})$ it enhances the oscillation probability in one of the channels and suppresses it in the other. Thus, comparing the neutrino signal against the anti-neutrino signal in very long baseline experiments gives a powerful tool to determine $\text{sgn}(\Delta m^2_{31})$.

In this dissertation we study the effects of multi-Higgs doublets on the properties of the neutrino sector and heavy quark systems. The dissertation is organised as follows: In the rest of the introduction we present a general background of two-Higgs-doublet model (2HDM), heavy quark systems, top forward-backward asymmetry, and neutrino sector. In the following chapters we discuss the phenomenological implications of the 2HDM in neutrino

mixing models, non-standard neutrino interactions, and heavy quarkonium system, as well as in the study of the top forward-backward asymmetry.

1.1 Higgs in the Standard Model and multi-Higgs-doublet models

The Higgs mechanism is a simple method for explaining the electroweak symmetry breaking and developing masses for the electroweak gauge bosons, the $W^{\pm}$ and the Z^0, as well as all elementary fermions; leptons and quarks. It was first proposed in 1964 by Higgs, Kibble, Guralnik, Hagen, Englert and Brout [5, 6, 7]. The Higgs mechanism has become the corner stone of the standard model for explaining the origin of the particle masses. In the SM, one complex doublet of scalar fields with a non trivial potential is introduced as

$$\Phi = \begin{pmatrix} \phi^+ \\ \phi^0 \end{pmatrix} = \begin{pmatrix} \phi_1 + i\phi_2 \\ \phi_3 + i\phi_4 \end{pmatrix} \tag{1.1}$$

to provide masses to both the weak force carriers and the elementary matter particles. The Higgs doublet transforms as an $SU(2)_L$ doublet, and its weak hypercharge is $Y = 1$. The price of proposing the Higgs mechanism is the presence of just one new massive Higgs particle or Higgs boson.

The Higgs Lagrangian consists of three terms: the scalar potential, the kinetic term, and the Yukawa terms

$$\begin{aligned} V(\Phi^+\Phi) &= \mu^2(\Phi^+\Phi) + \lambda(\Phi^+\Phi)^2, \\ \pounds_{kin} &= (D_\mu\Phi)\,(D^\mu\Phi)^\dagger \quad ; \quad D_\mu \equiv \partial_\mu - \frac{ig'}{2}YW_\mu^4 - ig\tau_i W_\mu^i, \\ -\pounds_Y &= \eta_{ij}^U \overline{Q}_L \widetilde{\Phi} U_R + \eta_{ij}^D \overline{Q}_L \Phi D_R + \eta_{ij}^\ell \overline{\ell}_L \Phi E_R + h.c. \end{aligned} \tag{1.2}$$

where μ^2 and λ are free parameters of the theory. W_μ^i with $i = 1, 2, 3$ are the four-vector fields (gauge eigenstates), associated with the three generators τ_i of $SU(2)_L$ symmetry. On the other hand, W_μ^4 is the four-vector field associated to the Y generator i.e. the $U(1)_Y$ symmetry. g and g' are the coupling strengths associated with W_μ^i and W_μ^4 , respectively. $\overline{Q}_L$ is the left-handed quark doublet, U_R, D_R are the right-handed singlets of the up and down sectors of quarks. $\overline{\ell}_L$ is the left-handed lepton doublet, E_R is the right-handed singlet of the down sector of leptons. The Yukawa couplings $\eta_{ij}^{U,D,\ell}$ define the vertices and, consequently, the Feynman rules of the Lagrangian where i, j are family indices. The spontaneous symmetry breaking describes systems where the Lagrangian obeys certain symmetries, but the lowest energy solutions do not exhibit that symmetry. The Higgs potential generates

the spontaneous symmetry breaking when $\mu^2 < 0$. The above potential is the most general renormalizable potential invariant under the SM symmetry group $SU(2)_L \times U(1)_Y$. The kinetic term describes the interactions between scalar particles and vector bosons, and provides the masses for the latter when the Higgs field acquires a vacuum expectation value (VEV). The Yukawa Lagrangian describes the interaction among the Higgs bosons and fermions.

Even though the standard model offers a very successful description of strong and electroweak interactions, it fails in providing an explanation for issues such as the gauge group, the number of families, the dynamics of flavor and the mechanism of mass generation, among others. This suggests the SM is not a fundamental theory but a part of a more complete theory. There are many extensions of the SM have been proposed. Several such models, like supersymmetry, contain an extended Higgs sector. The simplest extended Higgs sector is a two Higgs doublet model (2HDM) which constitutes of two, instead of one, complex scalar doublets as

$$\Phi_1 = \begin{pmatrix} \phi_1^+ \\ \phi_1^0 \end{pmatrix}, \quad \Phi_2 = \begin{pmatrix} \phi_2^+ \\ \phi_2^0 \end{pmatrix}, \tag{1.3}$$

with hypercharges ($Y_1 = Y_2 = 1$). In the so-called 2HDM-II model Φ_1 couples to the up-type and Φ_2 to the down-type quarks respectively. Upon spontaneous symmetry breaking, the neutral components of Φ_1 and Φ_2 acquire vacuum expectation values

$$\langle \Phi_1 \rangle = \frac{v_1}{\sqrt{2}}, \quad \langle \Phi_2 \rangle = \frac{v_2}{\sqrt{2}} e^{i\xi}. \tag{1.4}$$

So it is more convenient to parametrize the doublets in the following way

$$\Phi_1 = \begin{pmatrix} \phi_1^+ \\ \frac{h_1 + v_1 + i g_1}{\sqrt{2}} \end{pmatrix} \; ; \; \Phi_2 = \begin{pmatrix} \phi_2^+ \\ \frac{h_2 + v_2 + i g_2}{\sqrt{2}} \end{pmatrix} \tag{1.5}$$

where ξ is a phase parameter and

$$\begin{aligned} g_1 &= \sqrt{2} Im(\phi_1^0), \quad g_2 = \sqrt{2} Im(\phi_2^0), \\ h_1 &= \sqrt{2} \left(Re(\phi_1^0) - v_1 \right), \quad h_2 = \sqrt{2} \left(Re(\phi_2^0) - v_2 \right). \end{aligned} \tag{1.6}$$

The mass eigenstastes are obtained from the gauge eigenstates defined in (1.5) by the following transformations

$$
\begin{aligned}
\begin{pmatrix} \cos\beta & \sin\beta \\ -\sin\beta & \cos\beta \end{pmatrix} \begin{pmatrix} \phi_1^{\pm} \\ \phi_2^{\pm} \end{pmatrix} &= \begin{pmatrix} G^{\pm} \\ H^{\pm} \end{pmatrix}, \\
\begin{pmatrix} \cos\alpha & \sin\alpha \\ -\sin\alpha & \cos\alpha \end{pmatrix} \begin{pmatrix} h_1 \\ h_2 \end{pmatrix} &= \begin{pmatrix} H^0 \\ h^0 \end{pmatrix}, \\
\begin{pmatrix} \cos\beta & \sin\beta \\ -\sin\beta & \cos\beta \end{pmatrix} \begin{pmatrix} g_1 \\ g_2 \end{pmatrix} &= \begin{pmatrix} G^0 \\ A^0 \end{pmatrix}. \qquad (1.7)
\end{aligned}
$$

Only three of the eight original scalar degrees of freedom (corresponding to two complex doublet) are reabsorbed in transforming the originally massless vector bosons into massive ones, i.e. three Goldstone bosons ($G^{\pm}, G^0$) corresponding to $W^{\pm}, Z$, respectively. The remaining five degrees of freedom correspond to physical degrees of freedom in the form of: two neutral CP-even scalars (H^0, h^0), one neutral pseudoscalar (CP-odd) A^0, and two charged scalar fields ($H^{\pm}$). A key parameter of the model is the ratio of the vacuum expectation values

$$
\tan\beta = \frac{v_2}{v_1}. \qquad (1.8)
$$

The Higgs potential which spontaneously breaks $SU(2)_L \times U(1)_Y$ down to $U(1)_{EM}$ is [8]

$$
\begin{aligned}
V_{2HD}(\Phi_1,\, \Phi_2) &= \lambda_1(\Phi_1^{\dagger}\Phi_1 - v_1^2)^2 + \lambda_2(\Phi_2^{\dagger}\Phi_2 - v_2^2)^2 \\
&+ \lambda_3 \left[(\Phi_1^{\dagger}\Phi_1 - v_1^2) + (\Phi_2^{\dagger}\Phi_2 - v_2^2)\right]^2 \\
&+ \lambda_4 \left[(\Phi_1^{\dagger}\Phi_1)(\Phi_2^{\dagger}\Phi_2) - (\Phi_1^{\dagger}\Phi_2)(\Phi_2^{\dagger}\Phi_1)\right] \\
&+ \lambda_5 \left[\mathrm{Re}(\Phi_1^{\dagger}\Phi_2) - v_1 v_2 \cos\xi\right]^2 + \lambda_6 \left[\mathrm{Im}(\Phi_1^{\dagger}\Phi_2) - v_1 v_2 \sin\xi\right]^2, \qquad (1.9)
\end{aligned}
$$

where λ_i are real parameters (by hermiticity). The kinetic Lagrangian and the most general gauge invariant Lagrangian that couples the Higgs fields to fermions read

$$
\begin{aligned}
\pounds_{kin} &= (D_\mu \Phi_1)^{+}(D^\mu \Phi_1) + (D_\mu \Phi_2)^{+}(D^\mu \Phi_2), \\
-\pounds_Y &= \eta_{ij}^{U,0} \overline{Q}_{iL}^0 \widetilde{\Phi}_1 U_{jR}^0 + \eta_{ij}^{D,0} \overline{Q}_{iL}^0 \Phi_1 D_{jR}^0 + \xi_{ij}^{U,0} \overline{Q}_{iL}^0 \widetilde{\Phi}_2 U_{jR}^0 + \xi_{ij}^{D,0} \overline{Q}_{iL}^0 \Phi_2 D_{jR}^0 + \\
&\quad \eta_{ij}^{E,0} \overline{l}_{iL}^0 \Phi_1 E_{jR}^0 + \xi_{ij}^{E,0} \overline{l}_{iL}^0 \Phi_2 E_{jR}^0 + h.c., \qquad (1.10)
\end{aligned}
$$

where $\widetilde{\Phi}_{1,2} \equiv i\sigma_2 \Phi_{1,2}$, η_{ij}^0 and ξ_{ij}^0 are non diagonal 3×3 matrices and i, j denote family indices. D_R^0 refers to the three down-type weak isospin quark singlets $D_R^0 \equiv (d_R^0, s_R^0, b_R^0)^T$, U refers to the three up-type weak isospin quark singlets $U_R^0 \equiv (u_R^0, c_R^0, t_R^0)^T$ and E_R^0 to the three

charged leptons. Finally, $\overline{Q}^0_{iL}$, $\overline{l}^0_{iL}$ denote the quark and lepton weak isospin left-handed doublets respectively. The superscript "0" indicates that the fields are not mass eigenstates yet.

The real CP-even sector contains two physical Higgs scalars (H^0, h^0) which mix through the following mass-squared matrix

$$\mathcal{M} = \begin{pmatrix} 4v_1^2(\lambda_1+\lambda_3)+v_2^2\lambda_5 & (4\lambda_3+\lambda_5)v_1v_2 \\ (4\lambda_3+\lambda_5)v_1v_2 & 4v_2^2(\lambda_2+\lambda_3)+v_1^2\lambda_5 \end{pmatrix}. \tag{1.11}$$

At tree level, the masses of the scalar and pseudoscalar degrees of freedom satisfy the following relations:

$$\begin{aligned} M^2_{H^\pm} &= \lambda_4(v_1^2+v_2^2), \\ M^2_{A^0} &= \lambda_6(v_1^2+v_2^2), \\ M^2_{H^0,h^0} &= \frac{1}{2}\left(\mathcal{M}_{11}+\mathcal{M}_{22} \pm \sqrt{(\mathcal{M}_{11}-\mathcal{M}_{22})^2+4\mathcal{M}_{12}^2}\right), \end{aligned} \tag{1.12}$$

and the mixing angle α is obtained as

$$\begin{aligned} \sin 2\alpha &= \frac{2\mathcal{M}_{12}}{\sqrt{(\mathcal{M}_{11}-\mathcal{M}_{22})^2+4\mathcal{M}_{12}^2}}, \\ \cos 2\alpha &= \frac{\mathcal{M}_{11}-\mathcal{M}_{22}}{\sqrt{(\mathcal{M}_{11}-\mathcal{M}_{22})^2+4\mathcal{M}_{12}^2}}. \end{aligned} \tag{1.13}$$

1.2 Heavy quarkonium decay

On 4 July 2012 both of the CERN experiments CMS and ATLAS announced they had independently made the same discovery of new boson state with mass 125.3 ± 0.6 GeV in CMS [9] and 126.5 GeV in ATLAS [10]. Using the combined analysis, both experiments reached a local significance of 5σ significance. After the discovery of the boson state, it is widely anticipated that physics beyond the standard model or new physics (NP) will be discovered soon at experiments such as the LHC. This NP might contain additional Higgs bosons beyond the SM Higgs, new gauge bosons, or new quarks and leptons. It is generally believed that these new particles will be heavy with masses from the weak scale ~ 100 GeV to a TeV. However, light scalars and vector bosons with masses in the GeV range or even lower are not ruled out. For instance, light scalar states coming from a primary higgs with non SM decays can be consistent with existing experimental constraints [11]. One of the ways to probe these light states is to look at decays of particles with masses in the 10 GeV

range such as the Υ. Data from the present and future B factories can be used to search for these states and/or to put constraints on models that predict such states.

It is also possible to probe these light states via the η_b decays. The pseudoscalar $b\bar{b}$ bound state in the 1S configuration, the η_b, was observed in BaBar by two different experiments. First, it was seen in the decay of $\Upsilon(3S) \to \gamma\eta_b$ [12] with a signal significance greater than 10 standard deviations (σ). The η_b was observed in the photon energy spectrum using (109 ± 1) million $\Upsilon(3S)$ events and the hyperfine $\Upsilon(1S) - \eta_b$ mass splitting was measured to be $71.4^{+2.3}_{-3.1}(\text{stat}) \pm 2.7(\text{syst})$ MeV from the mass $m(\eta_b) = 9388.9^{+3.1}_{-2.3}\,(\text{stat}) \pm 2.7\,(\text{syst})$ MeV. Soon after, it was also seen in $\Upsilon(2S) \to \gamma\eta_b$ [13] by another group in BaBar, and the hyperfine mass splitting was determined to be $67.4^{+4.8}_{-4.6}(\text{stat}) \pm 2.0(\text{syst})$ MeV from the mass $m(\eta_b) = 9392.9^{+4.6}_{-4.8}\,(\text{stat}) \pm 1.9\,(\text{syst})$ MeV. In the past, since the discovery of the $\Upsilon(nS)$ resonances [14] in 1977, various experimental environments [15, 16, 17] have been used to seek the ground state η_b but without success. Many theoretical models have attempted to predict the mass of η_b. Lattice NRQCD [18, 19] predicts the hyperfine splitting to be $E^{lat}_{hfs} = 61 \pm 14$ MeV and correspondingly the mass to be $m_{\eta_b} = 9383(4)(2)$ MeV which is in agreement with the experimental results. The calculations of perturbative QCD based models [19, 20] predict the hyperfine splitting to be $E^{QCD}_{hfs} = 39 \pm 11(\text{th})^{+9}_{-8}(\delta\alpha_s)$ MeV which is smaller than the measured values. Experiments at BaBar have also searched for a low-mass Higgs boson in $\Upsilon(3S) \to \gamma A^0$, $A^0 \to \tau^+\tau^-$ [21] with data sample containing 122 million $\Upsilon(3S)$ events. In the same analysis, constraint on the branching ratio for $\eta_b \to \tau^+\tau^-$ was reported as $\mathcal{BR}(\eta_b \to \tau^+\tau^-) < 8\%$ at 90% confidence level (C.L.).

Here we explore the decay $\eta_b \to \tau^+\tau^-$ as a probe for a light pseudoscalar or a light axial vector state. We estimate the standard model branching ratio for this decay to be $\sim 4 \times 10^{-9}$. We show that considerably larger branching ratios, up to the present experimental limit of $\sim 8\%$, is possible in models with a light pseudoscalar or a light axial vector state.

1.3 Forward-backward asymmetry in top physics

The top quark with its high mass may play a crucial role in electroweak symmetry breaking. Hence the top sector may be sensitive to new physics effects that could be revealed through careful measurements of top quark properties. The top quark pair production in proton-antiproton collisions at the Tevatron collider with a center-of-mass (CM) energy of $\sqrt{s} = 1.96$ TeV is dominated by the partonic process $q\bar{q} \to t\bar{t}$. Recently the CDF experiment has reported a measurement of forward-backward asymmetry in $t\bar{t}$ production which appears to deviate from the standard model predictions. The CDF collaboration measured the forward-backward asymmetry (A_{FB}) in top quark pair production in the $t\bar{t}$

rest frame to be $A_{FB}^{t\bar{t}} = 0.475 \pm 0.774$ for $M_{t\bar{t}} > 450$ GeV [22], which is 3.4 σ deviations from the next-to leading order (NLO) SM prediction $A_{FB}^{t\bar{t}} = 0.088 \pm 0.013$ [23, 24, 25, 26]. The DØ collaboration also observed a larger than predicted asymmetry [27].

The current measurement of the top quark pair production cross section from 4.6 fb^{-1} of data at CDF is

$$\sigma_{t\bar{t}} \quad = \quad (7.50 \pm 0.48) pb\,, \tag{1.14}$$

for $m_t = 172.5$ GeV [28], in good agreement with their SM predictions by Langenfeld *et al.* $\sigma_{t\bar{t}} = 7.46^{+0.66}_{-0.80}$ pb [29], Cacciari *et al.* $\sigma_{t\bar{t}} = 7.26^{+0.78}_{-0.86}$ pb [30], Kidonakis $\sigma_{t\bar{t}} = 7.29^{+0.79}_{-0.85}$ pb [31], and recent Ahrens *et al.*'s significantly low value $\sigma_{t\bar{t}} = 6.30 \pm 0.19^{0.31}_{-0.23}$ pb [32]. Hence new physics models that aim to explain the A_{FB} measurement must not change the production cross section appreciably. Many NP models that affect A_{FB}, either via s-channel [33] or t-channel exchange of new particles [34] have been proposed to explain the forward-backward anomaly. Here we will study the forward-backward asymmetry measurement in the presence of Z' boson contribution. We consider a flavor-changing tuZ' coupling which can contribute to $t\bar{t}$ production in the t-channel including tensor term in the coupling, and study the effects on the top $A_{\rm FB}$.

1.4 Neutrino oscillation

Neutrino oscillation is a quantum mechanical phenomenon of lepton flavor changing for a neutrino with energy E travelling some distance L between the source and detector. Neutrino oscillation has been observed in various experiments. This phenomenon is not expected in the standard model because neutrinos are massless in this theory and it is always possible to choose a physical basis where the leptonic Yukawa couplings are diagonal. Neutrino mass is the most potent evidence of existing physics beyond the standard model.

1.4.1 Current experimental situation

The first experimental observation of the electron neutrino was in 1956 in the nuclear fission products in the nuclear reactor beta decay. Neutrino was first postulated in 1930 by Wolfgang Pauli in order to preserve the conservation of energy, conservation of momentum, and conservation of angular momentum (spin) in β-decay $n \to p + e^- + \bar{\nu}_e$. Soon later, the muon neutrino ν_μ was discovered. It was assumed to be the same neutrino that was discovered in the beta decay till Schwarz, Steinberger and Lederman performed a neutrino experiment to prove the existence of two kinds of neutrinos through the pion decay $\pi^+ \to \mu^+ + \nu_\mu$.

parameter	best fit	1σ range	2σ range	3σ range
$\Delta m^2_{21} \cdots [10^{-5}\text{eV}^2]$	7.62	7.43–7.81	7.27–8.01	7.12–8.20
$\lvert\Delta m^2_{31}\rvert \cdots [10^{-3}\text{eV}^2]$	2.55 2.43	$2.46 - 2.61$ $2.37 - 2.50$	$2.38 - 2.68$ $2.29 - 2.58$	$2.31 - 2.74$ $2.21 - 2.64$
$\sin^2\theta_{12}$	0.320	0.303–0.336	0.29–0.35	0.27–0.37
$\sin^2\theta_{23}$	0.613 $(0.427)^1$ 0.600	0.400-0.461 (0.573–0.635) 0.569–0.626	0.38–0.66 0.39–0.65	0.36–0.68 0.37–0.67
$\sin^2\theta_{13}$	0.0246 0.0250	0.0218–0.0275 0.0223–0.0276	0.019–0.030 0.020–0.030	0.017–0.033
δ	0.80π -0.03π	$0 - 2\pi$	$0 - 2\pi$	$0 - 2\pi$

Table 1.1. Neutrino oscillation parameters summary. For Δm^2_{31}, $\sin^2\theta_{23}$, $\sin^2\theta_{13}$, and δ the upper (lower) row corresponds to normal (inverted) neutrino mass hierarchy. [1] This is a local minimum in the first octant of θ_{23} with $\Delta\chi^2 = 0.02$ with respect to the global minimum

The conception of the standard model, established in the mid 1970s, postulated that the fermions, consisting of the electron, muon, tau and the neutrinos, form a doublet structure such that the electron is grouped with ν_e, the muon is grouped with ν_μ and the tau is grouped with ν_τ. The third type of neutrino, ν_τ was observed in 2000 by the DONUT collaboration [35]. The experiment used a neutrino beam created by $D_s \to \tau\bar{\nu}_\tau$ and the decay of τ into another ν_τ.

The last decades have been extremely successful for the field of neutrino physics. It was not until 1998 that the existence of neutrino oscillations was finally established experimentally by the Super-Kamiokande experiment in Japan for atmospheric neutrinos [36]. In 2002, the SNO collaboration demonstrated that the solar neutrino problem i.e. the major discrepancy between measurements of the numbers of neutrinos flowing through the Earth and theoretical models of the solar interior [37] is solved by solar neutrino oscillations [38]. Throughout the last decades, measurements by Super-Kamiokande [39], by the reactor experiments KamLAND [40] and CHOOZ [41] and by the accelerator experiments K2K [42] and MINOS [43] have confirmed our picture of neutrino oscillations and have provided precise values or tight constraints for most of the oscillation parameters. The experiments have shown that the angles of lepton mixing are relatively larger than their counterparts in the quark sector.

Recent data from the Double Chooz [44], Daya Bay [45], RENO [46] experiments as well as latest T2K [1] and MINOS [2] experiments have yield a nonzero values for θ_{13}. The best

fit values for the mixing angles are given as [47]

$$\begin{aligned}
\sin^2\theta_{12} &= 0.320, \\
\sin^2\theta_{23} &= 0.613\ (0.600)\ \text{(for normal (inverted) hierarchy)}, \\
\sin^2\theta_{13} &= 0.0246\ (0.0250)\ \text{(for normal (inverted) hierarchy)}.
\end{aligned} \tag{1.15}$$

The summary of neutrino oscillation results [47] can be found in table 1.1 which provides best fit points, 1σ errors, and the allowed intervals at 2 and 3σ for the three-flavor oscillation parameters. There are several papers that have attempted to explain the recent θ_{13} results [48, 49].

Neutrino oscillation experiments are only sensitive to mass squared differences. Thus, they cannot provide information on the absolute neutrino masses. However, kinematical studies of the electron spectrum in nuclear β-decay [50] produce upper limit to the absolute neutrino masses ≤ 2.3 eV (95% C.L.). Also, cosmological observations constrain the absolute masses to lie below ~ 0.2 eV [51]. On the other hand, the neutrinoless double beta decay experiments [52] put a bound at the level of 0.35 eV (90% C.L.) in the case of neutrinos with Majorana mass terms.

Several experiments have searched for new effects beyond the framework of three massive neutrinos with standard model interactions. Till now, no evidence for such effects has been found yet. Instead, constraints have been derived on non-standard neutrino interactions [53], neutrino decay [54], neutrino decoherence [55], oscillations into sterile neutrinos (i.e. neutrinos not coupling to the Z boson) [56] and other exotic scenarios.

1.4.2 Mixing and oscillation parameters

There are two different bases of the neutrino field, flavor basis $\nu_\alpha(\alpha = e, \mu, \tau)$ which associate with the charged lepton partners in the charged weak interactions and has no definite mass as the mass matrix of neutrinos are non-diagonal, and the mass basis $\nu_i(i = 1, 2, 3)$ which have definite masses and are the eigenstates of the free Hamiltonian. The fact of lepton mixing has been firmly established through a variety of solar, atmospheric, and terrestrial neutrino oscillation experiments [57]. The charged current interaction can be written in the flavor basis as

$$-\frac{g}{\sqrt{2}}\bar{l}_\alpha\gamma^\mu(1-\gamma_5)\nu_\alpha W_\mu. \tag{1.16}$$

If the charged lepton and neutrino Yukawa matrices are non-diagonal, using the transformation between the flavor and mass fields the charged current interaction can be written

as

$$-\frac{g}{\sqrt{2}}\bar{l}_i\gamma^\mu(1-\gamma_5)U_{\alpha i}\nu_i W_\mu. \tag{1.17}$$

If the charged lepton Yukawa matrix is diagonal, the charged current interaction can be given as

$$-\frac{g}{\sqrt{2}}\bar{l}_\alpha\gamma^\mu(1-\gamma_5)U_{\alpha i}\nu_i W_\mu, \tag{1.18}$$

where the mixing between the two bases of the neutrino field can be described by the relationship

$$|\nu_\alpha\rangle = \sum_{i=1}^{n} U_{\alpha i}|\nu_i\rangle, \tag{1.19}$$

where U is the unitary leptonic mixing matrix. The well known parametrization of the neutrino mixing matrix is known as Pontecorvo-Maki-Nakagawa-Sakata (PMNS) matrix, U_{PMNS} [58]:

$$U_{PMNS} = \begin{pmatrix} c_{12}c_{13} & s_{12}c_{13} & s_{13}e^{-i\delta} \\ -s_{12}c_{23} - c_{12}s_{23}s_{13}e^{i\delta} & c_{12}c_{23} - s_{12}s_{23}s_{13}e^{i\delta} & s_{23}c_{13} \\ s_{12}s_{23} - c_{12}c_{23}s_{13}e^{i\delta} & -c_{12}s_{23} - s_{12}c_{23}s_{13}e^{i\delta} & c_{23}c_{13} \end{pmatrix} K, \tag{1.20}$$

where $s_{13} \equiv \sin\theta_{13}$, $c_{13} \equiv \cos\theta_{13}$ with θ_{13} being the reactor angle, $s_{12} \equiv \sin\theta_{12}$, $c_{12} \equiv \cos\theta_{12}$ with θ_{12} being the solar angle, $s_{23} \equiv \sin\theta_{23}$, $c_{23} \equiv \cos\theta_{23}$ with θ_{23} being the atmospheric angle, δ is the Dirac CP violating phase, and $K = diag(1, e^{i\phi_1}, e^{i\phi_2})$ contains additional (Majorana) CP violating phases ϕ_1, ϕ_2, which are physically relevant if neutrinos are Majorana particles. Experiments have put no constraints on the Majorana phases, therefore, we usually ignore them. The experiments have shown that the angles of lepton mixing are relatively larger than their counterparts in the quark sector.

In order to calculate the probability of flavor changing we need to consider the evaluation of the eigenstates in time [59]. Suppose a given source is producing a neutrino flux of given flavor $|\nu_\alpha\rangle$ at zero time and zero position $t = 0 = x$ then the neutrino state at a later time t will be given by

$$|\nu_\alpha(t)\rangle = \sum_{i=1}^{n} U^*_{\alpha i}|\nu_i(t)\rangle = \sum_{i=1}^{n} U^*_{\alpha i}e^{-iE_i t}|\nu_i(0)\rangle, \tag{1.21}$$

where E_i are the energy eigenvalues associated with the individual neutrino mass eigenstates

ν_i. The oscillation probability $P_{\alpha\beta}$ for the flavor transition $\alpha \to \beta$ is given by

$$\begin{aligned} P_{\alpha\beta}(t) &= |\langle \nu_\beta | \nu_\alpha(t) \rangle|^2 \\ &= \sum_{i=1}^{n} \sum_{j=1}^{m} J^{ij}_{\alpha\beta} e^{-i(E_i - E_j)t}, \end{aligned} \tag{1.22}$$

where the Jarlskog CP-odd invariant $J^{ij}_{\alpha\beta}$ is written as

$$J^{ij}_{\alpha\beta} \equiv U_{\beta i} U^*_{\alpha i} U^*_{\beta j} U_{\alpha j}. \tag{1.23}$$

For ultra relativistic neutrinos with small mass one can assume $p_i \equiv p \simeq E$ and we have

$$E_i = \sqrt{p_i^2 + m_i^2} \simeq p + \frac{m_i^2}{2p} = E + \frac{m_i^2}{2E}, \tag{1.24}$$

or

$$E_i - E_j = \frac{\Delta m^2_{ji}}{2E}, \tag{1.25}$$

where $\Delta m^2_{ji} = m_i^2 - m_j^2$. Let us suppose that t is the travel time of the ultra relativistic neutrinos from the source to the detector with L is the distance traveled. In the natural unit, $c = 1$, we can consider that $t \cong L$, thus

$$(E_i - E_j)t = \frac{\Delta m^2_{ji} L}{2E}. \tag{1.26}$$

Now, the transition probability can be written as

$$\begin{aligned} P_{\alpha\beta} &= \sum_{i,j} U_{\beta i} U^*_{\alpha i} U^*_{\beta j} U_{\alpha j} e^{-i\frac{\Delta m^2_{ji} L}{2E}} \\ &= \sum_{i} |U_{\alpha i}|^2 |U_{\beta i}|^2 + 2\mathrm{Re} \sum_{i>j} \left(U_{\beta i} U^*_{\alpha i} U^*_{\beta j} U_{\alpha j} \right) e^{-i\frac{\Delta m^2_{ji} L}{2E}}. \end{aligned} \tag{1.27}$$

From the orthogonality relation $\langle \nu_j | \nu_i \rangle = \delta_{ij}$ one can obtain the following relation

$$\sum_{i} |U_{\alpha i}|^2 |U_{\beta i}|^2 = \delta_{\alpha\beta} - 2\mathrm{Re} \sum_{i>j} \left(U_{\beta i} U^*_{\alpha i} U^*_{\beta j} U_{\alpha j} \right), \tag{1.28}$$

then

$$\begin{aligned} P_{\alpha\beta} &= \delta_{\alpha\beta} - 2\mathrm{Re}\sum_{i>j}\left(U_{\beta i}U^*_{\alpha i}U^*_{\beta j}U_{\alpha j}\right) + 2\mathrm{Re}\sum_{i>j}\left(U_{\beta i}U^*_{\alpha i}U^*_{\beta j}U_{\alpha j}\right)e^{-i\frac{\Delta m^2_{ji}L}{2E}} \\ &= \delta_{\alpha\beta} - 2\mathrm{Re}\sum_{i>j}\left(U_{\beta i}U^*_{\alpha i}U^*_{\beta j}U_{\alpha j}\right)(1-e^{-i\frac{\Delta m^2_{ji}L}{2E}}). \end{aligned} \tag{1.29}$$

Since for any complex numbers a and b, Re(ab)=Re(a)Re(b)-Im(a)Im(b), then

$$\begin{aligned} P_{\alpha\beta} &= \delta_{\alpha\beta} - 2\mathrm{Re}\sum_{i>j}\left(U_{\beta i}U^*_{\alpha i}U^*_{\beta j}U_{\alpha j}\right)\left(1-\cos\frac{\Delta m^2_{ji}L}{2E} + i\sin\frac{\Delta m^2_{ji}L}{2E}\right) \\ &= \delta_{\alpha\beta} - 2\sum_{i>j}\mathrm{Re}\left(U_{\beta i}U^*_{\alpha i}U^*_{\beta j}U_{\alpha j}\right)\left(1-\cos\frac{\Delta m^2_{ji}L}{2E}\right) + 2\sum_{i>j}\mathrm{Im}\left(U_{\beta i}U^*_{\alpha i}U^*_{\beta j}U_{\alpha j}\right)\sin\frac{\Delta m^2_{ji}L}{2E} \\ &= \delta_{\alpha\beta} - 4\sum_{i>j}\mathrm{Re}\left(U_{\beta i}U^*_{\alpha i}U^*_{\beta j}U_{\alpha j}\right)\sin^2\frac{\Delta m^2_{ji}L}{4E} + 2\sum_{i>j}\mathrm{Im}\left(U_{\beta i}U^*_{\alpha i}U^*_{\beta j}U_{\alpha j}\right)\sin\frac{\Delta m^2_{ji}L}{2E}. \end{aligned} \tag{1.30}$$

Similarly, for the antineutrino oscillation probability $\bar{\nu}_\alpha \to \bar{\nu}_\beta$

$$P_{\alpha\beta} = \delta_{\alpha\beta} - 4\sum_{i>j}\mathrm{Re}\left(U_{\beta i}U^*_{\alpha i}U^*_{\beta j}U_{\alpha j}\right)\sin^2\frac{\Delta m^2_{ji}L}{4E} - 2\sum_{i>j}\mathrm{Im}\left(U_{\beta i}U^*_{\alpha i}U^*_{\beta j}U_{\alpha j}\right)\sin\frac{\Delta m^2_{ji}L}{2E}. \tag{1.31}$$

For two flavor oscillation, let us assume ν_e and ν_μ be the flavor eigenstates and ν_1 and ν_2 be the mass eigenstates with masses m_1 and m_2, respectively. We can parametrize the mixing between the two bases as follows

$$\begin{aligned} |\nu_e(t=0)\rangle = |\nu_e\rangle &= \cos\theta|\nu_1\rangle + \sin\theta|\nu_2\rangle, \\ |\nu_\mu(t=0)\rangle = |\nu_\mu\rangle &= -\sin\theta|\nu_1\rangle + \cos\theta|\nu_2\rangle. \end{aligned} \tag{1.32}$$

where θ is the mixing angle. The transition probability can be written as

$$\begin{aligned} P(\nu_e\to\nu_\mu) &= |\langle\nu_\mu|\nu_e(t)\rangle|^2 \\ &= \left(-\sin\theta\cos\theta + \sin\theta\cos\theta e^{-i\frac{\Delta m^2 L}{2E}}\right)^2 \\ &= \sin^2\theta\cos^2\theta|1-e^{-i\frac{\Delta m^2 L}{2E}}|^2 \\ &= \sin^2 2\theta\sin^2\left(1.27\Delta m^2\frac{L}{E}\right), \end{aligned} \tag{1.33}$$

where the units of m^2, L, and E are given in terms of GeV.

1.4.3 Patterns of neutrino mixing matrix

Unlike the CKM matrix that can be thought of as a perturbation about the identity matrix the leading term in the leptonic mixing contains large mixing angles. The distribution of the flavors in the mass eigenstates, corresponding to the best fit values of the mixing angles, has shown that the leading order mixing method is a successful way to describe the lepton mixing. The most common patterns that have been discussed in the literatures to describe the lepton mixing, which may arise from discrete symmetries, are called; democratic (DC) [60, 61], bimaximal (BM) [62, 63], and tri-bimaximal (TBM) [64, 65, 66] mixing matrix. However, current experiments indicate deviations from these standard zeroth order forms

$$U_{TBM} = \begin{pmatrix} \sqrt{\frac{2}{3}} & \frac{1}{\sqrt{3}} & 0 \\ -\frac{1}{\sqrt{6}} & \frac{1}{\sqrt{3}} & \frac{1}{\sqrt{2}} \\ \frac{1}{\sqrt{6}} & -\frac{1}{\sqrt{3}} & \frac{1}{\sqrt{2}} \end{pmatrix}, \quad U_{BM} = \begin{pmatrix} \frac{1}{\sqrt{2}} & \frac{1}{\sqrt{2}} & 0 \\ -\frac{1}{2} & \frac{1}{2} & \frac{1}{\sqrt{2}} \\ \frac{1}{2} & -\frac{1}{2} & \frac{1}{\sqrt{2}} \end{pmatrix}, \quad U_{DC} = \begin{pmatrix} \frac{1}{\sqrt{2}} & \frac{1}{\sqrt{2}} & 0 \\ \frac{1}{\sqrt{6}} & -\frac{1}{\sqrt{6}} & -\sqrt{\frac{2}{3}} \\ -\frac{1}{\sqrt{3}} & \frac{1}{\sqrt{3}} & -\sqrt{\frac{2}{3}} \end{pmatrix}. \tag{1.34}$$

All the above patterns in Eq. 1.34 suppose vanishing θ_{13}. This assumption contradicts the recent observations of θ_{13} being significant. In Ref. [67] it has been shown that it is possible to get appropriate neutrino mixing angles that may fit the recent data if one assumes some general modification of the neutrino BM/TBM/DC mixing patterns. Several papers have discussed the recent data [48, 49]. Some of those studies have considered deviations from the charged lepton sector [48, 68].

Over the last ten years, the TBM neutrino mixing pattern has attracted copious attention with many model builders attempting to reconstruct it via symmetries and auxiliary fields. Most remarkable examples are models with discrete (e.g. A_4, Δ_{27}) and continuous (e.g. $SO(3), SU(3)$) family symmetries. Some recent examples of models can be found in [69]. It should be noted that many of these models are often quite complicated and require additional constraints on the particle content or a non-trivial Higgs sector for them to be viable. However, the tribimaximal structure presents a relatively simple manifestation of the neutrino mixing matrix that is more or less consistent with current experimental bounds. In the light of this, it is theoretically appealing to take $U_{\rm TBM}$ (with or without the Majorana phases) as the starting point in any model building or analyses involving the neutrino mass matrix.

1.5 Mechanisms of neutrino mass generation

After the experiments have emphasized the phenomenon of neutrino oscillation, we have become confident that there is physics beyond standard model to explain the neutrino masses and oscillation. The see-saw mechanism is the most natural way for generating neutrino masses beyond the SM. Some other models of neutrino masses have been studied. The masses of neutrinos are relatively unknown. Experiments which put kinematic limits on the neutrino mass directly are difficult to conduct and put weak limits [70]. However, the abundant sources of neutrinos, from stars and atmosphere, help in understanding the properties of neutrinos further. In the see-saw mechanism, the small neutrino masses are generated via a large scale of new particles masses. This scale could be in the range of the grand unification energy. But it is also acceptable to introduce particles with masses in the TeV scale in the see-saw mechanism, which makes the origin of neutrino mass generation testable in the LHC.

1.5.1 Scale of absolute neutrino mass

From neutrino oscillation experiments, two out of three neutrino states must be massive. But, these experiments measure mass squared differences and do not indicate the scale of the absolute neutrino mass. However, other ways are possible to provide us with some hints about the neutrino mass values. Here, we discuss three of those methods; single beta decay, neutrino-less double beta decay and cosmology experiments.

Sensitivity of the $\boldsymbol{\beta}$-spectrum to $\boldsymbol{m^2(\nu_e)}$

Since in the β-decay we observe only the kinetic energy E of the β particle we are measuring actually a sum of β spectra, leading each with probability P_i to a final state of excitation energy V_i of the daughter and with probability $|U_{ej}|^2$ to a neutrino mass eigenstate $m(\nu_j)$. The differential decay rate of the single β-decay is

$$\begin{aligned}\frac{\mathrm{d}R}{\mathrm{d}E} &= N\frac{G_f^2}{2\pi^3\hbar^7 c^5}\cos^2(\Theta_c)|M|^2F(E,\mathrm{Z}+1)\cdot \\ &\quad p(E+m_e\mathrm{c}^2)\sum_{ij}P_i(E_0-V_i-E)\cdot \\ &\quad |U_{ej}|^2\sqrt{(E_0-V_i-E)^2-m_{\nu_j}^2\mathrm{c}^4}. \end{aligned} \tag{1.35}$$

Here N is the number of mother nuclei, G_f the universal Fermi coupling constant, Θ_c the Cabibbo angle, M the nuclear decay matrix element, $F(E,\mathrm{Z}+1)$ the Fermi function, p the electron momentum, m_e the electron mass and E_0 the Q value of the tritium T_2 decay minus the recoil energy of the daughter. E_0 marks the endpoint of the β spectrum in case of zero

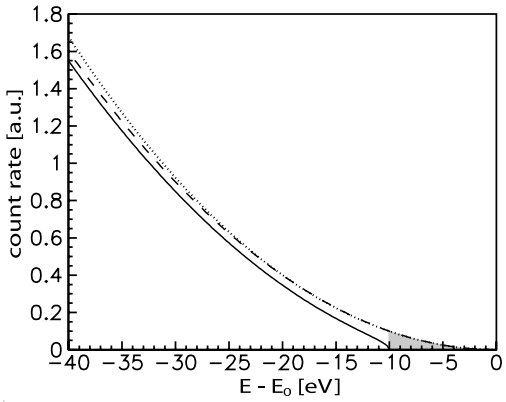

Figure 1.1. Tritium β spectrum close to the endpoint E_0. The dotted and the dashed line correspond to $m(\nu_e) = 0$, the solid one to $m(\nu_e) = 10$ eV/c^2. In case of the dashed and the solid line only the decay into the electronic ground state of the daughter is considered. For $m(\nu_e)$=10 eV/c^2 the missing decay rate in the last 10 eV below E_0 (shaded region) is a fraction of $2{\cdot}10^{-10}$ of the total decay rate, scaling as $m^3(\nu_e)$.

neutrino mass where E_0=(18574.3±1.7) eV [71].

The last 2 terms in (1.35) are the total energy E_ν and the momentum p_ν of the neutrino. They represent the neutrino phase space and give rise to the parabolic increase of the β spectrum below E_0 for vanishing neutrino mass, shown in Fig. 1.1 by the dotted and dashed line. The solid line shows the effect of degenerate neutrino masses $m_{\nu_j} = m_{\nu_e}$= 10 eV. In case of the dashed and the solid line only the decay into the electronic ground state of the daughter is considered. For m_{ν_e}= 10 eV the missing decay rate in the last 10 eV below E_0 is a fraction of $2{\times}10^{-10}$ of the total decay rate.

We learn from these numbers that the tiny useful high energy end of the spectrum is threatened by an enormous majority at lower energies. However, it can be rejected safely by an electrostatic filter which can be passed only by electrons with a kinetic energy E larger than a potential barrier qU to be climbed. Any momentum analyzing, e.g. magnetic spectrometer cannot guarantee this strict rejection since scattering events may introduce tails to both sides of the resolution function.

Neutrino-less double beta decay ($0\nu\beta\beta$)

If two neutrons have decayed into two protons without producing two electron anti-neutrinos, as in the regular beta decay, the process can be mediated by an exchange of a light Majorana neutrino and called neutrino-less double beta decay ($0\nu\beta\beta$), see Fig. 1.2,

$$(A, Z) \rightarrow (A, Z + 2) + e + e, \tag{1.36}$$

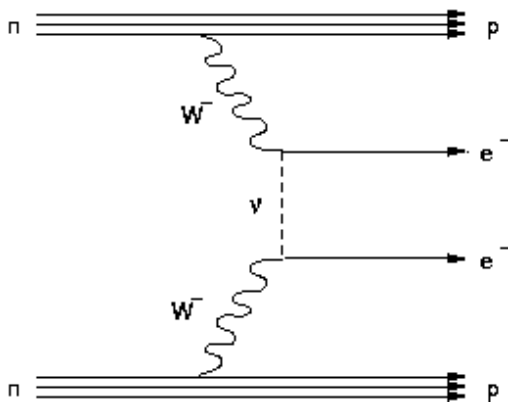

Figure 1.2. Neutrino-less double beta decay ($0\nu\beta\beta$).

where Z is the atomic number and A is the mass number. Neutrinoless double-beta decay would lead to violation of total lepton number conservation. However, the existence of $0\nu\beta\beta$-decay requires Majorana neutrino mass, no matter what the actual mechanism is. The decay rate of $0\nu\beta\beta$-decay has the general form (see Ref. [72])

$$\Gamma^{0\nu}(A,Z) = |m_{\beta\beta}|^2 |M(A,Z)|^2 G^{0\nu}(E_0,Z), \tag{1.37}$$

where $M(A,Z)$ is the nuclear matrix element and $G^{0\nu}(E_0,Z)$ is the phase-space factor (E_0 is the energy release), and $m_{\beta\beta}$ is the effective Majorana mass [73], which depends on neutrino masses m_i and on U_{ei},

$$m_{\beta\beta} \equiv \sum_{i=1}^{3} U_{ei}^2 \, m_i \ . \tag{1.38}$$

By analyzing the resultant electron energy spectrum, one can probe this quantity. The above relation gives an upper limit on the absolute neutrino mass scale. Two groups, Mainz [74] and Troitsk [75], have reported bounds of $m_\nu < 2.3$ eV and $m_\nu < 2.5$ eV, respectively. An upcoming experiment, KATRIN [76], is expected to have a sensitivity down to about 0.2 eV. There are several groups such as the Heidelberg-Moscow [77] and IGEX [78] collaborations who have conducted experiments with ^{76}Ge. The more recent CUORICINO experiment [79] use ^{130}Te to test for this. There is no confirmed observation for the neutrinoless double β-decay. The best upper bounds on the decay lifetimes are presently provided by CUORICINO whose results are translated to

$$m_\nu \equiv m_{\beta\beta} < 0.19 - 0.68 \text{ eV} \ \ (90\% \text{ C.L.}) \ . \tag{1.39}$$

Upcoming experiments like CUORE [80], GERDA [81] and Majorana [82] are expected to further improve these results with projected sensitivity of about 0.05 eV.

Neutrino masses from cosmology

During the epoch of structure formation, free-streaming neutrinos with a large mass is assumed to have significant effects on the growth of structure and, consequently, on the eventual galaxy power spectrum. Thus, an accurate measurement of neutrinos could help put limits on the scale of absolute neutrino mass given by the standard theory of structure formation. Studying the data from the Wilkinson Microwave Anisotropy Probe (WMAP) and the Sloan Digital Sky Survey (SDSS) has found that the sum of neutrino masses, assuming three species, is constrained by $\sum_i |m_i| \lesssim 0.6$ [83] and 1.6 eV [84], respectively, at a confidence level of about 95%. Since the observed squared-mass splittings $(\Delta m^2_{12}, \Delta m^2_{23})$ imply that $|m_i - m_j| \ll \mathcal{O}(0.1)$ eV for any i and j, taking $\sum_i |m_i| \lesssim 0.6$ gives an absolute upper bound for each individual neutrino mass of about

$$|m_i| \lesssim 0.2 \text{ eV} \quad (95\% \text{ C.L.}) \quad \text{for all } i \,. \tag{1.40}$$

This estimation agrees with the least upper bound imposed by the CUORICINO experiment, which further confirms that the absolute neutrino mass scale must be in the sub-eV range.

1.5.2 See-saw mechanism

Neutrinos are extremely light and, hence, this might suggest a unique mass generation mechanism to explain the smallness of mass in a natural way. The first reasonable attempt, see-saw mechanism, was between late 1970's and early 1980's [85]. One of the simplest way to extend the SM to accommodate neutrino masses is to introduce right-handed (RH) components ν_R for neutrinos. The Dirac mass term for neutrinos is written as $\frac{1}{2} m_{\rm D} \overline{\nu_L} \nu_R + h.c.$. This is not the only term allowed for neutrino masses. Since neutrinos are neutral particles, the RH components are singlets under all the SM gauge symmetries. Thus, the Majorana mass term $\frac{1}{2} M_{\rm R} \overline{(\nu_R)^c} \nu_R + h.c.$ is allowed, where the superscript c denotes charge conjugation, see appendix 8. The overall mass term for neutrinos can then be written in a matrix form as

$$\mathcal{L}_{\rm mass} = -\frac{1}{2} \begin{pmatrix} \overline{\nu_L} & \overline{(\nu_R)^c} \end{pmatrix} \begin{pmatrix} 0 & m_{\rm D} \\ m_{\rm D} & M_{\rm R} \end{pmatrix} \begin{pmatrix} (\nu_L)^c \\ \nu_R \end{pmatrix} + h.c. \tag{1.41}$$

Here, the above Lagrangian is assumed to be gauge invariant, thus, the upper left component of the mass matrix is zero because it is not possible to add a Majorana mass term for left-handed fields without breaking gauge invariance.

By assuming that the Majorana mass is much larger than the Dirac mass, i.e. $M_{\rm R} \gg m_{\rm D}$,

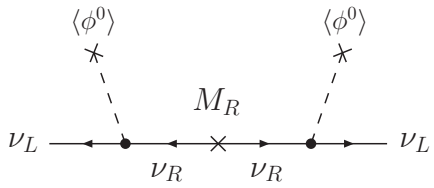

Figure 1.3. Diagram representing the type I seesaw realisation of the small Majorana mass.

diagonalizing the mass matrix yields the following two mass eigenvalues

$$m_\nu \cong -m_{\rm D}^T M_{\rm R}^{-1} m_{\rm D}, \quad M_\nu \cong M_{\rm R}. \tag{1.42}$$

The first eigenvalue corresponds to a light neutrino mass while the second eigenvalue corresponds to the mass of a heavy Majorana neutrino. Roughly speaking, plugging a Dirac mass at the electroweak scale, $m_{\rm D} = 100$ GeV, with a heavy neutrino mass close to the unification scale, say $M_{\rm R} = 10^{14}$ GeV, leads to a light neutrino mass of order $m_\nu = 0.1$ eV. This version of the see-saw mechanism with the additional RH neutrinos is referred to as the type-I see-saw mechanism. The Lagrangian that describes this type can be written as follows

$$\mathcal{L}_{\text{type-I}} = i\overline{\nu_{Ri}}\gamma_\mu\partial^\mu\nu_{Ri} - h_{\alpha i}\overline{\ell_{L\alpha}}\nu_{Ri}\tilde{\Phi} - \frac{1}{2}M_{{\rm R}i}\overline{(\nu_{Ri})^c}\nu_{Ri} + h.c.\ , \tag{1.43}$$

where $\alpha = e, \mu, \tau$, three new fields $\nu_{Ri},\ i = 1, 2, 3$, a Majorana mass matrix $M_{\rm R}$ and a Yukawa coupling matrix h have been introduced. The effective interaction of the above Lagrangian can schematically be described by the diagram in Fig. 1.3.

Instead of introducing right handed components to explain the neutrino masses, we could extend the SM by adding a heavy Higgs triplet [86]

$$\Delta = \begin{pmatrix} \Delta^-/\sqrt{2} & \Delta^{--} \\ \Delta^0 & -\Delta^-/\sqrt{2} \end{pmatrix}\ , \tag{1.44}$$

with the Lagrangian

$$\mathcal{L}_{\text{type-II}} = \frac{Y_\Delta}{2}\,\overline{\ell_L^c}\, i\tau_2\,\Delta\,\ell_L + \mu_\Delta\,\phi^T\Delta\,\phi + M_\Delta^2\,{\rm Tr}(\Delta^\dagger\Delta) + {\rm h.c.} \tag{1.45}$$

This gives rise to the diagram shown in Fig. 1.4a. This generates a Majorana mass term for the left handed neutrinos $\frac{1}{2}m_{\rm L}\overline{(\nu_L)^c}\nu_L + h.c.$ where $m_{\rm L} = Y_\Delta\langle\Delta\rangle$. The corresponding mass term has the weak isospin $I = 1$ and violates the lepton number by two units $\Delta L = 2$. By considering non-zero value for m_L in Eq. 1.41 the resultant light neutrino mass matrix can

be written in the form

$$m_\nu = m_L - m_{\rm D}^T M_{\rm R}^{-1} m_{\rm D}. \tag{1.46}$$

The above form refers to the mixed see-saw, when the first term dominates it refers to as the type-II see-saw mechanism [87].

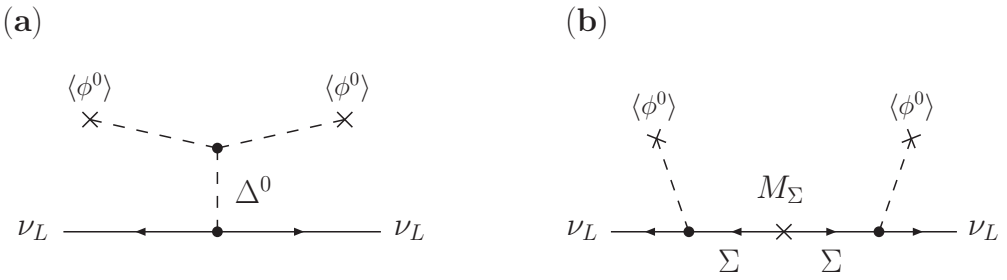

Figure 1.4. (a) The process induced by the type II seesaw Lagrangian that will give rise to small neutrino Majorana masses. (b) The corresponding process in the type III seesaw case with heavy triplet fermion Σ instead.

The above two versions of the see-saw mechanism are not the only types, another possibility is to introduce heavy triplet fermions

$$\Sigma = \begin{pmatrix} \Sigma^- & \Sigma^0/\sqrt{2} \\ \Sigma^0/\sqrt{2} & \Sigma^+ \end{pmatrix} . \tag{1.47}$$

and interact with the ordinary lepton doublets via Yukawa couplings [88] with hypercharge $Y = 0$. The corresponding Lagrangian for this model is given by

$$\mathcal{L}_{\text{type-III}} = Y_\Sigma\, \overline{\ell}_L\, i\tau_2\, \Sigma\, \phi + M_\Sigma\, {\rm Tr}\left(\overline{\Sigma^c}\, \Sigma\right) + {\rm h.c.}\,, \tag{1.48}$$

where Y_Σ is the Yukawa coupling. This gives rise to the diagram shown in Fig. 1.4b, and after integrating out the heavy Σ field, one obtains the desired form for the seesaw neutrino mass

$$m_\nu = \, Y_\Sigma \, \frac{\langle\phi^0\rangle^2}{M_\Sigma}\, Y_\Sigma^T \,. \tag{1.49}$$

Hence by setting $M_\Sigma \gg \langle\phi^0\rangle$, one can explain the smallness of neutrino masses, and as a result, this is often referred to as the type III seesaw mechanism [88].

1.5.3 Models of neutrino masses at TeV scale

Although, the see-saw mechanism successfully explains the smallness of neutrino masses, there have been other ways to extending the standard model by the enlargement of the Higgs

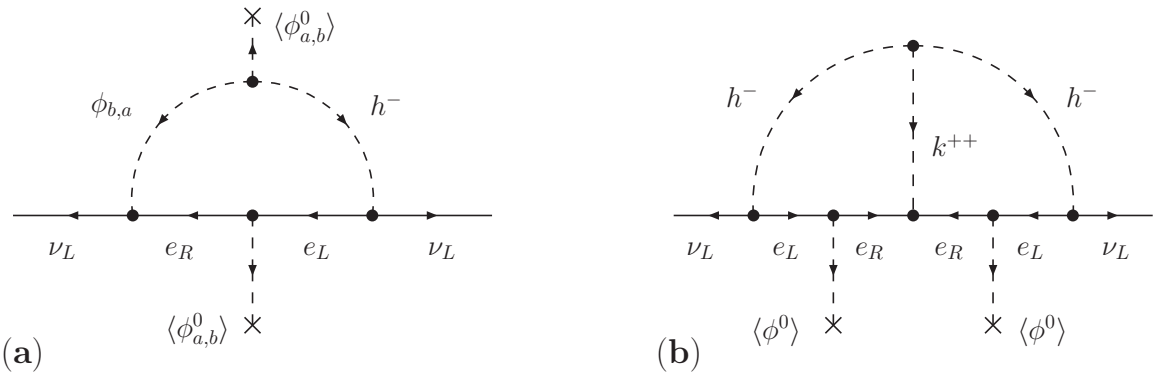

Figure 1.5. (a) One-loop correction graph of the Zee model that generates a neutrino Majorana mass. (b) Two-loop diagram of the Babu-Zee model that contributes to the neutrino Majorana mass term.

sector and having the newly introduced charged scalars coupling to the LH lepton doublets. Here, we will review some of the those models.

Radiative corrections

In this mechanism, the neutrinos are massless at the tree level, but acquire a small mass at the one-loop level because of the loop suppression. Here we discuss two models. One can modify the scalar sector of the model by adding two (or more) $SU(2)_L$ Higgs doublets, all with the same hypercharge ($Y(\phi) = 1$) and a charged scalar singlet h^- which has $Y(h^-) = -2$. Neutrino masses are now generated radiatively and thus are naturally small. This model is called the Zee model [89]. Then, the scalar field h^- can couple to the LH lepton doublets and, also, a cubic coupling term between h^- and other doublets can be there as follows:

$$\begin{aligned} \mathcal{L}^{\rm Z}_{\rm yuk} &= \kappa\, \epsilon_{ij}\, \overline{\ell}^{\,i}_L\, (\ell^j_L)^c\, h^- + \text{h.c.}\,, \\ \mathcal{L}^{\rm Z}_{\rm cubic} &= \mu_{ab}\, \epsilon_{ij}\, \phi^i_a\, \phi^j_b\, h^- + \text{h.c.}\,, \end{aligned} \tag{1.50}$$

where i, j are indices in $SU(2)_L$ and ϵ_{ij} denotes the Levi-Civita tensor. Also, $a, b = 1, 2, \ldots$ are labels for the different Higgs doublets. In this case, the Majorana mass term can be induced using the tree-level interactions of 1.50 and the standard Higgs Yukawa ($\overline{\ell}_L\, \phi_{a,b}\, e_R$) via the one-loop diagram shown in Fig. 1.5a. By choosing carefully certain scale of the Higgses vacuum expectation values and assuming a small coupling for κ tiny neutrino masses can be generated.

Babu-Zee model [90] is another version of the radiative corrections method. The model contains two charged scalar singlets; one singly charged (h^-) and the other doubly charged

(k^{++})in addition to the SM Higgs doublet. The interaction Lagrangian is given by:

$$\mathcal{L}_{\rm int}^{\rm BZ} = \kappa\,\epsilon_{ij}\,\overline{\ell}_L^i\,(\ell_L^j)^c\,h^- + \lambda\,\overline{(e_R)^c}\,e_R\,k^{++} + \mu\,k^{++}\,h^-\,h^- + Y_e\,\overline{\ell}_L\,\phi\,e_R + \text{h.c.}\,, \tag{1.51}$$

where κ, λ and Y_e are dimensionless coupling constants while constant μ has a dimension of mass. These interactions give rise to Majorana neutrino masses at the two-loop level as shown in Fig. 1.5b.

Inverse seesaw mechanism

In the so-called inverse seesaw mechanism [91] one uses a similar idea to the see-saw model by introducing a singlet scalar field S for each generation besides a RH neutrino ν_R. Here, the Majorana mass term for ν_R is not proposed. Thus, the 9×9 mass matrix can be generated, in the basis of $(\nu_L,\ \nu_R,\ S)$, as follows

$$M_\nu = \begin{pmatrix} 0 & M_D & 0 \\ M_D^T & 0 & M_{NS} \\ 0 & M_{NS} & M_S \end{pmatrix}. \tag{1.52}$$

In the case of

$$M_S \ll M_D \ll M_{NS}, \tag{1.53}$$

one may have a large Dirac mass, M_D, and TeV scale RH neutrino masses. The effective light neutrino mass matrix is then given by, to the leading order,

$$M_{(\text{eff})} \simeq (M_D M_{NS}^{-1}) M_S (M_D M_{NS}^{-1})^T. \tag{1.54}$$

Thus, the smallness of the neutrino masses is due to the smallness of the lepton number violation coupling, M_S, which is lower than the EW scale. Viable effective neutrino masses can be obtained with $M_{NS} \sim \mathcal{O}(1\ \text{TeV})$, $M_D \sim \mathcal{O}(100\ \text{GeV})$, and $M_S \sim \mathcal{O}(0.1\ \text{keV})$.

Higher dimensional operator approach

In the seesaw mechanism, the neutrino masses are generated by dimension-5 effective operators,

$$\frac{HHLL}{\Delta}. \tag{1.55}$$

It is supposed that Majorana neutrino masses are generated at the cutoff scale of the new physics which is commonly defined at the GUT scale in order to sufficiently suppress the effective light neutrino masses. In the presence of some new symmetry, neutrino masses are

generated only at high mass dimensionalities while operators with lower mass dimensionalities are forbidden [92]. In this case, the operators generically have the suppression factor in terms of some power p of the ratio of VEV of the scalar field, ϕ, that breaks the new symmetry to the cutoff scale of the symmetry scale, $\left(\frac{\langle\phi\rangle}{\Delta}\right)^p$. If the dimensionality is high enough, the cutoff scale of the new physics can be on the order of a TeV.

1.6 Neutrino symmetries of nature

Symmetry is the main ingredient in particle physics to understand several phenomena. Abelian as well as non-Abelian discrete symmetries are used in model building in order to control allowed couplings and to study the flavor physics beyond the standard model. The quark and lepton masses and mixing angles have been studied in the framework of the flavor symmetries which are presented to control the Yukawa couplings. The study of neutrino masses and mixing [93] has stimulated interests in flavor symmetries. Non-Abelian discrete symmetries are studied as a tool for model building to derive experimental values of quark/lepton masses and mixing angles.

1.6.1 2-3 and Z_n

The 2-3, or $\mu-\tau$, is a symmetry in which the matrix elements of the neutrino mass matrix $\mathcal{M}_\nu$ is invariant under the interchange of the flavor basis vectors $|e\rangle \leftrightarrow |e\rangle$ and $|\mu\rangle \leftrightarrow -|\tau\rangle$. The minus sign in this transformation is introduced to conventionally generate only positive mixing angles. With this symmetry,

$$\begin{aligned} \mathcal{M}_\nu^{e\mu} &= -\mathcal{M}_\nu^{e\tau}, \\ \mathcal{M}_\nu^{\mu\mu} &= \mathcal{M}_\nu^{\tau\tau}, \\ \mathcal{M}_\nu^{\mu\tau} &= \mathcal{M}_\nu^{\tau\mu}. \end{aligned} \tag{1.56}$$

Thus, we may parametrize $\mathcal{M}_\nu$ by four parameters as in

$$\mathcal{M}_\nu = \begin{pmatrix} a & b & -b \\ b & f & e \\ -b & e & f \end{pmatrix}. \tag{1.57}$$

The two conditions in 1.56 implies $s_{13} = 0$ and $s_{23} = 1/\sqrt{2}$, and the unitary matrix that diagonalize the mass matrix is equal to

$$U = \begin{pmatrix} c_{12} & s_{12} & 0 \\ -\frac{1}{\sqrt{2}}s_{12} & \frac{1}{\sqrt{2}}c_{12} & \frac{1}{\sqrt{2}} \\ \frac{1}{\sqrt{2}}s_{12} & -\frac{1}{\sqrt{2}}c_{12} & \frac{1}{\sqrt{2}} \end{pmatrix} = \begin{pmatrix} 1 & 0 & 0 \\ 0 & \frac{1}{\sqrt{2}} & \frac{1}{\sqrt{2}} \\ 0 & -\frac{1}{\sqrt{2}} & \frac{1}{\sqrt{2}} \end{pmatrix} \cdot \begin{pmatrix} c_{12} & s_{12} & 0 \\ -s_{12} & c_{12} & 0 \\ 0 & 0 & 1 \end{pmatrix}. \quad (1.58)$$

The neutrino mass-squared difference values $(\Delta m_{12})^2 \ll (\Delta m_{23})^2$ demonstrate that $m_1 \approx m_2$ then it is much more natural to have a 1-2 symmetry [94] rather than a 2-3 symmetry. For this reason, the 2-3 symmetry in 1.56 might seem to be totally unnatural. Nevertheless, it turns out that the 2-3 symmetry on $\mathcal{M}_\nu$ given by 1.56 places no restriction whatsoever on the neutrino masses m_i, so this 2-3 symmetry on $\mathcal{M}_\nu$ is not contradictory to a 1-2 symmetry on the mass spectrum. Moreover, the 2-3 symmetry gives rise naturally to the right mixing of neutrinos.

The suggested structure of the neutrino mass matrix in the 2-3 symmetric limit leads to an additional symmetry of the mass matrix such as the Abelian discrete cyclic group Z_n. The Z_n group is defined as the group of n elements $\{A_1, A_2, \ldots, A_n\}$ such that for each element in the group $A_i^n = I$ where I is the identity matrix. The Z_n group can be represented as discrete rotations, whose generator corresponds to $2\pi/n$ rotation. For example, the group Z_2 consists of two elements $\{e, a\}$ where $a^2 = e$. The transformation of the element a under the Z_2 group could be even or odd i.e. $a \to \pm a$. The Z_4 group consists of four elements e, a, b, c where $a^4 = b^4 = c^4 = e$. The transformation of the Z_4 symmetry in the standard basis is given as $x \to \pm y$ or $x \to \pm iy$ for $x, y = a, b, c$.

1.6.2 A_4

The A_4 group is the symmetry of a tetrahedron as shown in Figure 1.6 and it is the smallest non-Abelian group. All of the 12 elements of the A_4 are denoted as

They are classified by the conjugacy classes as

$$\begin{aligned} C_1 &: \quad \{a_1\}, & h = 1, \\ C_3 &: \quad \{a_2, a_3, a_4\}, & h = 2, \\ C_4 &: \quad \{b_1, b_2, b_3, b_4\}, & h = 3, \\ C_{4'} &: \quad \{c_1, c_2, c_3, c_4\}, & h = 3, \end{aligned}$$

where we denote the orders of each element in the conjugacy class by h, where $a^h = e$. There are four conjugacy classes and there must be four irreducible representations. Using

$$a_1 = \begin{pmatrix} 1 & 0 & 0 \\ 0 & 1 & 0 \\ 0 & 0 & 1 \end{pmatrix}, \quad a_2 = \begin{pmatrix} 1 & 0 & 0 \\ 0 & -1 & 0 \\ 0 & 0 & -1 \end{pmatrix}, \quad a_3 = \begin{pmatrix} -1 & 0 & 0 \\ 0 & 1 & 0 \\ 0 & 0 & -1 \end{pmatrix},$$
$$a_4 = \begin{pmatrix} -1 & 0 & 0 \\ 0 & -1 & 0 \\ 0 & 0 & 1 \end{pmatrix}, \quad b_1 = \begin{pmatrix} 0 & 0 & 1 \\ 1 & 0 & 0 \\ 0 & 1 & 0 \end{pmatrix}, \quad b_2 = \begin{pmatrix} 0 & 0 & 1 \\ -1 & 0 & 0 \\ 0 & -1 & 0 \end{pmatrix},$$
$$b_3 = \begin{pmatrix} 0 & 0 & -1 \\ 1 & 0 & 0 \\ 0 & -1 & 0 \end{pmatrix}, \quad b_4 = \begin{pmatrix} 0 & 0 & -1 \\ -1 & 0 & 0 \\ 0 & 1 & 0 \end{pmatrix}, \quad c_1 = \begin{pmatrix} 0 & 1 & 0 \\ 0 & 0 & 1 \\ 1 & 0 & 0 \end{pmatrix},$$
$$c_2 = \begin{pmatrix} 0 & 1 & 0 \\ 0 & 0 & -1 \\ -1 & 0 & 0 \end{pmatrix}, \quad c_3 = \begin{pmatrix} 0 & -1 & 0 \\ 0 & 0 & 1 \\ -1 & 0 & 0 \end{pmatrix}, \quad c_4 = \begin{pmatrix} 0 & -1 & 0 \\ 0 & 0 & -1 \\ 1 & 0 & 0 \end{pmatrix}. \quad (1.59)$$

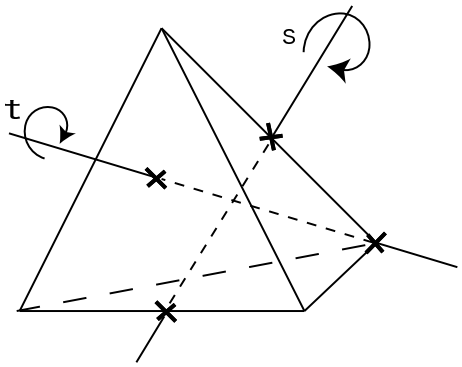

Figure 1.6. The A_4 symmetry of tetrahedron.

the orthogonality relation

$$\sum_{n=1}^{4} m_n^2 = m_1^2 + m_2^2 + m_3^2 + m_4^2 = 12, \quad (1.60)$$

where m_n is the dimension of the n-irreducible representations. Solving this equation one can obtain the solution $(m_1, m_2, m_3, m_4) = (1, 1, 1, 3)$. That is, the A_4 group has three singlets, **1**, **1**$'$, and **1**$''$, and a single triplet **3**, where the triplet corresponds to (1.59).

We denote $a_1 = e$, $a_2 = s$ and $b_1 = t$. A_4 can also be defined as the group generated by the two elements s and t obeying the relations:

$$s^2 = t^3 = (st)^3 = e. \quad (1.61)$$

It is straightforward to write all of a_i, b_i and c_i elements by s and t. Then, the conjugacy

classes are rewritten as

$$\begin{array}{lll} C_1: & \{e\}, & h=1, \\ C_3: & \{s, tst^2, t^2st\}, & h=2, \\ C_4: & \{t, ts, st, sts\}, & h=3, \\ C_{4'}: & \{t^2, st^2, t^2s, tst\}, & h=3. \end{array} \tag{1.62}$$

It immediately seen that one-dimensional unitary representations are given by:

$$\begin{array}{lll} \mathbf{1}: & s=1, & t=1, \\ \mathbf{1}': & s=1, & t=e^{i4\pi/3} \equiv \omega^2, \\ \mathbf{1}'': & s=1, & t=e^{i2\pi/3} \equiv \omega. \end{array} \tag{1.63}$$

The characters are shown in Table 1.2. Next, we consider the characters for the triplet representation. Obviously, the matrices in Eq. (1.59) correspond to the triplet representation. Thus, we can obtain their characters. Its result is also shown in Table 1.2.

	h	χ_1	$\chi_{1'}$	$\chi_{1''}$	χ_3
C_1	1	1	1	1	3
C_3	2	1	1	1	-1
C_4	3	1	ω	ω^2	0
$C_{4'}$	3	1	ω^2	ω	0

Table 1.2. Characters of A_4 representations

On the representation **3**, these generators are represented as

$$s = \begin{pmatrix} 1 & 0 & 0 \\ 0 & -1 & 0 \\ 0 & 0 & -1 \end{pmatrix}, \quad t = \begin{pmatrix} 0 & 0 & 1 \\ 1 & 0 & 0 \\ 0 & 1 & 0 \end{pmatrix}. \tag{1.64}$$

In the above basis, s is diagonal and t is non-diagonal. Next, we consider another basis [95] in which t is diagonal while s is non-diagonal. In this basis, we denote the generators as s' and t' to replace s and t, respectively,

$$s'^2 = t'^3 = (s't')^3 = e \ . \tag{1.65}$$

and these generators are represented as

$$s' = \frac{1}{3}\begin{pmatrix} -1 & 2 & 2 \\ 2 & -1 & 2 \\ 2 & 2 & -1 \end{pmatrix}, \quad t' = \begin{pmatrix} 1 & 0 & 0 \\ 0 & \omega^2 & 0 \\ 0 & 0 & \omega \end{pmatrix}, \tag{1.66}$$

for the representation **3**. These bases are related by the following unitary transformation matrix U_ω

$$U_\omega = \frac{1}{\sqrt{3}}\begin{pmatrix} 1 & 1 & 1 \\ 1 & \omega & \omega^2 \\ 1 & \omega^2 & \omega \end{pmatrix}. \tag{1.67}$$

We can write the elements s' and t' as

$$s' = U_\omega^\dagger s U_\omega = \frac{1}{3}\begin{pmatrix} -1 & 2 & 2 \\ 2 & -1 & 2 \\ 2 & 2 & -1 \end{pmatrix}, \quad t' = U_\omega^\dagger t U_\omega = \begin{pmatrix} 1 & 0 & 0 \\ 0 & \omega^2 & 0 \\ 0 & 0 & \omega \end{pmatrix}. \tag{1.68}$$

Recalling the 4 irreducible representations **1**, **1′**, **1″**, and **3** respectively, the multiplication rules are obtained as follows

$$\begin{aligned} &\mathbf{3} \times \mathbf{3} = \mathbf{1} + \mathbf{1}' + \mathbf{1}'' + \mathbf{3} + \mathbf{3} \\ &\mathbf{1} \times \mathbf{1} = \mathbf{1}, \;\; \mathbf{1}' \times \mathbf{1}' = \mathbf{1}'', \;\; \mathbf{1}' \times \mathbf{1}'' = \mathbf{1}, \;\; \mathbf{1}'' \times \mathbf{1}'' = \mathbf{1}' \end{aligned} \tag{1.69}$$

If $\mathbf{3} \sim (a_1, a_2, a_3)$ is a triplet transforming by the matrices in eq. (1.64) we have that under s: $s(a_1, a_2, a_3)^t = (a_1, -a_2, -a_3)^t$ (here the upper index t indicates transposition) and under t: $t(a_1, a_2, a_3)^t = (a_2, a_3, a_1)^t$. Then, from two such triplets $\mathbf{3}_a \sim (a_1, a_2, a_3)$, $\mathbf{3}_b \sim (b_1, b_2, b_3)$ the irreducible representations obtained from their product are:

$$\begin{aligned} \mathbf{1} &= a_1 b_1 + a_2 b_2 + a_3 b_3 \\ \mathbf{1}' &= a_1 b_1 + \omega^2 a_2 b_2 + \omega a_3 b_3 \\ \mathbf{1}'' &= a_1 b_1 + \omega a_2 b_2 + \omega^2 a_3 b_3 \\ \mathbf{3} &\sim (a_2 b_3, a_3 b_1, a_1 b_2) \\ \mathbf{3} &\sim (a_3 b_2, a_1 b_3, a_2 b_1) \end{aligned} \tag{1.70}$$

In fact, take for example the expression for $\mathbf{1}'' = a_1 b_1 + \omega a_2 b_2 + \omega^2 a_3 b_3$. Under s it is invariant and under t it goes into $a_2 b_2 + \omega a_3 b_3 + \omega^2 a_1 b_1 = \omega^2[a_1 b_1 + \omega a_2 b_2 + \omega^2 a_3 b_3]$ which is exactly

the transformation corresponding to $\mathbf{1}''$.

1.7 Nonstandard neutrino interactions

Neutrino oscillation results have confirmed that neutrinos are massive and lepton flavors are mixed. This opens a window for searching new physics beyond the standard model. Besides the standard matter effects [96, 97], the possibility of having non-standard neutrino interactions (NSIs) is opened up. The existence of neutrino masses and mixing requires physics beyond the standard model (SM). Hence it is not unexpected that neutrinos could have non-standard interactions (NSI). The effects of NSI have been widely considered in neutrino phenomenology [98, 99, 100, 101, 102, 103, 104, 105, 106, 107, 108, 109, 110, 111, 112]. Based on expectation of new physics at TeV scale, such non-standard interactions with matter possessed by neutrinos have been proposed and extensively discussed [113, 114, 115, 116, 117, 118]. The experimental constraints on NSI are summarized in [119, 120]. The importance of NSI for neutrino oscillation physics has been pointed out in a pioneering work by Grossman [121]. The NSI impact has been studied on solar neutrinos [122, 123, 124, 125], atmospheric neutrinos [126, 127, 128, 129, 130, 131], conventional and upgraded neutrino beams [132, 133, 134, 135, 136, 103, 137], neutrino factories [133, 138, 139, 140, 141, 142, 143, 144, 145], beta beams [146], supernova neutrinos [147, 148, 149], cosmological relic neutrinos [150], e^+e^- colliders [151], neutrino-electron scattering [152], and neutrino-nucleus scattering [153, 154].

At low energy, the CC and NC neutrino weak interactions can be described by effective dimension six operators like

$$\begin{aligned} \mathcal{L}^{\rm CC} &= \frac{G_F}{\sqrt{2}} \left[\bar{\nu}_\alpha \gamma^\rho (1-\gamma^5) \ell_\alpha\right] \left[\bar{f}' \gamma_\rho (1-\gamma^5) f\right], \\ \mathcal{L}^{\rm NC} &= \frac{G_F}{\sqrt{2}} \left[g_L^\nu \bar{\nu}_\alpha \gamma^\rho (1-\gamma^5) \nu_\alpha\right] \left[g_L^f \left(\bar{f} \gamma_\rho (1-\gamma^5) f\right) + g_R^f \left(\bar{f} \gamma_\rho (1+\gamma^5) f\right)\right], \end{aligned} \quad (1.71)$$

where G_F is the Fermi constant, ν_α is the neutrino field of flavor α, ℓ_α is the corresponding charged lepton field, and f, f' are fermions. The effective operators of the non-standard interactions have a structure similar to Eq. (1.71). If we consider only lepton number conserving operators, the most general NSI Lagrangian reads

$$\mathcal{L}_{\rm NSI} = \mathcal{L}_{V\pm A} + \mathcal{L}_{S\pm P} + \mathcal{L}_T, \quad (1.72)$$

where the different terms are classified according to their Lorentz structure in the following

way:

$$\begin{aligned}
\mathcal{L}_{V\pm A} &= \frac{G_F}{\sqrt{2}}\sum_{f,f'}\varepsilon_{\alpha\beta}^{f,f',V\pm A}\left[\bar{\nu}_\beta\gamma^\rho(1-\gamma^5)\ell_\alpha\right]\left[\bar{f}'\gamma_\rho(1\pm\gamma^5)f\right] \\
&+ \frac{G_F}{\sqrt{2}}\sum_{f}\varepsilon_{\alpha\beta}^{f,V\pm A}\left[\bar{\nu}_\alpha\gamma^\rho(1-\gamma^5)\nu_\beta\right]\left[\bar{f}\gamma_\rho(1\pm\gamma^5)f\right] + \text{h.c.}, \\
\mathcal{L}_{S\pm P} &= \frac{G_F}{\sqrt{2}}\sum_{f,f'}\varepsilon_{\alpha\beta}^{f,f',S\pm P}\left[\bar{\nu}_\beta(1+\gamma^5)\ell_\alpha\right]\left[\bar{f}'(1\pm\gamma^5)f\right], \\
\mathcal{L}_{T} &= \frac{G_F}{\sqrt{2}}\sum_{f,f'}\varepsilon_{\alpha\beta}^{f,f',T}\left[\bar{\nu}_\beta\sigma^{\rho\tau}\ell_\alpha\right]\left[\bar{f}'\sigma_{\rho\tau}f\right].
\end{aligned} \tag{1.73}$$

The dimensionless NSI parameters ε's represent the strength of the nonstandard interactions relative to G_F. Note that we deal with the SM neutrinos which are purely left-handed particles. This constraint on the neutrino chirality forbids $\nu\nu ff$ terms in $\mathcal{L}_{S\pm P}$ and $\mathcal{L}_T$. If the nonstandard interactions are supposed to be mediated by new state with a mass of order $M_{\rm NSI}$, the effective vertices in Eq. (1.73) will be suppressed by $1/M_{\rm NSI}^2$ in the same way as the standard weak interactions are suppressed by $1/M_{\rm W}^2$. Therefore we expect that

$$|\varepsilon| \sim \frac{M_{\rm W}^2}{M_{\rm NSI}^2}. \tag{1.74}$$

NSI effects enter the neutrino oscillation at production, propagation, and detection processes. For simplicity, we are going to discuss the NSI effect by considering the following effective weak interaction

$$\mathcal{L}_{\rm NSI} = \frac{G_F}{\sqrt{2}}\sum_{f,P}\varepsilon_{\alpha\beta}^{fP}\left(\bar{\nu}_\alpha\gamma^\mu L\nu_\beta\right)\left(\bar{f}\gamma_\mu Pf\right) \ , \tag{1.75}$$

where $P = \{L, R\}$ is a projection operator. In order to introduce the effective mixing parameters in the presence of the non-standard interactions, we start from neutrino oscillations in vacuum. The evolution in time of a neutrino mass eigenstate $|\nu(t)\rangle$ can be described by

$$\mathrm{i}\frac{\mathrm{d}}{\mathrm{d}t}|\nu(t)\rangle = H|\nu(t)\rangle \ , \tag{1.76}$$

where H is the Hamiltonian of the system. For neutrinos traveling in vacuum, the Hamiltonian in the ultra-relativistic limit $E \gg m_i$ is

$$H = \frac{1}{2E}U\,\mathrm{diag}\left(0, \Delta m_{21}^2, \Delta m_{31}^2\right)U^\dagger \ , \tag{1.77}$$

Thus, the neutrino oscillation probability from a neutrino flavor α to a neutrino flavor β is given by

$$P_{\alpha\beta} \equiv |S_{\alpha\beta}(t,t_0)|^2 = \left| \sum_i U_{\beta i} U^*_{\alpha i} e^{-i\frac{m_i^2 L}{2E}} \right|^2 \ . \tag{1.78}$$

The effective Hamiltonian responsible for neutrino propagation in matter, disregarding the neutral current contributions, is given by

$$\tilde{H}_{\alpha\beta} = H_{\alpha\beta} + a\left(\delta_{\alpha e}\delta_{\beta e} + \varepsilon_{\alpha\beta}\right) \ , \tag{1.79}$$

where $a = \sqrt{2}G_F N_e$ is the matter parameter arises from coherent forward scattering, N_e denotes the electron number density along the neutrino trajectory in matter, and the NSI parameters $\varepsilon_{\alpha\beta}$ are defined as

$$\varepsilon_{\alpha\beta} = \sum_{f,P} \varepsilon^{fP}_{\alpha\beta} \frac{N_f}{N_e} \ , \tag{1.80}$$

with N_f being the number density of a fermion of type f. The effective Hamiltonian in matter can be written similar to the vacuum Hamiltonian in Eq. (1.77) as

$$\tilde{H} = \frac{1}{2E} \tilde{U} \mathrm{diag}\left(\tilde{m}_1^2, \tilde{m}_2^2, \tilde{m}_3^2\right) \tilde{U}^\dagger \ , \tag{1.81}$$

where $\tilde{m}_i^2$ denote the effective mass-squared eigenvalues of neutrinos and $\tilde{U}$ is the unitary mixing matrix in matter. Assuming a constant matter density profile, which is close to reality, one can obtain the transition probability with matter effects including the NSI contribution

$$P_{\alpha\beta} \equiv |S_{\beta\alpha}(t,t_0)|^2 = \left| \sum_i \tilde{U}^*_{\beta i} \tilde{U}_{\alpha i} e^{-\mathrm{i}\frac{\tilde{m}_i^2 L}{2E}} \right|^2 \ . \tag{1.82}$$

From Eqs. (1.78, 1.82), the neutrino oscillation probability in vacuum and in matter have the same form with replacing the vacuum parameters U and m_i^2 by the effective parameters $\tilde{U}$ and $\tilde{m}_i^2$. Thus, the key point turns out to be the diagonalization of the effective Hamiltonian $\tilde{H}$ and figuring out the explicit relations of the effective parameters.

After discussing the NSI effects in the propagation process of neutrinos, now in order to complete the picture we need to introduce the contributions of the NSIs at the production and detection processes. In most of the viable models for NSIs, the source and detector effects are simultaneously taken into account. Now, the NSI parameters at sources and

detectors can be defined as [155, 138, 156]

$$|\nu^s_\alpha\rangle = |\nu_\alpha\rangle + \sum_{\beta=e,\mu,\tau} \varepsilon^s_{\alpha\beta}|\nu_\beta\rangle = (1+\varepsilon^s)\tilde{U}|\nu_i\rangle\,, \tag{1.83}$$

$$\langle\nu^d_\beta| = \langle\nu_\beta| + \sum_{\alpha=e,\mu,\tau} \varepsilon^d_{\alpha\beta}\langle\nu_\alpha| = \langle\nu_i|\tilde{U}^\dagger[1+(\varepsilon^d)^\dagger]\,, \tag{1.84}$$

where the superscripts 's' and 'd' denote source and detector, respectively, and $|\nu_i\rangle$ is a neutrino mass eigenstate. Note that the states $|\nu^s_\alpha\rangle$ and $\langle\nu^d_\beta|$ are not orthonormal states due to the NSIs. The matrices ε^s and ε^d are arbitrary and non-unitary in general. They are not necessarily the same matrix since different physical processes take place at the source and the detector. If the production and detection processes are exactly the same process with the same participating fermions (e.g. β-decay and inverse β-decay), then the same matrix enters as $\varepsilon^s = \left(\varepsilon^d\right)^\dagger$, or on the form of matrix elements, $\varepsilon^s_{\alpha\beta} = \varepsilon^d_{\alpha\beta} = (\varepsilon^s_{\beta\alpha})^* = (\varepsilon^d_{\beta\alpha})^*$ [156]. For example, in the case of non-unitarity effects (which can be considered as a type of NSIs, see e.g. Ref. [157]) in the minimal unitarity violation model [158, 159, 160, 161, 162, 163] $\varepsilon^s = \left(\varepsilon^d\right)^\dagger$. Thus, it is important to keep in mind that these matrices are model-dependent parameters.

The transition probabilities are then modified in general as[2]

$$\begin{aligned}
P_{\alpha\beta} &= \left|\left[\left(1+\varepsilon^d\right)^T \cdot S(t,t_0) \cdot \left(1+\varepsilon^s\right)^T\right]_{\beta\alpha}\right|^2, \\
&= \left|\sum_{\gamma,\delta,i} \left(1+\varepsilon^d\right)_{\gamma\beta} \left(1+\varepsilon^s\right)_{\alpha\delta} \tilde{U}_{\delta i}\tilde{U}^*_{\gamma i} e^{-\mathrm{i}\frac{\tilde{m}^2_i L}{2E}}\right|^2, \\
&= \sum_{i,j} \tilde{\mathcal{J}}^i_{\alpha\beta}\tilde{\mathcal{J}}^{j*}_{\alpha\beta} - 4\sum_{i>j} \mathrm{Re}(\tilde{\mathcal{J}}^i_{\alpha\beta}\tilde{\mathcal{J}}^{j*}_{\alpha\beta}) \sin^2\left(\frac{\Delta\tilde{m}^2_{ij}L}{4E}\right) \\
&+ 2\sum_{i>j} \mathrm{Im}(\tilde{\mathcal{J}}^i_{\alpha\beta}\tilde{\mathcal{J}}^{j*}_{\alpha\beta}) \sin\left(\frac{\Delta\tilde{m}^2_{ij}L}{2E}\right),
\end{aligned} \tag{1.85}$$

where

$$\tilde{\mathcal{J}}^i_{\alpha\beta} = \tilde{U}^*_{\alpha i}\tilde{U}_{\beta i} + \sum_\gamma \varepsilon^s_{\alpha\gamma}\tilde{U}^*_{\gamma i}\tilde{U}_{\beta i} + \sum_\gamma \varepsilon^d_{\gamma\beta}\tilde{U}^*_{\alpha i}\tilde{U}_{\gamma i} + \sum_{\gamma,\delta} \varepsilon^s_{\alpha\gamma}\varepsilon^d_{\delta\beta}\tilde{U}^*_{\gamma i}\tilde{U}_{\delta i}\,. \tag{1.86}$$

In fact, an important feature of Eq. (1.85) is that when $\alpha \neq \beta$, the first term is generally non-vanishing, which means that a neutrino flavor transition would already happen at the source before the oscillation process has taken place. This is known as the *zero-distance effect*

[2]Here we have neglected the normalization factors, which are needed in order to normalize the quantum states.

[164]. It could be measured with a near detector close to the source. Note that Eq. (1.85) is also usable to describe neutrino oscillations with a non-unitary mixing matrix, e.g. in the minimal unitarity violation model [158].

CHAPTER 2

PROBING LIGHT PSEUDOSCALAR, AXIAL VECTOR STATES THROUGH $\eta_b \to \tau^+\tau^-$

2.1 Introduction

In this work we will be interested in probing light scalar and spin 1 states via η_b decays. As the η_b is a pseudoscalar, a light pseudoscalar and a spin 1 state with axial vector coupling can directly couple to η_b. We will assume the pseudoscalar to couple to the mass of the fermion as is usually the case for Higgs coupling to fermions. Hence, the η_b which is a $b\bar{b}$ bound state has advantages over the η_c and η/η' mesons which are $c\bar{c}$ and $q\bar{q}(q = u, d, s)$ bound states, respectively. The η_b is expected to be a sensitive probe of a light axial vector state. This follows from the fact that the longitudinal polarization of the axial vector, $\epsilon_L^\mu \sim k^\mu$, when k^μ the momentum of the vector boson is much larger than its mass. Consequently, the effective axial vector-fermion pair coupling is proportional to the fermion mass for the longitudinal polarization.

In this work we will study the process $\eta_b \to \tau^+\tau^-$ mediated by a pseudoscalar (A^0) or an axial vector (U). In the SM this process can only go through a Z exchange at tree level and is highly suppressed with a branching ratio $\sim 4 \times 10^{-9}$. There is also a higher order contribution to $\eta_b \to \tau^+\tau^-$ in the SM, via two intermediate photons. The branching ratio for this process is also tiny $\sim 10^{-10}$. Hence, a measurement of $BR[\eta_b \to \tau^+\tau^-]$ larger than the SM rate will be a signal of new states. One can also probe the states $A^0(U)$ in Υ decays. To search for light $A^0(U)$ states in Υ decays one generally considers the decay chains, $\Upsilon \to A^0(U)\gamma$ ($A^0(U) \to \tau^+\tau^-$) [21]. In other words, the $A^0(U)$ is assumed to be produced on-shell. One then looks for a peak in the invariant mass of the τ pairs. The experimental

measurement/constraint of $BR[\Upsilon \to A^0(U)\gamma] \times BR[A^0(U) \to \tau^+\tau^-]$ can be converted into a measurement/constraint on the coupling of the $A^0(U)$ to $b\bar{b}$, and hence on model parameters, if the $BR[A^0(U) \to \tau^+\tau^-]$ is used as an input [165]. Clearly as $m_{A^0(U)} > m_\Upsilon$, the $A^0(U)$ can no longer be produced on-shell and the rate for $\Upsilon \to \tau^+\tau^-\gamma$ will fall and consequently the constraints on the model parameters will be weaker. Note that the constraint $m_{A^0} < 2m_B$ needs to be assumed in the very particular case where the CP-even Higgs mass $m_h < 114$ GeV and $h \to 2A^0$ dominates over $h \to 2m_b$ [11]. In general $m_{A^0} > 2m_B$ is also possible. We will just assume the existence of light pseudoscalar and axial vector states close to the η_b mass but they can have masses that are greater than or less than $2m_b$.

The η_b has only been seen in the radiative decays $\Upsilon \to \gamma\eta_b$. Hence, the decay $\eta_b \to \tau^+\tau^-$ has only been studied via the decay $\Upsilon \to \tau^+\tau^-\gamma$. However, the decay $\eta_b \to \tau^+\tau^-$ can be studied independently from the process $\Upsilon \to \tau^+\tau^-\gamma$ as the η_b can be produced from various other processes such as two-photon collisions, $\gamma\gamma \to \eta_b$ [16], and in two parton collisions [17, 166], in hadron colliders like the Tevatron and the LHC. The process $\eta_b \to \tau^+\tau^-$ has several advantages over Υ decays in probing $A^0(U)$ states specially when $A^0(U)$ is off-shell which is always the case when $m_{A^0(U)} > m_\Upsilon$. First, unlike the η_b which can couple directly to $A^0(U)$, the Υ can only couple to $A^0(U)$ in conjunction with another state- usually a photon. Hence, the Υ couplings are second order and therefore it can decay only to the $\tau^+\tau^-\gamma$ state with a rate much smaller than the rate for $\eta_b \to \tau^+\tau^-$. However, the Υ states are narrower than the η_b, which may compensate partially the larger rate for $\eta_b \to \tau^+\tau^-$ relative to $\Upsilon \to \tau^+\tau^-\gamma$ in the branching ratio measurements. Secondly, an important distinction between $\Upsilon \to \tau^+\tau^-\gamma$ and $\eta_b \to \tau^+\tau^-$ is that the former decay can also proceed as a radiative decay in the SM while the latter decay is highly suppressed in the SM as indicated above. Adapting the expression used to estimate the SM branching ratio for $J/\psi \to e^+e^-\gamma$ [167], with the γ emitted from the final state electrons, to the decay $\Upsilon \to \tau^+\tau^-\gamma$, the rate for this decay in the SM is,

$$d\Gamma_{\Upsilon\to\tau^+\tau^-\gamma} = d\Gamma_{\Upsilon\to\tau^+\tau^-}\beta'^3\frac{2\alpha}{\pi}\frac{dE'_\gamma}{E'_\gamma}\frac{s'}{s}\frac{1-cos^2\theta'_{\gamma\tau}}{(1-\beta'^2cos^2\theta'_{\gamma\tau})^2}d\Omega'_\gamma, \tag{2.1}$$

with

$$d\Gamma_{\Upsilon\to\tau^+\tau^-} = \frac{3}{3+\lambda}(1+\lambda\cos^2\theta'_\tau)\Gamma_{\Upsilon\to\tau^+\tau^-}\frac{d\Omega'_\tau}{4\pi}. \tag{2.2}$$

Here E'_γ represents the γ energy, θ'_γ and $\phi'_\gamma(\Omega'_\gamma)$ the γ angles, and θ'_τ and $\phi'_\tau(\Omega'_\tau)$ the τ angles, all in the $\tau^+\tau^-$ c.m. frame. β' is the τ velocity and $\theta'_{\gamma\tau}$ is the angle between the τ and γ directions, also in the $\tau^+\tau^-$ c.m. frame while s' is the $\tau^+\tau^-$ invariant mass squared and s is

the Υ invariant mass squared. The parameter λ is determined from the experimental data to be (0.88 ± 0.19) [167]. Using the branching ratio for $\Upsilon \to \tau^+\tau^- = 2.6 \times 10^{-2}$ [168] we estimate the branching ratio for $\Upsilon \to \tau^+\tau^-\gamma = 4.4 \times 10^{-3}$ with $E_\gamma > 100$ MeV.

Naively, the rate for $\Upsilon \to \tau^+\tau^-\gamma$ through an off-shell A^0, from a 2HDM of type II, relative to the SM rate for $\Upsilon \to \tau^+\tau^-\gamma$ is $\sim \frac{g^4 \tan^4\beta m_b^2 m_\tau^2}{16 e^4 M_W^4}$. Therefore, for large $\tan\beta \sim 28$ the SM and the NP rates may be comparable. However given the hadronic uncertainties in estimating the SM and the NP rates for $\Upsilon \to \tau^+\tau^-\gamma$, it will be difficult to distinguish between the NP and the SM contributions. Hence, searching for $A^0(U)$ with $m_{A^0(U)} > m_\Upsilon$ in $\Upsilon \to \tau^+\tau^-\gamma$ will be very difficult because of the large SM background. Note that even in e^+e^- machines like the B-factories where the η_b is produced through the decay $\Upsilon \to \gamma\eta_b$, the product of branching ratios $BR[\Upsilon \to \gamma\eta_b] \times [\eta_b \to \tau^+\tau^-]$ is tiny in the SM because of the highly suppressed $BR[\eta_b \to \tau^+\tau^-] \sim 4 \times 10^{-9}$. Using the measured $BR[\Upsilon \to \gamma\eta_b] \sim 5 \times 10^{-4}$ [12, 13] one obtains $BR[\Upsilon \to \gamma\eta_b] \times [\eta_b \to \tau^+\tau^-] \sim 2 \times 10^{-12}$ which is very difficult to measure. In the presence of new physics this product of branching ratios is enhanced and can reach $\lesssim 10^{-5}$. Hence the observation of $\Upsilon \to \gamma\tau^+\tau^-$, with the τ pairs coming from η_b, at branching ratios much larger than the SM expectations will be signal for new light states. In summary, the large SM background in $\Upsilon \to \tau^+\tau^-\gamma$ and a tiny SM contribution to $\eta_b \to \tau^+\tau^-$ makes the later decay potentially a better probe for $A^0(U)$ than the former if the decays proceed through the off-shell exchange of $A^0(U)$.

There are good theoretical motivations for the existence of a light CP-odd A^0 Higgs boson or an axial vector boson U with masses, m_{A^0} and m_U respectively, in the GeV range or below. There has been interest in the $m_{A^0} < 2m_B$ region, for which a light Higgs, h, with SM-like WW, ZZ and fermionic couplings can have mass $m_h \sim 100$ GeV while still being consistent with LEP data by virtue of $h \to A^0A^0$. This scenario could even explain the $2.3\,\sigma$ excess in the $e^+e^- \to Z + 2b$ channel for $M_{2b} \sim 100$ GeV [169]. Such a light pseudoscalar Higgs can naturally arise in extensions of MSSM with additional singlet scalars and fermions (gauge-singlet supermultiplets) known as Next-to-Minimal Supersymmetric Model (NMSSM) [170]. Constraints on models with a light A^0 state have been studied recently within a 2HDM framework with certain assumptions about the coupling and in NMSSM [165, 171, 172].

Our goal will not be to work in a specific model but we will assume the couplings of the A^0 to the b quark and the τ lepton to be the same as in the 2HDM. We will assume this 2HDM is part of some extension of the SM. Hence, we will not strictly follow the bounds and constraints obtained in some specific extension of the SM which includes the 2HDM, but will choose values for the parameters in our calculation which are similar to constraints on these parameters in specific NP models. The process $\eta_b \to \tau^+\tau^-$ will proceed through

an off-shell A^0 and we will consider both $m_{A^0} < m_{\eta_b}$ and $m_{A^0} > m_{\eta_b}$. In general, there will be mixing between A^0 and the η_b and as the pseudoscalar state gets close to the η_b mass the mixing between the states will become important [173]. The calculation of this mixing is model dependent and while there are estimates of this mixing in simple quark models the mixing may be very different in other approaches to the bound state problem in QCD. Hence, we will not take into account mixing in our analysis. Therefore, our results will be reliable when the A^0 mass is away from the η_b mass. We will further assume that the A^0 is narrow and neglect its width in our calculations. This approximation will be good as long as m_{A^0} is sufficiently away from the η_b mass. When A^0 is produced on-shell both mixing and width effects will become important and our results will not be reliable.

There are also models, for example within SUSY with extra gauged $U(1)$, which have a light axial vector state [174]. These light states can also mediate the process $\eta_b \to \tau^+\tau^-$. Constraints on these models have been studied [175, 176, 177, 178, 179]. We will consider $\eta_b \to \tau^+\tau^-$ through the exchange of the axial vector U. To perform our calculations we will choose the model discussed in [176, 179] and neglect the width of the U-boson. Finally, we note that there are recent dark matter models [180] that also contain light scalar (pseudoscalar) and vector (axial vector) states which may be probed via $\eta_b \to \tau^+\tau^-$. The HyperCP collaboration has some events for the decay $\Sigma^+ \to p\mu^+\mu^-$ which may be interpreted as evidence for a light pseudoscalar state [181]. In this work we perform the calculations of the decay $\eta_b \to \tau^+\tau^-$ in the SM and in models with a light pseudoscalar A^0 and a light axial vector U state. Next, we present our conclusion after the numerical results of the branching ratios for $\eta_b \to \tau^+\tau^-$.

2.2 $\eta_b \to \tau^+\tau^-$ in the SM and NP

In this section we will study $\eta_b \to \tau^+\tau^-$ in the SM and in models of NP. The η_b is a pseudoscalar and cannot couple to γ directly. Hence, in the SM, $\eta_b \to \tau^+\tau^-$ can only proceed through the exchange of a Z at tree level and we will calculate the branching ratio for this process in the SM . This decay can also proceed at higher order in the SM through intermediate two photon states.

In the presence of NP $\eta_b \to \tau^+\tau^-$ can proceed through the exchange of a light pseudoscalar or a light spin 1 boson with axial vector coupling. We will consider these two NP scenarios in this section. The various tree level contribution to the $\eta_b \to \tau^+\tau^-$ in the SM and NP are shown in Fig. 2.1 and Fig. 2.2, respectively.

We begin with $\eta_b \to \tau^+\tau^-$ in the SM. We show, in Fig. 2.1, the decay process $\eta_b \to \tau^+\tau^-$ via the Z-boson exchange and through the two photon intermediate states. The decay rate

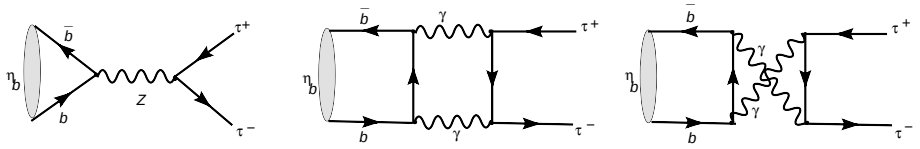

Figure 2.1. Various processes contributing to $\eta_b \to \tau^+\tau^-$ in the SM.

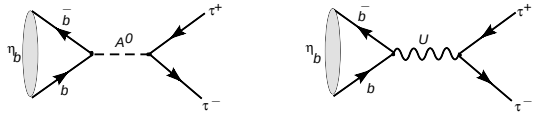

Figure 2.2. Various processes contributing to $\eta_b \to \tau^+\tau^-$ in NP.

for the tree level Z exchange process can be obtained as,

$$\Gamma^Z(\eta_b \to \tau^+\tau^-) \;=\; \frac{G_F^2 M_W^4 m_\tau^2 f_{\eta_b}^2 m_{\eta_b}}{16\pi \cos^4\theta_W}\beta_\tau\Big(1-\frac{m_{\eta_b}^2}{M_Z^2}\Big)^2|a_Z|^2, \tag{2.3}$$

where θ_W denotes the Weinberg angle, $\beta_\tau = \sqrt{1-\left(\frac{2m_\tau}{m_{\eta_b}}\right)^2}$ is the velocity of the τ lepton in the η_b rest frame and

$$|a_Z|^2 \;\equiv\; \frac{1}{(m_{\eta_b}^2 - M_Z^2)^2 + M_Z^2\Gamma_Z^2}. \tag{2.4}$$

The decay constant f_{η_b} in Eq. 2.3 is defined as [182],

$$\langle 0\bar{b}(0)\gamma_\mu\gamma_5 b(0)\rangle\eta_b(q) \;=\; i f_{\eta_b} q_\mu. \tag{2.5}$$

The process $\eta_b \to \tau^+\tau^-$ can also go via two photon intermediate states as shown in diagram Fig. 2.1. This diagram is dominated by the imaginary part [183] which we can estimate using unitarity [184] to obtain,

$$\Gamma^{2\gamma}[\eta_b \to \tau^+\tau^-] \;\geq\; \frac{\alpha^2}{2\beta_\tau}\left[\frac{m_\tau}{m_{\eta_b}}\ln\frac{(1+\beta_\tau)}{(1-\beta_\tau)}\right]^2\Gamma[\eta_b \to \gamma\gamma], \tag{2.6}$$

where α is the electromagnetic fine structure constant. One can calculate $\Gamma[\eta_b \to \gamma\gamma]$ as,

$$\Gamma[\eta_b \to \gamma\gamma] \;=\; \frac{\pi\alpha^2 m_{\eta_b} f_{\eta_b}^2}{81 m_b^2}, \tag{2.7}$$

where we have used the heavy quark limit for the b quark. Since the 2γ exchange contribution is mostly imaginary relative to the Z exchange contribution therefore to a good

approximation the total width $\Gamma_t[\eta_b \to \tau^+\tau^-]$ is ,

$$\Gamma_t[\eta_b \to \tau^+\tau^-] \approx \Gamma^Z[\eta_b \to \tau^+\tau^-] + \Gamma^{2\gamma}[\eta_b \to \tau^+\tau^-]. \quad (2.8)$$

We now turn to NP models and begin with the 2HDM. The couplings of the down-type quarks D and charged leptons ℓ with A^0 in the generic 2HDM model are given by [185]

$$\mathcal{L}^{D,\ell}_{A^0} = \frac{igF_{A^0}}{2M_W}(\bar{D}M_D^{diag}\gamma_5 D + \bar{\ell}M_l^{diag}\gamma_5\ell)A^0, \quad (2.9)$$

where F_{A^0} is a model-dependent parameter, $M_D^{diag} = (m_d, m_c, m_b)$ and $M_\ell^{diag} = (m_e, m_\mu, m_\tau)$ are the diagonal mass matrices of D and ℓ, respectively. We will consider $F_{A^0} > 1$ in our analysis. In the case of 2HDM type (II) $F_{A^0} \equiv \tan\beta$ while in 2HDM type (I) $F_{A^0} \equiv -\cot\beta$.

In Fig. 2.2(a) we show the decay process $\eta_b \to \tau^+\tau^-$ via the exchange of the CP-odd Higgs scalar A^0. The decay rate for this process can be obtained as,

$$\Gamma^{A^0}(\eta_b \to \tau^+\tau^-) = \frac{G_F^2 m_\tau^2 f_{\eta_b}^2 m_{\eta_b}^5}{16\pi}\beta_\tau |a_{A^0}|^2, \quad (2.10)$$

where the invariant coefficient a_{A^0} depends on the mass m_{A^0} as,

$$|a_{A^0}|^2 \equiv \frac{F_{A^0}^4}{(m_{\eta_b}^2 - m_{A^0}^2)^2}. \quad (2.11)$$

We have assumed that the decay width Γ_{A^0} for the A^0 is negligible. In Eq. 2.10, we have used,

$$\langle 0|\bar{b}(0)\gamma_5 b(0)\rangle \eta_b(q) = \frac{if_{\eta_b}m_{\eta_b}^2}{2m_b}, \quad (2.12)$$

where f_{η_b} has been defined in Eq. 2.5.

Finally, we move to NP models that contain a light spin 1 boson with axial vector couplings. In Fig. 2.2(b) we show the decay process $\eta_b \to \tau^+\tau^-$ via the exchange of the light neutral gauge boson U. We write down a model independent Lagrangian for the U-boson but we assume the structure of the Lagrangian to be similar to the one discussed in Ref. [176, 177, 178]. We take the U couplings to the down-type quarks and charged leptons to be given by

$$\mathcal{L}_U^{D,\ell} = f_A^{D,\ell}(\bar{D}\gamma^\mu\gamma_5 D + \bar{\ell}\gamma^\mu\gamma_5\ell)U_\mu, \quad (2.13)$$

with the axial coupling

$$f_A^{D,\ell} = 2^{-\frac{3}{4}} G_F^{\frac{1}{2}} m_U F_U, \tag{2.14}$$

where m_U denotes the mass of U-boson and F_U denotes a model-dependent parameter. In the specific model [176, 177, 178], $F_U \equiv \cos\zeta \tan\beta$.

Again, we will be interested in $F_U > 1$. The decay rate for $\eta_b \to \tau^+\tau^-$ can be obtained as

$$\Gamma^U(\eta_b \to \tau^+\tau^-) = \frac{G_F^2 m_\tau^2 f_{\eta_b}^2 m_{\eta_b}}{16\pi} \beta_\tau (m_U^2 - m_{\eta_b}^2)^2 F_U^4 |a_U|^2, \tag{2.15}$$

where

$$|a_U|^2 = \frac{1}{(m_{\eta_b}^2 - m_U^2)^2 + m_U^2 \Gamma_U^2}. \tag{2.16}$$

Eq. 2.16 can be expanded as,

$$|a_U|^2 = \frac{1}{(m_{\eta_b}^2 - m_U^2)^2} (1 - x^2 + \dots), \tag{2.17}$$

if $x = \frac{\Gamma_U/m_U}{(1-m_{\eta_b}^2/m_U^2)} < 1$.

Neglecting x, Eq. 2.15 reduces to

$$\Gamma^U(\eta_b \to \tau^+\tau^-) = \frac{G_F^2 m_\tau^2 f_{\eta_b}^2 m_{\eta_b}}{16\pi} \beta_\tau F_U^4. \tag{2.18}$$

Thus, Eq. 2.18 shows that the decay width for $\eta_b \to \tau^+\tau^-$ does not depend on m_U in the approximation of neglecting the width of the U-boson. This result is easy to understand. If one increases the mass of the U then the matrix element for $\eta_b \to \tau^+\tau^-$ is suppressed due to propagator effects. However, the coupling, which is proportional to m_U, increases to compensate for this suppression. The fact that the width for $\eta_b \to \tau^+\tau^-$ is independent of m_U only holds because the η_b is a pseudoscalar.

The result of Eq. 2.18 does not make sense as m_U gets sufficiently large as the couplings in Eq. 2.14 becomes non-perturbative. Requiring the couplings to be ≤ 1 one gets the constraints $m_U \leq \frac{4M_W}{gF_U}$. Hence for $F_U \sim 50$ one can get m_U to be in the GeV range.

It is interesting to note that in the up sector the behavior for the decay width is different.

The coupling of the vector boson to the up type quark, U, is given by

$$\mathcal{L}_U = f_A^{UP} \bar{U} \gamma^\mu \gamma_5 U U_\mu, \tag{2.19}$$

with the axial coupling of the up-type quarks

$$f_A^{UP} = 2^{-\frac{3}{4}} G_F^{\frac{1}{2}} m_U F'_U. \tag{2.20}$$

In the model of Ref. [176, 177, 178], $F'_U \equiv \cos\zeta \cot\beta$.

For instance, the branching ratio $\mathcal{BR}(\eta_c \to \mu^+\mu^-)$ does not depend on m_U or on $\tan\beta$ and is given as,

$$\Gamma^U(\eta_c \to \mu^+\mu^-) = \frac{G_F^2 m_\mu^2 f_{\eta_c}^2 m_{\eta_c}}{16\pi} \bar{\beta}_\tau \cos^4\zeta. \tag{2.21}$$

where $\bar{\beta}_\tau = \sqrt{1 - \left(\frac{2m_\mu}{m_{\eta_c}}\right)^2}$ and f_{η_c} is the η_c decay constant. We can see from Eq. 2.21 that the branching ratio $\mathcal{BR}(\eta_c \to \mu^+\mu^-)$ is much smaller than $\mathcal{BR}(\eta_b \to \tau^+\tau^-)$ if $\tan\beta > 1$ because of the absence of the factor $\tan^4\beta$ in the rate for $\eta_c \to \mu^+\mu^-$.

2.3 Numerical analysis

In this section we present our numerical results. We take the average $\eta_b(1S)$ mass to be $m_{\eta_b} = 9390.8 \pm 3.2$ MeV [13], the decay constant $f_{\eta_b} = (705 \pm 27)$ MeV [186] and the width to be $\Gamma_{\eta_b} \approx 10$ MeV [187].

In the SM, at tree level, $\eta_b \to \tau^+\tau^-$ goes through the exchange of a Z-boson and we obtain a tiny branching ratio $\mathcal{BR}^Z(\eta_b \to \tau^+\tau^-) = 3.8 \times 10^{-9}$. In our calculation we have used $\Gamma_Z = 2.4952 \pm 0.0023$ GeV [168]. For the two photon contribution to $\eta_b \to \tau^+\tau^-$, we obtain, using Eq. 2.6 and Eq. 2.7, $\mathcal{BR}^{2\gamma}[\eta_b \to \tau^+\tau^-] \geq 4.6 \times 10^{-10}$ for $m_b = 4.8$ GeV. Using Eq. 2.8 the total branching ratio for $\eta_b \to \tau^+\tau^-$ is $\approx 4.3 \times 10^{-9}$.

In Fig. 2.3, we plot the logarithm of the branching ratio for $\eta_b \to \tau^+\tau^-$ mediated by the pseudoscalar A^0 in a generic 2HDM model. The branching ratio, $\mathcal{BR}^{A^0}$, is plotted for various values of the A^0 mass, which we take from 0.1 to 20 GeV, and for various values of F_{A^0}. As the mass of the A^0 approaches the mass of the η_b the branching ratio increases and blows up at $m_{A^0} = m_{\eta_b}$. This behavior clearly does not represent the physical situation because in this region the width of the A^0 and mixing effects of the A^0 with η_b become important and regularize the A^0 contribution. We observe in Fig. 2.3 that the branching ratio $\sim F_{A^0}^4$ is very sensitive to F_{A^0}. The branching ratio is relatively less sensitive to the mass m_A^0. We see

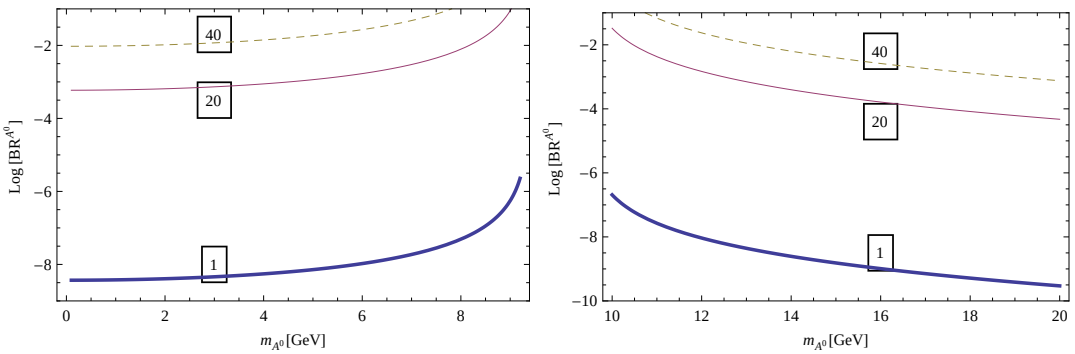

Figure 2.3. The logarithm of $\mathcal{BR}^{A^0}(\eta_b \to \tau^+\tau^-)$ as a function of m_{A^0} for different values of F_{A^0} and $m_{A^0} \in [0.1, 20]$ GeV.

from the plots in Fig. 2.3 that the branching ratio for $\eta_b \to \tau^+\tau^-$, through the A^0 exchange, can be considerably larger than the SM branching ratios and can vary from $\sim 10^{-8}$ to the experimental bound of 8 % for $F_{A^0} = 40$. Since we have neglected the width and mixing effects our predictions are no longer reliable as the mass of the A^0 approaches the mass of the η_b. The mixing effects are model dependent and as an example, for the model for mixing employed in Ref. [173], the effects of mixing are important in the m_{A^0} mass range of $9.4-10.5$ GeV. We see from Fig. 2.3 that even outside this range the branching ratio for $\eta_b \to \tau^+\tau^-$ can be significant and we expect the same to be true also in the mass range where mixing effects are important.

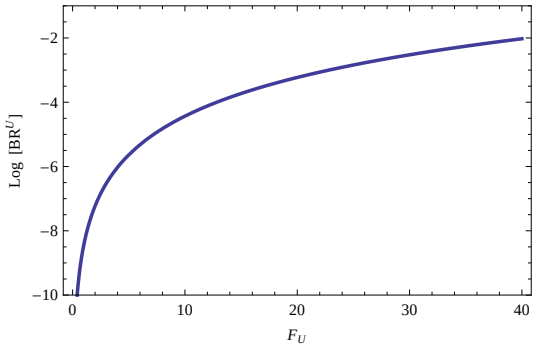

Figure 2.4. The logarithm of $\mathcal{BR}^U(\eta_b \to \tau^+\tau^-)$ as a function of F_U.

As discussed in the previous section, the branching ratio for the decay $\mathcal{BR}^U(\eta_b \to \tau^+\tau^-)$ is independent of the mass of the gauge boson U in the approximation of neglecting the width of the U-boson. We next plot in Fig. 2.4 the logarithm of the branching ratio for $\eta_b \to \tau^+\tau^-$ versus F_U. Working in a specific model [176, 177, 178] $F_U \equiv \cos\zeta \tan\beta$, we plot the branching ratio versus the invisibility factor $\cos\zeta$ for different values of $\tan\beta$ in Fig. 2.5. Again we observe that the branching ratio can vary over a wide range and can be much

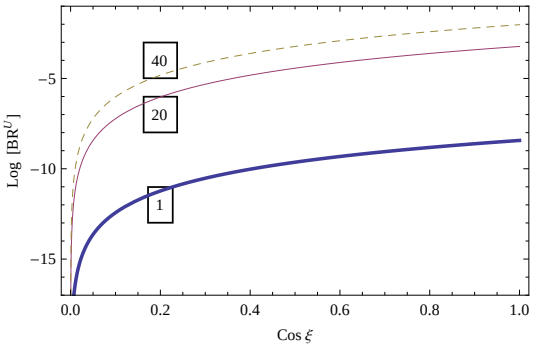

Figure 2.5. The logarithm of $\mathcal{BR}^U(\eta_b \to \tau^+\tau^-)$ as a function of $\cos\zeta$ for different values of $\tan\beta$ and $\cos\zeta \in [0,1]$.

larger than the SM prediction.

2.4 Conclusion

In this work we explored the decay $\eta_b \to \tau^+\tau^-$ as a probe for a light pseudoscalar or a light axial vector state. We estimated the SM branching ratios for $\eta_b \to \tau^+\tau^-$ via the Z exchange and the two photon intermediate state and found it to be very small at $\sim 4\times10^{-9}$. We then considered the decay process $\eta_b \to \tau^+\tau^-$ mediated via the pseudoscalar Higgs boson A^0 in a 2HDM-type NP model. We found that the branching ratio for $\eta_b \to \tau^+\tau^-$ can be substantially larger than the SM prediction and can reach the experimental bound of 8 %. Working in a specific model containing a light axial vector state, U, a similar result was obtained for the branching ratio of $\eta_b \to \tau^+\tau^-$. We also obtained an interesting result that the $\mathcal{BR}^U(\eta_b \to \tau^+\tau^-)$ is independent of the mass of U-boson if the width of the U is neglected. This result followed from the fact that the axial U-boson couplings to fermions were proportional to the mass m_U and the fact that η_b is a pseudoscalar. A constraint on the U-boson mass could be obtained by requiring its coupling to fermions to be ≤ 1. In light of the results obtained in the work an experimental measurement of the branching ratio for $\eta_b \to \tau^+\tau^-$ is strongly desirable as this measurement might reveal the presence of light, $\sim$ GeV, pseudoscalar or axial vector states. The experimental measurements of $\eta_b \to \tau^+\tau^-$ may be feasible at planned high luminosity B factories and at hadron colliders such as the Tevatron and the LHC, especially if the branching ratios are much larger than the SM rate.

CHAPTER 3

THE TOP FORWARD BACKWARD ASYMMETRY WITH GENERAL Z' COUPLINGS

3.1 Introduction

The measurement of the top forward-backward asymmetry in $t\bar{t}$ production measured at the Tevatron shows deviation from the Standard Model prediction. A $u \to t$ transition via a flavor changing Z' can explain the data. We consider the model with a Z' boson with the most general form of the tuZ' interaction which includes vector-axial vector as well as tensor type couplings and study how these couplings affect the top forward-backward asymmetry. This coupling can contribute to $t\bar{t}$ production at the Tevatron via the t-channel exchange of the Z' boson (see Fig. 3.1(a)). The A_{FB} measurement can be explained with a light Z' with a mass around 150 GeV and flavor changing tuZ' coupling of $g_{utZ'} \sim O(g)$ where g is the weak coupling. One can take higher Z' masses which requires larger $g_{utZ'} \geq 1$ values [188].

Flavor changing neutral current(FCNC) effects in the SM are tiny and to date there are no experimental evidence of FCNC effects beyond those expected from the SM. There are some anomalies in the B system which might require new physics to resolve but the NP generated FCNC effects that are needed in the B system are much smaller than the one needed to resolve the top A_{FB} [189]. A tree level dbZ' or a sbZ' coupling is strongly suppressed by $B_{d,s}$ mixing. A tree level $tq'Z'$ coupling, where $q' = u, c, t$, will generate an effective $bqZ'(q = d, s)$ coupling through a vertex correction involving the W exchange [190] (see Fig. 3.1(b)). The B_q mixing constraints on these effective vertices would then lead to constraints on the $tq'Z'$ coupling. The vertex corrections are divergent and can be regulated by a cut-off Λ which represents the scale of NP in an effective theory framework. In NP models where there are

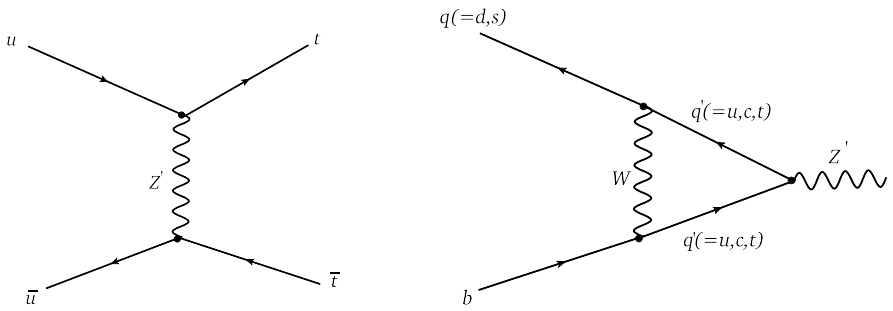

Figure 3.1. Left panel(a): Tree level $t\bar{t}$ production diagram involving the Z' exchange. Right panel(b): Tree level diagram with $tq'Z'$ coupling ($q' = u, c, t$) which generates an effective bqZ' (q =d,s) coupling through a vertex correction involving the W exchange.

no bare bqZ' couplings the vertex corrections with a chosen Λ can be used to constrain the $tq'Z'$ coupling from B_q mixing measurements. We will take the scale of new physics to be $\sim TeV$. In specific complete models Λ will represent the mass of some new particles. In models of NP where there are bare bqZ' couplings the vertex correction will renormalize the bare bqZ' vertices to produce the renormalized vertices U_{qb}. These renormalized vertices can then be fitted to B_q mixing data. Assuming the vertex corrections to be less than or at most the same size of the bare couplings one we can obtain bounds on the tqZ' couplings by requiring the generated bqZ' coupling to be $\leq U_{qb}$. It is possible to have models where large bare bqZ' couplings cancel with large vertex corrections to produce small renormalized bqZ' vertices consistent with experiments. We will not consider these finely tuned model.

When the vertex corrections are computed one finds that right handed tuZ' couplings do not contribute to B_q mixing in the limit of setting the up quark mass to zero. We note that ttZ' couplings do not have such suppression and will contribute to B_q mixing via the vertex corrections. Even though the ttZ' coupling does not contribute to the top A_{FB}, in specific models of NP this coupling may be related to the the FCNC coupling tuZ' [191]. It turns out the B_q mixing constraints on ttZ' are weak because of the small CKM elements $V_{ts(d)}$ and not because of right handed couplings. The $tqZ'(q = u, c, t)$ couplings via box diagrams can produce an effective $\bar{d}(\bar{s})b\bar{u}u$ operator that can contribute to decays like $B \to K(K^*)\pi(\eta, \eta'\rho)$ or $B \to \pi(\rho)\pi(\rho)$ e.t.c decays. The effects of these new operators can be observed in CP violating and/or triple product measurements [192]. However these effective operators only modify the SM Wilson's co-efficients in the SM effective Hamiltonian and so the CP violating predictions and /or triple product measurements should be similar to the SM for a reasonable choice of $tqZ'(q = u, c, t)$ couplings.

We will next consider the most general tuZ' couplings including both vector, axial vector and tensor couplings($\sim \frac{\sigma_{\mu\nu}q^\nu}{m_t}$) and study the effect of these couplings on the top A_{FB}.

The interesting feature about these tensor couplings are that we can avoid the B_q mixing constraints due to the suppressions of these operators at low energies [193]. The momentum dependence of these operators imply that at the b quark scale these operators will be suppressed by $\sim m_b/m_t$ and consequently the B_q mixing constraints will be weak for these operators.

In the next section we discuss the $B_q(q = d, s)$ constraints on the tuZ' operators. In the following section we introduce the general tuZ'coupling including tensor terms and study the effects in the top A_{FB}. This is followed by the section on the $t \to uZ'$ branching ratio calculations and, finally, summarize the results of this work.

3.2 Constraints on $tq'(= u, t)Z'$ couplings from $B_{q(=d,s)}$ mixing

In general, new physics contributions to the mass difference between neutral B_q meson mass eigenstates (ΔM_q) can be constrained by the ΔM_q experimental results. In the SM, B_q^0-$\bar{B}_q^0$ mixing occurs at the one loop level by the flavor changing weak interaction box diagrams. The mixing amplitude M_{12}^q is related to the mass difference ΔM_q via $\Delta M_q = 2|M_{12}^q|$. The recent theoretical estimations for the mass differences of B_s^0-$\bar{B}_s^0$ and B_d^0-$\bar{B}_d^0$ mixing [194] at 1σ confidence level(CL) are

$$(\Delta M_s)^{SM} = 16.8^{+2.6}_{-1.5}\,\mathrm{ps}^{-1}\,, \qquad (\Delta M_d)^{SM} = 0.555^{+0.073}_{-0.046}\,\mathrm{ps}^{-1}. \tag{3.1}$$

The latest measurements of mass difference by CDF [195] and DØ [196] for B_s mixing are

$$\begin{aligned} \Delta M_{B_s} &= (17.77 \pm 0.10(\mathrm{stat.}) \pm 0.07(\mathrm{syst.}))\,\mathrm{ps}^{-1} \\ \Delta M_{B_s} &= (18.53 \pm 0.93(\mathrm{stat.}) \pm 0.30(\mathrm{syst.}))\,\mathrm{ps}^{-1}\,. \end{aligned} \tag{3.2}$$

The HFAG value for the mass difference of B_d^0-$\bar{B}_d^0$ mixing is $\Delta M_{B_d}(\mathrm{exp}) = (0.507 \pm 0.004)\,\mathrm{ps}^{-1}$ [197]. The experimental results for the mass differences of both B_s^0-$\bar{B}_s^0$ and B_d^0-$\bar{B}_d^0$ mixing are consistent with their SM expectations. Hence, the mass difference results can provide strong constraints on NP contributions.
In this section we will consider the $B_{d,s}$ mixing constraints on the $tq'(= u, t)Z'$ couplings.

3.2.1 *tuZ' left-handed coupling*

The most general Lagrangian for flavor changing tuZ' transition is [198]

$$\mathcal{L}_{tuZ'} = \bar{u}\Big[\gamma^\mu(a + b\gamma_5) + i\frac{\sigma_{\mu\nu}}{m_t}q^\nu(c + d\gamma_5)\Big]tZ'_\mu\,, \tag{3.3}$$

where $q = p_t - p_u$. In general the couplings a, b, c and d are complex and can be momentum dependent (form factors). In this work we will take the couplings to be constants with no momentum dependence. Consider the tuZ' vertex with $a = -b = g^L_{tu}$, and c=d=0 in Eq. (3.3). This generates effective $bqZ'(q = d, s)$ coupling at one loop level due to W exchange. We obtain the bqZ' coupling in the Pauli-Villars regularization as

$$\mathcal{L}_{Z'} = U_{qb}\bar{q}\gamma^\mu(1-\gamma_5)bZ'_\mu\,, \tag{3.4}$$

where the contribution of the vertex correction in Fig. 3.1 is given by

$$\delta\Gamma^\mu(p,p') \;=\; g'\int \frac{d^4k}{(2\pi)^4}\bar{u}(p')\frac{(-g_{\nu\rho}+q_\nu q_\rho/q^2)\gamma^\nu(1-\gamma_5)(\not{k}'+m_t)\gamma^\mu(1-\gamma_5)\not{k}\gamma^\rho(1-\gamma_5)}{((p-k)^2-M_W^2+i\varepsilon)\,(k'^2-m_t^2+i\varepsilon)\,(k^2+i\varepsilon)}u(p), \tag{3.5}$$

where

$$g' = g^L_{tu}\frac{-iG_F}{\sqrt{2}}M_W^2(V^*_{uq}V_{tb}+V^*_{tq}V_{ub}), \tag{3.6}$$

and leads to the effective coupling

$$U_{qb} \;=\; g^L_{tu}\,\frac{G_F}{\sqrt{2}}M_W^2(V^*_{uq}V_{tb}+V^*_{tq}V_{ub})\frac{1}{8\pi^2}\Big[\frac{x_t Log[\frac{\Lambda^2}{m_t^2}]-Log[\frac{\Lambda^2}{M_W^2}]}{(x_t-1)}\Big]. \tag{3.7}$$

where $\Lambda \sim$ TeV is a cut-off scale, and $x_t = m_t^2/M_W^2$. The function U_{qb} includes only the contribution from the W boson, and the contribution of the associated Goldston boson in the SM is the order of m_u/M_W. Note that for B_d mixing the coupling g^L_{tu} is associated with the CKM factor $V^*_{ud}V_{tb} \sim 1$, and thus one can expect a strong constraint on g^L_{tu} from the mass difference ΔM_d.

A tree-level exchange of the Z' generates the $\Delta B = 2$ effective Lagrangian responsible for the neutral B_q meson mixing

$$\mathcal{H}^{\Delta B=2}_{Z'} = \frac{U^2_{qb}}{M^2_{Z'}}\eta_{Z'}(\bar{q}b)_{V-A}(\bar{q}b)_{V-A}\,, \tag{3.8}$$

where $(\bar{q}b)_{V-A} = \bar{q}\gamma^\mu(1-\gamma_5)b$, and the QCD correction factor $\eta_{Z'} = [\alpha_s(M_{Z'})/\alpha_s(m_b)]^{6/23}$. The Z' contribution to the B_q mixing amplitude can be introduced in the matrix element by using the vacuum insertion method as

$$M_{Z'} = \frac{U^2_{qb}}{M^2_{Z'}}\eta_{Z'}\langle B^0_q|(\bar{q}\gamma^\mu(1-\gamma_5)b)^2|\bar{B}^0_q\rangle, \tag{3.9}$$

where

$$\begin{aligned}\langle B_q^0|(\bar{q}\gamma^\mu(1-\gamma_5)b)^2|\bar{B}_q^0\rangle &= \sum_n \langle B_q^0|\bar{q}\gamma^\mu(1-\gamma_5)b|n\rangle\langle n|\bar{q}\gamma_\mu(1-\gamma_5)b|\bar{B}_q^0\rangle, \\ &\equiv B_B\langle B_q^0|\bar{q}\gamma^\mu(1-\gamma_5)b|0\rangle\langle 0|\bar{q}\gamma_\mu(1-\gamma_5)b|\bar{B}_q^0\rangle, \\ &= B_B|\langle 0|\bar{q}\gamma^\mu\gamma_5 b|B_q^0\rangle|^2, \\ &= \frac{8}{3}B_B f_{B_q}^2 m_{B_q}^2, \end{aligned} \tag{3.10}$$

where B_B is the bag factor and f_{B_q} is the decay constant. The mixing amplitude is given by

$$[M_{12}^q]^{Z'} = \frac{|M_{Z'}|}{2m_{B_q}}, \tag{3.11}$$

where $1/2m_{B_q}$ is a normalization factor. Thus

$$[M_{12}^q]^{Z'} = \frac{4}{3}\frac{U_{qb}^2}{M_{Z'}^2}\eta_{Z'}m_{B_q}f_{B_q}^2 B_q. \tag{3.12}$$

In the presence of new physics, the mixing amplitude M_{12}^q can be parameterized by complex parameters Δ_q [194]

$$M_{12}^q = [M_{12}^q]^{SM,}\Delta_q. \tag{3.13}$$

In our case, $\Delta_q = |\Delta_q|e^{i\phi_q^\Delta} = 1 + [M_{12}^q]^{Z'}/[M_{12}^q]^{SM}$. A global analysis on the parameters $|\Delta_q|$ and ϕ_q^Δ for $B_d - \bar{B}_d$ and $B_s - \bar{B}_s$ mixing are carried out in [194]. The best fit results for Δ_d and Δ_s in this analysis at 1 σ CL (scenario I) are

$$|\Delta_d| = 0.747^{+0.195}_{-0.082}, \qquad \phi_d^\Delta = -12.9^{+3.8^\circ}_{-2.7}, \tag{3.14}$$

and

$$|\Delta_s| = 0.887^{+0.143}_{-0.064}, \qquad \phi_s^\Delta = -51.6^{+14.2^\circ}_{-9.7} \quad \text{or} \quad -130.0^{+13^\circ}_{-12}. \tag{3.15}$$

The Δ_d constraint in Eq. (3.14) on the coupling g_{tu}^L at $\bar{m}_t(\bar{m}_t) = (165.017 \pm 1.156 \pm 0.11)$ GeV [194], $\beta^{SM} = 27.2^{+1.1^\circ}_{-3.1}$ [194], and $M_{Z'} = 150$ GeV is shown in Fig. 3.2. The numerical values of all other theoretical inputs can be found in [194]. They are varied within 1 σ errors in the fit. The cut-off scale Λ is varied between 300 GeV to 2 TeV . The green scatter points in Fig. 3.2 satisfy only $|\Delta_d|$ in Eq. (3.14), while blue points satisfy both $|\Delta_d|$ and ϕ_d^Δ in

Eq. (3.14). The results indicates that B_d mixing can strongly constrain the tuZ' coupling g^L_{tu} even at $\Lambda = 300$ GeV. In particular we note that the maximum value for $|g^L_{tu}|$ is around 0.2 and is associated with a large phase. In fact there are no real g^L_{tu} that satisfy the B_d constraint.

On the other hand, Fig. 3.3 suggests that the constraints from B_s mixing on the tuZ' coupling g^L_{tu} are weaker ($\sim O(1)$) even at $\Lambda = 2$ TeV. This can be understood from the fact that the B_s mixing contribution in this case is associated with the CKM factor $V^*_{us}V_{tb}$ and is suppressed. The (green, blue, red) scatter points in Fig. 3.3 are constrained by ($|\Delta_s|$, ($|\Delta_s|$ and $\phi^\Delta_s = -51.6^{+14.2^\circ}_{-9.7}$), ($|\Delta_s|$ and $\phi^\Delta_s = -130.0^{+13^\circ}_{-12}$) in Eq. (3.15). The large negative phase ϕ^Δ_s prefers large g^L_{tu} values.

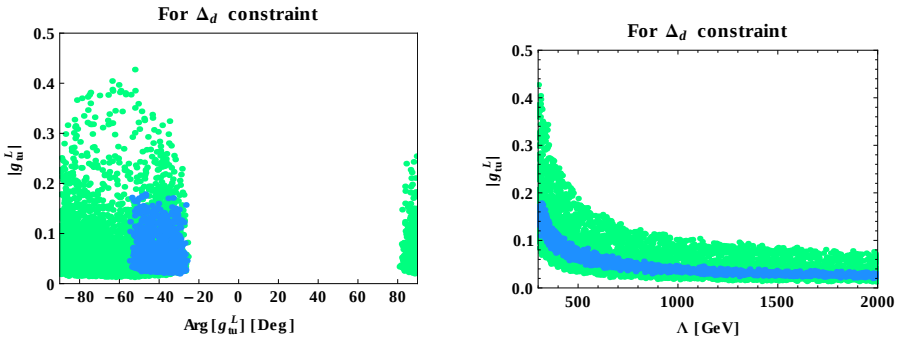

Figure 3.2. $|g^L_{tu}|$ **vs Arg**$[g^L_{tu}]$**[Deg] (left panel) and** $|g^L_{tu}|$ **vs** Λ**[GeV] (right panel) for** B_d **mixing. Green scatter points are constrained by** $|\Delta_d|$**. Blue scatter points are constrained by** $|\Delta_d|$ **and** ϕ^Δ_d**.**

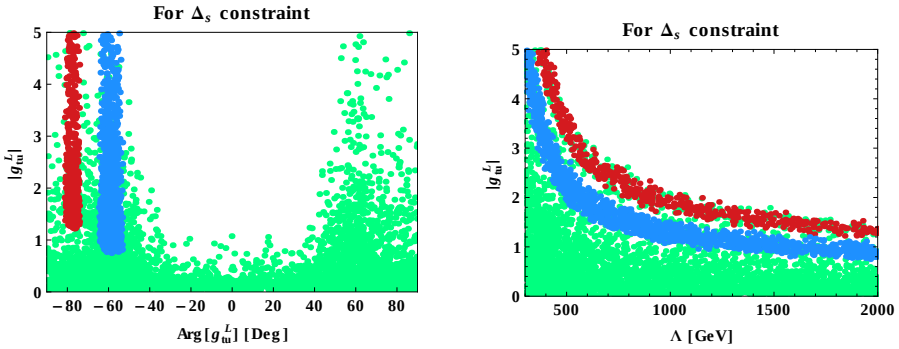

Figure 3.3. $|g^L_{tu}|$ **vs Arg**$[g^L_{tu}]$**[Deg] (left panel) and** $|g^L_{tu}|$ **vs** Λ**[GeV] (right panel) for** B_s **mixing. Green scatter points are constrained by** $|\Delta_s|$**. Blue scatter points are constrained by** $|\Delta_d|$ **and** $\phi^\Delta_d = -51.6^{+14.2^\circ}_{-9.7}$**. Red scatter points are constrained by** $|\Delta_d|$ **and** $\phi^\Delta_d = -130.0^{+13^\circ}_{-12}$**.**

3.2.2 *tuZ' right-handed coupling*

We now consider the tuZ' vertex with right handed couplings, $a = b = g_R$, and c=d=0. The contribution of this vertex to M_{12} is suppressed by m^2_u/m^2_W. Hence, the right handed

coupling g_R cannot be constrained by B_q mixing.

Finally as indicated in the earlier section, the left and the right handed couplings generate via the box diagram effective $\bar{q}b\bar{u}u(\ q = d, s)$ operators. These operator can be constrained by observables in non-leptonic B meson decays like $B \to \pi\pi/K\pi$. These operators change the Wilson's co-efficients of the SM effective Hamiltonian with the change being $\sim 10^{-2}$ at the scale $\mu = M_W$ for $M_{Z'} = 150$ GeV and $g^L_{tu}, g^R_{tu} \sim O(g)$. Since the generated NP physics operator structures are similar to the SM there are no easy way to detect their presence. A detailed fit to all the non-leptonic data may provide constraints on the couplings $g^{L,R}_{tu}$, which we do not perform in this work. Some analysis along this line has been done for tdW' coupling in [199].

3.2.3 *ttZ' coupling*

For completeness, next we consider B_q mixing constraints on the ttZ' couplings. The Lagrangian for the ttZ' interaction is

$$\mathcal{L}_{ttZ'} = \bar{t}[g^L_{tt}\gamma^\mu(1-\gamma_5) + g^R_{tt}\gamma^\mu(1+\gamma_5)]tZ'_\mu. \tag{3.16}$$

Again, we evaluate the one-loop diagram (see Fig. 3.1(b)) in the Pauli-Villars regularization and obtain the effective Lagrangian for bq(=d,s)Z' interaction as

$$\mathcal{L}'_{Z'} = U'_{qb}\bar{q}\gamma^\mu(1-\gamma_5)bZ'_\mu\,, \tag{3.17}$$

where

$$U'_{qb} = \frac{G_F}{\sqrt{2}}M_W^2 V_{tq}V_{tb}f_{tt}(\Lambda, x_t)\,, \tag{3.18}$$

with

$$f_{tt}(\Lambda, x_t) = \frac{1}{(4\pi^2)}\int_0^1 dx\int_0^{1-y} dy\Big[g^L_{tt}\Big(Log[\frac{x\Lambda^2}{M_W^2 D_{tt}}] + \frac{1}{2}\frac{x_t^2}{D_{tt}}\Big) + g^R_{tt}x_t\Big(\frac{1}{2}Log[\frac{x\Lambda^2}{M_W^2 D_{tt}}] + \frac{1}{D_{tt}}\Big)\Big]\,, \tag{3.19}$$

and $D_{tt} = x + (1-x)x_t$. The function f_{tt} includes both the W boson and the associated Goldston boson contributions. The ttZ' contribution to the B_q mixing amplitude is

$$[M^q_{12}]^{Z'} = \frac{4}{3}\frac{[U'_{qb}]^2}{M^2_{Z'}}\eta_{Z'}m_{B_q}f^2_{B_q}B_q. \tag{3.20}$$

Both $B_d - \bar{B}_d$ and $B_s - \bar{B}_s$ constraints in Eqs. (3.14) and (3.15) can allow large $\sim O(1)$ values for $g_{tt}^{L,R}$.

3.3 Top quark forward-backward asymmetry

In this section we calculate the top A_{FB} keeping in mind the constraints derived on the coupling from the previous section. The most general Lagrangian for a flavor changing tuZ' interaction is given in Eq. (3.3). This interaction can contribute to $u\bar{u} \to t\bar{t}$ scattering amplitude through the t-channel exchange of the Z' boson (see Fig. 3.1(a)). The SM and Z' matrix elements are

$$\begin{aligned} M_{\rm SM} &= \frac{g_s^2 (t^a)_{ji} (t^a)_{lk}}{\hat{s}} \left(\bar{v}_{\bar{u}_j}(p_2)\gamma^\mu u_{u_i}(p_1)\right) \left(\bar{u}_{t_l}(p_3)\gamma_\mu v_{\bar{t}_k}(p_4)\right), \\ M_{Z'} &= \frac{1}{\hat{t} - M_{Z'}^2 + iM_{Z'}\Gamma_{Z'}} \\ &\quad \left[\bar{u}_{t_l}(p_3)\left(\gamma_\mu(a+b\gamma_5) + i\frac{\sigma_{\mu\nu}}{m_t}q^\nu(c+d\gamma_5)\right)u_{u_i}(p_1)\right](-g^{\mu\alpha} + q^\mu q^\alpha/q^2) \\ &\quad \left[\bar{v}_{\bar{u}_j}(p_2)\left(\gamma_\alpha(a+b\gamma_5) + i\frac{\sigma_{\alpha\beta}}{m_t}q^\beta(c+d\gamma_5)\right)v_{\bar{t}_k}(p_4)\right]. \end{aligned} \tag{3.21}$$

The tree-level differential cross section for $q\bar{q} \to t\bar{t}$ process in the $t\bar{t}$ c.m. frame including both the SM and for Z' contributions is

$$\frac{d\hat{\sigma}}{d\cos\theta} = \frac{\beta_t}{32\pi\hat{s}}(\mathcal{A}_{SM} + \mathcal{A}_{SM-Z'} + \mathcal{A}_{Z'}), \tag{3.22}$$

where $\hat{s} = (p_q + p_{\bar{q}})^2$ is the squared c.m. energy of the $t\bar{t}$ system, $\beta_t = \sqrt{1 - 4m_t^2/\hat{s}}$, and the polar angle θ is the relative angle between direction of motion of the outgoing top-quark and the incoming q-quark. The quantities $\mathcal{A}_{SM}$, $\mathcal{A}_{SM-Z'}$, and $\mathcal{A}_{Z'}$ denote the leading order SM, the interference between the SM and Z', and the pure Z' scattering amplitudes, respectively. These amplitudes can be obtained in terms of kinematic variables θ and $\hat{s}$ as

$$\begin{aligned} \mathcal{A}_{SM} &= \frac{2g_s^4}{9}\left[1 + c_\theta^2 + \frac{4m_t^2}{\hat{s}}\right], \\ \mathcal{A}_{SM-Z'} &= \frac{2g_s^2}{9}\left[\frac{\hat{t} - M_{Z'}^2}{(\hat{t} - M_{Z'}^2)^2 + M_{Z'}^2\Gamma_{Z'}^2}\right](f_1 + f_2), \\ \mathcal{A}_{Z'} &= \frac{1}{4}\left[\frac{1}{(\hat{t} - M_{Z'}^2)^2 + M_{Z'}^2\Gamma_{Z'}^2}\right](f_3 + f_4 + f_5). \end{aligned} \tag{3.23}$$

Where $c_\theta = \beta_t \cos\theta$, and $\hat{t} = (p_q - p_t)^2 = -\hat{s}/2(1-\beta_t \cos\theta) + m_t^2$. The functions f_is (i = 1..5) can be found in Appendix. 9. Here we assume the couplings a, b, c and d to be real. Our results for $\bar{t}t$ production are obtained by the convolution of the analytic differential cross section of Eq. (3.22) with the CTEQ-5L parton distribution functions [200] implemented in Mathematica. We expect the MSTW 2008 [201] parton distributions to give compatible results.

The forward-backward asymmetry of the top quark in the $t\bar{t}$ c.m. frame is defined as [202]

$$A_{FB}^{t\bar{t}} = \frac{\sigma_F - \sigma_B}{\sigma_F + \sigma_B}, \tag{3.24}$$

where

$$\sigma_F = \int_0^1 \frac{d\sigma}{d\cos\theta} d\cos\theta, \quad \sigma_B = \int_{-1}^0 \frac{d\sigma}{d\cos\theta} d\cos\theta. \tag{3.25}$$

In our analysis, we choose some representative values for the couplings a, b, c, and d to generate large forward-backward asymmetry $A_{FB}^{t\bar{t}}$ for high $M_{t\bar{t}}$ (> 450 GeV) without distorting the shape of the mass spectrum $d\sigma_{t\bar{t}}/dM_{t\bar{t}}$. We fix the renormalization and factorization scales at $\mu_R = \mu_F = m_t$. We evaluate $A_{FB}^{t\bar{t}}$ which includes the NLO SM and the Z' contributions at $m_t = 172.5$ GeV. Also, we apply a QCD K-factor K = 1.3 to the tree-level cross section in order to match the SM prediction for $\sigma_{t\bar{t}}$. We consider the Z' boson with mass $M_{Z'} = 150$ GeV and width $\Gamma_{Z'} = 0$ for the numerical analysis.

3.3.1 Pure vector-axial vector couplings: $a = \mp b$, and $c = d = 0$

This case has already been considered before [34] but only right handed couplings were considered. Here we will consider both right and left handed couplings. We take the representative values of the couplings $a = -b = |g_{tu}^L| = 0.257$, and $c = d = 0$. This value for g_{tu}^L satisfies the $|\Delta_d|$ constraint but not the phase ϕ_d^Δ constraints from B_d mixing (see Fig. 3.2). For these values $A_{FB}^{t\bar{t}}$ can be explained within one σ error of its measurement for $M_{t\bar{t}} > 450$ GeV. In Fig. 3.4, we show the $M_{t\bar{t}}$ distribution for the $t\bar{t}$ observables $A_{FB}^{t\bar{t}}$, and $\sigma_{t\bar{t}}$. The differential distribution, $d\sigma_{t\bar{t}}/dM_{t\bar{t}}$, has been measured in eight different energy bins of $M_{t\bar{t}}$ for $m_t = 175$ GeV in Ref. [203]. Our distribution of $d\sigma_{t\bar{t}}/dM_{t\bar{t}}$ is consistent with the measurements. Since the partonic scattering amplitudes in this case (see Appendix. 9) depends on b^2 and b^4 terms, our results hold for right handed couplings also, i.e $a = b = |g_{tu}^R| = 0.257$, and $c = d = 0$.

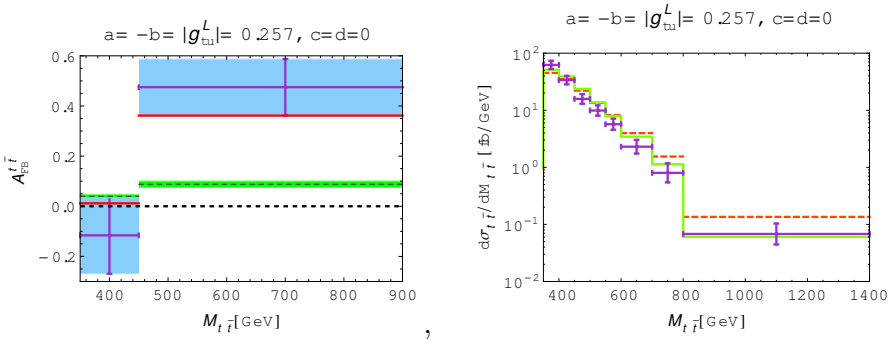

Figure 3.4. Left panel: $M_{t\bar{t}}$ distribution of $A_{FB}^{t\bar{t}}$ in the two energy ranges [350,450]GeV and [450,900]GeV of invariant mass $M_{t\bar{t}}$. Green band: the SM prediction. Blue band with 1σ error bars: the unfolded CDF measurement [22]. Red line: the SM with Z' exchange prediction for $(a = -b = 0.257, c = d = 0)$. Right panel: $M_{t\bar{t}}$ distribution of $d\sigma_{t\bar{t}}/dM_{t\bar{t}}$ [in fb/GeV] for eight different energy bins of $M_{t\bar{t}}$. Green line: the NLO SM prediction. Blue band with 1σ error bars: the unfolded CDF measurement [203]. Red line: the SM with Z' exchange prediction for above values of couplings at $m_t = 175$ GeV.

3.3.2 General case: all couplings are present

In this section we consider the most general tuZ' couplings. We showed earlier that the left handed coupling are strongly constrained from B_d mixing and there are no real values of g_{tu}^L that satisfy the B_d mixing constraint. We now investigate the effect of the couplings c and d on the A_{FB} predictions.

3.3.3 Pure tensor couplings : $a = b = 0$, $c = \pm d$

We consider the case of pure tensor couplings. In this scenario we can avoid the B_q mixing constraints as the effects of the tensor couplings are suppressed by $\frac{m_b}{m_t}$ at the b mass scale. The SM and Z' interference contribution $\mathcal{A}_{SM-Z'}$ in Eq. (3.23) vanishes in this case. The functions f_4 and f_5 in pure Z' contribution $\mathcal{A}_{Z'}$ are also zero, and f_3 is order of $(c\hat{s}/m_t)^2$. The mass spectrum for $A_{FB}^{t\bar{t}}$ is shown in Fig. 3.5(a) for only $c = \pm d$ couplings $(c = \pm d = 0.5)$. The results indicate that Z' contribution cannot reproduce the A_{FB} measurement within one σ for $M_{t\bar{t}} > 450$ GeV even at a low $M_{Z'} = 100$ GeV (yellow lines) value.

3.3.4 All the couplings are same order

Finally we consider the case where all couplings are of the same order. We choose the representative values of the couplings $a = -b = |g_{tu}^L| = 0.239$, and $c = d = 0.148$. Again this value for g_{tu}^L will satisfy the $|\Delta_d|$ constraint but not the phase ϕ_d^{Δ} constraints from B_d mixing (see Fig. 3.2). In Fig. 3.6, we show the $M_{t\bar{t}}$ distribution for the $t\bar{t}$ observables $A_{FB}^{t\bar{t}}$, and $\sigma_{t\bar{t}}$. We note that $A_{FB}^{t\bar{t}}$ can be explained within one σ error of its measurement for $M_{t\bar{t}} > 450$

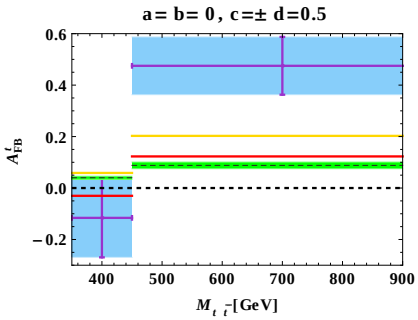

Figure 3.5. $M_{t\bar{t}}$ **distribution of** $A_{FB}^{t\bar{t}}$**. Green band: The SM prediction. Blue band with** 1σ **error bars : CDF measurement. Red and yellow lines: The SM with** Z' **exchange prediction at** $M_{Z'} = 150$ **GeV, and** $M_{Z'} = 100$ **GeV, respectively for** $a = b = 0$ **and** $c = \pm d = 0.5$

GeV. The distribution $d\sigma_{t\bar{t}}/dM_{t\bar{t}}$ is also consistent with the measurements. Similar results are obtained with $a = b = |g_{tu}^{R}| = 0.245$, and $c = d = 0.148$ as shown in Fig. 3.7. The conclusion is that the inclusion of the tensor couplings do not have a significant effect on the top A_{FB} and they can only slightly lower the values of the couplings a and b realtive to their values in the pure case, with no tensor couplings, discussed earlier. The presence of the tensor couplings may have an important impact on the polarization measurement in $t\bar{t}$ production [204].

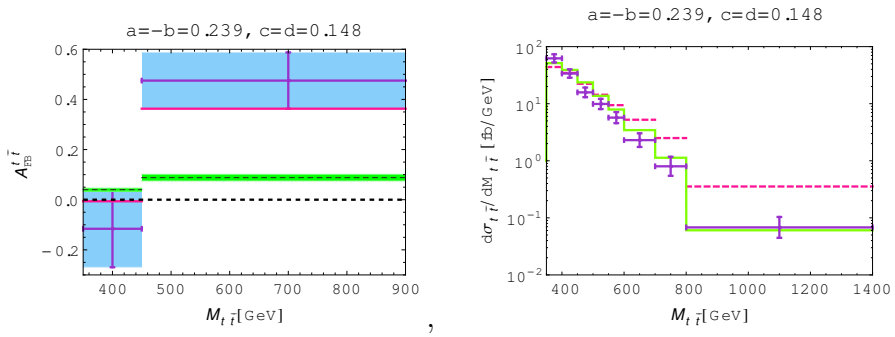

Figure 3.6. $M_{t\bar{t}}$ **distributions of** $A_{FB}^{t\bar{t}}$ **and** $d\sigma_{t\bar{t}}/dM_{t\bar{t}}$ **[in fb/GeV]. Pink lines: the SM with** Z' **exchange prediction for** $(a = -b = 0.239,\ c = d = 0.148)$**. The same conventions as in Fig. 3.4 used for other lines.**

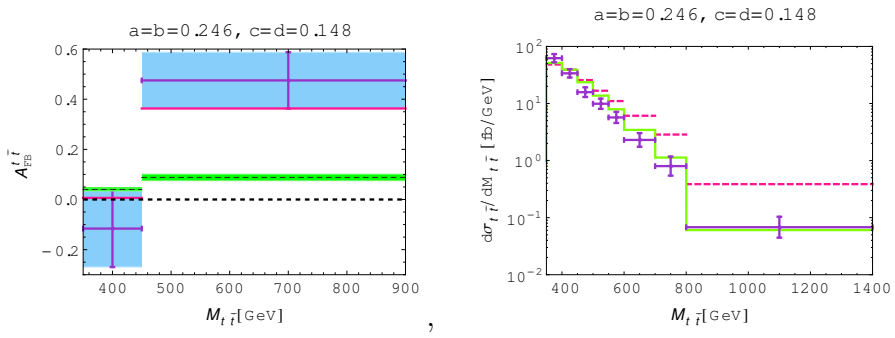

Figure 3.7. $M_{t\bar{t}}$ **distributions of** $A_{FB}^{t\bar{t}}$ **and** $d\sigma_{t\bar{t}}/dM_{t\bar{t}}$ **[in fb/GeV]. Pink lines: the SM with** Z' **exchange prediction for** ($a = b = 0.245$, **and** $c = d = 0.148$). **The same conventions as in Fig. 3.4 used for other lines.**

3.4 $t \to uZ'$ Branching ratio

In this section we consider the decay width for $t \to uZ'$. The invariant amplitude and decay width with the most general tuZ' coupling are given by,

$$\begin{aligned} M(t \to uZ') &= \bar{u}_u(p_2)\left[\gamma_\mu(a+b\gamma_5) + i\frac{\sigma_{\mu\nu}}{m_t}p_3^\nu(c+d\gamma_5)\right]u_t(p_1)\epsilon_\lambda^{\mu*}(p_3), \\ \Gamma(t \to uZ') &= \frac{1}{16\pi m_t}\left(1-\frac{m_{Z'}^2}{m_t^2}\right)\left(\frac{m_t^2}{m_{Z'}^2}-1\right)\left[(m_t^2+2m_{Z'}^2)(a^2+b^2)\right. \\ &\quad \left. -6m_{Z'}^2(ac-bd) + m_{Z'}^2(\frac{m_{Z'}^2}{m_t^2}+2)(c^2+d^2)\right]. \end{aligned} \tag{3.26}$$

The branching ratio is defined as,

$$BR_{tuZ'} = \frac{\Gamma[t \to cZ']}{\Gamma[m_t]}. \tag{3.27}$$

For the top width we use $\Gamma(m_t) \approx \Gamma(t \to bW)$ which is given by,

$$\Gamma(t \to bW) = \frac{G_F}{8\pi\sqrt{2}}|V_{tb}|^2 m_t^3\left(1-\frac{m_W^2}{m_t^2}\right)\left(1+\frac{m_W^2}{m_t^2}-2\frac{m_W^4}{m_t^4}\right). \tag{3.28}$$

In Fig. 3.8 we show the variation of $t \to uZ'$ branching ratio with $M_{Z'}$ for different couplings. For couplings $a = \pm b = 0.257$, and $c = d = 0$ (red dashed line), we get $BR_{tuZ'} \sim$ 6% at $m_t = 172.5$ GeV, for a = - b = 0.239, c = -d = 0.148 (blue dashed line), $BR_{tuZ'}$ is 6.9%, and for a = b = 0.246, c = d = 0.148 (pink dashed line), $BR_{tuZ'}$ is 7.2%. These branching ratios may be observable at the LHC [188].

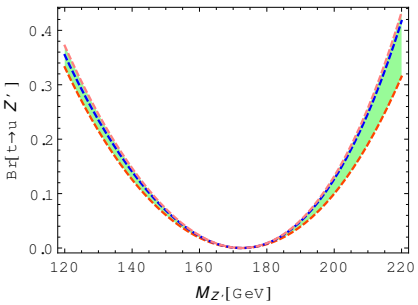

Figure 3.8. $BR_{Z'}$ **vs** $M_{Z'}$**. Red dashed line is for** $a = \pm b = 0.257$**, and c = d =0. Blue dashed line is for a = -b = 0.239, c = -d = 0.148. Pink dashed line is for a = b = 0.246, c = d = 0.148.**

3.5 Conclusion

A large forward backward asymmetry in $t\bar{t}$ production, about a 3.4σ away from the SM prediction, has been reported by the CDF collaboration. A Z' with flavor changing tuZ' coupling can explain this anomaly. In this work we considered $B_{d,s}$ constraints on the $tq'Z'$ couplings ($q' = u, t$). These constraints resulted from the bounds on the effective $b(s, d)Z'$ vertices generated from vertex corrections involving the tuZ' couplings. We found that the right handed couplings were generally not tightly constrained but the left handed couplings were tightly bound from the $B_{d,s}$ mixing data. We then considered the most general tuZ' coupling including tensor terms and found that the tensor terms did not affect the top A_{FB} in a significant manner. Finally we computed the branching ratio for the $t \to uZ'$ transition and found it to be in the percentage range.

CHAPTER 4

THE CHARGED LEPTON MASS MATRIX AND NON-ZERO θ_{13} WITH TEV SCALE NEW PHYSICS

4.1 Introduction

The leptonic mixing arises from the overlap of matrices that diagonalize the charged lepton and the neutrino mass matrices. Many approaches to studying the leptonic mixing start in the basis where the charged lepton mass is diagonal. Our approach to obtaining the leading order leptonic mixing as well as deviations from it starts from the charged lepton sector. A recent attempt to understand θ_{13} from the charged lepton sector can be found in Ref. [48] and in the past corrections to the leptonic mixing from the charged lepton sector were considered in Ref. [205]. An approach to suppress flavor changing neutral current effects (FCNC) in the quark sector, based on shared flavor symmetry, was proposed in Ref. [206]. As an example of this shared symmetry the decoupled $2-3$ symmetry was used for the down quark sector to suppress FCNC effects and explain anomalies [207] observed in the B meson system. In the decoupled limit the first generation is decoupled from the other two generations. We extend this decoupled $2-3$ symmetry to the charged lepton sector. This is a reasonable extension given the fact that the down quark and charged leptons exhibit similar hierarchical structure and they may be combined in representations of GUT groups.

One of the central ideas of this approach is the requirement that the mass matrices, in a symmetric limit, be diagonalized by unitary matrices composed of pure numbers independent of the parameters of the mass matrices. This is similar to the idea of form diagonalizable matrices discussed in Ref. [208]. If one starts with a $2-3$ symmetric mass matrix for the charged lepton sector and requires it to be diagonalized by unitary matrices of pure numbers

one recovers the decoupled $2-3$ symmetry. In the neutrino sector we assume the third generation to be decoupled from the first two generations. With real entries in the neutrino mass matrix it is diagonalized by a rotation matrix and the resulting leptonic mixing has a $\mu-\tau$ symmetry. Requiring the mass matrix to be diagonalized by pure numbers can lead to, among other structures, the BM and the TBM leptonic mixing depending on the structure of the chosen mass matrix.

In the bimaximal case, to generate the mixing matrices in the charged lepton and the neutrino sector, we present a Lagrangian that extends the SM by three right handed neutrinos, an additional Higgs doublet and two singlet scalar fields.[1] The Lagrangian uses the same class of Z_2 symmetries as has been used in Ref [210]. However, the structure as well as the phenomenology of our model is very different from the above mentioned papers. The Lagrangian is constructed to have a $2-3$ symmetry, Z_2^{23}, along with two additional Z_2 symmetries Z_2^e and Z_2^D. The neutrino masses and mixing are generated through the usual see-saw mechanism. The presence of the $Z_2^{23}\times Z_2^e$ symmetries leads to the decoupled $2-3$ symmetry in the charged lepton sector and fixes the interactions of the right handed neutrinos with the singlet scalar fields. The presence of the Z_2^D symmetry forces the neutrinos to acquire Dirac masses by coupling to a second Higgs doublet which has a different Z_2^D transformation than the usual SM Higgs doublet that give masses to the charged leptons. The full Lagrangian is symmetric under the product of the Z_2 symmetries, $Z_2^{23}\times Z_2^e\times Z_2^D$.

In tri-bimaximal case, we introduce a Lagrangian that extends the SM particle content by three right-handed neutrinos, three complex singlet scalar fields, and an additional Higgs doublet. The symmetry group of the SM is extended by the product of the symmetries $Z_4\times U(1)$. The Z_4 symmetry serves to have a $2-3$ symmetric Yukawa matrix in the charged lepton sector and yields the mass matrices in the charged lepton and neutrino sector to have decoupled structures. We present a global $U(1)$ symmetry which equates certain couplings of the charged leptons and neutrinos as we relate the couplings to the $U(1)$ charges. The $U(1)$ symmetry forbids the Majorana masses of the right-handed neutrinos. The Majorana neutrino masses are generated via the v.e.v of the singlet scalars and the $U(1)$ gets broken spontaneously. Without altering the lepton mixing, an additional Majorana mass term is introduced to protect one of the neutrino masses from blowing up.

The neutrino masses and mixing arise when the Higgs doublets and the singlet scalars acquire v.e.v's and break the symmetries of the Lagrangian. The leptonic mixing is predicted to be either of bimaximal or tri-bimaximal type when the singlet scalars acquire the same v.e.v. If the v.e.v of the second Higgs doublet is small enough $\sim MeV$ then the see-saw scale

[1] Recent motivations for considering two Higgs doublet models can be found in Ref. [209].

as well as the masses of the singlet scalars can be in the TeV range.

Symmetry breaking in both cases is introduced in the charged lepton sector by higher dimensional operators that break the decoupled $2-3$ symmetry but generate a $2-3$ symmetric mass matrix except for a single breaking generated by the muon mass. In the neutrino sector, symmetry breaking is introduced by breaking the alignment of the v.e.v's of the singlet scalars by terms in the effective potential. The corrections to leptonic mixing go as $\sim \frac{v^2}{\omega^2}$ where v is the v.e.v of the SM Higgs and ω the scale of the singlet scalar v.e.v's. If $\omega \sim$ TeV then the corrections to the leptonic mixing are enough to explain the experimental observations.

broken spontaneously. Without altering the lepton mixing, an additional Majorana mass term is introduced to protect one of the neutrino masses from blowing up.

Here, we begin with studying the flavor symmetric limit in the lepton sector that leads to the BM and TBM mixing. In the following two sections we present the Lagrangians that are invariant under the underlying symmetry groups in both the BM and TBM cases, and study the effects of symmetry breaking in the charged lepton and neutrino sector to generate the realistic leptonic mixing matrix. Finally, we show the numerical results in each case and summarize the results.

4.2 The leptonic mixing in the symmetric limit

We start with the charged lepton sector, and assume that the Yukawa matrix is $2-3$ symmetric [211]. The Yukawa couplings of the charged leptons are given by

$$Y^L = \begin{pmatrix} l_{11} & l_{12} & -l_{12} \\ l_{12} & l_{22} & l_{23} \\ -l_{12} & l_{23} & l_{22} \end{pmatrix}. \tag{4.1}$$

The above Yukawa matrix can be diagonalized as

$$\begin{aligned} U^\dagger Y^L U &= Y^L_{diag}, \\ U &= \begin{pmatrix} 1 & 0 & 0 \\ 0 & \frac{1}{\sqrt{2}} & \frac{1}{\sqrt{2}} \\ 0 & -\frac{1}{\sqrt{2}} & \frac{1}{\sqrt{2}} \end{pmatrix} \cdot \begin{pmatrix} \cos\theta & \sin\theta & 0 \\ -\sin\theta & \cos\theta & 0 \\ 0 & 0 & 1 \end{pmatrix}, \end{aligned} \tag{4.2}$$

where the mixing angle θ is determined by the positive solution to

$$\tan\theta = \frac{2\sqrt{2}l_{12}}{l_{22}-l_{23}-l_{11}\pm\sqrt{(l_{22}-l_{23}-l_{11})^2+8l_{12}^2}}. \tag{4.3}$$

The eigenvalues of Y^L are $\frac{1}{2}[l_{11}+l_{22}-l_{23}\pm\sqrt{(l_{11}-l_{22}+l_{23})^2+8l_{12}^2}]$ and $l_{22}+l_{23}$. According to our assumption, the elements of the matrix that diagonalizes Y^L must be pure numbers in the symmetric limit. It is clear that we can achieve that by setting $l_{12}=0$ ($\theta=0$) in Eq. 4.3. This generates the decoupled 2-3 symmetry [206], as the flavor symmetry in the charged lepton sector in which the first generation is decoupled from the second and third generations.

One can represent the Yukawa matrix with the decoupled 2-3 symmetry by Y_{23}^L as

$$Y_{23}^L = \begin{pmatrix} l_{11} & 0 & 0 \\ 0 & \frac{1}{2}l_{22} & \frac{1}{2}l_{23} \\ 0 & \frac{1}{2}l_{23} & \frac{1}{2}l_{22} \end{pmatrix}. \tag{4.4}$$

This Yukawa matrix Y_{23}^L is diagonalized by the unitary matrix W_{23}^l given by

$$W_{23}^l = \begin{pmatrix} 1 & 0 & 0 \\ 0 & -\frac{1}{\sqrt{2}} & \frac{1}{\sqrt{2}} \\ 0 & \frac{1}{\sqrt{2}} & \frac{1}{\sqrt{2}} \end{pmatrix}. \tag{4.5}$$

Note that this matrix differs from the one in Eq. 4.2 in the limit $\theta=0$ by an irrelevant diagonal phase matrix. Writing the diagonalized Yukawa matrix as Y_{23d}^L we have

$$Y_{23d}^L = W_{23}^{l\dagger}Y_{23}^L W_{23}^l = \begin{pmatrix} l_{11} & 0 & 0 \\ 0 & \frac{1}{2}(l_{22}-l_{23}) & 0 \\ 0 & 0 & \frac{1}{2}(l_{22}+l_{23}) \end{pmatrix}. \tag{4.6}$$

The charged lepton masses are given by

$$\begin{aligned} m_e &= \pm\frac{v_1}{\sqrt{2}}l_{11}, \\ m_\mu &= \pm\frac{v_1}{\sqrt{2}}\frac{(l_{22}-l_{23})}{2}, \\ m_\tau &= \pm\frac{v_1}{\sqrt{2}}\frac{(l_{22}+l_{23})}{2}. \end{aligned} \tag{4.7}$$

Since $m_\mu << m_\tau$ there has to be a fine tuned cancellation between l_{22} and l_{23} to produce the muon mass. Hence, it is more natural to consider the symmetry limit $l_{22} = l_{23}$ which leads to $m_\mu = 0$. The Yukawa matrix which leads to the zero muon mass within the decoupled 2-3 symmetry is

$$Y_{23}^L = \begin{pmatrix} l_{11} & 0 & 0 \\ 0 & \frac{1}{2}l_T & \frac{1}{2}l_T \\ 0 & \frac{1}{2}l_T & \frac{1}{2}l_T \end{pmatrix}. \tag{4.8}$$

In the neutrino sector we assume that, in the symmetric limit, $\mathcal{M}_\nu$ has the general structure

$$\mathcal{M}_\nu = \begin{pmatrix} a & d & 0 \\ d & b & 0 \\ 0 & 0 & c \end{pmatrix}, \tag{4.9}$$

where all the parameters are real. This can be diagonalized by the matrix

$$\begin{aligned} W_{12}^\nu &= \begin{pmatrix} c_{12} & s_{12} & 0 \\ s_{12} & -c_{12} & 0 \\ 0 & 0 & 1 \end{pmatrix}, \\ s_{12} &\equiv \sin\theta_{12}, \quad c_{12} \equiv \cos\theta_{12}, \end{aligned} \tag{4.10}$$

where

$$\tan 2\theta_{12} = \frac{2d}{(a-b)}. \tag{4.11}$$

We can then calculate U_{PMNS}^s as

$$U_{PMNS}^s = U_\ell^\dagger U_\nu, \tag{4.12}$$

with

$$\begin{aligned} U_\ell &= W_{23}^l, \\ U_\nu &= W_{12}^\nu, \end{aligned} \tag{4.13}$$

where W_{23}^l and W_{23}^ν are given in Eq. 4.5 and in Eq. 4.10.

This gives

$$U^{s}_{PMNS} = \begin{pmatrix} c_{12} & s_{12} & 0 \\ -\frac{1}{\sqrt{2}}s_{12} & \frac{1}{\sqrt{2}}c_{12} & \frac{1}{\sqrt{2}} \\ \frac{1}{\sqrt{2}}s_{12} & -\frac{1}{\sqrt{2}}c_{12} & \frac{1}{\sqrt{2}} \end{pmatrix}, \tag{4.14}$$

which is just the $\mu - \tau$ symmetric leptonic mixing. If we require θ_{12} in Eq. 4.11 to be independent of the parameters a, b and d, then, we either have $a = b$ which leads to $\theta_{12} = \pi/4$ and generates the BM mixing

$$\mathcal{M}_{\nu} = \begin{pmatrix} a & d & 0 \\ d & a & 0 \\ 0 & 0 & c \end{pmatrix}. \tag{4.15}$$

with mass eigenvalues

$$\mathcal{M}^{d}_{\nu} = diag\ (a + d,\ a - d,\ c). \tag{4.16}$$

or $d = k(a-b)$ and in particular we obtain the tri-bimaximal mixing with $\sin\theta_{12} = \frac{1}{\sqrt{3}}$ where $k = \sqrt{2}$ and

$$\mathcal{M}_{\nu} = \begin{pmatrix} a & \sqrt{2}(a-b) & 0 \\ \sqrt{2}(a-b) & b & 0 \\ 0 & 0 & c \end{pmatrix}. \tag{4.17}$$

The mass eigenvalues are given by

$$\mathcal{M}^{d}_{\nu} = diag\ (2a - b,\ 2b - a,\ c). \tag{4.18}$$

We see that the neutrino mass matrix exhibits decoupling of the first two generations from the third one. We will study both cases here in this work.

4.3 Bimaximal mixing

In this section, we use the bimaximal structure as the mixing matrix in the flavor symmetric limit. We present the Lagrangian required to generate the BM pattern. Finally, we study the effect of breaking the flavor symmetry on both sectors and show the numerical results.

4.3.1 The Lagrangian in the symmetric limit

Here, we present a simple Lagrangian that generates the mixing matrices considered in the previous section. We find that the model naturally generates the BM mixing though the TBM mixing can also be obtained but with introducing different flavor symmetries. Our phenomenology will be done in the scenario in which the leptonic mixing is BM in the symmetric limit.

We will use the seesaw mechanism to obtain the neutrino masses. Our model extends the SM by an additional Higgs doublet and two singlet scalars. The particle content of the model is given as

- three left-handed lepton doublets D_{α_L}, where α denotes $e,\ \mu$, and τ,
- three right-handed charged-lepton singlet α_R, and
- three right-handed neutrino singlets $\nu_{\alpha R}$.

In the scalar sector, we employ

- two Higgs doublets ϕ_j with vacuum expectation values, v.e.v, $\langle 0|\phi_j^0|0\rangle = \frac{v_j}{\sqrt{2}}$ and
- two real singlet scalar fields ϵ_1 and ϵ_2, with v.e.v's $\langle 0|\epsilon_k^0|0\rangle = w_k$.

The symmetries of the Lagrangian are introduced as

$$\begin{aligned}
Z_2^{23} \ &: \ D_{\mu_L} \leftrightarrow -D_{\tau_L},\ \mu_R \leftrightarrow -\tau_R,\ \nu_{\mu R} \leftrightarrow -\nu_{\tau R}, \\
&\quad\ D_{e_L} \to D_{e_L},\ e_R \to e_R,\ \nu_{eR} \to \nu_{eR}, \\
&\quad\ \epsilon_1 \to -\epsilon_1,\ \epsilon_2 \to \epsilon_2,\ \phi_1 \to \phi_1,\ \phi_2 \to \phi_2, \\
Z_2^e \ &: \ \nu_{eR},\ e_R,\ D_{e_L},\ \epsilon_1,\ \epsilon_2, \quad \text{(Change sign, and the rest of the fields remain same)} \\
Z_2^D \ &: \ \nu_{eR},\ \nu_{\mu R},\ \nu_{\tau R},\ \phi_2, \quad \text{(Change sign, and the rest of the fields remain same).}
\end{aligned} \tag{4.19}$$

The most general Lagrangian consistent with the symmetries is

$$\begin{aligned}
\mathcal{L}_Y \ &= \ y_1 \bar{D}_{e_L} e_R \phi_1 + y_2 \left(\bar{D}_{\mu_L}\mu_R + \bar{D}_{\tau_L}\tau_R\right)\phi_1 + y_3\left(\bar{D}_{\mu_L}\tau_R + \bar{D}_{\tau_L}\mu_R\right)\phi_1 \\
&+ \ \left[y_4 \bar{D}_{e_L}\nu_{eR} + y_5\left(\bar{D}_{\mu_L}\nu_{\mu R} + \bar{D}_{\tau_L}\nu_{\tau R}\right)\right]\tilde{\phi}_2 + h.c.,
\end{aligned} \tag{4.20}$$

$$\begin{aligned}\mathcal{L}_M &= \frac{1}{2}\left[M\nu_{eR}^T C^{-1}\nu_{eR} + M_P\nu_{\mu R}^T C^{-1}\nu_{\mu R} + M_P\nu_{\tau R}^T C^{-1}\nu_{\tau R}\right] \\ &- \frac{1}{2}y\nu_{eR}^T C^{-1}\left(\nu_{\mu R}\frac{(a\epsilon_1 + b\epsilon_2)}{\sqrt{2}} + \nu_{\tau R}\frac{(a\epsilon_1 - b\epsilon_2)}{\sqrt{2}}\right) + h.c. \end{aligned} \tag{4.21}$$

Here, $\tilde{\phi}_i \equiv i\sigma_2\phi_i^*$ is the conjugate Higgs doublet and we have chosen to work in a basis where the Dirac mass matrix for the neutrinos is diagonal. We can simplify the Lagrangian in several ways. First, we can redefine $a\epsilon_1 \to \epsilon_1$ and $b\epsilon_2 \to \epsilon_2$. Second, to reduce the number of parameters we can impose an approximate symmetry of the Lagrangian. A $SU(3)$ symmetry where the right handed singlet fields and the left handed doublet fields transform as the $SU(3)$ triplets leads to $y_4 = y_5 = y_D$. The $SU(3)$ symmetry is only satisfied by the Dirac mass term for the neutrinos and is broken by the other terms in the Lagrangian. Third, we will require the Lagrangian to be invariant under the transformation of the right-handed charged leptons ($\mu_R \leftrightarrow -\tau_R, e_R \to -e_R, \phi_1 \to -\phi_1$), with all other fields remaining unchanged. This symmetry requires $y_2 = y_3$ leading to vanishing μ mass. The μ mass is introduced later as a symmetry breaking term. Finally, we will set the Majorana mass terms $M = M_P$. We can then rewrite the Lagrangian as

$$\begin{aligned}\mathcal{L}_Y &= y_1\bar{D}_{e_L}e_R\phi_1 + y_2\left(\bar{D}_{\mu_L}\mu_R + \bar{D}_{\tau_L}\tau_R\right)\phi_1 + y_2\left(\bar{D}_{\mu_L}\tau_R + \bar{D}_{\tau_L}\mu_R\right)\phi_1 \\ &+ y_D\left[\bar{D}_{e_L}\nu_{eR} + \bar{D}_{\mu_L}\nu_{\mu R} + \bar{D}_{\tau_L}\nu_{\tau R}\right]\tilde{\phi}_2 + h.c., \end{aligned} \tag{4.22}$$

$$\begin{aligned}\mathcal{L}_M &= \frac{1}{2}M\left[\nu_{eR}^T C^{-1}\nu_{eR} + \nu_{\mu R}^T C^{-1}\nu_{\mu R} + \nu_{\tau R}^T C^{-1}\nu_{\tau R}\right] \\ &- \frac{1}{2}y\nu_{eR}^T C^{-1}\left(\nu_{\mu R}\frac{(\epsilon_1 + \epsilon_2)}{\sqrt{2}} + \nu_{\tau R}\frac{(\epsilon_1 - \epsilon_2)}{\sqrt{2}}\right) + h.c. \end{aligned} \tag{4.23}$$

The most general scalar potential V that is invariant under $Z_2^{23} \times Z_2^e \times Z_2^D$ is given by

$$\begin{aligned}V &= -\mu_1^2\epsilon_1^2 - \mu_2^2\epsilon_2^2 + \lambda_1\epsilon_1^4 + \lambda_2\epsilon_2^4 + \lambda_1'\epsilon_1^2\epsilon_2^2 \\ &+ \sigma_1\epsilon_1^2|\phi_1|^2 + \sigma_2\epsilon_1^2|\phi_2|^2 + \sigma_3\epsilon_2^2|\phi_1|^2 + \sigma_4\epsilon_2^2|\phi_2|^2 + V_{2HD}(\phi_1,\ \phi_2), \end{aligned} \tag{4.24}$$

where $V_{2HD}(\phi_1,\ \phi_2)$ is the potential of the two Higgs doublets,

$$\begin{aligned}V_{2HD}(\phi_1,\ \phi_2) &= -\mu_{\phi_1}^2\phi_1^\dagger\phi_1 - \mu_{\phi_2}^2\phi_2^\dagger\phi_2 + \lambda_{\phi_1}(\phi_1^\dagger\phi_1)^2 + \lambda_{\phi_2}(\phi_2^\dagger\phi_2)^2 + \lambda_{\phi_{12}}\left(\phi_1^\dagger\phi_1 + \phi_2^\dagger\phi_2\right)^2 \\ &+ \lambda_{\phi_{12}}'\left(\phi_1^\dagger\phi_1 - \phi_2^\dagger\phi_2\right)^2 + \lambda_{\phi_{21}}\left((\phi_1^\dagger\phi_1)(\phi_2^\dagger\phi_2) - (\phi_1^\dagger\phi_2)(\phi_2^\dagger\phi_1)\right) \\ &+ \lambda_{\phi_{21}}'\left((\phi_1^\dagger\phi_1)(\phi_2^\dagger\phi_2) + (\phi_1^\dagger\phi_2)(\phi_2^\dagger\phi_1)\right). \end{aligned} \tag{4.25}$$

If we impose an additional symmetry to the above potential such as $\epsilon_1 \leftrightarrow \epsilon_2$, then the potential takes the form

$$\begin{aligned} V &= -\mu^2\left(\epsilon_1^2+\epsilon_2^2\right)+\left(\epsilon_1^2+\epsilon_2^2\right)\sum_{i=1}^{2}\sigma_i\phi_i^\dagger\phi_i+\lambda\left(\epsilon_1^2+\epsilon_2^2\right)^2 \\ &+ \lambda'\left(\epsilon_1^2-\epsilon_2^2\right)^2+V_{2HD}(\phi_1,\ \phi_2). \end{aligned} \tag{4.26}$$

We can parametrize the v.e.v's of the singlet scalars as follows

$$\langle 0\left|\epsilon_1\right|0\rangle = w\cos\gamma \qquad \text{and} \qquad \langle 0\left|\epsilon_2\right|0\rangle = w\sin\gamma. \tag{4.27}$$

Thus, the only term that depends on γ is

$$f(\gamma)\equiv\lambda' w^4\cos^2 2\gamma. \tag{4.28}$$

By minimizing $f(\gamma)$, one gets

$$\cos 2\gamma = 0. \tag{4.29}$$

Thus

$$\langle 0\left|\epsilon_1\right|0\rangle = \langle 0\left|\epsilon_2\right|0\rangle = \frac{w}{\sqrt{2}}. \tag{4.30}$$

By minimizing the above potential one can find the parameter w and the v.e.v's of the two Higgs doublets which are nonzero and different in the symmetric limit

$$\begin{aligned} v_1 &= \sqrt{\frac{\alpha_1}{2\beta_1}}, \\ v_2 &= \sqrt{\frac{\alpha_2}{2\beta_2}}, \end{aligned} \tag{4.31}$$

where

$$\begin{aligned}
\alpha_1 &= 4\lambda(\lambda_{\phi_{12}}\mu_{\phi_1}^2 + \lambda_{\phi_2}\mu_{\phi_1}^2 - \lambda'_{\phi_{21}}\mu_{\phi_2}^2 - \lambda_{\phi_{12}}\mu_{\phi_2}^2 + \lambda'_{\phi_{12}}(\mu_{\phi_1}^2 + \mu_{\phi_2}^2)) - 2\lambda_{\phi_{12}}\mu^2\sigma_1 \\
&- 2\lambda_{\phi_2}\mu^2\sigma_1 + 2\lambda'_{\phi_{21}}\mu^2\sigma_2 + 2\lambda_{\phi_{12}}\mu^2\sigma_2 + \mu_{\phi_2}^2\sigma_1\sigma_2 - \mu_{\phi_1}^2\sigma_2^2 - 2\lambda'_{\phi_{12}}\mu^2(\sigma_1+\sigma_2), \\
\beta_1 &= 4\lambda(-\lambda'^2_{\phi_{21}} - 2\lambda'_{\phi_{21}}\lambda_{\phi_{12}} + \lambda_{\phi_1}\lambda_{\phi_{12}} + \lambda_{\phi_1}\lambda_{\phi_2} + \lambda_{\phi_{12}}\lambda_{\phi_2} + \lambda'_{\phi_{12}}(2\lambda'_{\phi_{21}} + \lambda_{\phi_1} + 4\lambda_{\phi_{12}} \\
&+ \lambda_{\phi_2})) - \lambda_{\Phi_{12}}\sigma_1^2 - \lambda_{\phi_2}\sigma_1^2 + 2\lambda'_{\phi_{21}}\sigma_1\sigma_2 + 2\lambda_{\phi_{12}}\sigma_1\sigma_2 - \lambda_{\phi_1}\sigma_2^2 - \lambda_{\phi_{12}}\sigma_2^2 - \lambda'_{\phi_{12}}(\sigma_1+\sigma_2)^2, \\
\alpha_2 &= 4\lambda(\lambda_{\phi_{12}}\mu_{\phi_2}^2 + \lambda_{\phi_1}\mu_{\phi_2}^2 - \lambda'_{\phi_{21}}\mu_{\phi_1}^2 - \lambda_{\phi_{12}}\mu_{\phi_1}^2 + \lambda'_{\phi_{12}}(\mu_{\phi_2}^2 + \mu_{\phi_1}^2)) - 2\lambda_{\phi_{12}}\mu^2\sigma_2 \\
&- 2\lambda_{\phi_1}\mu^2\sigma_2 + 2\lambda'_{\phi_{21}}\mu^2\sigma_1 + 2\lambda_{\phi_{12}}\mu^2\sigma_1 + \mu_{\phi_1}^2\sigma_2\sigma_1 - \mu_{\phi_2}^2\sigma_1^2 - 2\lambda'_{\phi_{12}}\mu^2(\sigma_2+\sigma_1), \\
\beta_2 &= 4\lambda(-\lambda'^2_{\phi_{21}} - 2\lambda'_{\phi_{21}}\lambda_{\phi_{12}} + \lambda_{\phi_2}\lambda_{\phi_{12}} + \lambda_{\phi_2}\lambda_{\phi_1} + \lambda_{\phi_{12}}\lambda_{\phi_1} + \lambda'_{\phi_{12}}(2\lambda'_{\phi_{21}} + \lambda_{\phi_2} + 4\lambda_{\phi_{12}} \\
&+ \lambda_{\phi_1})) - \lambda_{\Phi_{12}}\sigma_2^2 - \lambda_{\phi_1}\sigma_2^2 + 2\lambda'_{\phi_{21}}\sigma_2\sigma_1 + 2\lambda_{\phi_{12}}\sigma_2\sigma_1 - \lambda_{\phi_2}\sigma_1^2 - \lambda_{\phi_{12}}\sigma_1^2 - \lambda'_{\phi_{12}}(\sigma_2+\sigma_1)^2.
\end{aligned} \tag{4.32}$$

Also, the parameter w can simply be written as follows

$$w^2 = \frac{\mu^2 - (\sigma_1|v_1|^2 + \sigma_2|v_2|^2)}{2\lambda}, \tag{4.33}$$

which shows that the v.e.v of the singlet scalars is independent of $(v_1,\ v_2)$ when $\sigma_1 = \sigma_2 = 0$.

The explicit form of the Yukawa matrix, Y_{23}^L, and the Dirac neutrino mass matrix can be written from the Lagrangian (4.20) as follows

$$Y_{23}^L = \frac{v_1}{\sqrt{2}}\begin{pmatrix} y_1 & 0 & 0 \\ 0 & y_2 & y_2 \\ 0 & y_2 & y_2 \end{pmatrix}, \tag{4.34}$$

$$M_D = \mathrm{diag}(A, A, A), \quad \text{with } A = y\frac{v_2}{\sqrt{2}}. \tag{4.35}$$

Also, the Majorana mass matrix can be obtained from Eq. (4.85) as follows

$$M_R = \begin{pmatrix} M & -v_w & 0 \\ -v_w & M & 0 \\ 0 & 0 & M \end{pmatrix}, \tag{4.36}$$

with $v_w = yw$. Using the seesaw formula [212], the neutrino mass matrix is given as

$$\mathcal{M}_\nu = -M_D^T M_R^{-1} M_D. \tag{4.37}$$

Then $\mathcal{M}_\nu$ has the structure

$$\mathcal{M}_\nu = \begin{pmatrix} X & G & 0 \\ G & X & 0 \\ 0 & 0 & Z \end{pmatrix}, \tag{4.38}$$

where

$$X = -\frac{A^2 M}{M^2 - v_w^2},\ G = -\frac{A^2 v_w}{M^2 - v_w^2},\ Z = -\frac{A^2}{M}. \tag{4.39}$$

By diagonalizing Eq. 4.90, we obtain the neutrino masses as

$$\begin{aligned} m_1 &= -\frac{A^2}{M + v_w}, \\ m_2 &= -\frac{A^2}{M - v_w}, \\ m_3 &= -\frac{A^2}{M}. \end{aligned} \tag{4.40}$$

Note that from the above equations one can estimate the scale of the v.e.v, v_2, of the second Higgs doublet ϕ_2. As the absolute neutrino masses are in the eV scale, therefore, v_2 has to be in the MeV scale if the see-saw scale (M) is in the TeV range. The mass relations satisfy the relation

$$\frac{1}{m_1} + \frac{1}{m_2} = \frac{2}{m_3}. \tag{4.41}$$

Similar relations among the masses are discussed in Ref. [213]. We can use the above sum-rule to obtain an upper limit for the heaviest mass, $|m_3| \leq \frac{2|m_1||m_2|}{||m_1|+|m_2||}$ for the normal hierarchy or $|m_2| \leq \frac{|m_1||m_3|}{|2|m_1|-|m_3||}$ for the inverted hierarchy.

4.3.2 Symmetry breaking

The breaking of the flavor symmetries in the charged lepton and the neutrino sectors will cause deviation from the BM form, and we study these deviations in this section.

Charged Lepton Sector

In the charged lepton sector we break the decoupled $2-3$ symmetry by adding the following higher dimensional terms

$$O_1 = c y_2 \bar{D}_{\mu_L} \mu_R \phi_1 \frac{\phi_1^\dagger \phi_1}{\Lambda^2}, \tag{4.42}$$

and

$$O_2 = y' \left(\bar{D}_{e_L} \mu_R - \bar{D}_{e_L} \tau_R + \bar{D}_{\mu_L} e_R - \bar{D}_{\tau_L} e_R \right) \phi_1 \frac{\phi_1^\dagger \phi_1}{\Lambda^2}. \tag{4.43}$$

The operator O_2 breaks the decoupled $2-3$ symmetry, $Z_2^{23} \times Z_2^e$, but is still $2-3$ symmetric. The operator O_1 explicitly breaks the $2-3$ symmetry, Z_2^{23}, and generates the muon mass. To generate explicit $2-3$ breaking we have introduced the higher dimensional operator in the position of the muon field, 2-2 element, in the Yukawa matrix which is the most straightforward way to generate the muon mass. Introducing this operator in the 3-3 position generates the same numerical solutions for the correction angles. But introducing it in the 2-3 or 3-2 positions does not generate physical values for the mixing angles. Even introducing $2-3$ symmetric terms in (2-2, 3-3) or (2-3, 3-2) generates either unphysical mixing angles or gives very large correction mixing angles that do not lead to successful phenomenology.

In the presence of the higher dimensional terms the charged lepton Yukawa matrix has the following form

$$Y^L = \begin{pmatrix} l_{11} & l_{12} & -l_{12} \\ l_{12} & \frac{1}{2} l_T (1 + 2\kappa_l) & \frac{1}{2} l_T \\ -l_{12} & \frac{1}{2} l_T & \frac{1}{2} l_T \end{pmatrix}, \tag{4.44}$$

with $\kappa_l = c v_1^2 / 2\Lambda^2$ and $l_{12} = y' v_1^3 / 2\sqrt{2}\Lambda^2$ after the Higgs field gets it's v.e.v. Three relations can be obtained among the Y^L matrix elements

$$\begin{aligned} Y^L_{12} &= -Y^L_{13}, \\ Y^L_{23} &= Y^L_{33}, \\ Y^L_{22} &= (1 + 2\kappa_l) Y^L_{23}. \end{aligned} \tag{4.45}$$

We can solve for the unitary matrix, U_l, that diagonalizes Y^L in Eq. 4.44. We write,

$$U_l = W^l_{23} R^l_{23} R^l_{13} R^l_{12}, \tag{4.46}$$

where

$$\begin{aligned} R^l_{12} &= \begin{pmatrix} c_{12l} & s_{12l} & 0 \\ -s_{12l} & c_{12l} & 0 \\ 0 & 0 & 1 \end{pmatrix}, \\ c_{12l} &= \cos\theta_{12l}; s_{12l} = \sin\theta_{12l}, \end{aligned} \tag{4.47}$$

$$
\begin{aligned}
R^l_{13} &= \begin{pmatrix} c_{13l} & 0 & s_{13l}e^{-i\delta} \\ 0 & 1 & 0 \\ -s_{13l}e^{i\delta} & 0 & c_{13l} \end{pmatrix}, \\
c_{13l} &= \cos\theta_{13l}; s_{13l} = \sin\theta_{13l},
\end{aligned} \tag{4.48}
$$

$$
\begin{aligned}
R^l_{23} &= \begin{pmatrix} 1 & 0 & 0 \\ 0 & c_{23l} & s_{23l} \\ 0 & -s_{23l} & c_{23l} \end{pmatrix}, \\
c_{23l} &= \cos\theta_{23l}; s_{23l} = \sin\theta_{23l}.
\end{aligned} \tag{4.49}
$$

The Yukawa matrix, Y^L, can be written as

$$
Y^L = U_l Y^L_d U^\dagger_l, \tag{4.50}
$$

with

$$
Y^L_d = \begin{pmatrix} l_e & 0 & 0 \\ 0 & l_\mu & 0 \\ 0 & 0 & l_\tau \end{pmatrix}. \tag{4.51}
$$

Applying the relations in Eq. 4.45 to the Y^L matrix elements in Eq. 4.50 using Eq. 4.46, one can solve for the corrections of the mixing angles. Two ways can be used to find the angles, analytically or numerically. Solving for the mixing angles analytically, see details in appendix 10, can determine the size of the Yukawa matrix parameters in Eq. 4.44

$$
\begin{aligned}
z_\mu &\equiv \frac{m_\mu}{m_\tau}, \\
\kappa_l &= z z_\mu, \\
l_{12} &\approx \sqrt{\frac{z_\mu}{2}}(l_e - l_\mu), \\
l_T &\approx (l_\tau - l_\mu)(1 - \frac{1}{2}(z z_\mu)^2).
\end{aligned} \tag{4.52}
$$

with $z \sim 2$. It is interesting to note that

$$
\kappa = \frac{c v_1^2}{2\Lambda^2} = z z_\mu \tag{4.53}
$$

which fixes $\Lambda \sim$ TeV. We assume that the charged lepton corrections are "CKM-like", i.e.

$$\sin\theta_{12l} \approx \lambda, \quad \sin\theta_{23l} \approx A\lambda^2, \quad \sin\theta_{13l} \approx B\lambda^3, \tag{4.54}$$

where A, B are real and of order one, with λ is the sine of the Cabibbo angle, $\lambda = \sin\theta_C \simeq 0.227$. Numerical solution for the above relations presents some numerical results for various z values that generate appropriate correction angles, with assuming $\delta = \pi$,

- For $z = 2.0$: $s_{12l} \approx \pm 0.34,\ s_{13l} \approx \pm 0.0011,\ s_{23l} \approx -0.059$,
- For $z = 2.06$: $s_{12l} \approx \pm 0.3,\ s_{13l} \approx \pm 0.001,\ s_{23l} \approx -0.061$,
- For $z = 2.2$: $s_{12l} \approx \pm 0.2,\ s_{13l} \approx \pm 0.00075,\ s_{23l} \approx -0.065$,

We expand the angles in Eq. 1.20 as

$$s_{13} = \frac{r}{\sqrt{2}}, \quad s_{12} = \frac{1}{\sqrt{2}}(1+s), \quad s_{23} = \frac{1}{\sqrt{2}}(1+a), \tag{4.55}$$

where the three real parameters r, s, a describe the deviations of the reactor, solar, and atmospheric angles from their bimaximal values. We use global fits of the conventional mixing parameters $(s,\ a)$ [214] that can be translated into 3σ ranges and the mixing parameter r with 2.5σ significance (90% C.L.) [1]

$$0.12 < r < 0.39,\ -0.29 < s < -0.14,\ -0.15 < a < 0.16. \tag{4.56}$$

To first order in r, s, a, the lepton mixing matrix can be written as,

$$U \approx \begin{pmatrix} \frac{1}{\sqrt{2}}(1-s) & \frac{1}{\sqrt{2}}(1+s) & \frac{1}{\sqrt{2}} r e^{-i\delta} \\ -\frac{1}{2}(1+s-a+\frac{r}{\sqrt{2}}e^{i\delta}) & \frac{1}{2}(1-s-a-\frac{r}{\sqrt{2}}e^{i\delta}) & \frac{1}{\sqrt{2}}(1+a) \\ \frac{1}{2}(1+s+a-\frac{r}{\sqrt{2}}e^{i\delta}) & -\frac{1}{2}(1-s+a+\frac{r}{\sqrt{2}}e^{i\delta}) & \frac{1}{\sqrt{2}}(1-a) \end{pmatrix}, \tag{4.57}$$

which is similar to the parametrization in Ref. [215] with the TBM mixing. We have assumed that $\delta = \pi$ where the present data prefers a negative value for s [215] and r is positive, in our discussion we do not consider CP violation. Now, we can write the parameters $(r,\ s,\ a)$ in terms of the elements of the mixing matrix

$$\begin{aligned} s &= -1 + \sqrt{2}U_{12}, \\ r &= \sqrt{2}(1+s-a+2U_{21}), \\ a &= -1 + \sqrt{2}U_{23}. \end{aligned} \tag{4.58}$$

From the details in appendix 10, one obtains

$$\begin{aligned} s &\approx -\frac{1}{\sqrt{2}}(s_{12l}+s_{13l}), \\ r &\approx s_{12l}-s_{13l}, \\ a &\approx -s_{23l}. \end{aligned} \tag{4.59}$$

From the above equations one can get the deviation parameters as follows

- For $z=2.0$: $s\approx -0.24,\ r\approx 0.34,\ a\approx 0.059$,
- For $z=2.06$: $s\approx -0.21,\ r\approx 0.30,\ a\approx 0.061$,
- For $z=2.2$: $s\approx -0.14,\ r\approx 0.20,\ a\approx 0.065$.

The above results demonstrate that the contributions from the charged lepton sector can accommodate the T2K data of θ_{13} as well as the other mixing angles.

Neutrino sector

In this section we consider deviations of the BM mixing from the neutrino sector. We maintain the invariance of the Majorana Lagrangian under the symmetry group in Eq. 4.81 and generate the deviation from the BM matrix by breaking the $\epsilon_1 \leftrightarrow \epsilon_2$ symmetry in Eq. 4.26 by introducing the most general dimension four symmetry breaking terms in the potential

$$\left(\epsilon_1^2-\epsilon_2^2\right)\sum_{i=1}^{2}\sigma_i'\phi_i^\dagger\phi_i+\varrho\left(\epsilon_1^2-\epsilon_2^2\right)\left(\epsilon_1^2+\epsilon_2^2\right).^2 \tag{4.60}$$

We require that all terms in the symmetry breaking potential are of the same size which results in $\rho\sim\frac{v^2}{w^2}\sigma_i'$ where v is the electroweak v.e.v with $v^2=v_1^2+v_2^2$ and ω is the scale of the v.e.v's of the singlet scalars. Thus, the potential is

$$\begin{aligned} V &= -\mu^2\left(\epsilon_1^2+\epsilon_2^2\right)+\left(\epsilon_1^2+\epsilon_2^2\right)\sum_{i=1}^{2}\sigma_i\phi_i^\dagger\phi_i+\lambda\left(\epsilon_1^2+\epsilon_2^2\right)^2+\lambda'\left(\epsilon_1^2-\epsilon_2^2\right)^2 \\ &+ \left(\epsilon_1^2-\epsilon_2^2\right)\sum_{i=1}^{2}\sigma_i'\phi_i^\dagger\phi_i+\varrho\left(\epsilon_1^2-\epsilon_2^2\right)\left(\epsilon_1^2+\epsilon_2^2\right)+V_{2HD}(\phi_1,\ \phi_2). \end{aligned} \tag{4.61}$$

[2] The most general symmetry breaking terms can be expressed in terms of the form in Eq. 4.93 and symmetry conserving terms that can be absorbed in the symmetric potential.

Now, parameterizing the v.e.v's as in Eq. 4.27 and minimizing the potential leads to

$$\begin{aligned} \cos 2\gamma &= -\frac{\varrho w^2 + (\sigma_1'|v_1|^2 + \sigma_2'|v_2|^2)}{2\lambda' w^2}, \\ w^2 &= \frac{2\lambda'(\mu^2 - (\sigma_1|v_1|^2 + \sigma_2|v_2|^2)) + \varrho(\sigma_1'|v_1|^2 + \sigma_2'|v_2|^2)}{4\lambda\lambda' - \varrho^2}. \end{aligned} \tag{4.62}$$

Keeping in mind the size of the various co-efficients in the symmetry breaking potential discussed above, we find that $\cos 2\gamma \approx 0$ up to corrections of order $\frac{v^2}{\omega^2}$. We assume that w is in the TeV scale and with v in the EW scale the symmetry breaking corrections are of the right size to explain the experimental numbers.

We shift the v.e.v's of the two singlet scalars ($w_1 \neq w_2$) up to the first order of the symmetry breaking parameter. Then, the Majorana neutrino mass matrix in Eq. 4.36 takes the form

$$M_R = \begin{pmatrix} M & -v_{wp} & -v_{wn} \\ -v_{wp} & M & 0 \\ -v_{wn} & 0 & M \end{pmatrix}, \tag{4.63}$$

where

$$\begin{aligned} v_{wp} &= \frac{y}{\sqrt{2}}(w_1 + w_2), \\ v_{wn} &= \frac{y}{\sqrt{2}}(w_1 - w_2). \end{aligned} \tag{4.64}$$

We write the v.e.v's of the singlet scalars after symmetry breaking as

$$\begin{aligned} w_1 &= \frac{w + \rho_1}{\sqrt{2}}, \\ w_2 &= \frac{w + \rho_2}{\sqrt{2}}, \end{aligned} \tag{4.65}$$

where ρ_1 and ρ_2 are small quantities and

$$\rho_1 = -\rho_2 = \frac{w\tau}{2}. \tag{4.66}$$

Up to the first order of the symmetry breaking parameter τ,

$$\tau \equiv -\frac{\varrho w^2 + (\sigma_1'|v_1|^2 + \sigma_2'|v_2|^2)}{2\lambda' w^2}, \tag{4.67}$$

one gets

$$\begin{aligned} v_{wp} &= v_w, \\ v_{wn} &= \frac{\tau}{2} v_w. \end{aligned} \tag{4.68}$$

It turns out that breaking the $\epsilon_1 \leftrightarrow \epsilon_2$ symmetry to generate different v.e.v's for the singlet scalars is not sufficient to break the almost degeneracy of $(m_1,\ m_2)$ to satisfy the squared mass difference measurements. Therefore, we introduce an additional term in the Lagrangian which is consistent with the symmetries of the Lagrangian,

$$M_1 \left[\nu_{\mu R}^T C^{-1} \nu_{\mu R} + \nu_{\tau R}^T C^{-1} \nu_{\tau R} \right]. \tag{4.69}$$

Thus

$$M_R = \begin{pmatrix} M & -v_w & -\frac{\tau}{2} v_w \\ -v_w & M' & 0 \\ -\frac{\tau}{2} v_w & 0 & M' \end{pmatrix}, \tag{4.70}$$

where $M' = M + M_1$.

The neutrino mass matrix in Eq. 4.90 changes to be

$$\mathcal{M}_\nu = \begin{pmatrix} X' & G' & P' \\ G' & Y' & W' \\ P' & W' & Z' \end{pmatrix}, \tag{4.71}$$

where

$$\begin{aligned} X' &= -\frac{4A^2 M'}{4MM' - v_w^2(4+\tau^2)}, \\ Y' &= -\frac{A^2(4MM' - v_w^2\tau^2)}{M'(4MM' - v_w^2(4+\tau^2))}, \\ Z' &= -\frac{4A^2(MM' - v_w^2)}{M'(4MM' - v_w^2(4+\tau^2))}, \\ G' &= -\frac{4A^2 v_w}{4MM' - v_w^2(4+\tau^2)}, \\ P' &= -\frac{2A^2 v_w \tau}{4MM' - v_w^2(4+\tau^2)}, \\ W' &= -\frac{2A^2 v_w^2 \tau}{M'(4MM' - v_w^2(4+\tau^2))}. \end{aligned} \tag{4.72}$$

By diagonalizing Eq. 4.108, one gets the mass eigenvalues

$$\begin{aligned} m_1 &= -\frac{2A^2\left((M+M') - \sqrt{M^2 - 2MM' + M'^2 + v_w^2(4+\tau^2)}\right)}{4MM' - v_w^2(4+\tau^2)}, \\ m_2 &= -\frac{2A^2\left((M+M') + \sqrt{M^2 - 2MM' + M'^2 + v_w^2(4+\tau^2)}\right)}{4MM' - v_w^2(4+\tau^2)}, \\ m_3 &= -\frac{A^2}{M'}. \end{aligned} \tag{4.73}$$

Now, we can diagonalize the mass matrix in Eq. 4.108 using the unitary matrix $U_\nu = W_{12}^\nu R_{23}^\nu R_{12}^\nu$ with,

$$\begin{aligned} R_{12}^\nu &= \begin{pmatrix} c_{12\nu} & s_{12\nu} & 0 \\ -s_{12\nu} & c_{12\nu} & 0 \\ 0 & 0 & 1 \end{pmatrix}, \\ c_{12\nu} &= \cos\theta_{12\nu}; s_{12\nu} = \sin\theta_{12\nu}, \\ R_{23}^\nu &= \begin{pmatrix} 1 & 0 & 0 \\ 0 & c_{23\nu} & s_{23\nu} \\ 0 & -s_{23\nu} & c_{23\nu} \end{pmatrix}, \\ c_{23\nu} &= \cos\theta_{23\nu}; s_{23\nu} = \sin\theta_{23\nu}. \end{aligned} \tag{4.74}$$

The mass matrix elements in Eq. 4.109 satisfy the two relations

$$\begin{aligned} X'(Z'-Y') &= P'^2 - G'^2, \\ G'P'(Z'-Y') &= W'(P'^2 - G'^2). \end{aligned} \tag{4.75}$$

By applying the above relations to the matrix elements of

$$\mathcal{M}_\nu = U_\nu \mathcal{M}_\nu^d U_\nu^\dagger, \tag{4.76}$$

one can obtain the mixing angles

$$\begin{aligned} s_{23\nu} &= \sqrt{\frac{2m_1(m_2-m_3)}{m_2(m_1-m_3)}}, \\ s_{12\nu} &= \sqrt{\frac{-m_1m_2 + 2m_1m_3 - m_2m_3}{2m_3(m_1-m_2)}}. \end{aligned} \tag{4.77}$$

Eventually, we obtain the elements of the lepton mixing matrix $U_{PMNS} = U_l^\dagger U_\nu$ with $U_\ell = W_{23}^l R_{23}^l R_{13}^l R_{12}^l$ and $U_\nu = W_{12}^\nu R_{23}^\nu R_{12}^\nu$. The deviation parameters $(s,\ r,\ a)$ can be obtained from Eq. 4.115 as follows

$$\begin{aligned} s &\approx -\frac{1}{\sqrt{2}}(s_{12l} + s_{13l}) + s_{12\nu}, \\ r &\approx s_{12l} - s_{13l} - s_{23\nu}, \\ a &\approx -s_{23l} + \frac{1}{\sqrt{2}} s_{23\nu}. \end{aligned} \tag{4.78}$$

4.3.3 Numerical results

From the neutrino mass matrix (4.15), one observes that in the degenerate case, when $m_1 \approx m_2 \approx m_3$, $a \approx c$, $d \approx 0$ which means that the neutrino mass matrix is already diagonalized as $\mathcal{M}_\nu \approx \text{diag}\,(a, a, a)$. That means the lepton mixing matrix does not include a contribution from the neutrino sector, and the resultant leptonic mixing is inconsistent with the experimental data. Thus, in the symmetric limit our model excludes the case of the degenerate neutrino masses. Even, after symmetry breaking, the degenerate case in Eq. 4.110 leads to vanishing the v.e.v's of the singlet scalar fields which does not lead to successful phenomenology.

The numerics goes as following; we choose masses (m_1, m_2, m_3) which satisfy the experimental values of the squared mass differences

$$\begin{aligned} \Delta m_{21}^2 &= m_2^2 - m_1^2 = (7.59 \pm 0.20) \times 10^{-5} eV^2, \\ \Delta m_{32}^2 &= |m_3^2 - m_2^2| = (2.43 \pm 0.13) \times 10^{-3} eV^2. \end{aligned} \tag{4.79}$$

We substitute those mass values in (r, s, a) in Eq. 4.115, using $(s_{12\nu},\ s_{23\nu})$ given in Eq. 4.111 and $(s_{12l},\ s_{23l},\ s_{13l})$ in sec. 4.3.2. If the results satisfy the experimental constraints in Eq. 4.113, we plot the possible values of the absolute masses and the mixing angles. By using Eq. 4.110, we calculate values for the Lagrangian parameters $(v_w,\ A,\ M,\ M')$ which generate the values of the absolute masses obtained from the graphs. From the graphs, one finds that $(v_w,\ M,\ M')$ are obtained in the TeV scale and A in the MeV range.

Three mass-dependent neutrino observables are probed in different types of experiments. The sum of absolute neutrino masses $m_{cosm} \equiv \Sigma m_i$ is probed in cosmology, the kinetic electron neutrino mass in beta decay (M_β) is probed in direct search for neutrino masses, and the effective mass (M_{ee}) is probed in neutrinoless double beta decay experiments with the decay rate for the process $\Gamma \propto M_{ee}^2$. In terms of the "bare" physical parameters m_i and

$U_{\alpha i}$, the observables are given by [213]

$$\begin{aligned} \Sigma m_i &= |m_1| + |m_2| + |m_3|, \\ M_{ee} &= ||m_1||U_{e1}|^2 + |m_2||U_{e2}|^2 e^{i\phi_1} + |m_3||U_{e3}|^2 e^{i\phi_2}|, \\ M_\beta &= \sqrt{|m_1|^2|U_{e1}|^2 + |m_2|^2|U_{e2}|^2 + |m_3|^2|U_{e3}|^2}. \end{aligned} \tag{4.80}$$

In our analysis we ignore the Majorana phases ($\phi_1,\ \phi_2$) and plot M_β versus Σm_i and M_{ee} versus m_{light}, where m_{light} is the lightest neutrino mass.

In Figs. (4.1, 4.2, 4.3) we assume specific values of z with the corresponding correction mixing angles ($s_{13l},\ s_{12l},\ s_{23l}$) and plot the absolute masses and the mixing angles which satisfy the neutrino mixing constraints. By choosing a value for the symmetry breaking term τ, we plot the parameters ($v_w,\ A,\ M,\ M'$) that satisfy the squared mass difference measurements. This model supports the normal mass hierarchy as shown in the graphs with the scale of the neutrino masses in the few meV to ~ 50 meV range. The results agree with the recent T2K data which find a relatively large θ_{13}. The graphs show that the see-saw scale ($M,\ M'$) are in the TeV range, and the second Higgs that couples to the right-handed neutrinos has v.e.v v_2, included in A, in the MeV scale. Also, they indicate that the v.e.v of the singlet scalar fields v_w is in the TeV scale. The graphs show that $\Sigma m_i \approx 0.06$ eV and $M_{ee} < M_\beta$ and $M_{ee} < 0.35$ eV [216]. Various other mechanisms to generate the neutrino masses with TeV scale new physics are mentioned in Ref. [217].

4.4 Tri-bimaximal mixing

We have seen in the previous section how this model introduced the bimaximal structure to study the neutrino mixing. Here, in this section we present the tri-bimaximal pattern and compare the results obtained from the two patterns.

4.4.1 The Lagrangian in the symmetric limit

The Lagrangian that describes this model will be discussed in this section. It is assumed to be invariant under the product of the symmetries $Z_4 \times U(1)$. The Yukawa Lagrangian exhibits $\mu - \tau$ symmetry, which can be represented by a Z_4 symmetry. We use the see-saw mechanism to generate the neutrino masses. The particle content of the model is similar to the BM case in the fermionic sector. In the scalar sector, we employ two Higgs doublets ϕ_j, like in the BM case, and three complex singlet scalar fields ϵ_k with v.e.v's $\langle 0|\epsilon_k^0|0\rangle =$

w_k, $k = 1, 2, 3$. The symmetry of the Lagrangians is assumed as

$$\begin{aligned} Z_4 \;:\; & D_{\mu_L} \leftrightarrow -D_{\tau_L},\ \mu_R \leftrightarrow -\tau_R,\ \nu_{\mu R} \leftrightarrow -\nu_{\tau R}, \\ & \nu_{eR} \to i\nu_{eR},\ e_R \to ie_R,\ D_{e_L} \to iD_{e_L}, \\ & \epsilon_1 \to -i\epsilon_1,\ \epsilon_2 \to i\epsilon_2,\ \epsilon_3 \to -\epsilon_3,\ \phi_1 \to \phi_1,\ \phi_2 \to \phi_2, \\ U(1) \;:\; & \left\{\nu_{(e,\mu,\tau)R},\ e_R,\ (\mu,\tau)_R,\ D_{(e,\mu,\tau)_L},\ \epsilon_{(1,2,3)},\ \phi_1, \phi_2\right\} = \left\{\frac{1}{3}, \frac{7}{3}, \frac{4}{3}, \frac{4}{3}, \frac{2}{3}, 0, -1\right\}. \end{aligned} \tag{4.81}$$

The most general Lagrangian invariant under the underlined symmetry is given by

$$\begin{aligned} \mathcal{L}_Y &= y_1 \bar{D}_{e_L} e_R \phi_2 + \left[y_2 \left(\bar{D}_{\mu_L}\mu_R + \bar{D}_{\tau_L}\tau_R\right) + y_2 \left(\bar{D}_{\mu_L}\tau_R + \bar{D}_{\tau_L}\mu_R\right)\right] \phi_1 \\ &+ y_D \left[\bar{D}_{e_L}\nu_{eR} + \bar{D}_{\mu_L}(\nu_{\mu R} + \nu_{\tau R}) + \bar{D}_{\tau_L}(\nu_{\mu R} + \nu_{\tau R})\right] \tilde{\phi}_2 \\ &+ \frac{1}{2} y \bar{\nu}_{eR} \left(\nu^c_{\mu R} \frac{(\epsilon_1 + \epsilon_2)}{\sqrt{2}} + \nu^c_{\tau R} \frac{(\epsilon_1 - \epsilon_2)}{\sqrt{2}}\right) \\ &+ \frac{1}{2} y\ \bar{\nu}_{eR}\ \nu^c_{eR}\ \epsilon_3 + h.c. \end{aligned} \tag{4.82}$$

Here, $\tilde{\phi}_j \equiv i\sigma_2 \phi^*_j$ is the conjugate Higgs doublet. The Z_4 symmetry yields the decoupling structure in the charged lepton and neutrino mass matrices. In our model we relate the couplings to the $U(1)$ charges as $y = cq$ where y is a coupling, q is a $U(1)$ charge, and c is a constant. This leads to a universal coupling to the right-handed neutrinos and to the charged leptons.

The phenomenology of the above Lagrangian with the off-diagonal elements $\bar{D}_{\mu_L}\nu_{\tau R} + \bar{D}_{\tau_L}\nu_{\mu R}$ can be studied. But in this model we choose to work with diagonal Dirac neutrino mass matrix M_D to make the model even simpler. For this, we impose an approximate symmetry of the Lagrangian. A global $SO(3)$ flavour symmetry is introduced in a way that the transformations of the fields are given as follows:

$$\begin{pmatrix} e_R \\ \mu_R \\ \tau_R \end{pmatrix},\ \begin{pmatrix} D_{e_L} \\ D_{\mu_L} \\ D_{\tau_L} \end{pmatrix},\ \begin{pmatrix} \nu_{eR} \\ \nu_{\mu R} \\ \nu_{\tau R} \end{pmatrix},\ \begin{pmatrix} \epsilon_1 \\ \epsilon_2 \\ \epsilon_3 \end{pmatrix},\ \phi_1,\ \phi_2. \tag{4.83}$$

In the above Lagrangian, the $SO(3)$ symmetry is only satisfied by the Dirac mass terms for the neutrinos and is broken by the other terms in the way that the Yukawa Lagrangian is invariant under the symmetry product $Z_4 \times U(1)$. The implications of proposing the $SO(3)$ flavour symmetry in the lepton sector will be discussed in a separate work. By implementing these particle assignment we find that the off-diagonal elements $\bar{D}_{\mu_L}\nu_{\tau R} +$

$\bar{D}_{\tau_L}\nu_{\mu R}$ are forbidden leading to a diagonal Dirac mass matrix. We can then rewrite the above Lagrangian as

$$\begin{aligned}
\mathcal{L}_Y &= y_1\bar{D}_{e_L}e_R\phi_2 + \left[y_2\left(\bar{D}_{\mu_L}\mu_R + \bar{D}_{\tau_L}\tau_R\right) + y_2\left(\bar{D}_{\mu_L}\tau_R + \bar{D}_{\tau_L}\mu_R\right)\right]\phi_1 \\
&+ y_D\left[\bar{D}_{e_L}\nu_{eR} + \bar{D}_{\mu_L}\nu_{\mu R} + \bar{D}_{\tau_L}\nu_{\tau R}\right]\tilde{\phi}_2 \\
&+ \frac{1}{2}y\bar{\nu}_{eR}\left(\nu^c_{\mu R}\frac{(\epsilon_1+\epsilon_2)}{\sqrt{2}} + \nu^c_{\tau R}\frac{(\epsilon_1-\epsilon_2)}{\sqrt{2}}\right) \\
&+ \frac{1}{2}y\ \bar{\nu}_{eR}\ \nu^c_{eR}\ \epsilon_3 + h.c. \qquad (4.84)
\end{aligned}$$

When the singlet scalar fields acquire their v.e.v's, the $U(1)$ symmetry gets broken spontaneously and the neutrinos obtain their Majorana masses [218]. One of the neutrino masses blows up, therefore, we need to introduce a Majorana mass term as a $U(1)$ symmetry breaking term, which is not going to change the mixing,

$$\mathcal{L}_M = \frac{1}{2}M\left[\bar{\nu}_{eR}\nu^c_{eR} + \bar{\nu}_{\mu R}\nu^c_{\mu R} + \bar{\nu}_{\tau R}\nu^c_{\tau R}\right] + h.c. \qquad (4.85)$$

he above Majorana mass term is invariant under the $SO(3)$ symmetry. The would-be-Goldstone bosons could be generated due to the spontaneous symmetry breaking of the global $U(1)$ symmetry by the v.e.v's of the singlet scalars. They can acquire masses through the explicit symmetry breaking of $U(1)$. Studying the effects of breaking the $U(1)$ symmetry is beyond the main goal of this work.

The most general scalar potential V that is invariant under the above symmetry product $Z_4 \times U(1) \times SO(3)$ is

$$\begin{aligned}
V &= -\mu^2\left(|\epsilon_1|^2 + |\epsilon_2|^2 + |\epsilon_3|^2\right) + \left(|\epsilon_1|^2 + |\epsilon_2|^2 + |\epsilon_3|^2\right)\sum_{i=1}^{2}\sigma_i\phi_i^\dagger\phi_i \\
&\quad +\lambda\left(|\epsilon_1|^2 + |\epsilon_2|^2 + |\epsilon_3|^2\right)^2 + V_{2HD}(\phi_1,\ \phi_2), \qquad (4.86)
\end{aligned}$$

where $V_{2HD}(\phi_1,\ \phi_2)$ is the potential of the two Higgs doublets in Eq. 4.25. One can easily verify that the v.e.v's of the Higgs doublets are different and non-zero in the symmetric limit.

We can minimize the potential to get the v.e.v's ($\langle 0|\epsilon_k^0|0\rangle = w_k$) as follows

$$\begin{aligned}
\left.\frac{\partial V}{\partial|\epsilon_1|}\right|_{\min} &= -2\mu^2 w_1 + 2w_1 \sum_{i=1}^{2} \sigma_i v_i^\dagger v_i + 4\lambda w_1 \left(w_1^2 + w_2^2 + w_3^2\right) = 0, \\
\left.\frac{\partial V}{\partial|\epsilon_2|}\right|_{\min} &= -2\mu^2 w_2 + 2w_2 \sum_{i=1}^{2} \sigma_i v_i^\dagger v_i + 4\lambda w_2 \left(w_1^2 + w_2^2 + w_3^2\right) = 0, \\
\left.\frac{\partial V}{\partial|\epsilon_3|}\right|_{\min} &= -2\mu^2 w_3 + 2w_3 \sum_{i=1}^{2} \sigma_i v_i^\dagger v_i + 4\lambda w_3 \left(w_1^2 + w_2^2 + w_3^2\right) = 0. \qquad (4.87)
\end{aligned}$$

One can notice that the three equations are not independent. Thus, we have the three v.e.v's are the same and equal to

$$w^2 = \frac{\mu^2 - (\sigma_1|v_1|^2 + \sigma_2|v_2|^2)}{6\lambda}, \qquad (4.88)$$

where $w_k = w$ for $k = 1, 2, 3$. The explicit form of the charged lepton Yukawa matrix and the Majorana and Dirac neutrino mass matrices can be written from Lagrangian (8.61) as follows

$$\begin{aligned}
Y_{23}^L &= \frac{v_1}{\sqrt{2}} \begin{pmatrix} y_1 v_2/v_1 & 0 & 0 \\ 0 & y_2 & y_2 \\ 0 & y_2 & y_2 \end{pmatrix}, \\
M_R &= \begin{pmatrix} M + \sqrt{2} v_w & 2v_w & 0 \\ 2v_w & M & 0 \\ 0 & 0 & M \end{pmatrix}, \quad \text{with } v_w = y\frac{w}{\sqrt{2}}, \\
M_D &= \text{diag}(A, A, A), \quad \text{with } A = y\frac{v_2}{\sqrt{2}}. \qquad (4.89)
\end{aligned}$$

Using the see-saw formula 4.37, Then $\mathcal{M}_\nu$ has the structure

$$\mathcal{M}_\nu = \begin{pmatrix} X & G & 0 \\ G & Y & 0 \\ 0 & 0 & Z \end{pmatrix}, \qquad (4.90)$$

where

$$\begin{aligned}
X &= -\frac{A^2 M}{M^2 + \sqrt{2} M v_w - 4v_w^2}, \; Y = -\frac{A^2(M + \sqrt{2} v_w)}{M^2 + \sqrt{2} M v_w - 4v_w^2}, \\
G &= \frac{2A^2 v_w}{M^2 + \sqrt{2} M v_w - 4v_w^2}, \; Z = -\frac{A^2}{M}. \qquad (4.91)
\end{aligned}$$

One can easily verifies that the relation $G = \sqrt{2}(X - Y)$ in Eq. 4.17 is satisfied. The mass eigenvalues $(2X - Y, 2Y - X, Z)$ can be written as

$$\begin{aligned} m_1 &= -\frac{A^2}{M + 2\sqrt{2}v_w}, \\ m_2 &= -\frac{A^2}{M - \sqrt{2}v_w}, \\ m_3 &= -\frac{A^2}{M}. \end{aligned} \tag{4.92}$$

From the above equations one can estimate the range of the v.e.v v_2 where $A = yv_2/\sqrt{2}$. As the absolute neutrino masses are in the eV scale, therefore, v_2 has to be in the MeV scale if the see-saw scale (M) is in the TeV range. The mass eigenvalues satisfy the relation 4.41, and similarly to the BM case the upper limit for the heaviest mass $|m_3| \leqslant \frac{3|m_1||m_2|}{|2|m_1|+|m_2||}$ for the normal hierarchy or $|m_2| \leqslant \frac{2|m_1||m_3|}{|3|m_1|-|m_3||}$ for the inverted hierarchy.

4.4.2 Symmetry Breaking

The breaking of flavor symmetries in the charged lepton and neutrino sector cause deviations from the TBM form. Symmetry breaking in the charged lepton sector has been considered in section 4.3.2. We evaluated the correction angles numerically. In this section we are going to consider deviations of the TBM structure from the neutrino sector.

We are going to break the $SO(3)$ symmetry, which has led to equal v.e.v's in the symmetric limit, and maintain the other symmetries of the Lagrangian. We will break the symmetry by introducing symmetry breaking terms of dimension four. We can present a large number of symmetry breaking terms. The most straightforward way is to break the alignment of the v.e.v's of $(\epsilon_1,\ \epsilon_2)$ which, in turn, violate the decoupling in the neutrino mass matrix. Here, we introduce the most general form of symmetry breaking terms

$$\xi \left(|\epsilon_1|^2 - |\epsilon_2|^2\right)^2 + \left(|\epsilon_1|^2 - |\epsilon_2|^2\right) \sum_{i=1}^{2} \rho_i \phi_i^\dagger \phi_i + \varrho \left(|\epsilon_1|^4 - |\epsilon_2|^4\right). \tag{4.93}$$

The most general symmetry breaking terms can be expressed in terms of the form in Eq. 4.93 and symmetry conserving terms that can be absorbed in the symmetric potential. Thus, the

scalar potential including all the terms of the form in Eq. 4.93 is given as follows

$$\begin{aligned} V &= -\mu^2\left(|\epsilon_1|^2+|\epsilon_2|^2+|\epsilon_3|^2\right)+\left(|\epsilon_1|^2+|\epsilon_2|^2+|\epsilon_3|^2\right)\sum_{i=1}^{2}\sigma_i\phi_i^\dagger\phi_i \\ &+ \xi\left(|\epsilon_1|^2-|\epsilon_2|^2\right)^2+\left(|\epsilon_1|^2-|\epsilon_2|^2\right)\sum_{i=1}^{2}\rho_i\phi_i^\dagger\phi_i+\varrho\left(|\epsilon_1|^4-|\epsilon_2|^4\right) \\ &+ \xi'\left(|\epsilon_1|^2+|\epsilon_2|^2\right)^2+\left(|\epsilon_1|^2+|\epsilon_2|^2\right)\sum_{i=1}^{2}\rho_i'\phi_i^\dagger\phi_i+\varrho'\left(|\epsilon_1|^4+|\epsilon_2|^4\right) \\ &+ \lambda\left(|\epsilon_1|^2+|\epsilon_2|^2+|\epsilon_3|^2\right)^2+V_{2HD}(\phi_1,\,\phi_2). \end{aligned} \tag{4.94}$$

We can parametrize the v.e.v's of the singlet scalars as

$$\langle 0\,|\epsilon_1|\,0\rangle=\beta_1\cos\gamma,\quad \langle 0\,|\epsilon_2|\,0\rangle=\beta_1\sin\gamma,\ \text{and}\quad \langle 0\,|\epsilon_3|\,0\rangle=\beta_2. \tag{4.95}$$

We require that all terms in the symmetry breaking potential are of the same size which results in, from Eq. 4.93, $\varrho\sim\frac{v^2}{\beta_1^2}\rho_i$ and $\xi\sim\frac{v^2}{\beta_1^2\cos 2\gamma}\rho_i$ where $v^2=v_1^2+v_2^2$ is the EW scale. The only terms that depend on γ are

$$f(\gamma)=\xi\beta_1^4\cos^2 2\gamma+\beta_1^2\cos 2\gamma\sum_{i=1}^{2}\rho_i|v_i|^2+\varrho\beta_1^4\cos 2\gamma+\varrho'\beta_1^4\left(\frac{1+\cos^2 2\gamma}{2}\right). \tag{4.96}$$

After minimizing the potential, one can get the parameters of the v.e.v's as follows

$$\begin{aligned} \cos 2\gamma &= -\frac{\varrho\beta_1^2+(\rho_1|v_1|^2+\rho_2|v_2|^2)}{(2\xi+\varrho')\beta_1^2}, \\ \beta_1^2 &= \frac{|v_1|^2(\varrho\rho_1-\rho_1'(2\xi+\varrho'))+|v_2|^2(\varrho\rho_2-\rho_2'(2\xi+\varrho'))}{-\varrho^2+2\xi(2\xi'+\varrho')+\varrho'(2\xi'+\varrho')}, \\ \beta_2^2 &= \frac{\beta_2'^2}{-2\lambda(-\varrho^2+2\xi(2\xi'+\varrho')+\varrho'(2\xi'+\varrho'))}, \end{aligned} \tag{4.97}$$

where

$$\begin{aligned} \beta_2'^2 &\equiv -\mu^2(-\varrho^2+2\xi(2\xi'+\varrho')+\varrho'(2\xi'+\varrho')) \\ &+ |v_1|^2(\sigma_1(-\varrho^2+2\xi(2\xi'+\varrho')+\varrho'(2\xi'+\varrho'))+2\lambda(\varrho\rho_1-\rho_1'(2\xi+\varrho'))) \\ &+ |v_2|^2(\sigma_2(-\varrho^2+2\xi(2\xi'+\varrho')+\varrho'(2\xi'+\varrho'))+2\lambda(\varrho\rho_2-\rho_2'(2\xi+\varrho'))). \end{aligned} \tag{4.98}$$

Then, we find that the following relation is satisfied

$$\beta_2^2 + \beta_1^2 = 3w^2. \tag{4.99}$$

In Eq. 4.97, since $\varrho \sim \frac{v^2}{\beta_1^2}\rho_i$ that leads to $\cos 2\gamma \approx 0$ up to corrections of v^2/β_1^2 where v is the EW scale and we assume β_1 in the TeV range in order to produce a sizable symmetry breaking parameter. However, we consider in our analysis the first order correction to $\cos 2\gamma$ ($\cos 2\gamma \approx \tau$) where the symmetry breaking term is defined by

$$\tau \equiv -\frac{\varrho\beta_1^2 + (\rho_1|v_1|^2 + \rho_2|v_2|^2)}{(2\xi + \varrho')\beta_1^2}. \tag{4.100}$$

This leads to shifting the v.e.v's of the two singlet scalars ($\langle 0\,|\epsilon_1|\,0\rangle \neq \langle 0\,|\epsilon_2|\,0\rangle$) up to the first order of τ. Then, the Majorana neutrino mass matrix takes the form

$$M_R = \begin{pmatrix} M + v_{\beta_2} & v_{\beta_{1p}} & v_{\beta_{1n}} \\ v_{\beta_{1p}} & M & 0 \\ v_{\beta_{1n}} & 0 & M \end{pmatrix}, \tag{4.101}$$

where $v_{\beta_i} = y\beta_i$ and

$$\begin{aligned} v_{\beta_{1p}} &= \frac{y}{\sqrt{2}}(\langle 0\,|\epsilon_1|\,0\rangle + \langle 0\,|\epsilon_2|\,0\rangle), \\ v_{\beta_{1n}} &= \frac{y}{\sqrt{2}}(\langle 0\,|\epsilon_1|\,0\rangle - \langle 0\,|\epsilon_2|\,0\rangle). \end{aligned} \tag{4.102}$$

We write the v.e.v's of the singlet scalars after symmetry breaking as

$$\begin{aligned} \langle 0\,|\epsilon_1|\,0\rangle &= \frac{\beta_1}{\sqrt{2}}\left(1 + \frac{\tau}{2}\right), \\ \langle 0\,|\epsilon_2|\,0\rangle &= \frac{\beta_1}{\sqrt{2}}\left(1 - \frac{\tau}{2}\right), \end{aligned} \tag{4.103}$$

then

$$\begin{aligned} v_{\beta p} &= v_{\beta_1}, \\ v_{\beta n} &= \frac{\tau}{2}v_{\beta_1}. \end{aligned} \tag{4.104}$$

Note that, from the discussion below Eq. 4.95 and using Eq. 4.100 one finds

$$\xi \sim \frac{v^2}{\beta_1^2\tau}\rho_i \sim \frac{\varrho}{\tau} \tag{4.105}$$

which leads to $\xi \simeq 10\varrho$ for $\tau = 0.1$.

The results of the model have to satisfy the neutrino oscillation measurements. Although the numerical results show that breaking the $SO(3)$ symmetry in the scalar potential, see Eq. 4.93, is not sufficient to break the *slight* equality of $(m_1,\ m_2)$ to satisfy the Δm^2_{12} measurement. Therefore, we introduce additional terms to the Dirac mass term for the neutrinos which *minimally* break the $SO(3)$ symmetry,

$$\frac{1}{2}\left[M_1 \bar{\nu}_{eR}\nu^c_{eR} + M_2\left(\bar{\nu}_{\mu R}\nu^c_{\mu R} + \bar{\nu}_{\tau R}\nu^c_{\tau R}\right)\right] + h.c. \tag{4.106}$$

By presenting the above terms we have broken the $SO(3)$ symmetry in the whole Yukawa Lagrangian and the scalar potential. Note that the above terms break the $U(1)$ symmetry too. Thus

$$M_R = \begin{pmatrix} M' + v_{\beta_2} & v_{\beta_1} & \frac{\tau}{2}v_{\beta_1} \\ v_{\beta_1} & M'' & 0 \\ \frac{\tau}{2}v_{\beta_1} & 0 & M'' \end{pmatrix}, \tag{4.107}$$

where $M' = M + M_1$ and $M'' = M + M_2$. Using the see-saw formula (4.37), the neutrino mass matrix is given by

$$\mathcal{M}_\nu \ = \ \begin{pmatrix} X' & G' & P' \\ G' & Y' & W' \\ P' & W' & Z' \end{pmatrix}, \tag{4.108}$$

where

$$\begin{aligned}
X' &= -\frac{4A^2M''}{4M'M'' + 4M''v_{\beta_2} - v^2_{\beta_1}(4+\tau^2)}, \\
Y' &= -\frac{A^2(4M'M'' + 4M''v_{\beta_2} - v^2_{\beta_1}\tau^2)}{M''(4M'M'' + 4M''v_{\beta_2} - v^2_{\beta_1}(4+\tau^2))}, \\
Z' &= -\frac{4A^2(M'M'' + M''v_{\beta_2} - v^2_{\beta_1})}{M''(4M'M'' + 4M''v_{\beta_2} - v^2_{\beta_1}(4+\tau^2))}, \\
G' &= \frac{4A^2v_{\beta_1}}{4M'M'' + 4M''v_{\beta_2} - v^2_{\beta_1}(4+\tau^2)}, \\
P' &= \frac{2A^2v_{\beta_1}\tau}{4M'M'' + 4M''v_{\beta_2} - v^2_{\beta_1}(4+\tau^2)}, \\
W' &= -\frac{2A^2v^2_{\beta_1}\tau}{M''(4M'M'' + 4M''v_{\beta_2} - v^2_{\beta_1}(4+\tau^2))}.
\end{aligned} \tag{4.109}$$

From Eqs. (4.108, 4.109), one gets the mass eigenvalues

$$\begin{aligned} m_1 &= -\frac{A^2}{4M'M'' + 4M''v_{\beta_2} - v_{\beta_1}^2(4+\tau^2)}\,[2(M' + M'' + v_{\beta_2}) \\ &\quad -2\sqrt{M'^2 + M''^2 - 2M'(M'' - v_{\beta_2}) - 2M''v_{\beta_2} + v_{\beta_2}^2 + v_{\beta_1}^2(4+\tau^2)}\Big]\,, \\ m_2 &= -\frac{A^2}{4M'M'' + 4M''v_{\beta_2} - v_{\beta_1}^2(4+\tau^2)}\,[2(M' + M'' + v_{\beta_2}) \\ &\quad +2\sqrt{M'^2 + M''^2 - 2M'(M'' - v_{\beta_2}) - 2M''v_{\beta_2} + v_{\beta_2}^2 + v_{\beta_1}^2(4+\tau^2)}\Big]\,, \\ m_3 &= -\frac{A^2}{M''}. \end{aligned} \tag{4.110}$$

We can diagonalize the mass matrix in Eq. 4.108 using the unitary matrix $U_\nu = W_{12}^\nu R_{23}^\nu R_{12}^\nu$ with Eq. 4.74. On can find relations between the mass matrix elements in Eq. 4.109 given by Eq. 4.75. Applying the relations 4.75 to the corresponding mass matrix elements of $\mathcal{M}_\nu = U_\nu \mathcal{M}_\nu^d U_\nu^\dagger$ with $U_\nu = W_{12}^\nu R_{23}^\nu R_{12}^\nu$, one can get the two mixing angles

$$\begin{aligned} s_{23\nu} &= \sqrt{\frac{3m_1(m_2 - m_3)}{m_2(m_1 - m_3)}}, \\ s_{12\nu} &= \sqrt{\frac{-2m_1m_2 + 3m_1m_3 - m_2m_3}{3m_3(m_1 - m_2)}}. \end{aligned} \tag{4.111}$$

Following Ref. [215], we expand the angles in Eq. 1.20 as

$$s_{13} = \frac{r}{\sqrt{2}}, \quad s_{12} = \frac{1}{\sqrt{3}}(1+s), \quad s_{23} = \frac{1}{\sqrt{2}}(1+a), \tag{4.112}$$

where the three real parameters r, s, a describe the deviations of the reactor, solar, and atmospheric angles from their tri-bimaximal values. We use global fits of the mixing parameters with 3σ significance [47]

$$0.18 < r < 0.26,\ -0.10 < s < 0.05,\ -0.15 < a < 0.17. \tag{4.113}$$

To first order in r, s, a the lepton mixing matrix can be written as [215],

$$U \approx \begin{pmatrix} \sqrt{\frac{2}{3}}(1 - \frac{1}{2}s) & \frac{1}{\sqrt{3}}(1+s) & \frac{1}{\sqrt{2}}re^{-i\delta} \\ -\frac{1}{\sqrt{6}}(1 + s - a + re^{i\delta}) & \frac{1}{\sqrt{3}}(1 - \frac{1}{2}s - a - \frac{1}{2}re^{i\delta}) & \frac{1}{\sqrt{2}}(1+a) \\ \frac{1}{\sqrt{6}}(1 + s + a - re^{i\delta}) & -\frac{1}{\sqrt{3}}(1 - \frac{1}{2}s + a + \frac{1}{2}re^{i\delta}) & \frac{1}{\sqrt{2}}(1-a) \end{pmatrix}. \tag{4.114}$$

We are not going to consider CP violation in this work, thus, we assume that $\delta = 0$. We can write the parameters $(r,\ s,\ a)$ in terms of the elements of the mixing matrix,

$$\begin{aligned} r &= -1 - s + a - \sqrt{6}U_{21}, \\ s &= -1 + \sqrt{3}U_{12}, \\ a &= -1 + \sqrt{2}U_{23}. \end{aligned} \tag{4.115}$$

Now, we can calculate the full deviation of the leptonic mixing coming from the charged lepton and neutrino sector. We obtain the elements of the lepton mixing matrix

$$U_{PMNS} = U_l^\dagger U_\nu, \tag{4.116}$$

with $U_\ell = W_{23}^l R_{23}^l R_{13}^l R_{12}^l$ and $U_\nu = W_{12}^\nu R_{23}^\nu R_{12}^\nu$. Thus, up to the first order one can get

$$\begin{aligned} r &\approx -s_{12l} + \sqrt{\frac{2}{3}} s_{23\nu} + s_{13l}, \\ s &\approx -s_{12l} + \sqrt{2} s_{12\nu} - s_{13l}, \\ a &\approx -s_{23l} + \sqrt{\frac{2}{3}} s_{23\nu}. \end{aligned} \tag{4.117}$$

In section 4.3.2, it was found that the contribution of the charged lepton sector, with $\delta = 0$, is give as

- For $z = 1.8$: $s_{12l} \approx \pm 0.44,\ s_{13l} \approx \mp 0.0012,\ s_{23l} \approx -0.053$,
- For $z = 1.7$: $s_{12l} \approx \pm 0.48,\ s_{13l} \approx \mp 0.0013,\ s_{23l} \approx -0.050$,

where z is an arbitrary parameter with a value around 2. We can check the contributions of the charged leptons, $U_\ell = W_{23}^l R_{23}^l R_{13}^l R_{12}^l$, without corrections from the neutrino sector, i.e. $U_\nu = W_{12}^\nu$. By substituting the above values in Eq. 4.117 up to the first order one gets

- For $z = 1.8$: $r \approx 0.44,\ s \approx 0.44,\ a \approx 0.053$,
- For $z = 1.7$: $r \approx 0.48,\ s \approx 0.48,\ a \approx 0.050$,

The results above do not match the experimental values where the charged lepton sector introduces a large correction to the mixing angles θ_{13} and θ_{12}. Thus, it becomes necessary to combine the contributions come from the charged lepton and neutrino sector in order to calculate the full deviation from the TBM mixing.

4.4.3 Numerical results

In the case of degenerate neutrino masses $m_1 \approx m_2 \approx m_3$, one can find from Eq. 4.18 that $a \approx b \approx c$. This leads to a diagonalized neutrino mass matrix $\mathcal{M}_\nu \approx \text{diag}\,(a, a, a)$. That means the lepton mixing matrix does not include a contribution from the neutrino sector, which is inconsistent with the experimental data. Thus, in the symmetric limit our model excludes the case of the degenerate neutrino masses.

The numerics goes following the method used in the BM case. The results support the normal mass hierarchy. The figures show that the scale of the neutrino masses is in the few meV to $\sim$ 50 meV range (meV= 10^{-3}eV). Also, the full contribution from both the charged lepton and neutrino sector accommodates the measurements of the mixing angles. The graphs (4.4, 4.5) show that the see-saw scales (M', M'') are in the TeV range, and the extra Higgs that generates the Dirac neutrino masses has v.e.v (v_2), included in A, in the MeV scale [3]. Also, they indicate that the v.e.v's of the singlet scalar fields ($v_{\beta 1}$, $v_{\beta 2}$) are in the TeV scale [4]. We plot M_β versus Σm_i and M_{ee} versus m_{light}, where m_{light} is the lightest neutrino mass which is m_1 in this model. The graphs show that $\Sigma m_i \approx 60$ meV and $M_{ee} < M_\beta$ and $M_{ee} < 0.40$ eV [216].

4.5 Conclusion

In this work we presented a model for leptonic mixing which accommodates the sizable neutrino mixing angle θ_{13} recently measured. We worked in a basis where the charged lepton mass matrix is not diagonal and proposed an explicit structure for the charged lepton mass matrix which is 2-3 symmetric except for a single breaking of this symmetry by the muon mass. We identified a flavor symmetric limit for the mass matrices where the first generation is decoupled from the other two in the charged lepton sector while in the neutrino sector the third generation is decoupled from the first two generations. The leptonic mixing in the symmetric limit was shown to have, among other structures, the bi-maximal (BM) and the tri-bimaximal (TBM) mixing.

In the BM case, a model that extended the SM by three right handed neutrinos, an extra Higgs doublet, and two singlet scalars was introduced to generate the leptonic mixing. In the symmetric limit the model had two Z_2 symmetries in addition to the $\mu-\tau$ symmetry and the BM leptonic mixing was obtained when the two singlet scalars got equal v.e.v's. Symmetry breaking effects were included in the charged lepton sector via higher dimensional operators that generated a $\mu - \tau$ symmetric mass matrix except for a single breaking due to the finite

[3] Higgs doublet with a small v.e.v has been discussed in the literatures [219].

[4] Several papers have introduced neutrino mixing models in the TeV scale (for review see Refs. [220]).

muon mass. In the neutrino sector, symmetry breaking was included via slightly different v.e.v's for the two singlet scalars. To explain the Δm^2 data, two different Majorana mass terms, one for ν_e and one for ν_μ and ν_τ, was used keeping in mind that the $\mu - \tau$ symmetry fixes the Majorana mass terms for the ν_μ and ν_τ to be the same.

In the TBM case, we fixed the neutrino mass matrix to have a decoupling of the first two generations from the third one, and under a certain condition we generated the lepton mixing in the symmetric limit with the TBM structure. This model was described by the Lagrangian that extended the SM by three right-handed neutrinos, an extra Higgs doublet, and three complex singlet scalar fields. Also, the symmetry group of the SM was extended by the product of the symmetries $Z_4 \times U(1)$. The symmetry breaking in the charged lepton sector did not fix the data by introducing a large contribution to the mixing angles θ_{13} and θ_{12}. Thereafter, by breaking the $SO(3)$ symmetry in the effective potential and violating the alignment of the v.e.v's of the singlet scalars, the contribution of the neutrino sector was introduced to accommodate the measurements.

A fit to the experimental measurements showed in both the cases that our model predicted normal hierarchy for the neutrino masses with the masses being in the few meV to ~ 50 meV range. The Majorana mass terms as well as the v.e.v's of the singlet scalar fields were predicted to be in the TeV scale and consequently the v.e.v of the second Higgs doublet was shown to be in the MeV range. We calculated predictions for the mass-dependent observables (Σm_i), (M_β) and (M_{ee}). We found that $\Sigma m_i \approx 0.06$ eV, $M_{ee} < M_\beta$, and $M_{ee} < 0.40$ eV.

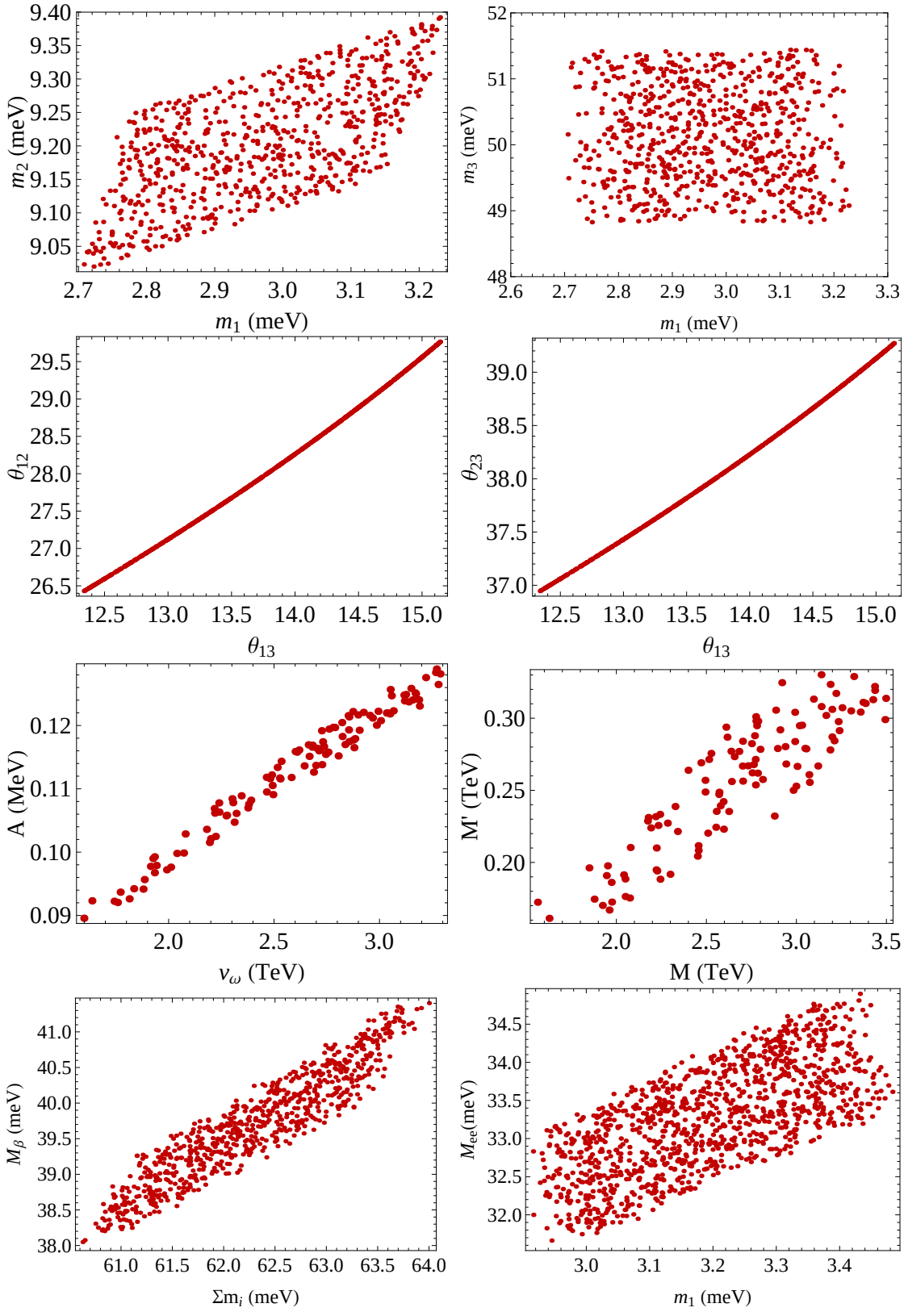

Figure 4.1. BM: Scatter plots for $z = 2.0$ with $s_{12l} \approx -0.34$, $s_{13l} \approx -0.0011$, and $s_{23l} \approx -0.059$. In the neutrino sector, we assume that $\tau = 0.1$. (meV $\equiv 10^{-3}$ eV)

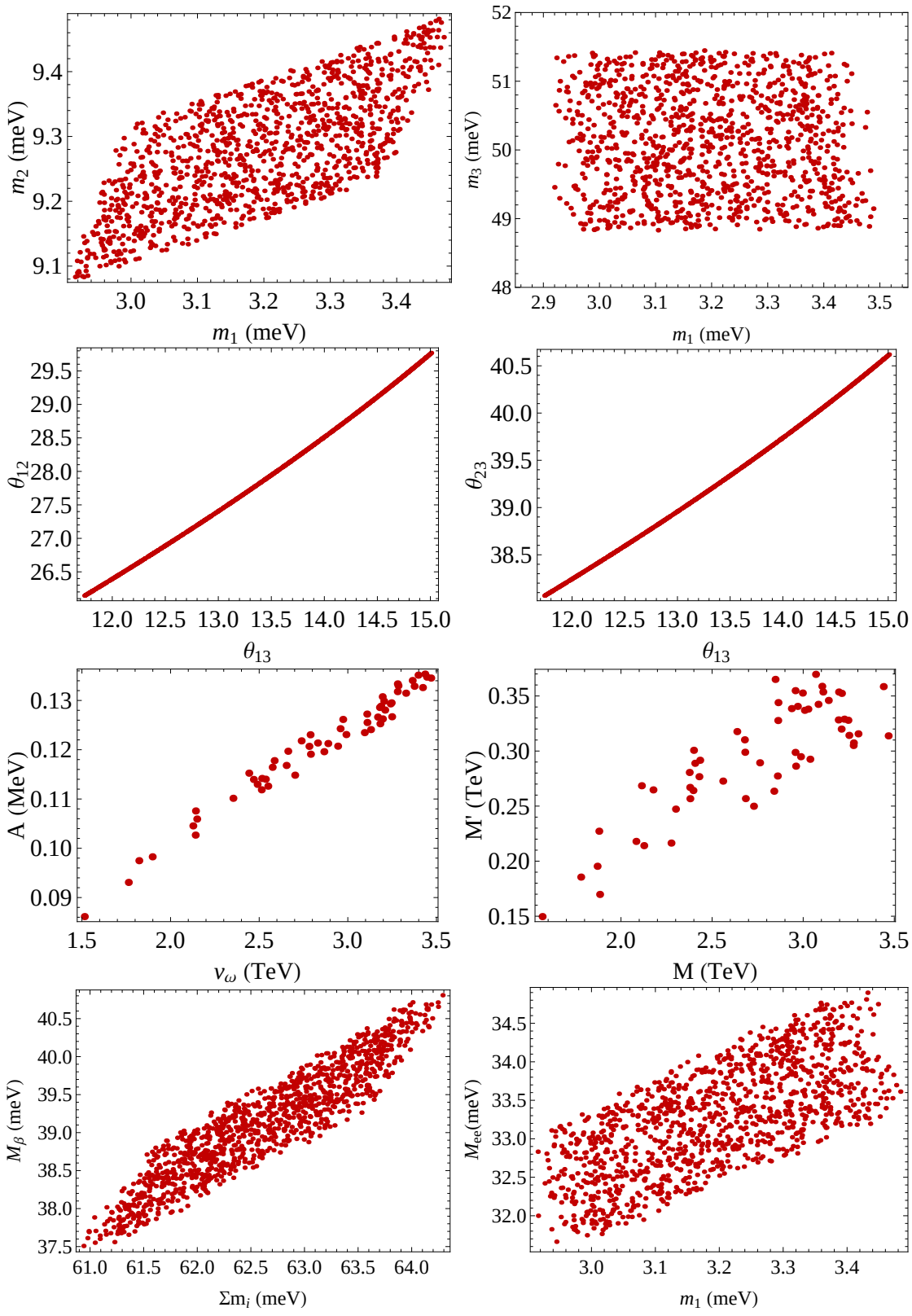

Figure 4.2. BM: Scatter plots for $z = 2.06$ with $s_{12l} \approx -0.3$, $s_{13l} \approx -0.001$, and $s_{23l} \approx -0.061$. In the neutrino sector, we assume that $\tau = 0.05$. (meV $\equiv 10^{-3}$ eV)

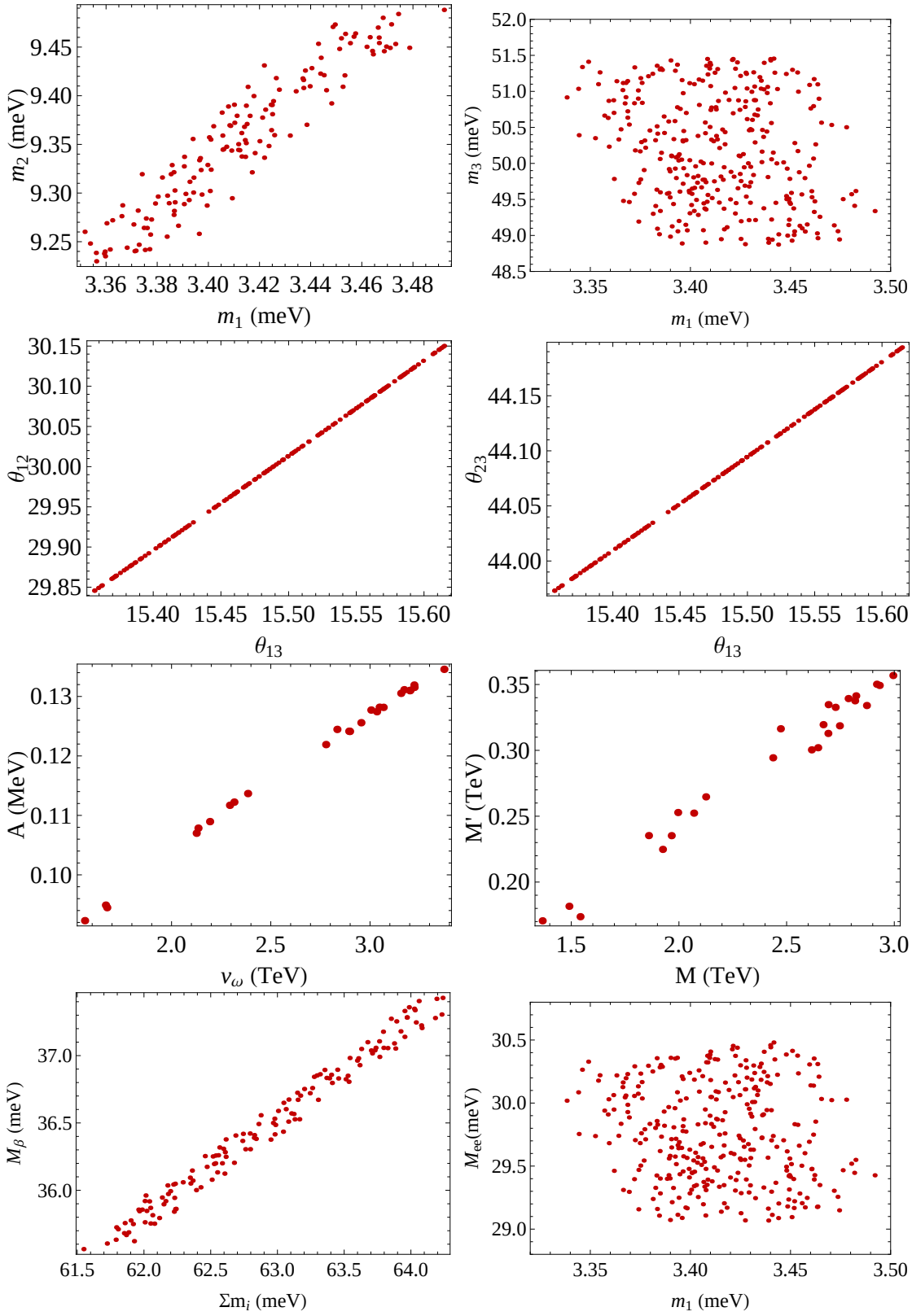

Figure 4.3. BM: Scatter plots for $z = 2.2$ with $s_{12l} \approx -0.2$, $s_{13l} \approx -0.00075$, and $s_{23l} \approx -0.065$. In the neutrino sector, we assume that $\tau = 0.1$. (meV $\equiv 10^{-3}$ eV)

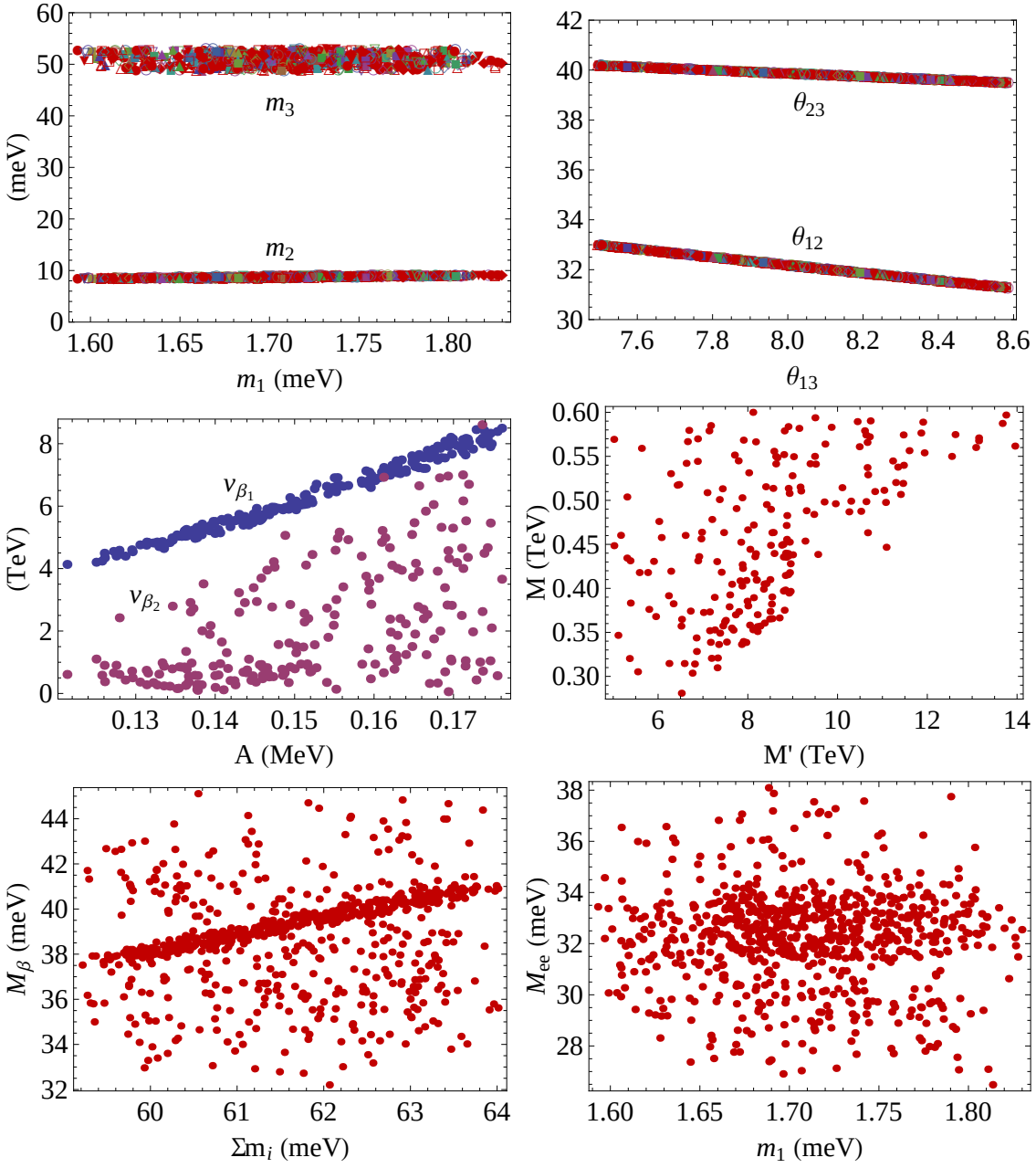

Figure 4.4. TBM: Scatter plot for $z = 1.8$ with $s_{12l} \approx -0.44$, $s_{13l} \approx 0.0012$, and $s_{23l} \approx -0.053$. In the neutrino sector, we take $\tau = 0.1$. (meV $= 10^{-3}$ eV)

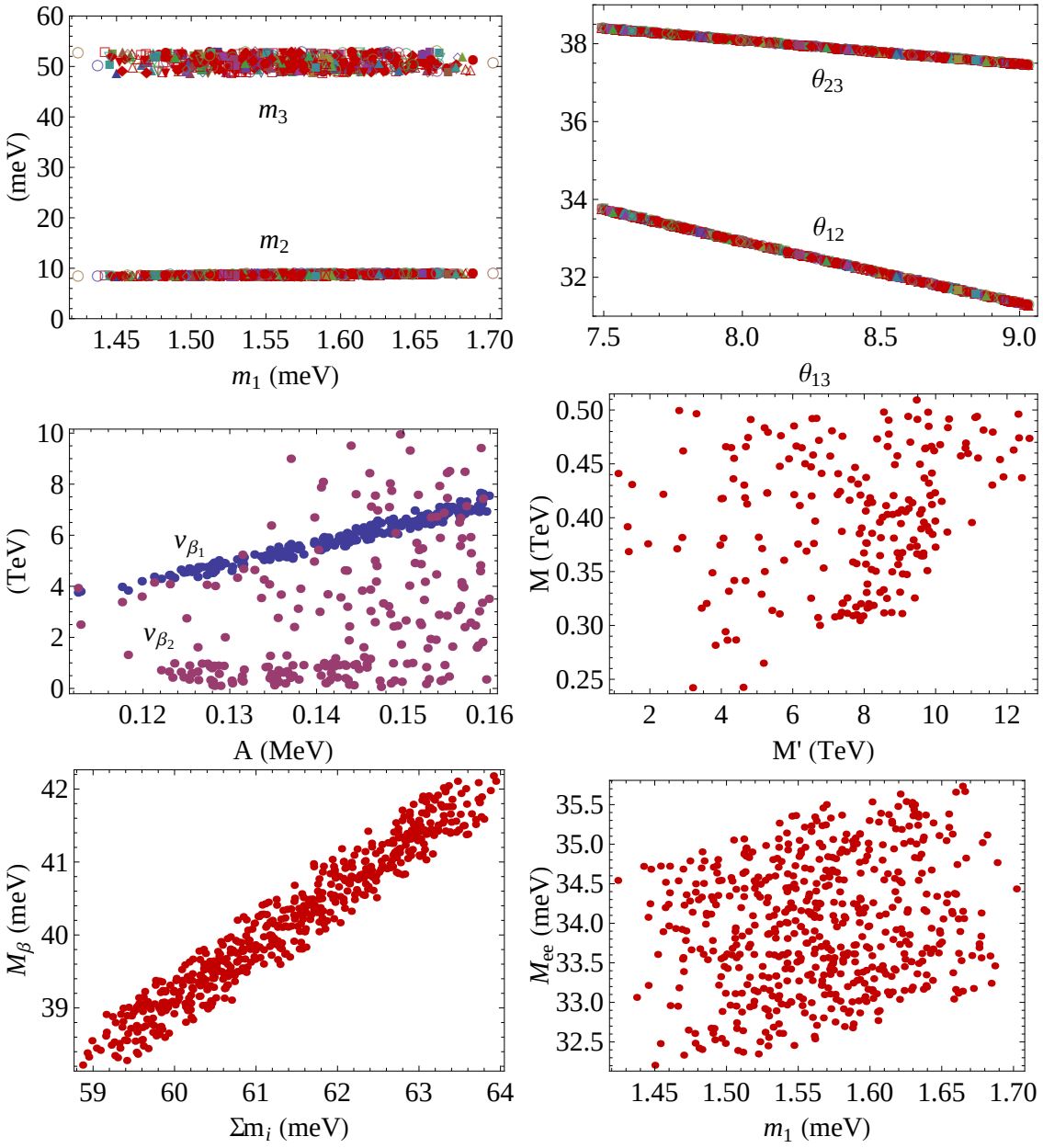

Figure 4.5. TBM: Scatter plot for $z = 1.7$ with $s_{12l} \approx -0.48$, $s_{13l} \approx 0.0013$, and $s_{23l} \approx -0.05$. In the neutrino sector, we take $\tau = 0.05$. (meV $= 10^{-3}$ eV)

CHAPTER 5

SCOTOGENIC A_4 NEUTRINO MODEL FOR NONZERO θ_{13} AND LARGE δ_{CP}

In 2006, a one-loop mechanism was introduced [221] linking neutrino mass with dark matter. The idea is very simple. The standard model of particle interactions is extended to include a second scalar doublet (η^+, η^-) which is odd under an exactly conserved Z_2 symmetry [222], as well as three neutral fermion singlets N_i which are also odd under Z_2. This requirement immediately allows the possibility of having the real (or imaginary) part of η^0 as a dark-matter candidate, which was first pointed out also in Ref. [221]. As shown in Fig. 1, this results in the radiative generation of seesaw Majorana neutrino masses from dark matter, i.e. scotogenic from the Greek 'scotos' meaning darkness.

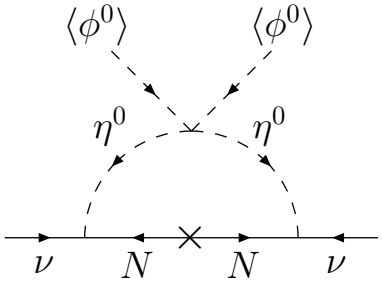

Figure 5.1. One-loop generation of scotogenic Majorana neutrino mass.

The non-Abelian discrete symmetry A_4 was introduced [223, 224, 225] to achieve the seemingly impossible, i.e. the existence of a lepton family symmetry consistent with the three very different charged-lepton masses m_e, m_μ, m_τ. It was subsequently shown [226] to be a natural theoretical framework for neutrino tribimaximal mixing, i.e. $\sin^2\theta_{23} = 1$,

$\tan^2\theta_{12} = 0.5$, and $\theta_{13} = 0$. This pattern was consistent with experimental data until recently, when the Daya Bay Collaboration reported [227] the first precise measurement of θ_{13}, i.e.

$$\sin^2 2\theta_{13} = 0.092 \pm 0.016(\text{stat}) \pm 0.005(\text{syst}), \tag{5.1}$$

followed shortly [228] by the RENO Collaboration, i.e.

$$\sin^2 2\theta_{13} = 0.113 \pm 0.013(\text{stat}) \pm 0.019(\text{syst}). \tag{5.2}$$

This means that tribimaximal mixing is not a good description, and more importantly, leptonic CP violation is now possible because $\theta_{13} \neq 0$, just as hadronic CP violation in the quark sector is possible because $V_{ub} \neq 0$.

Recently, it was shown [229] that A_4 is still a good symmetry for understanding this pattern, using a new simple variation of the original idea [226]. In that proposal, neutrinos acquire Majorana masses through their direct interactions with Higgs triplets. We study here instead the corresponding scenario with the radiative mechanism of Fig. 1.

The symmetry A_4 is that of the even permutation of four objects. It has twelve elements and is the smallest group which admits an irreducible three-dimensional representation. Its character table is given below. The basic multiplication rule of A_4 is

$$\underline{3} \times \underline{3} = \underline{1} + \underline{1}' + \underline{1}'' + \underline{3} + \underline{3}. \tag{5.3}$$

As first shown in Ref. [223], for $(\nu_i, l_i) \sim \underline{3}$, $l_i^c \sim \underline{1}, \underline{1}', \underline{1}''$, and $\Phi_i = (\phi_i^0, \phi_i^-) \sim \underline{3}$, the

class	n	h	χ_1	$\chi_{1'}$	$\chi_{1''}$	χ_3
C_1	1	1	1	1	1	3
C_2	4	3	1	ω	ω^2	0
C_3	4	3	1	ω^2	ω	0
C_4	3	2	1	0	0	–1

Table 5.1. Character table of A_4.

charged-lepton mass matrix is given by

$$\mathcal{M}_l = \begin{pmatrix} v_1 & 0 & 0 \\ 0 & v_2 & 0 \\ 0 & 0 & v_3 \end{pmatrix} \begin{pmatrix} 1 & 1 & 1 \\ 1 & \omega^2 & \omega \\ 1 & \omega & \omega^2 \end{pmatrix} \begin{pmatrix} f_1 & 0 & 0 \\ 0 & f_2 & 0 \\ 0 & 0 & f_3 \end{pmatrix}, \tag{5.4}$$

where $v_i = \langle \phi_i^0 \rangle$ and $\omega = e^{2\pi i/3} = -1/2 + i\sqrt{3}/2$. For $v_1 = v_2 = v_3 = v/\sqrt{3}$, we then obtain

$$\mathcal{M}_l = \frac{1}{\sqrt{3}} \begin{pmatrix} 1 & 1 & 1 \\ 1 & \omega^2 & \omega \\ 1 & \omega & \omega^2 \end{pmatrix} \begin{pmatrix} m_e & 0 & 0 \\ 0 & m_\mu & 0 \\ 0 & 0 & m_\tau \end{pmatrix}, \tag{5.5}$$

where $m_e = f_1 v$, $m_\mu = f_2 v$, $m_\tau = f_3 v$. The original A_4 symmetry is now broken to the residual symmetry Z_3, i.e. lepton flavor triality [230], with $e \sim 1$, $\mu \sim \omega^2$, $\tau \sim \omega$. This is a good symmetry of the Lagrangian as long as neutrino masses are zero. Exotic scalar decays are predicted and may be observable at the Large Hadron Collider (LHC) in some regions of parameter space [231, 232].

To obtain nonzero neutrino masses, we assign $\eta \sim \underline{1}$ and $N_i \sim \underline{3}$ under A_4. We also add the scalar singlets $\sigma_i \sim \underline{3}$ with nonzero $\langle \sigma_i \rangle$. The resulting 3×3 Majorana mass matrix for N_i is then

$$\mathcal{M}_N = \begin{pmatrix} A & F & E \\ F & A & D \\ E & D & A \end{pmatrix}, \tag{5.6}$$

which is the analog of

$$\mathcal{M}_\nu = \begin{pmatrix} a & f & e \\ f & a & d \\ e & d & a \end{pmatrix}, \tag{5.7}$$

considered in Ref. [229]. (A better way to enforce Eq. (6) is to postulate gauged $B - L$ and assume complex neutral scalars which transform as $\underline{1}$, $\underline{3}$ under A_4, in complete analogy to the scalar triplets of Ref. [229].) Instead of enforcing $E = F = 0$ which is required for tribimaximal mixing, we assume here that $F = -E$ which may be maintained by an interchange symmetry [226, 233].

Consider now the tribimaximal basis, i.e.

$$\begin{pmatrix} \nu_e \\ \nu_\mu \\ \nu_\tau \end{pmatrix} = \begin{pmatrix} \sqrt{2/3} & 1/\sqrt{3} & 0 \\ -1/\sqrt{6} & 1/\sqrt{3} & -1/\sqrt{2} \\ -1/\sqrt{6} & 1/\sqrt{3} & 1/\sqrt{2} \end{pmatrix} \begin{pmatrix} \nu_1 \\ \nu_2 \\ \nu_3 \end{pmatrix}. \tag{5.8}$$

Since $\nu_{1,2,3}$ are connected to $N_{1,2,3}$ through the identity matrix, we find

$$\mathcal{M}_N^{(1,2,3)} = \begin{pmatrix} A + D & 0 & 0 \\ 0 & A & C \\ 0 & C & A - D \end{pmatrix}, \tag{5.9}$$

where $C = (E-F)/\sqrt{2} = \sqrt{2}E$.

The diagram of Fig. 1 is exactly calculable from the exchange of $\mathrm{Re}(\eta^0)$ and $\mathrm{Im}(\eta^0)$ and is given by [221]

$$(\mathcal{M}_\nu)_{ij} = \sum_k \frac{h_{ik}h_{jk}M_k}{16\pi^2}\left[\frac{m_R^2}{m_R^2-M_k^2}\ln\frac{m_R^2}{M_k^2} - \frac{m_I^2}{m_I^2-M_k^2}\ln\frac{m_I^2}{M_k^2}\right], \tag{5.10}$$

where $\sum_k h_{ik}(h_{jk})^* = |h|^2\delta_{ij}$, and $m_{R,I}$ are the masses of $\sqrt{2}\mathrm{Re}(\eta^0)$ and $\sqrt{2}\mathrm{Im}(\eta^0)$, respectively. In the limit $m_R^2 - m_I^2 = 2\lambda_5 v^2$ is small compared to $m_0^2 = (m_R^2+m_I^2)/2$, and $m_0^2 << M_k^2$, Eq. (10) reduces to

$$(\mathcal{M}_\nu)_{ij} = \frac{\lambda_5 v^2}{8\pi^2}\sum_k \frac{h_{ik}h_{jk}}{M_k}\left[\ln\frac{M_k^2}{m_0^2} - 1\right]. \tag{5.11}$$

In the tribimaximal basis of Eq. (9), we then have

$$h_{ik} = h\begin{pmatrix}1 & 0 & 0\\ 0 & \cos\theta & -\sin\theta e^{i\phi}\\ 0 & \sin\theta e^{-i\phi} & \cos\theta\end{pmatrix}\begin{pmatrix}e^{i\alpha_1'/2} & 0 & 0\\ 0 & e^{i\alpha_2'/2} & 0\\ 0 & 0 & e^{i\alpha_3'/2}\end{pmatrix}, \tag{5.12}$$

with

$$\begin{pmatrix}\cos\theta & \sin\theta e^{i\phi}\\ -\sin\theta e^{-i\phi} & \cos\theta\end{pmatrix}\begin{pmatrix}A & C\\ C & A-D\end{pmatrix}\begin{pmatrix}\cos\theta & -\sin\theta e^{-i\phi}\\ \sin\theta e^{i\phi} & \cos\theta\end{pmatrix} = \begin{pmatrix}e^{i\alpha_2'}M_2 & 0\\ 0 & e^{i\alpha_3'}M_3\end{pmatrix}. \tag{5.13}$$

The neutrino mixing matrix U has 4 parameters: s_{12}, s_{23}, s_{13} and δ_{CP} [234]. We choose the convention $U_{\tau 1}, U_{\tau 2}, U_{e3}, U_{\mu 3} \to -U_{\tau 1}, -U_{\tau 2}, -U_{e3}, -U_{\mu 3}$ to conform with that of the tribimaximal mixing matrix of Eq. (8), then

$$\mathcal{M}_\nu^{(1,2,3)} = U_{TB}^T U\begin{pmatrix}e^{i\alpha_1}m_1' & 0 & 0\\ 0 & e^{i\alpha_2}m_2' & 0\\ 0 & 0 & m_3'\end{pmatrix}U^T U_{TB}, \tag{5.14}$$

where $m'_{1,2,3}$ are the physical neutrino masses, with

$$m'_2 = \sqrt{{m'_1}^2 + \Delta m^2_{21}}, \tag{5.15}$$

$$m'_3 = \sqrt{{m'_1}^2 + \Delta m^2_{21}/2 + \Delta m^2_{32}} \text{ (normal hierarchy)}, \tag{5.16}$$

$$m'_3 = \sqrt{{m'_1}^2 + \Delta m^2_{21}/2 - \Delta m^2_{32}} \text{ (inverted hierarchy)}. \tag{5.17}$$

We now diagonalize $\mathcal{M}_\nu^{(1,2,3)}$ using

$$U_\epsilon \mathcal{M}_\nu^{(1,2,3)} U_\epsilon^T = \begin{pmatrix} e^{i\alpha'_1} m'_1 & 0 & 0 \\ 0 & e^{i\alpha'_2} m'_2 & 0 \\ 0 & 0 & e^{i\alpha'_3} m'_3 \end{pmatrix}, \tag{5.18}$$

from which we obtain $U' = U_{TB} U_\epsilon^T$. To obtain U with the usual convention, we rotate the phases of the μ and τ rows so that $U'_{\mu 3} e^{-i\alpha'_3/2}$ is real and negative, and $U'_{\tau 3} e^{-i\alpha'_3/2}$ is real and positive. These phases are absorbed by the μ and τ leptons and are unobservable. We then rotate the $\nu_{1,2}$ columns so that $U'_{e1} e^{-i\alpha'_3/2} = U_{e1} e^{i\alpha''_1/2}$ and $U'_{e2} e^{-i\alpha'_3/2} = U_{e2} e^{i\alpha''_2/2}$, where U_{e1} and U_{e2} are real and positive. The physical relative Majorana phases of $\nu_{1,2}$ are then $\alpha_{1,2} = \alpha'_{1,2} + \alpha''_{1,2}$. The three angles and the Dirac phase are extracted according to

$$\tan^2\theta_{12} = |U'_{e2}/U'_{e1}|^2, \quad \tan^2\theta_{23} = |U'_{\mu 3}/U'_{\tau 3}|^2, \quad \sin\theta_{13} e^{-i\delta_{CP}} = U'_{e3} e^{-i\alpha'_3/2}. \tag{5.19}$$

The effective Majorana neutrino mass in neutrinoless double beta decay is then given by

$$m_{ee} = |U^2_{e1} e^{i\alpha_1} m'_1 + U^2_{e2} e^{i\alpha_2} m'_2 + U^2_{e3} m'_3|. \tag{5.20}$$

In Eq. (9), let A be real and positive by convention, then both C and D may be complex, i.e. $C = C_R + iC_I$ and $D = D_R + iD_I$. The 2×2 matrix of Eq. (13) can be solved exactly to yield

$$\tan\phi = \frac{C_R D_I - C_I D_R}{C_R(2A - D_R) - C_I D_I}, \tag{5.21}$$

$$\tan 2\theta = \frac{2[4A^2 C_R^2 - 4AC_R(C_R D_R + C_I D_I) + (C_R^2 + C_I^2)(D_R^2 + D_I^2)]^{1/2}}{2AD_R - (D_R^2 + D_I^2)}, \tag{5.22}$$

with

$$e^{i\alpha'_2} M_2 = \cos^2\theta A + 2\sin\theta\cos\theta e^{i\phi} C + \sin^2\theta e^{2i\phi}(A-D), \quad (5.23)$$

$$e^{i\alpha'_3} M_3 = \cos^2\theta(A-D) - 2\sin\theta\cos\theta e^{-i\phi} C + \sin^2\theta e^{-2i\phi} A. \quad (5.24)$$

The corresponding U' elements are

$$U'_{e1} = \sqrt{\frac{2}{3}}, \quad U'_{e2} = \frac{\cos\theta}{\sqrt{3}}, \quad U'_{e3} = -\frac{\sin\theta}{\sqrt{3}} e^{-i\phi}, \quad (5.25)$$

$$U'_{\mu 3} = -\frac{\cos\theta}{\sqrt{2}} - \frac{\sin\theta}{\sqrt{3}} e^{-i\phi}, \quad U'_{\tau 3} = \frac{\cos\theta}{\sqrt{2}} - \frac{\sin\theta}{\sqrt{3}} e^{-i\phi}. \quad (5.26)$$

If we absorb the scale factor $\lambda_5 h^2 v^2/8\pi^2$ into the parameters A, C, D as well as m_0, then the mass eigenvalues of Eq. (11) are given by

$$m'_k = \frac{1}{M_k}\left[\ln\frac{M_k^2}{m_0^2} - 1\right], \quad (5.27)$$

which are the ones used in Eqs. (14) and (18). Since m_0 is an unknown, having to do with the dark-matter scalar mass, we fix it by requiring $M_1/m_0 = 10$, where $M_1 = |A+D|$. If we input the five parameters A, C_R, C_I, D_R, D_I, we will obtain $m'_{1,2,3}$ as well as the three mixing angles and the three CP phases. For our numerical analysis, we set

$$\Delta m^2_{21} = 7.59 \times 10^{-5}\ \text{eV}^2, \quad \Delta m^2_{32} = 2.45 \times 10^{-3}\ \text{eV}^2, \quad (5.28)$$

and vary θ_{13} in the range

$$\sin^2 2\theta_{13} = 0.05 \text{ to } 0.15. \quad (5.29)$$

Following Ref. [229], we look for solutions with $\sin^2 2\theta_{23} = 0.92$ and 0.96. Whereas only normal hierarchy is allowed in the model of Ref. [229], we find solutions for both normal and inverted hierarchies, as well as quasi-degenerate solutions, as detailed below.

The predictions of this model regarding mixing angles are basically the same as in

Ref. [229] for the special case of $b = 0$ there. Using Eqs. (19), (25), and (26), we find

$$\tan^2\theta_{12} = \frac{1-3\sin^2\theta_{13}}{2}, \tag{5.30}$$

$$\tan^2\theta_{23} = \frac{\left(1-\frac{\sqrt{2}\sin\theta_{13}\cos\phi}{\sqrt{1-3\sin^2\theta_{13}}}\right)^2+\frac{2\sin^2\theta_{13}\sin^2\phi}{1-3\sin^2\theta_{13}}}{\left(1+\frac{\sqrt{2}\sin\theta_{13}\cos\phi}{\sqrt{1-3\sin^2\theta_{13}}}\right)^2+\frac{2\sin^2\theta_{13}\sin^2\phi}{1-3\sin^2\theta_{13}}}. \tag{5.31}$$

The conventionally defined Dirac CP phase is given by $\delta_{CP} = \phi + \alpha_3'/2$, where α_3' is defined in Eq. (18) and depends on the specific values of Eq. (9). For $\sin\theta_{13} = 0.16$, corresponding to $\sin^2 2\theta_{13} = 0.1$, this predicts $\tan^2\theta_{12} = 0.46$. If $Im(C) = 0$, then $\delta_{CP} = \alpha_3' = 0$, so this would predict $\sin^2 2\theta_{23} = 0.80$ which is of course ruled out. Using $\sin^2 2\theta_{23} > 0.92$, we find in this case $|\tan\phi| > 1.2$.

For each of the two values $\sin^2 2\theta_{23} = 0.92$ and 0.96, we obtain 5 representative solutions, all as functions of $\sin^2 2\theta_{13}$. Using Eq. (30), we plot $\sin^2 2\theta_{12}$ versus $\sin^2 2\theta_{13}$ in Fig. 5.2. The

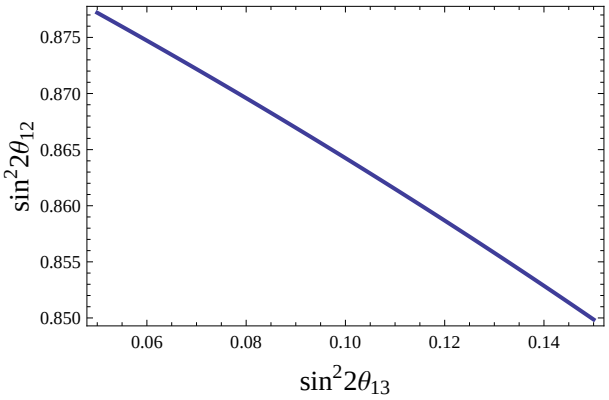

Figure 5.2. $\sin^2 2\theta_{12}$ **versus** $\sin^2 2\theta_{13}$**.**

characteristic features of the 5 solutions are listed in Table 2. For $Im(D) = 0$, we find one

solution	$Im(D)$	class	$\lvert\tan\delta_{CP}\rvert$	m_{ee}
I	0	IH	2.05	0.020
II	$Re(D)$	IH	4.64	0.022
III	0	NH	3.59	0.002
IV	0	QD	2.20	0.046
V	$Re(D)$	QD	1.84	0.051

Table 5.2. Five representative solutions. Three have $Im(D) = 0$**, and two have** $Im(D) = Re(D)$**. NH denotes normal hierarchy of neutrino masses, IH inverted, and QD quasi-degenerate. The values of** $|\tan\delta_{CP}|$ **and** m_{ee} **(in eV) are for** $\sin^2 2\theta_{23} = 0.96$ **and** $\sin^2 2\theta_{13} = 0.10$**.**

solution for inverted ordering of neutrino masses, and two solutions for normal ordering (one of which is quasi-degenerate). For $Im(D) = Re(D)$, we again find one solution for inverted ordering, but the only solution for normal ordering is quasi-degenerate.

In Fig. 3 we show the physical neutrino masses $m'_{1,2,3}$ and the effective mass in neutrinoless double beta decay m_{ee} (in eV) as well as the model parameters (in eV^{-1}) for solution (I) in the case $\sin^2 2\theta_{23} = 0.96$. In Figs. 4-7 we show the same quantities for solutions (II),(III),(IV),(V) in the cases of $\sin^2 2\theta_{23} = 0.92, 0.96, 0.92, 0.96$ respectively. Finally we show in Fig. 8 the values of $|\tan\delta_{CP}|$ for all 5 solutions in the case of $\sin^2 2\theta_{23} = 0.92$. It is clear that at $\sin^2 2\theta_{13} = 0.10$, large $|\tan\delta_{CP}|$ is predicted.

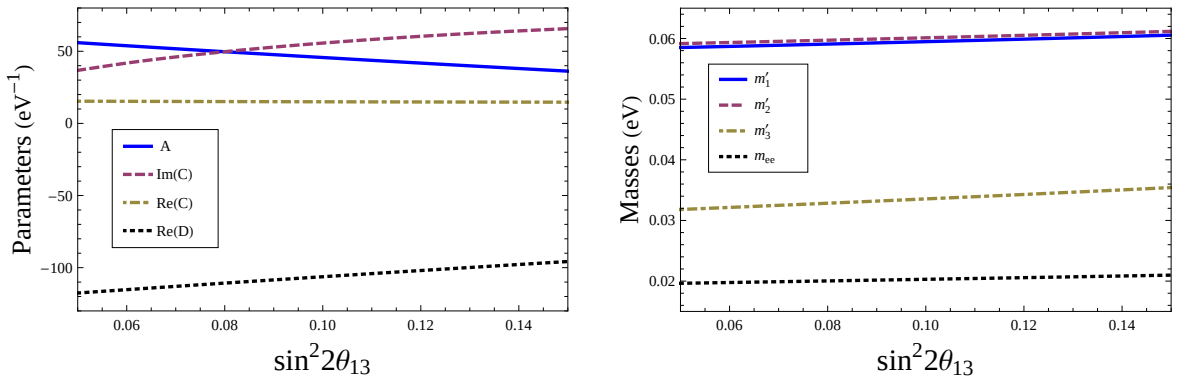

Figure 5.3. A_4 **parameters and the physical neutrino masses and effective neutrino mass** m_{ee} **in neutrinoless double beta decay for the inverted hierarchy with Im(D)=0 and** $\sin^2 2\theta_{23} = 0.96$**.**

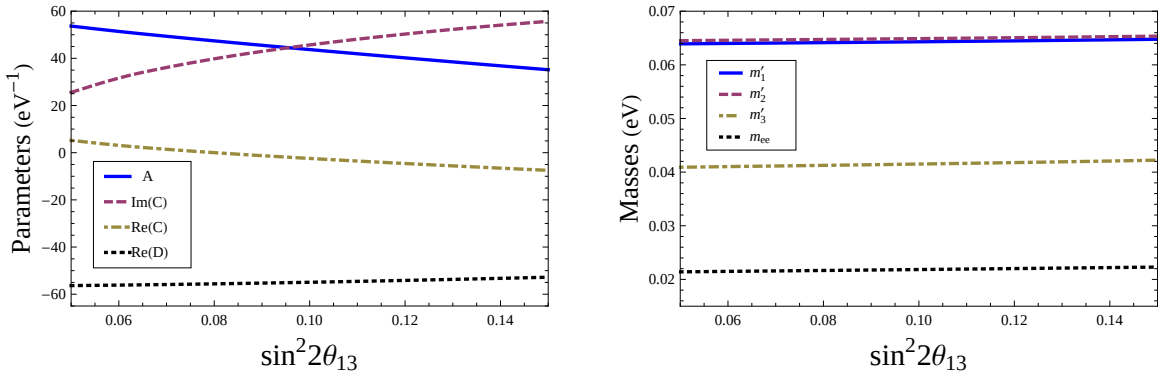

Figure 5.4. A_4 **parameters and the physical neutrino masses and effective neutrino mass** m_{ee} **in neutrinoless double beta decay for the inverted hierarchy with Im(D)=Re(D) and** $\sin^2 2\theta_{23} = 0.92$**.**

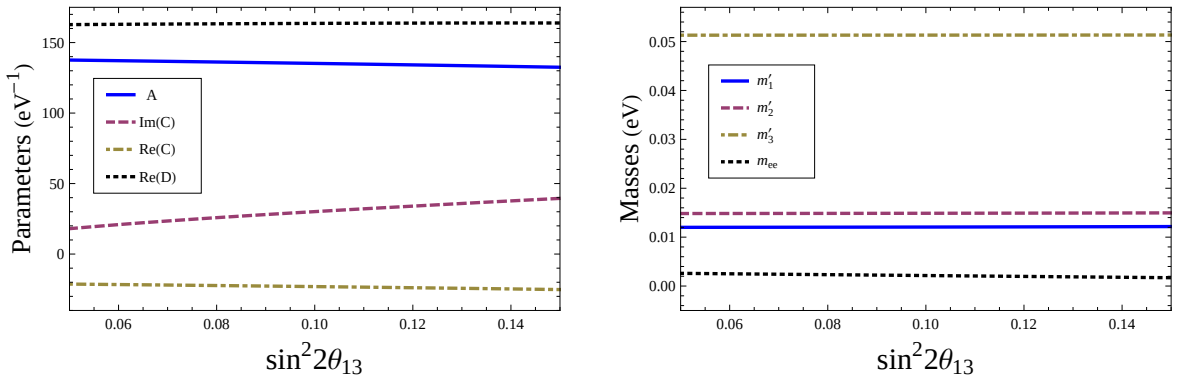

Figure 5.5. A_4 **parameters and the physical neutrino masses and effective neutrino mass** m_{ee} **in neutrinoless double beta decay for the normal hierarchy with Im(D)=0 and** $\sin^2 2\theta_{23} = 0.96$**.**

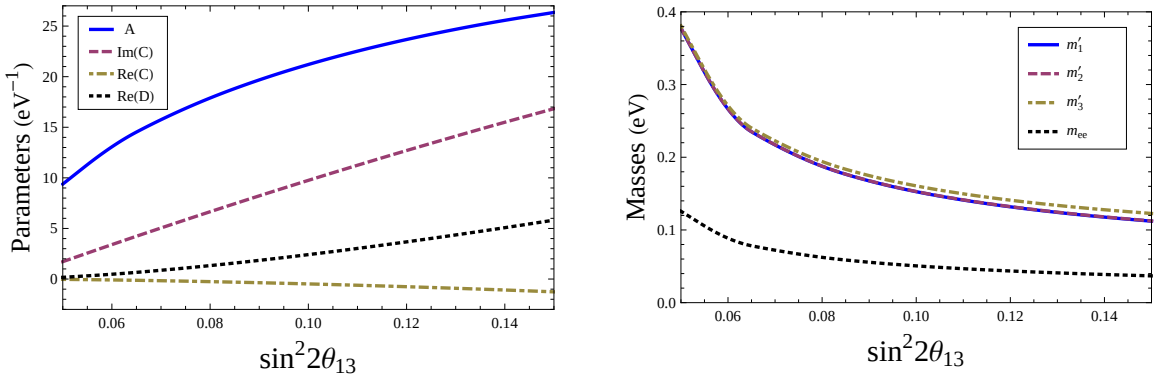

Figure 5.6. A_4 **parameters and the physical neutrino masses and effective neutrino mass** m_{ee} **in neutrinoless double beta decay for quasi-degenerate neutrino masses with Im(D)=0 and** $\sin^2 2\theta_{23} = 0.96$**.**

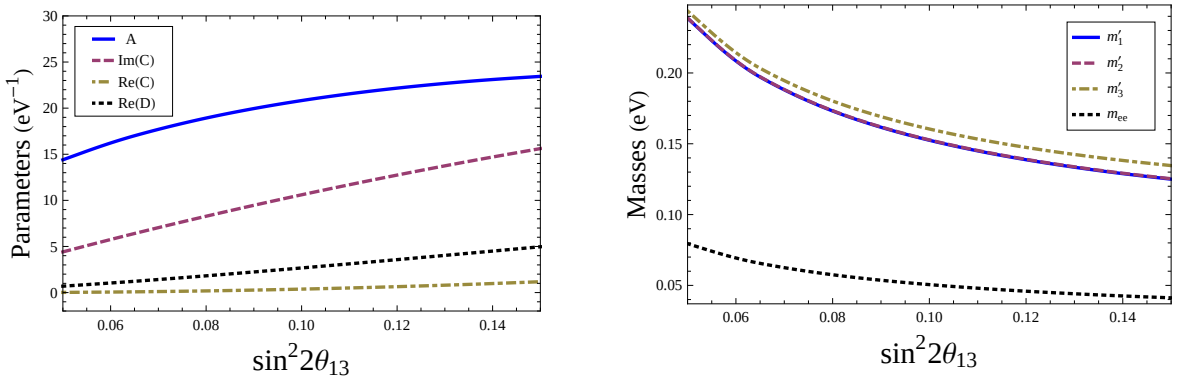

Figure 5.7. A_4 **parameters and the physical neutrino masses and effective neutrino mass** m_{ee} **in neutrinoless double beta decay for quasi-degenerate neutrino masses with Im(D)=Re(D) and** $\sin^2 2\theta_{23} = 0.96$**.**

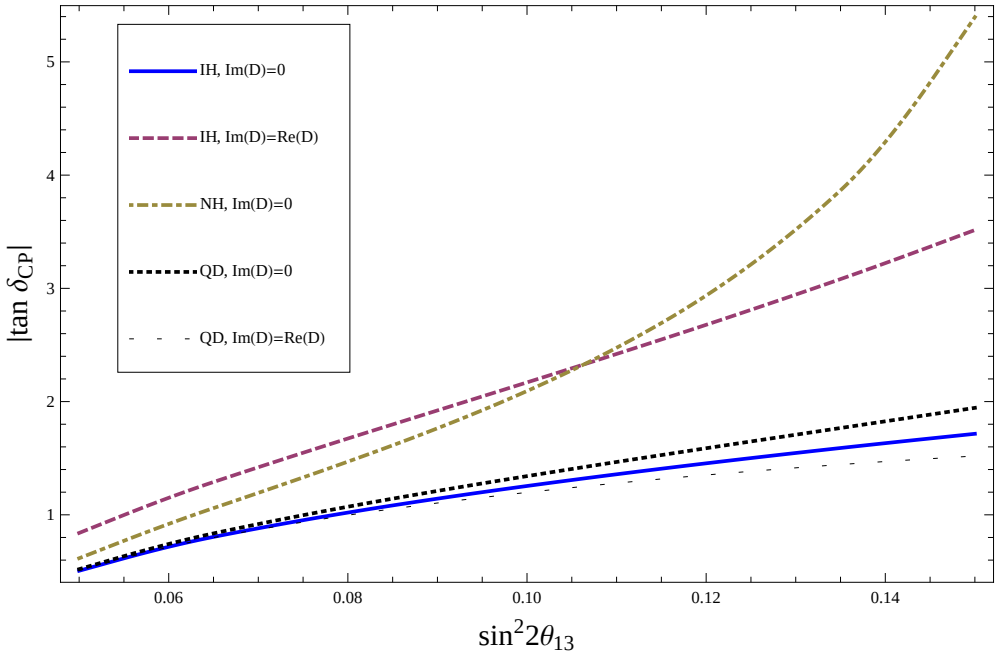

Figure 5.8. $|\tan\delta_{CP}|$ **versus** $\sin^2 2\theta_{13}$ **for** $\sin^2 2\theta_{23} = 0.92$**.**

CHAPTER 6

RADIATIVE SCALING NEUTRINO MASS WITH A_4 SYMMETRY

The origin of neutrino mass is the topic of many theoretical discussions. The consensus is that its smallness is due to some mass scale larger than the electroweak breaking scale of about 100 GeV. If there are no particles beyond those of the standard model lighter than this scale, then the well-known unique dimension-five opeartor [235]

$$\mathcal{L}_5 = \frac{-f_{ij}}{2\Lambda}(\nu_i\phi^0 - l_i\phi^+)(\nu_j\phi^0 - l_j\phi^+) + H.c. \tag{6.1}$$

induces Majorana neutrino masses as the Higgs scalar ϕ^0 acquires a nonzero vacuum expectation value $\langle\phi^0\rangle = v$, so that

$$(\mathcal{M}_\nu)_{ij} = \frac{f_{ij}v^2}{\Lambda}. \tag{6.2}$$

This shows that neutrino mass is seesaw in character, i.e. it is inversely proportional to some large scale Λ. The ultraviolet completion of this effective operator may be accomplished in three ways at tree level [236] using (I) heavy Majorana fermion singlets N_i, (II) a heavy scalar triplet (ξ^{++}, ξ^+, ξ^0), or (III) heavy Majorana fermion triplets $(\Sigma^+, \Sigma^0, \Sigma^0)_i$, commonly referred to as Type I, Type II, or Type III seesaw. There are also three one-particle-irreducible (1PI) one-loop realizations [236]. Recently the one-particle-reducible (1PR) diagrams have also been considered [237].

If there are new particles with masses below the elctroweak scale, such as fermion singlets ν_S with mass m_S, then neutrinos may acquire mass through their mixing with ν_S. However, this mechanism is still seesaw because m_ν is still inversely proportional to m_S. There is however an exception. It has been pointed out recently [238] that in the scotogenic model of radiative neutrino mass [221], it is possible to have m_ν directly proportional to m_S, and

there is no mixing between m_ν and m_S.

This model was proposed [221] in 2006 to connect neutrino mass with dark matter. The idea is very simple. Assume three neutral fermion singlets N_i as in the usual Type I seesaw [239], but let them be odd under a new Z_2 symmetry, so that there is no $(\nu_i\phi^0 - l_i\phi^+)N_j$ coupling and the effective operator of Eq. (1) is not realized. At this stage, N_i may have Majorana masses M_i, but ν_i is massless. However, they can be linked through the interaction $h_{ij}(\nu_i\eta^0 - l_i\eta^+)N_j$ where (η^+, η^0) is a new scalar doublet which is also odd under the aforementioned Z_2 [222]. Hence Majorana neutrino masses are generated in one loop as shown in Fig. 1. This mechanism has been called "scotogenic", from the Greek "scotos"

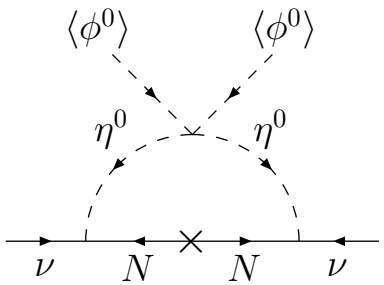

Figure 6.1. One-loop generation of scotogenic Majorana neutrino mass.

meaning darkness. Because of the allowed $(\lambda_5/2)(\Phi^\dagger\eta)^2 + H.c.$ interaction, $\eta^0 = (\eta_R + i\eta_I)/\sqrt{2}$ is split so that $m_R \neq m_I$. The diagram of Fig. 1 can be computed exactly [221], i.e.

$$(\mathcal{M}_\nu)_{ij} = \sum_k \frac{h_{ik}h_{jk}M_k}{16\pi^2}\left[\frac{m_R^2}{m_R^2 - M_k^2}\ln\frac{m_R^2}{M_k^2} - \frac{m_I^2}{m_I^2 - M_k^2}\ln\frac{m_I^2}{M_k^2}\right]. \tag{6.3}$$

A good dark-matter candidate is η_R as first pointed out in Ref. [221]. It was subsequently proposed by itself in Ref. [240] and studied in detail in Ref. [241]. The η doublet has become known as the "inert" Higgs doublet, but it does have gauge and scalar interactions even if it is the sole addition to the standard model.

The usual assumption for neutrino mass in Eq. (1) is

$$m_I^2 - m_R^2 << m_I^2 + m_R^2 << M_k^2, \tag{6.4}$$

in which case

$$(\mathcal{M}_\nu)_{ij} = \frac{\lambda_5 v^2}{8\pi^2}\sum_k \frac{h_{ik}h_{jk}}{M_k}\left[\ln\frac{M_k^2}{m_0^2} - 1\right], \tag{6.5}$$

where $m_0^2 = (m_I^2 + m_R^2)/2$ and $m_R^2 - m_I^2 = 2\lambda_5 v^2$ ($v = \langle\phi^0\rangle$). This scenario is often referred

to as the radiative seesaw. What was not realized in most applications of this model since 2006 is that there is another very interesting scenario, i.e.

$$M_k^2 << m_R^2,\ m_I^2. \tag{6.6}$$

Neutrino masses are then given by [238]

$$(\mathcal{M}_\nu)_{ij} = \frac{\ln(m_R^2/m_I^2)}{16\pi^2} \sum_k h_{ik} h_{jk} M_k. \tag{6.7}$$

This simple expression is actually very extraordinary, because neutrino mass is now not inversely proportional to some large scale. In that case, how do we understand the smallness of m_ν? The answer is lepton number. In this model, $(\nu, l)_i$ have lepton number $L = 1$ and N_k have $L = -1$, and L is conserved in all interactions except for the Majorana mass terms M_k which break L to $(-1)^L$. We may thus argue that M_k should be small compared to all other mass terms which conserve L, the smallest of which is the electron mass, $m_e = 0.511$ MeV. It is thus reasonable to have $M_k \sim 10$ keV, in which case $m_\nu \sim 0.1$ eV is obtained if $h^2 \sim 10^{-3}$ in Eq. (7). Each neutrino mass is then simply proportional to a linear combination of M_k according to Eq. (7). Their ratio is just a scale factor and small neutrino masses are due to this "scaling" mechanism. Note that the interesting special case where only M_1 is small has been considered previously [242, 243]. Note also that if $|m_I^2 - m_R^2| = 2|\lambda_5| v^2 << |m_I^2 + m_R^2|$, then $\ln(m_R^2/m_I^2)$ would be strongly suppressed, but this is not compulsory. For example, let $m_R = 240$ GeV, $m_I = 150$ GeV, then $|\lambda_5| = 0.58$ and $\ln(m_R^2/m_I^2) = 0.94$.

The scotogenic model [221] with large M_k, i.e. Eq. (5), has been extended recently [244] to include the well-known non-Abelian discrete symmetry A_4 [223, 224, 225]. Here we consider the case of Eq. (7). This assumption changes the phenomenology of N_k as well as (η^+, η^0) and may render this model to be more easily verifiable at the Large Hadron Collider (LHC). We let (η^+, η^0) be a singlet under A_4 and both (ν_i, l_i) and N_k to be triplets. In that case,

$$h_{ik} = h \delta_{ik}, \tag{6.8}$$

and

$$\mathcal{M}_\nu = \zeta \mathcal{M}_N, \tag{6.9}$$

where $\zeta = h^2 \ln(m_R^2/m_I^2)/16\pi^2$ is the scale factor. The soft breaking of A_4 which shapes $\mathcal{M}_N$ is then directly transmitted to $\mathcal{M}_\nu$.

One immediate consequence of this restricted scaling mechanism for neutrino mass is that if $M_{1,2,3}$ are all of order 10 keV, then the three neutrino masses are all of order 0.1 eV,

i.e. a quasidegenerate scenario. For example, if $m_1 = 0.1$ eV and is the lightest, then for $M_1 = 10$ keV, $M_3 = 10^5(m_1 + \sqrt{\Delta m^2_{31}}) = 14.85$ keV. Another immediate consequence is that the interactions of $N_{1,2,3}$ with the charged leptons through η^+ depend only on h and the mismatch between the charged-lepton mass matrix and the neutrino mass matrix, i.e. the experimentally determined neutrino mixing matrix $U_{l\nu}$. Hence $\mu \to e\gamma$ is highly suppressed because the leading term of its amplitude is proportional to $\sum_k h_{\mu k} h^*_{ek} = |h|^2 \sum_k U_{\mu k} U^*_{ek} = 0$. The next term $\sum_k U_{\mu k} U^*_{ek} M^2_k / m^2_{\eta^+}$ is nonzero but is negligibly small. This means that there is no useful bound on the η^+ mass from $\mu \to e\gamma$. *Note that A_4 may be replaced by any other flavor symmetry as long as it is possible to have Eq. (8) using the singlet and triplet representations of that symmetry.* As for the muon anomalous magnetic moment, it is given by [245]

$$\Delta a_\mu = -\frac{m^2_\mu |h|^2}{96\pi^2 m^2_{\eta^+}} = -1.18 \times 10^{-12} \left(\frac{|h|^2}{10^{-3}}\right) \left(\frac{100 \text{ GeV}}{m_{\eta^+}}\right)^2. \tag{6.10}$$

Since the experimental uncertaintly is 6×10^{-10}, this also does not give any useful bound on the η^+ mass.

If $\eta^\pm, \eta_R, \eta_I$ are of order 10^2 GeV, the interactions of N_k with the neutrinos and charged leptons are weaker than the usual weak interaction, hence N_k may be considered "sterile" and become excellent warm dark-matter candidates [246, 247]. However, unlike the usual sterile neutrinos [248] which mix with the active neutrinos, the lightest N_k here is absolutely stable. This removes one of the most stringent astrophysical constraints on warm dark matter, i.e. the absence of galactic X-ray emission from its decay, which would put an upper bound of perhaps 2.2 keV on its mass [249], whereas Lyman-α forest observations (which still apply in this case) impose a lower bound of perhaps 5.6 keV [250]. Such a stable sterile neutrino (called a "scotino") is also possible in an unusual left-right extension [251] of the standard model. Conventional left-right models where the $SU(2)_R$ neutrinos mix with the $SU(2)_L$ neutrinos have also been studied [252, 253, 254].

Since N_k are assumed light, muon decay proceeds at tree level through η^+ exchange, i.e. $\mu \to N_\mu e \bar{N}_e$. The inclusive rate is easily calculated to be

$$\Gamma(\mu \to N_\mu e \bar{N}_e) = \frac{|h|^4 m^5_\mu}{6144\pi^3 m^4_{\eta^+}}. \tag{6.11}$$

Since N_μ and $\bar{N}_e$ are invisible just as ν_μ and $\bar{\nu}_e$ are invisible in the dominant decay $\mu \to \nu_\mu e \bar{\nu}_e$ (with rate $G^2_F m^5_\mu / 192\pi^3$), this would change the experimental value of G_F. Using the

experimental uncertainty of 10^{-5} in the determination of G_F, we find

$$m_{\eta^+} > 70 \text{ GeV} \tag{6.12}$$

for $|h|^2 = 10^{-3}$. This is a useful bound on the η^+ mass, but it is also small enough so that η^+ may be observable at the LHC. The phenomenological bound on m_{η^+} from e^+e^- production at LEPII has been estimated [255] to be 70 – 90 GeV. A bound of 80 GeV was used in a previous study [256] of this model.

Whereas the lightest scotino, say N_1, is absolutely stable, $N_{2,3}$ will decay into N_1 through η_R and η_I. The decay rate of $N_3 \to N_1 \bar{\nu}_1 \nu_3$ is given by

$$\Gamma(N_3 \to N_1 \bar{\nu}_1 \nu_3) = \frac{|h|^4}{256\pi^3 M_3} \left(\frac{1}{m_R^2} + \frac{1}{m_I^2} \right)^2 \times \left(\frac{M_3^6}{96} - \frac{M_1^2 M_3^4}{12} + \frac{M_1^6}{12} - \frac{M_1^8}{96 M_3^2} + \frac{M_1^4 M_3^2}{8} \ln \frac{M_3^2}{M_1^2} \right). \tag{6.13}$$

Let $M_1 = 10$ keV, $M_3 = 14.85$ keV, $|h|^2 = 10^{-3}$, $m_R = 240$ GeV, $m_I = 150$ GeV, then this rate is 1.0×10^{-46} GeV, corresponding to a lifetime of 2.1×10^{14} y, which is much longer than the age of the Universe of $13.75 \pm 0.11 \times 10^9$ y. The lifetime of N_2 is even longer because $\Delta m^2_{21} << \Delta m^2_{31}$. Hence both N_2 and N_3 are stable enough to be components of warm dark matter. However, $N_{2,3} \to N_1 \gamma$ are negligible for the same reason that $\mu \to e\gamma$ is negligible, so they again have no galactic X-ray signatures.

Since η^+ may be as light as 70 GeV, it may be observable at the LHC. Assuming that the recently observed particle [257, 258] at the LHC is the Higgs boson H coming from (ϕ^+, ϕ^0), the decay $H \to \eta^+ \eta^-$ is not allowed for $m_H = 126$ GeV. However, $\eta^\pm$ will contribute to the $H \to \gamma\gamma$ rate, as already pointed out [259, 260, 261, 262]. What sets our model apart is the inclusive decay of $\eta^\pm \to l^\pm N_{1,2,3}$, which is of universal strength. At the LHC, the pair production of $\eta^+\eta^-$ will then lead to $l_i^+ l_j^-$ final states with equal probability for each flavor combination. For example, $e^+\mu^-$ and μ^+e^- will each occur 1/9 of the time. This signature together with the large missing energy of $N_{1,2,3}$ may allow it to be observed at the LHC. However, these events also come from W^+W^- production and their subsequent leptonic decays. If data show an excess of such events [263] over the standard-model prediction, it could be due to $\eta^+\eta^-$, but it may also simply come from an incorrect scale factor used in the standard-model calculation.

In the supersymmetric $SU(5)$ completion [264] of this model, there are exotic quarks which may be produced abundantly. Their decays into $\eta^\pm$ would have four leptons of different flavor in the final state. This may be a better signature of this model. Details will be given

elsewhere.

In conclusion, the scotogenic model [221] of neutrino mass with a solution [238] where there is no seesaw mechanism and $N_{1,2,3}$ have masses of order 10 keV has been implemented with the non-Abelian discrete symmetry A_4. The scotinos $N_{1,2,3}$ are good warm dark-matter candidates which can explain the structure of the Universe at all scales [246, 247]. Since N_1 is absolutely stable and the decays $N_{2,3} \to N_1 \gamma$ are negligible, the galactic X-ray upper bound of perhaps 2.2 keV on its mass [249] is avoided. It will also not be detected in terrestrial experiments. On the other hand, since this model requires an extra scalar doublet, and $\eta^\pm$ may be as light as 70 GeV, it may be tested at the LHC, especially if it is the decay product of an exotic quark.

CHAPTER 7

NONSTANDARD INTERACTIONS OF TAU NEUTRINO VIA CHARGED HIGGS AND W' CONTRIBUTION

7.1 Introduction

It has been established that NSI cannot be an explanation for the standard oscillation phenomena, but it may be present as a subleading effect. Many NSI involve flavor changing neutral current or charged current lepton flavor violating processes. In this work we consider charged current interactions involving a charged Higgs and a W' gauge boson in the tau-neutrino nucleon scattering as categorized according the value of the invariant mass into three subprocesses; quasielastic scattering processes $\nu_\tau + n \to \tau^- + p$ and $\bar{\nu}_\tau + p \to \tau^+ + n$, Δ-Resonance production $\nu_\tau + n \to \tau^- + \Delta^+$ and $\bar{\nu}_\tau + p \to \tau^+ + \Delta^0$, and deep inelastic scattering $\nu_\tau + N \to \tau^- + X$ and $\bar{\nu}_\tau + N \to \tau^+ + X$. In neutrino experiments, to measure the mixing angle the neutrino-nucleus interaction is assumed to be SM-like. If there is a charged Higgs or a W' contribution to this interaction, then there will be an error in the extracted mixing angle. We will calculate the error in the extracted mixing angle.

The reaction $\nu_\tau + N \to \tau^- + X$ is relevant for experiments like Super-Kamiokande (Super-K) [265, 266] and OPERA [267] that seek to measure $\nu_\mu \to \nu_\tau$ oscillation by the observation of the τ lepton . The above interaction is also important for the DONuT experiment [268] which measured the charged-current (CC) interaction cross section of the tau neutrino. The DONuT central-value results for a ν_τ scattering cross section show deviation from the standard model predictions by about 40% but with large experimental errors; thus, the measurements are consistent with the standard model. The new physics (NP) effects calculated in this work modify the SM cross sections by less than 10% and are therefore

consistent with the DONuT measurements. There have been recent measurements of the appearance of atmospheric tau neutrinos by Super-K [265] and by the OPERA Collaboration [267].

The reactor neutrino experiments such as Double Chooz [269], Daya Bay [270], and RENO [271] measure the mixing angle θ_{13} from the survival probability of an electron antineutrino, P($\bar{\nu}_e \to \bar{\nu}_e$). If high-energy Long Base Line (LBL) experiments (or atmospheric neutrino experiments scanning in the multi-GeV neutrino energy range) could measure θ_{13} via ν_τ appearance then the NP effects in $\nu_\tau + N \to \tau^- + X$ and $\bar{\nu}_\tau + N \to \tau^+ + X$ would impact the θ_{13} measurement and a mismatch between this measurement and that performed at the reactors could be a hint of a NSI in the former.

Generally, neutrino scattering contains contributions from various processes such as quasielastic scattering (QE), resonance scattering (RES), and deep inelastic scattering (DIS). Just above the threshold energy for τ production, which is 3.45 GeV [265, 266], the quasielastic interaction dominates in ν_τ scattering [272, 273]. At higher scattering energies other processes have to be included. For instance, the DIS is expected to be dominant above around 10 GeV [273], and so ν_τ scattering at the OPERA experiment, running at the average neutrino energy $E_\nu = 17$ GeV [267], will be dominated by DIS.

There are several reasons to consider NSI involving the (ν_τ, τ) sector. First, the third generation may be more sensitive to new physics effects because of their larger masses. As an example, in certain versions of the two Higgs doublet models (2HDM) the couplings of the new Higgs bosons are proportional to the masses, and so new physics effects are more pronounced for the third generation. Second, the constraints on NP involving the third generation leptons are somewhat weaker, allowing for larger new physics effects. Interestingly, the branching ratio of B decays to τ final states shows some tension with the SM predictions [275, 276] and this could indicate NP, possibly in the scalar or gauge boson sector [277]. Some examples of work that deals with NSI at the detector, though not necessarily involving the third family leptons, can be found in Refs. [278, 279, 280].

If there is NP involving the third generation leptons, one can search for it in B decays such as $B \to \tau\nu_\tau$, $B \to D^{(*)}\tau\nu_\tau$ [281], $b \to s\tau^+\tau^-$ etc. In general, the NP interaction in B decays may not be related to the one in $\nu_\tau + n \to \tau^- + p$ and $\bar{\nu}_\tau + p \to \tau^+ + n$, and so these scattering processes probe different NP. The same NP in $\nu_\tau + n \to \tau^- + p$ and $\bar{\nu}_\tau + p \to \tau^+ + n$ can be probed in τ decays [282], and we will consider the constraint on NP from this decay. However, in general, the scattering and the decay processes probe NP in different energy regions.

The form of NP in $\nu_\tau + N \to \tau^- + X$ involves the operator $\mathcal{O}_{NP} = \bar{u}\Gamma_i d\bar{\tau}\Gamma_j\nu_\tau$, where $\Gamma_{i,j}$

are some Dirac structures. The process $\bar{\nu}_\tau + N \to \tau^+ + X$ gets a contribution from $\mathcal{O}_{NP}^\dagger$. We will assume CP conserving NP in this work, and so the coefficients of the NP operators are real. The same NP operator can also contribute to hadronic tau decays $\tau^- \to \pi^- \nu_\tau$ and $\tau^- \to \rho^- \nu_\tau$, and the measured branching ratio of these decays can be used to constrain the couplings in the operator $\mathcal{O}_{NP}$. The ratio of the charged Higgs contribution to the SM in $\nu_\tau + N \to \tau^- + X$ and $\bar{\nu}_\tau + N \to \tau^+ + X$ is roughly (m_N/m_π) larger compared to the same ratio in $\tau^- \to \pi^- \nu_\tau$, where $m_{N,\pi}$ are the nucleon and pion masses. Hence, significant charged Higgs effects are possible in $\nu_\tau + N \to \tau^- + X$ and $\bar{\nu}_\tau + N \to \tau^+ + X$ even after imposing constraints from τ decays. We note that new interactions in the up and down quark sectors can be constrained if one assumes CKM unitarity. However, we do not consider this constraint as the NP in $\mathcal{O}_{NP}$ involves contributions from both the quark and the lepton sectors.

As noted above, at the quark level NSI in $\nu_\tau + N \to \tau^- + X$ and $\bar{\nu}_\tau + N \to \tau^+ + X$ involve the u and the d quarks. Often in the analysis of NSI, hadronization effects of the quarks via form factors are not included. As we show in our calculation the form factors play an important role in the energy dependence of the NP effects. In an accurate analysis one should also include nuclear physics effects which take into account the fact that the neutron and the proton are not free but bound in the nucleus. There is a certain amount of model dependence in this part of the analysis [283], and therefore we will not include nuclear effects in our calculation. Such effects can be easily incorporated once the free scattering cross sections are known.

This work is organized in the following way. In the next section, we present a model-independent analysis of NP effects. Then we discuss the kinematics of the interaction. In the following three sections, we consider charged Higgs and W' effects to the three processes quasi-elastic interaction, Δ resonance production and deep inelastic scattering in the neutrino-nucleon interactions $\nu_\tau + N \to \tau^- + X$ and $\bar{\nu}_\tau + N \to \tau^+ + X$. In the last section, we present our conclusions.

7.2 Model-independent analysis of new physics

The process $\nu_\tau + N \to \tau^- + X$ will impact the measurement of the oscillation probability for the $\nu_\mu \to \nu_\tau$ transition and hence the extraction of the mixing angle θ_{23}. The measurement of the atmospheric mixing angle θ_{23} relies on the following relationship [284]:

$$N(\nu_\tau) = P(\nu_\mu \to \nu_\tau) \times \Phi(\nu_\mu) \times \sigma_{\rm SM}(\nu_\tau)\,, \tag{7.1}$$

where $N(\nu_\tau)$ is the number of observed events, $\Phi(\nu_\mu)$ is the flux of muon neutrinos at the detector, $\sigma^{\rm SM}(\nu_\tau)$ is the total cross section of tau neutrino interactions with nucleons in the SM at the detector, and $P(\nu_\mu \to \nu_\tau)$ is the probability for the flavor transition $\nu_\mu \to \nu_\tau$. This probability is a function of $(E,\ L,\ \Delta m^2_{ij},\ \theta_{ij})$ with $i, j = 1, 2, 3$, where Δm^2_{ij} is the squared-mass difference, θ_{ij} is the mixing angle, E is the energy of neutrinos, and L is the distance traveled by neutrinos. The dominant term of the probability is

$$P(\nu_\mu \to \nu_\tau) \approx \sin^2 2\theta_{23} \cos^4 \theta_{13} \sin^2(\Delta m^2_{23} L/4E). \tag{7.2}$$

In the presence of NP, Eq. 7.1 is modified as

$$N(\nu_\tau) = P(\nu_\mu \to \nu_\tau) \times \Phi(\nu_\mu) \times \sigma_{\rm tot}(\nu_\tau), \tag{7.3}$$

with $\sigma_{\rm tot}(\nu_\tau) = \sigma_{\rm SM}(\nu_\tau) + \sigma_{\rm NP}(\nu_\tau)$, where $\sigma_{\rm NP}(\nu_\tau)$ refers to the additional terms of the SM contribution towards the total cross section. Hence, $\sigma_{\rm NP}(\nu_\tau)$ includes contributions from both the SM and NP interference amplitudes, and the pure NP amplitude. From Eqs. (7.1, 7.3), assuming θ_{13} to be small,[1]

$$\sin^2 2(\theta_{23}) \ = \ \sin^2 2(\theta_{23})_{SM} \frac{1}{1 + r_{23}}\,, \tag{7.4}$$

where $\theta_{23} = (\theta_{23})_{SM} + \delta_{23}$ is the actual atmospheric mixing angle, whereas $(\theta_{23})_{SM}$ is the extracted mixing angle assuming the SM ν_τ scattering cross section. Assuming negligible new physics effects in the $\mu - N$ interaction, the actual mixing angle θ_{23} is the same as the mixing angle extracted from the survival probability $P(\nu_\mu \to \nu_\mu)$ measurement. We will take the best-fit value for the mixing angle to be given by $\theta_{23} = 42.8^\circ$ [285]. In other words, the presence of new physics in a ν_τ-nucleon scattering will result in the mixing angle, extracted from a ν_τ appearance experiment, being different than the mixing angle from ν_μ survival probability measurements. The relationship between the ratio of the NP contribution to the SM cross section $r_{23} = \sigma_{NP}(\nu_\tau)/\sigma_{SM}(\nu_\tau)$ and δ_{23} can be expressed in a model-independent form as

$$r_{23} \ = \ \Big[\frac{\sin 2(\theta_{23})_{SM}}{\sin 2((\theta_{23})_{SM} + \delta_{23})}\Big]^2 - 1\,. \tag{7.5}$$

The reactor neutrino experiments can determine the mixing angle θ_{13} from the oscillation probability, $\mathrm{P}(\bar{\nu}_e \to \bar{\nu}_e)$. The probability of the tau antineutrino appearance $\bar{\nu}_e \to \bar{\nu}_\tau$ can be

[1]The presence of NP impacts the extraction of the combination $\sin^2 2\theta_{23} \cos^4 \theta_{13}$. The NP changes the extracted value of θ_{23} as well as θ_{13}. But we fix the value of θ_{13} as an input at this point.

used to extract θ_{13}. In this case the effect of NP contributions to the process $\bar{\nu}_\tau + N \to \tau^+ + X$ is pertinent. The relationship used in measuring θ_{13} will be given as

$$N(\bar{\nu}_\tau) = P(\bar{\nu}_e \to \bar{\nu}_\tau) \times \Phi(\bar{\nu}_e) \times \sigma_{\rm tot}(\bar{\nu}_\tau)\,, \tag{7.6}$$

where [286, 59, 287]

$$P(\bar{\nu}_e \to \bar{\nu}_\tau) \approx \sin^2 2\theta_{13} \cos^2\theta_{23} \sin^2(\Delta m^2_{13} L/4E). \tag{7.7}$$

Thus the relationship between the ratio of the NP contribution to the SM cross section $r_{13} = \sigma_{NP}(\bar{\nu}_\tau)/\sigma_{SM}(\bar{\nu}_\tau)$ and δ_{13} can be obtained in a model-independent form as

$$r_{13} \;=\; \Big[\frac{\sin 2(\theta_{13})_{SM}}{\sin 2((\theta_{13})_{SM} + \delta_{13})}\Big]^2 - 1\,. \tag{7.8}$$

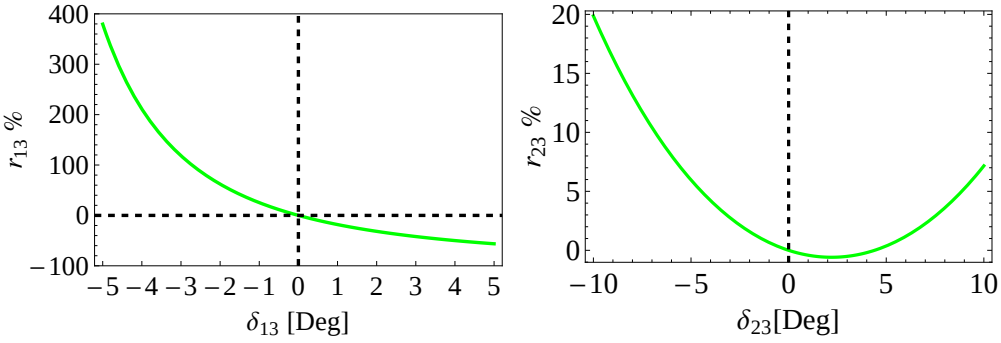

Figure 7.1. Correlation plot for $r_{23} = \sigma_{NP}(\nu_\tau)/\sigma_{SM}(\nu_\tau)\%$ versus $\delta_{23}[Deg]$, and $r_{13} = \sigma_{NP}(\bar{\nu}_\tau)/\sigma_{SM}(\bar{\nu}_\tau)\%$ versus $\delta_{13}[Deg]$.

In Fig. 7.1 we show the correlation between $r_{23(13)}\%$ and $\delta_{23(13)}$ [Deg]. One can see that $\delta_{23} \sim -5^\circ$ requires $r_{23} \sim 5\%$. But $\delta_{13} \sim -1^\circ$ requires $r_{13} \sim 25\%$. In the following sections, we consider specific models of NP to calculate r_{23} and r_{13}. We will consider a model with a charged Higgs and a W' model with both left- and right-handed couplings.

7.3 Kinematics and formalism

In the interactions $\nu_\tau(\bar{\nu}_\tau) + N \to \tau^-(\tau^+) + X$, we define the four-momenta of incoming neutrino (k), target nucleon (p) and produced τ lepton (k') in the laboratory frame. The hadronic invariant mass

$$W^2 = (p+q)^2, \tag{7.9}$$

where $q = k - k'$ is the four-momentum transfer, is defined in the allowed physical region

$$M \leq W \leq \sqrt{s} - m_\tau, \tag{7.10}$$

where $s = (k + p)^2$ is the center of mass energy and M is the average nucleon mass.

The three relevant subprocesses in the neutrino-nucleon interactions are classified according to the regions of the hadronic invariant mass W and the momentum transfer $q^2(= -Q^2)$ [272]. One can label QE (quasi-elastic scattering) when the hadronic invariant mass is equal to the nucleon mass $W = M$, RES (resonance production) when $M + m_\pi < W < W_{\rm cut}$, and IS (inelastic scattering) when $W_{\rm cut} < W < \sqrt{s} - m_\tau$. $W_{\rm cut}$, taken in the region 1.4 GeV$\sim$1.6 GeV, is an empirical boundary between RES and IS processes, to avoid double counting. The deep inelastic scattering DIS may be labeled within the IS region when $Q^2 \geq 1$ GeV^2, where the use of the parton model can be justified.

In this work, we consider Δ-resonance state production and neglect all the other higher resonance states which give small contributions [288, 289, 290]. One can write

$$W^2 = M^2 + t + 2p \cdot q, \tag{7.11}$$

with $p \cdot q = M(E_\nu^{cm} - E_l^{cm})$ where the energy and momentum of the lepton and the neutrino in the center of mass (cm) system are

$$\begin{aligned} E_\nu^{cm} &= \frac{(s - M^2)}{2\sqrt{s}}, \;\; p_l^{\rm cm} = \sqrt{(E_l^{cm})^2 - m_l^2}, \\ E_l^{cm} &= \frac{(s - M_\Delta^2 + m_l^2)}{2\sqrt{s}}, \end{aligned} \tag{7.12}$$

with $(m_l, \;\; M, \;\; M_\Delta)$ being the masses of the charged lepton, nucleon, and the Δ state, respectively. In the lab frame, the charged lepton energy is given by

$$E_l = \frac{t + 2ME_\nu + M^2 - M_\Delta^2}{2M}. \tag{7.13}$$

The threshold neutrino energy to create the charged lepton partner in the Δ-RES case is given by

$$E_{\nu_l}^{\rm th} = \frac{(m_l + M_\Delta)^2 - M_n^2}{2M_n}, \tag{7.14}$$

which gives $E_{\nu_l}^{\rm th} = 4.35$ GeV in the case of tau neutrino production. Using the allowed range of the invariant mass in the resonance production, the allowed region of the momentum

transfer $t \equiv -Q^2$ lies in the interval

$$(M+m_\pi)^2 - \left(M^2 + 2M(E_\nu^{\rm cm} - E_l^{\rm cm})\right) \leq t \leq W_{\rm cut}^2 - \left(M^2 + 2M(E_\nu^{\rm cm} - E_l^{\rm cm})\right). \quad (7.15)$$

In the following three sections, we consider charged Higgs and W' effects to the three processes quasi-elastic interaction, Δ resonance production and deep inelastic scattering in the neutrino-nucleon interactions $\nu_\tau + N \to \tau^- + X$ and $\bar{\nu}_\tau + N \to \tau^+ + X$.

7.4 Quasielastic neutrino interaction

In this section we will discuss the charged Higgs and W' effects to the quasi-elastic interaction.

7.4.1 Quasielastic neutrino interaction − SM

In this section we consider the SM contribution to $\nu_\tau + n \to \tau^- + p$ and $\bar{\nu}_\tau + p \to \tau^+ + n$. We first summarize the SM results for the quasielastic scattering of a neutrino on a free neutron target,

$$\nu_l(k) + n(p) \to l^-(k') + p(p'), \quad (7.16)$$

where k, k', p, and p' denote the four-momenta and l indicates the lepton e, μ, or τ. The spin-averaged matrix element squared for the above reaction is a convolution of spin-averaged leptonic and hadronic tensors $L^{\mu\nu}$ and $H^{\mu\nu}$:

$$|\bar{\mathcal{M}}|^2 = \frac{G_F^2}{2} L^{\mu\nu} H_{\mu\nu}. \quad (7.17)$$

The leptonic tensor calculation is straightforward, but the hadronic tensor involves nonperturbative effects. In order to calculate the hadronic tensor, we define the charged hadronic current for this process:

$$\begin{aligned} \langle p(p')|J_\mu^+|n(p)\rangle &= V_{ud}\, \langle p(p')|(V_\mu - A_\mu)|n(p)\rangle \\ &= V_{ud}\, \bar{p}(p')\Gamma_\mu n(p). \end{aligned} \quad (7.18)$$

The expressions for the matrix elements of the vector and axial-vector currents are summarized in terms of six form factors in the Appendix 11. Due to time reversal invariance, the form factors are real functions of $t = q^2$. When invariance under charge conjugation holds, two form factors vanish ($F_S = 0,\ F_T = 0$) [291]. The matrix element, then, can be written

as

$$\mathcal{M} = \frac{G_F \cos\theta_c}{\sqrt{2}} \bar{u}_l(k')\gamma^\mu(1-\gamma_5)u_{\nu_l}(k) \\ \bar{u}_{N'}(p')\left[F_1^V(t)\gamma_\mu + F_2^V(t) i\frac{\sigma_{\mu\nu}q^\nu}{2M} + F_A(t)\gamma_\mu\gamma_5 + F_P(t)\gamma_5\frac{q_\mu}{M}\right]u_N(p), \quad (7.19)$$

where N and N' are the initial and final nucleons, while l and ν_l are the final charged lepton and the initial neutrino. In our case $N = n$, $N' = p$, $l = \tau$, and $\nu_l = \nu_\tau$.

After evaluating $|\bar{\mathcal{M}}|^2$, one can obtain the SM differential cross section for the reaction in Eq. (7.16) [291],

$$\frac{d\sigma_{SM}(\nu_l)}{dt} = \frac{M^2 G_F^2 \cos^2\theta_c}{8\pi E_\nu^2}\Big[A_{SM} + B_{SM}\frac{(s-u)}{M^2} + C_{SM}\frac{(s-u)^2}{M^4}\Big], \quad (7.20)$$

where $G_F = 1.116637 \times 10^{-5}$ GeV^{-2} is the Fermi coupling constant, $\cos\theta_c = 0.9746$ is the cosine of the Cabibbo angle, M_W is the W boson mass, and E_ν is the incident neutrino energy. $M = (M_p + M_n)/2 \approx 938.9$ MeV is the nucleon mass, and we neglect the proton-neutron mass difference. The expressions for the coefficients f_{SM} $(f = A, B, C)$ are summarized in the Appendix 11. The Mandelstam variables are defined by $s = (k+p)^2$, $t = q^2 = (k-k')^2$, and $u = (k-p')^2$. The expressions for these variables in terms of E_ν and the lepton energy E_l are given in the Appendix 11.

The quasielastic scattering of an antineutrino on a free nucleon is given by

$$\bar{\nu}_l(k) + p(p) \to l^+(k') + n(p')\,. \quad (7.21)$$

The charged hadronic current becomes [272, 292]

$$\langle n(p')|J_\mu^-|p(p)\rangle = \langle p(p)|J_\mu^+|n(p')\rangle^\dagger \\ = V_{ud}\,\bar{n}(p')\tilde{\Gamma}_\mu p(p), \quad (7.22)$$

where

$$\tilde{\Gamma}_\mu(p,p') = \gamma_0\Gamma_\mu^\dagger(p',p)\gamma_0. \quad (7.23)$$

The relationship between the differential cross sections of $\nu_\tau + n \to \tau^- + p$ and $\bar{\nu}_\tau + p \to \tau^+ + n$ is [292, 293]

$$\frac{d\sigma_{SM}(\nu_l)}{dt}(s,t,u) = \frac{d\sigma_{SM}(\bar{\nu}_l)}{dt}(u,t,s). \quad (7.24)$$

Thus, the matrix element is given by Eq. 7.19, and the differential cross section, similarly to

Eq. 7.20, is given by

$$\frac{d\sigma_{SM}(\bar{\nu}_l)}{dt} = \frac{M^2 G_F^2 \cos^2\theta_c}{8\pi E_\nu^2}\Big[A_{SM} - B_{SM}\frac{(s-u)}{M^2} + C_{SM}\frac{(s-u)^2}{M^4}\Big]. \quad (7.25)$$

The negative sign of B_{SM} leads to a relatively smaller cross section for the antineutrino scattering.

7.4.2 Quasielastic neutrino interaction − Charged Higgs Effect

We consider here the charged Higgs contribution to $\nu_\tau + n \to \tau^- + p$ and $\bar{\nu}_\tau + p \to \tau^+ + n$. Charged Higgs particles appear in multi-Higgs models. In the SM the Higgs couples to the fermion masses, but in a general multi-Higgs model the charged Higgs may not couple to the mass. What is true in most models is that the coupling of the charged Higgs to the leptons is no longer universal. Hence, the extraction of θ_{23} and θ_{13} from $\nu_\mu \to \nu_\mu$ and $\bar{\nu}_e \to \bar{\nu}_e$ survival probabilities, respectively, will be different from $\nu_\mu \to \nu_\tau$ and $\bar{\nu}_e \to \bar{\nu}_\tau$ probabilities, respectively, in the presence of a charged Higgs effect.

The most general coupling of the charged Higgs is

$$\mathcal{L} = \frac{g}{2\sqrt{2}}\Big[V_{u_i d_j}\bar{u}_i(g_S^{u_i d_j} \pm g_P^{u_i d_j}\gamma^5)d_j + \bar{\nu}_i(g_S^{\nu_i l_j} \pm g_P^{\nu_i l_j}\gamma^5)l_j\Big]\ H^\pm, \quad (7.26)$$

where u_i and d_j refer to up and down type quarks, and ν_i and l_j refer to neutrinos and charged leptons. The other parameters are as follows: $g = e/\sin\theta_W$ is the SM weak coupling constant, $V_{u_i d_j}$ is the CKM matrix element, and $g_{S,P}$ are the scalar and pseudoscalar couplings of the charged Higgs to fermions. Here, in this work, we assume the couplings $g_{S,P}$ are real.

We will choose the couplings $g_{S,P}$, relevant for $\nu_\tau + n \to \tau^- + p$ and $\bar{\nu}_\tau + p \to \tau^+ + n$, to be given by the two Higgs doublet model of type II (2HDM II). In the 2HDM II these couplings are related to couplings in other sectors and so can be constrained by measurements in these other sectors. However, in our analysis, to keep things general we will not assume any relation between the couplings $g_{S,P}$ and the couplings in other sectors, thereby avoiding constraints from other sectors. To constrain the couplings $g_{S,P}$ we will only consider processes that are generated by $\mathcal{O}_{NP} = \bar{u}\Gamma_i d\bar{\tau}\Gamma_j\nu_\tau$. In the 2HDM II, constrains on the model parameters come from various sectors [294]. These constraints turn out to be similar but slightly stronger than the ones obtained in our analysis.

The coupling of charged Higgs boson ($H^\pm$) interactions to a SM fermion in the 2HDM II

is [295]

$$\mathcal{L} = \frac{g}{\sqrt{2}M_W}\sum_{ij}\Big[m_{u_i}\cot\beta\ \bar{u}_i V_{ij}P_{L,R}d_j + m_{d_j}\tan\beta\ \bar{u}_i V_{ij}P_{R,L}d_j + m_{l_j}\tan\beta\ \bar{\nu}_i P_{R,L}l_j\Big]H^{\pm}, \tag{7.27}$$

where $P_{L,R} = (1 \mp \gamma^5)/2$, and $\tan\beta$ is the ratio between the two vacuum expectation values (vev's) of the two Higgs doublets. Comparing Eq. (7.45) and Eq. (7.27), one can obtain

$$\begin{aligned} g_S^{u_i d_j} &= \left(\frac{m_{d_j}\tan\beta + m_{u_i}\cot\beta}{M_W}\right), \\ g_P^{u_i d_j} &= \left(\frac{m_{d_j}\tan\beta - m_{u_i}\cot\beta}{M_W}\right), \\ g_S^{\nu_i l_j} &= g_P^{\nu_i l_j} = \frac{m_{l_j}\tan\beta}{M_W}. \end{aligned} \tag{7.28}$$

Constraints on the size of the operator $\mathcal{O}_{NP} = \bar{u}\Gamma_i d\bar{\tau}\Gamma_j\nu_\tau$ can be obtained from the branching ratio of the decay $\tau^- \to \pi^-\nu_\tau$. In the presence of a charged Higgs, the branching ratio for this process is

$$Br^{SM+H}_{\tau^-\to\pi^-\nu_\tau} = Br^{SM}_{\tau^-\to\pi^-\nu_\tau}(1 + r_H^{\pi^2}), \tag{7.29}$$

where the charged Higgs contribution is

$$r_H^{\pi} = \Big(\frac{m_u - m_d\tan^2\beta}{m_u + m_d}\Big)\frac{m_\pi^2}{m_H^2}. \tag{7.30}$$

The SM branching ratio is related to the tau lepton width (Γ_τ) and the decay rate($\Gamma^{SM}_{\tau^-\to\pi^-\nu_\tau}$) as $Br^{SM}_{\tau^-\to\pi^-\nu_\tau} = \Gamma^{SM}_{\tau^-\to\pi^-\nu_\tau}/\Gamma_\tau$ with

$$\Gamma^{SM}_{\tau^-\to\pi^-\nu_\tau} = \frac{G_F^2}{16\pi}|V_{ud}|^2 f_\pi^2 m_\tau^3\Big(1 - \frac{m_\pi^2}{m_\tau^2}\Big)^2\delta_{\tau/\pi}. \tag{7.31}$$

Here $\delta_{\tau/\pi} = 1.0016 \pm 0.0014$ [296] is the radiative correction. Further, the SM branching ratio can also be expressed as [297]

$$Br^{SM}_{\tau^-\to\pi^-\nu_\tau} = 0.607 Br(\tau^- \to \nu_\tau e^-\bar{\nu}_e) = 10.82 \pm 0.02\%, \tag{7.32}$$

while the measured $Br(\tau^- \to \pi^-\nu_\tau)_{exp} = (10.91 \pm 0.07)\%$ [168]. In Fig. 7.2 we show the constraints on $m_H - \tan\beta$ from $\tau^- \to \pi^-\nu_\tau$. From Eq. 7.27 we can construct the NSI parameters defined in Ref [280] as $\varepsilon^{ud(L)}_{\tau\tau} \equiv \frac{m_u m_\tau}{m_H^2}$ and $\varepsilon^{ud(R)}_{\tau\tau} \equiv \frac{m_d m_\tau \tan^2\beta}{m_H^2}$. We find that the

constraints on the effective operator considered in this work are consistent with the one in Ref. [280]. Finally, we note that τ has a significant branching ratio to $\tau^- \to \rho^- \nu_\tau$ [168].

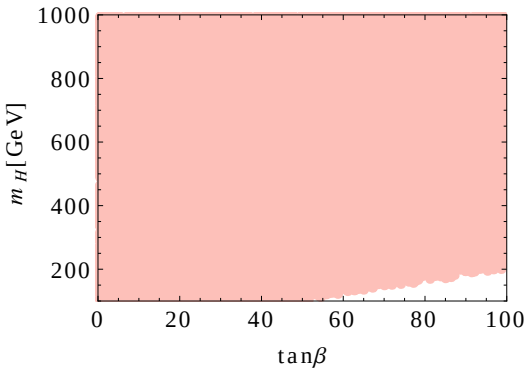

Figure 7.2. Constraint by $Br(\tau^- \to \pi^- \nu_\tau)$ at 95 % CL. The colored region is allowed.

However, a charged Higgs cannot contribute to this decay, and hence there is no constraint on the charged Higgs couplings from this decay [282].

Keeping in mind the constraints from Fig. (7.2), we calculate the charged Higgs contribution to $\nu_\tau + n \to \tau^- + p$. The modified differential cross section for the reaction in Eq. (7.16) is

$$\frac{d\sigma_{SM+H}}{dt} = \frac{M^2 G_F^2 \cos^2\theta_c}{8\pi E_\nu^2}\Big[A_H + B_H \frac{(s-u)}{M^2} + C_{SM}\frac{(s-u)^2}{M^4}\Big], \tag{7.33}$$

where $x_H = m_W^2/M_H^2$, $A_H = A_{SM} + 2x_H Re(A_H^I) + x_H^2 A_H^P$, and $B_H = B_{SM} + 2x_H Re(B_H^I)$. Superscripts I and P denote the SM-Higgs interference and pure Higgs contributions, respectively. The expressions for the quantities $A_H^{I,P}$ and B_H^I are given in the Appendix 11. The terms A_H^I and B_H^I are proportional to the tiny neutrino mass, and we will ignore them in our calculation. Note that this happens because we have chosen the couplings to be given by the 2HDM II. With general couplings of the charged Higgs, these interference terms will be present. The charged Higgs contribution relative to the SM $r_H^{23} = \frac{\sigma_H(\nu_\tau)}{\sigma_{SM}(\nu_\tau)}$ is proportional to t because of the dominant term $x_t G_P^2$, where $x_t = t/4M^2$ (see the Appendix 11 for more details). Consequently, r_H^{23} is proportional to the incident neutrino energy (see Fig. (7.3)). The deviation δ_{23} is negative, as there is no interference with the SM; hence, the cross section for $\nu_\tau + n \to \tau^- + p$ is always larger than the SM cross section. This means that, if the actual θ_{23} is close to maximal, then experiments should measure θ_{23} larger than the maximal value in the presence of a charged Higgs contribution.

The differential cross section for the interaction $\bar{\nu}_\tau + p \to \tau^+ + n$ has the same form as Eq. 7.33 in the limit of a massless neutrino. The hadronic current in this case is the complex

conjugate of the one in the Appendix 11. The ratio $r_H^{13} = \frac{\sigma_H(\bar{\nu}_\tau)}{\sigma_{SM}(\bar{\nu}_\tau)}$, as well as the deviation δ_{13}, is shown in Fig. 7.4. As θ_{13} is a small angle, large $\tan\beta$ and small charged Higgs mass are preferred to produce an observable deviation δ_{13}. For instance, we find $\delta_{13} \approx 1^\circ$ and $r_H^{13} \approx 30\%$ at $E_\nu = 8$ GeV, $M_H = 200$ GeV, and $\tan\beta = 100$.

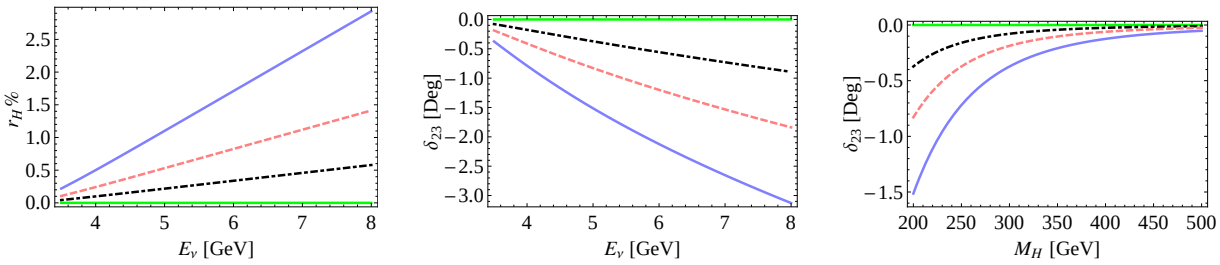

Figure 7.3. Variation of $r_H^{23}\%$ with E_ν and variation of δ_{23} with M_H and E_ν. The green line corresponds to the SM prediction. The black (dotdashed), pink (dashed), and blue (solid) lines correspond to $\tan\beta = 40, 50, 60$. The right figure is evaluated at $E_\nu = 5$ GeV, while the left figures are evaluated at $M_H = 200$ GeV. Here, we use the best-fit value $\theta_{23} = 42.8^\circ$ [285].

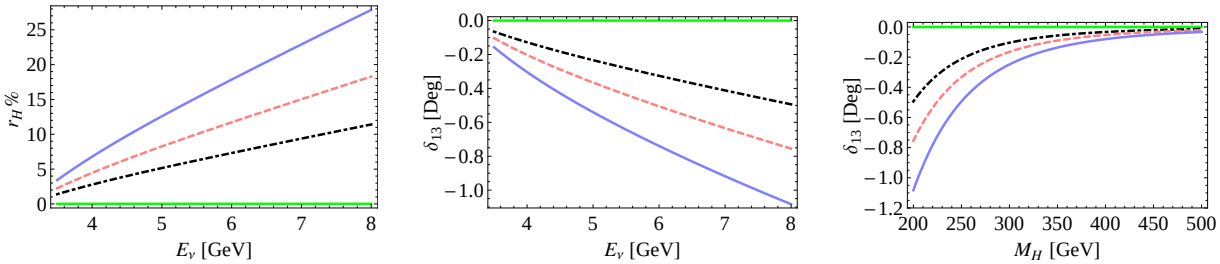

Figure 7.4. Variation of $r_H^{13}\%$ with E_ν and the variation of δ_{13} with M_H and E_ν. The green line corresponds to the SM prediction. The black (dotdashed), pink (dashed), and blue (solid) lines correspond to $\tan\beta = 80, 90, 100$. The right figure is evaluated at $E_\nu = 8$ GeV, while the left figures are evaluated at $M_H = 200$ GeV. Here, we use the inverted hierarchy value $\theta_{13} = 9.1^\circ$ [47].

7.4.3 Quasielastic neutrino interaction - W' model

Many extensions of the SM contain a W' gauge boson. We next consider modification to $\nu_\tau + n \to \tau^- + p$ and $\bar{\nu}_\tau + p \to \tau^+ + n$ in models with a W'. There are limits on the W' mass from direct searches to final states involving an electron and muon assuming SM couplings for the W' [168]. These limits generally do not apply to the W' coupling to ν_τ and τ which is relevant for our calculation.

The lowest dimension effective Lagrangian of W' interactions to the SM fermions has the form

$$\mathcal{L} = \frac{g}{\sqrt{2}} V_{f'f} \bar{f}' \gamma^\mu (g_L^{f'f} P_L + g_R^{f'f} P_R) f W'_\mu + h.c., \tag{7.34}$$

where f' and f refer to the fermions and $g_{L,R}^{f'f}$ are the left- and the right-handed couplings of the W'. For a SM-like W' boson, $g_L^{f'f} = 1$ and $g_R^{f'f} = 0$. We will assume $g_{L,R}^{f'f}$ to be real. Constraints on the couplings in Eq. (7.54) come from the hadronic τ decays. We will consider constraints from the decays $\tau^- \to \pi^-\nu_\tau$ and $\tau^- \to \rho^-\nu_\tau$.

The branching ratio for $\tau^- \to \pi^-\nu_\tau$ is

$$Br^{SM+W'}_{\tau^-\to\pi^-\nu_\tau} = Br^{SM}_{\tau^-\to\pi^-\nu_\tau}(1 + r^{\pi}_{W'})^2\,, \tag{7.35}$$

where the W' contribution is

$$r^{\pi}_{W'} = x_{W'} g_L^{\tau\nu}(g_L^{ud} - g_R^{ud})\,, \tag{7.36}$$

and $x_{W'} = m_W^2/M_{W'}^2$. The branching ratio for the $\tau^- \to \rho^-\nu_\tau$ process is

$$Br^{SM+W'}_{\tau^-\to\rho^-\nu_\tau} = Br^{SM}_{\tau^-\to\rho^-\nu_\tau}(1 + r^{\rho}_{W'})^2\,, \tag{7.37}$$

with the W' contribution

$$r^{\rho}_{W'} = x_{W'} g_L^{\tau\nu}(g_L^{ud} + g_R^{ud})\,. \tag{7.38}$$

The SM branching ratio is related to the decay rate as $Br^{SM}_{\tau^-\to\rho^-\nu_\tau} = \Gamma^{SM}_{\tau^-\to\rho^-\nu_\tau}/\Gamma_\tau$ with

$$\Gamma^{SM}_{\tau^-\to\rho^-\nu_\tau} = \frac{G_F^2}{16\pi}|V_{ud}|^2 f_\rho^2 m_\tau^3\Big(1 - \frac{m_\rho^2}{m_\tau^2}\Big)^2\Big(1 + \frac{2m_\rho^2}{m_\tau^2}\Big)\,, \tag{7.39}$$

where $f_\rho = 223$ MeV [298]. Further, the SM branching ratio can also be expressed as [297]

$$Br^{SM}_{\tau^-\to\rho^-\nu_\tau} = 1.23 Br(\tau^- \to \nu_\tau e^-\bar{\nu}_e) = 21.92 \pm 0.05\%\,. \tag{7.40}$$

The measured branching ratio is $Br(\tau^- \to \rho^-\nu_\tau)_{exp} = (23.1 \pm 0.98)\%$ [168].

Figures 7.5 and 7.6 show the allowed regions for the W' couplings. The couplings are uniformly varied in the range $[-2, 2]$ and constrained by the measured $\tau^- \to \pi^-\nu_\tau$ and $\tau^- \to \rho^-\nu_\tau$ branching ratios with 1σ errors. From Eqs. (7.36, 7.38), the case with a pure left-handed W' coupling is allowed, as shown in Figs. (7.5, 7.6). The constraints on the effective operator are consistent with the one in Ref. [280]. From Eq. 7.54 the NSI parameter $\varepsilon_{\tau\tau}^{ud(L,R)}$ defined in Ref. [280] is given as $\varepsilon_{\tau\tau}^{ud(L,R)} \equiv g_L^{\tau\nu} g_{(L,R)}^{ud}(\frac{M_W}{M_{W'}})^2$.

In the presence of the W' gauge boson, we can obtain the modified differential cross

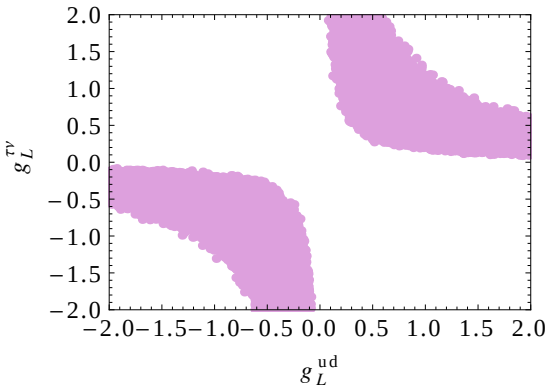

Figure 7.5. The constraints on the W' couplings without right-handed coupling at $M_{W'} = 500 - 1000$ GeV. The constraints are from $\tau^- \to \pi^-\nu_\tau$ and $\tau^- \to \rho^-\nu_\tau$ branching ratios. The errors in the branching ratios are varied within 1σ. The colored regions are allowed.

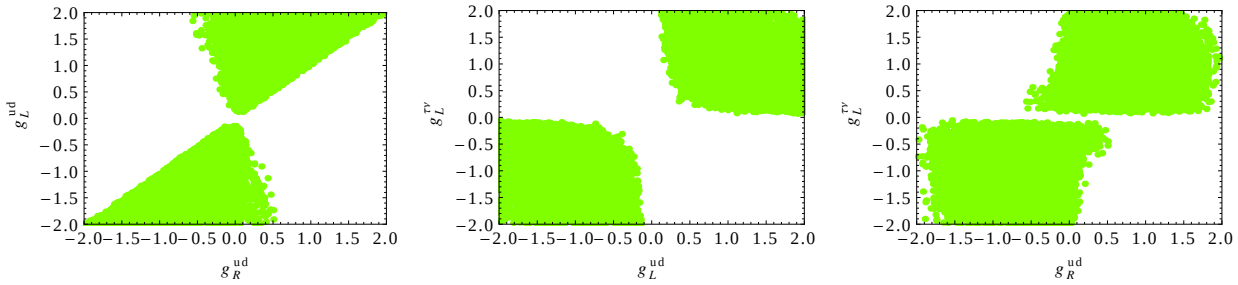

Figure 7.6. The constraints on the W' couplings with both left- and right-handed couplings at $M_{W'} = 500 - 1000$ GeV. The constraints are from $\tau^- \to \pi^-\nu_\tau$ and $\tau^- \to \rho^-\nu_\tau$ branching ratios. The errors in the branching ratios are varied within 1σ. The colored regions are allowed.

section for the reaction $\nu_\tau + n \to \tau^- + p$ as

$$\frac{d\sigma_{SM+W'}(\nu_\tau)}{dt} = \frac{M^2 G_F^2 \cos^2\theta_c}{8\pi E_\nu^2}\Big[A' + B'\frac{(s-u)}{M^2} + C'\frac{(s-u)^2}{M^4}\Big], \tag{7.41}$$

where the coefficients A', B', C' include both the SM and W' contributions. The expressions for these coefficients are given in the Appendix 11.

For a SM-like W' boson, with right-handed couplings ignored, the structure of the differential cross section is similar to the one in the SM case. Hence, the W' contribution relative to the SM $r_{W'}^{23} = \frac{\sigma_{W'}(\nu_\tau)}{\sigma_{SM}(\nu_\tau)}$ does not depend on the incident neutrino energy E_ν. We find $r_{W'}^{23} \sim 5\%$ at $M_{W'} = 500$ GeV from the hadronic tau decay constraints in Fig. (7.5). The variation of δ_{23} with the W' mass is shown in Fig. (7.7). In this case, δ_{23} is always negative and can reach up to -5° at $M_{W'} = 500$ GeV. Note that δ_{23} does not dependent on E_ν either.

Next, we consider the right-handed couplings also. The variation of $r_{W'}^{23}\%$ with $M_{W'}$ in this case is shown in Fig. (7.8). The $r_{W'}^{23}\%$ values are mostly positive which, in turn, leads

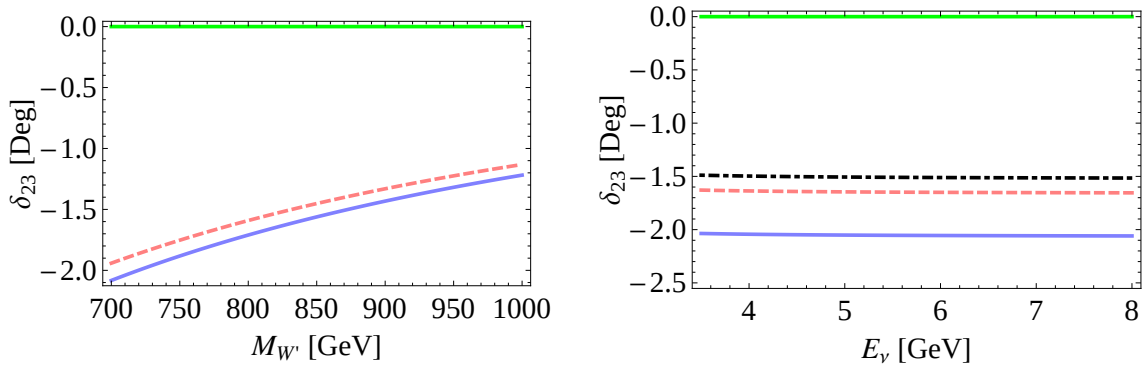

Figure 7.7. The left (right) panel illustrates the deviation δ_{23} with the W' mass (E_ν) when only left-handed W' couplings are present. The lines show predictions for some representative values of the W' couplings $(g_L^{\tau\nu_\tau}, g_L^{ud})$ taken from Fig. (7.5). The green line corresponds to the SM prediction. The blue (solid, lower) line in the left figure corresponds to (0.69, 0.89) at $E_\nu = 5$ GeV, and the blue (solid, lower) line in the right figure corresponds to (1.42, 0.22) at $M_{W'} = 500$ GeV. Here, we use the best-fit value $\theta_{23} = 42.8^\circ$ [285].

to δ_{23} being mostly negative. We find that $r^{23}_{W'}\%$ depends slightly on the neutrino energy. The variation of δ_{23} with the W' mass and E_ν are shown in Fig. (7.9).

The W' contribution to the interaction $\bar{\nu}_\tau + p \to \tau^+ + n$ leads to the following differential cross section:

$$\frac{d\sigma_{SM+W'}(\bar{\nu}_\tau)}{dt} = \frac{M^2 G_F^2 \cos^2\theta_c}{8\pi E_\nu^2}\Big[A' - B'\frac{(s-u)}{M^2} + C'\frac{(s-u)^2}{M^4}\Big]. \tag{7.42}$$

The differential cross section of the antineutrino scattering is relatively smaller than the corresponding one for the neutrino scattering because of the negative sign of the B coefficient. Thus, the value of the ratio $r^{13}_{W'} = \frac{\sigma_{W'}(\bar{\nu}_\tau)}{\sigma_{SM}(\bar{\nu}_\tau)}$ is smaller than the corresponding ratio, $r^{23}_{W'}$. Because of the smallness of θ_{13} and $r^{13}_{W'}$, the NP effect on the extraction of θ_{13} is small. Achieving large $r^{13}_{W'}$ within the constraints given in Fig. 7.6 is difficult in this model. This means the effect of the NP contribution in δ_{13} is very small and we do not plot the results of this calculations.

7.5 Δ-Resonance production

In this section we will discuss the charged Higgs and W' effects to the Δ-Resonance production.

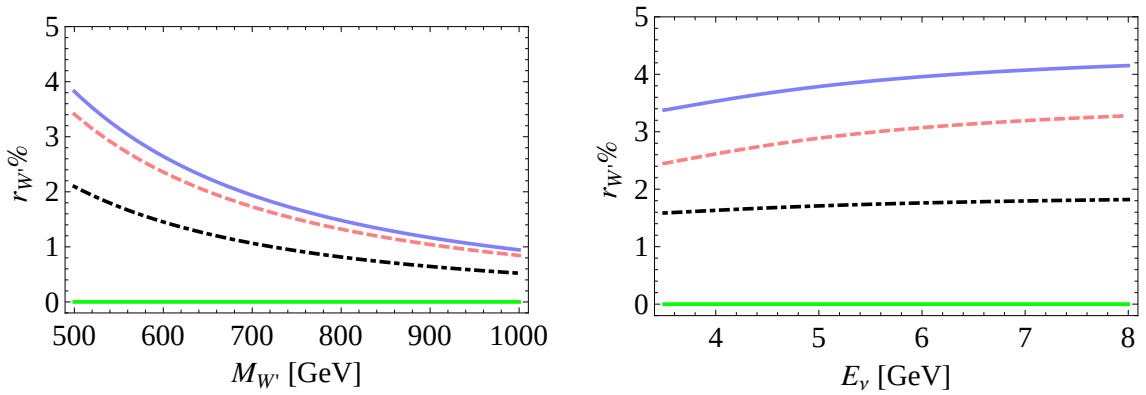

Figure 7.8. The left (right) panel illustrates the variation of $r^{23}_{W'}$% in $\nu_\tau + n \to \tau^- + p$ scattering with the W' mass (E_ν) when both left- and right-handed W' couplings are present. The lines show predictions for some representative values of the W' couplings $(g_L^{\tau\nu_\tau}, g_L^{ud}, g_R^{ud})$ taken from Fig. (7.6). The green line corresponds to the SM prediction. The blue (solid, upper) line in the left figure corresponds to (-0.94 , -1.13 , -0.85) at $E_\nu = 5$ GeV, and the blue (solid, upper) line in the right figure corresponds to (1.23 , 0.84 , 0.61) at $M_{W'} = 500$ GeV. Here, we use the best-fit value $\theta_{23} = 42.8°$ [285].

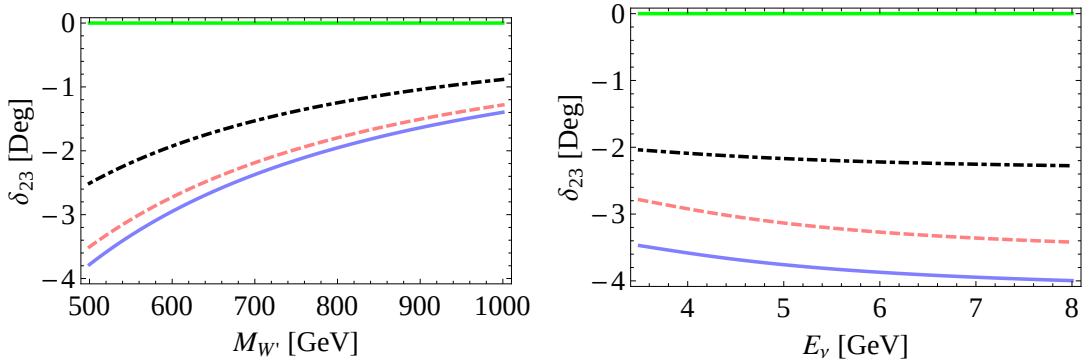

Figure 7.9. The left (right) panel illustrates the deviation δ_{23} with the W' mass (E_ν) when both the left- and right-handed W' couplings are present. The lines show predictions for some representative values of the W' couplings $(g_L^{\tau\nu_\tau}, g_L^{ud}, g_R^{ud})$ taken from Fig. (7.6). The green line corresponds to the SM prediction. The blue (solid, lower) line in the left figure corresponds to (-0.94 , -1.13 , -0.85) at $E_\nu = 5$ GeV, and the blue (solid, lower) line in the right figure corresponds to (1.23 , 0.84 , 0.61) at $M_{W'} = 500$ GeV. Here, we use the best-fit value $\theta_{23} = 42.8°$ [285].

7.5.1 Δ-Resonance production − SM

Neutrino-nucleon scattering produces many possible resonance states, one of which is the Δ-state. We consider here the SM cross section for the two processes which include ν_τ and $\bar{\nu}_\tau$,

$$\begin{aligned} \nu_\tau + n &\to \tau^- + \Delta^+, \\ \bar{\nu}_\tau + p &\to \tau^+ + \Delta^0. \end{aligned} \tag{7.43}$$

from the Hagiwara model [272]. That will represent the starting point of our original computation of NP effects due to charged Higgs and W'. Details of the SM cross section calculations can be found in Ref. [272]. The hadronic tensor is written as

$$W_{\mu\nu}^{\rm RES} = \frac{\cos^2\theta_c}{4}\,{\rm Tr}\left[P^{\beta\alpha}\Gamma_{\mu\alpha}(\not{p}+M)\overline{\Gamma}_{\nu\beta}\right]\frac{1}{\pi}\,\frac{W\Gamma(W)}{(W^2-M_\Delta^2)^2+W^2\Gamma^2(W)}. \tag{7.44}$$

Within the kinematical region of $M+m_\pi < W < W_{\rm cut}$ with $W_{\rm cut}=1.4$ GeV, we estimate the total cross section of the Δ production (Δ-RES) process by integrating over E_τ and $\cos\theta$.

7.5.2 Δ-Resonance production − Charged Higgs Effect

We consider here the charged Higgs contribution to $\nu_\tau + n \to \tau^- + \Delta^+$ and $\bar{\nu}_\tau + p \to \tau^+ + \Delta^0$. As considered in the previous section, we choose the couplings of charged Higgs interactions to the SM fermions to be given by the two Higgs doublet model of type II (2HDM II) [295]

$$\mathcal{L} \;=\; \frac{g}{2\sqrt{2}}\left[V_{u_id_j}\bar{u}_i(g_S^{u_id_j}\pm g_P^{u_id_j}\gamma^5)d_j + \bar{\nu}_i(g_S^{\nu_il_j}\pm g_P^{\nu_il_j}\gamma^5)l_j\right]\,H^\pm, \tag{7.45}$$

where u_i and d_j refer to up and down type quarks, and ν_i and l_j refer to neutrinos and the corresponding charged leptons. The other parameters are as follows: $g = e/\sin\theta_W$ is the SM weak coupling constant, $V_{u_id_j}$ is the CKM matrix element, and $g_{S,P}$ are the scalar and pseudoscalar couplings of the charged Higgs to fermions. Here, in this work, we assume the couplings $g_{S,P}$ are real and given as

$$\begin{aligned}
g_S^{u_id_j} &= \left(\frac{m_{d_j}\tan\beta + m_{u_i}\cot\beta}{M_W}\right),\\
g_P^{u_id_j} &= \left(\frac{m_{d_j}\tan\beta - m_{u_i}\cot\beta}{M_W}\right),\\
g_S^{\nu_il_j} &= g_P^{\nu_il_j} = \frac{m_{l_j}\tan\beta}{M_W},
\end{aligned} \tag{7.46}$$

where $\tan\beta$ is the ratio between the two vev's of the two Higgs doublets. From Eq. 7.45 we can construct the NSI parameters defined in Ref [299] as $\varepsilon_{\tau\tau}^{ud(L)} \equiv \frac{m_u m_\tau}{m_H^2}$ and $\varepsilon_{\tau\tau}^{ud(R)} \equiv \frac{m_d m_\tau \tan^2\beta}{m_H^2}$.

The (pseudo-)scalar hadronic current J for the processes $\nu_\tau + n \to \tau^- + \Delta^+$ and $\bar{\nu}_\tau + p \to$

$\tau^+ + \Delta^0$ in the 2HDM II is defined by

$$J = \langle \Delta^+(p')|\hat{J}|n(p)\rangle = \langle \Delta^0(p')|\hat{J}|p(p)\rangle = \bar{\psi}^{\alpha}_{\Delta^+}(p')\,\Gamma_\alpha\,u_n(p), \tag{7.47}$$

where the vertex Γ_α is expressed as

$$\Gamma_\alpha = g_S^{u_i d_j} G_V X_\alpha + g_P^{u_i d_j} G_A Y_\alpha \gamma^5. \tag{7.48}$$

Applying the equation of motion, one can obtain the hadronic matrix elements for the scalar and pseudoscalar currents

$$\begin{aligned} \langle \Delta^+(p')|\bar{u}d|n(p)\rangle &= \bar{\psi}^{\alpha}_{\Delta^+}(p') G_V X_\alpha u_n(p), \\ -\langle \Delta^+(p'))|\bar{u}\gamma_5 d|n(p)\rangle &= \bar{\psi}^{\alpha}_{\Delta^+}(p') G_A Y_\alpha \gamma_5 u_n(p)\,, \end{aligned} \tag{7.49}$$

where X_α and Y_α are 4-vectors and

$$\begin{aligned} G_V(t) &= \frac{C_5^A(t) + C_6^A(t)\; t/M^2}{m_u - m_d}, \\ G_A(t) &= 0, \\ X_\alpha &= q_\alpha. \end{aligned} \tag{7.50}$$

The hadronic contribution can be written as

$$W^{\rm RES} = \frac{\cos^2\theta_c}{4}\,{\rm Tr}\left[P^{\beta\alpha}\Gamma_\alpha(\not{p} + M)\overline{\Gamma}_\beta\right]\frac{1}{\pi}\,\frac{W\Gamma(W)}{(W^2 - M_\Delta^2)^2 + W^2\Gamma^2(W)}. \tag{7.51}$$

We use here the constraints on the NP parameters ($M_H,\ \tan\beta$) discussed in previous section to calculate the cross sections. The ratios between the charged Higgs contributions to the two processes $\nu_\tau + n \to \tau^- + \Delta^+$ and $\bar{\nu}_\tau + p \to \tau^+ + \Delta^0$ relative to the SM cross sections $r_H^{23} = \frac{\sigma_H(\nu_\tau)}{\sigma_{SM}(\nu_\tau)}$ and $r_H^{13} = \frac{\sigma_H(\bar{\nu}_\tau)}{\sigma_{SM}(\bar{\nu}_\tau)}$, respectively, can be obtained within the kinematical interval $M + m_\pi < W < 1.4$ GeV. The hadronic contribution to the matrix element is proportional to $q_\alpha (= X_\alpha)$ which varies within the small interval in Eq. 11.11. Thus, we require relatively large values of the NP parameter $\tan\beta$ to enhance the NP contributions. The ratios r_H^{23} and r_H^{13} decrease with increasing the incident neutrino energy and the charged Higgs mass, see Figs. (7.10, 7.12). The deviations δ_{23} and δ_{13} of the atmospheric and reactor mixing angles, respectively, are negative as there is no interference term with the SM, see Figs. (7.11, 7.13). Hence, the total cross sections for $\nu_\tau + n \to \tau^- + \Delta^+$ and $\bar{\nu}_\tau + p \to \tau^+ + \Delta^0$ are always larger than the SM cross section. This means that, if the actual θ_{23} is close to maximal, then experiments should measure θ_{23} larger than the maximal value in the presence of a charged

Higgs contribution. As an example, we find that $\delta_{23} \approx -5^\circ$ and $r_H^{23} \approx 6\%$ at $E_\nu = 4$ GeV, $M_H = 200$ GeV, and $\tan\beta = 60$. As θ_{13} is a small angle, the deviation δ_{13} for similar set of parameters is small. For instance, we find $\delta_{13} \approx -0.3^\circ$ and $r_H^{13} \approx 6.5\%$ at $E_\nu = 4$ GeV, $M_H = 200$ GeV, and $\tan\beta = 60$.

In Fig. 7.14 we show the δ_{23} result taking into account the atmospheric neutrino flux $\Phi(E_\nu)$ for Kamioka where the Super-Kamiokande experiment is located [300]. In this case the actual mixing angle θ_{23} is given as

$$\sin^2 2\theta_{23} = \sin^2 2\theta_{23}^{SM} R_H^{23} \tag{7.52}$$

where

$$R_H^{23} = \int \sin^2 \frac{\Delta m_{23}^2 L}{E_\nu} \Phi(E_\nu) \frac{d\sigma^{SM}(E_\nu, t)}{dt} dt dE_\nu \Big/ \int \sin^2 \frac{\Delta m_{23}^2 L}{E_\nu} \Phi(E_\nu) \frac{d\sigma^{tot}(E_\nu, t)}{dt} dt dE_\nu \tag{7.53}$$

with $\sigma^{tot} = \sigma^{SM} + \sigma^{NP}$. The atmospheric neutrino flux in Ref. [300] is calculated averaged over all directions in the 3-dimensional scheme. We fixed the neutrino production height [301] at an average height with 99% of accumulated probability for the production height. We integrate over the incoming neutrino energy from the threshold energy to 20 GeV. We find that the effect of the neutrino flux does not significantly modify the results - of order 0.1 degree.

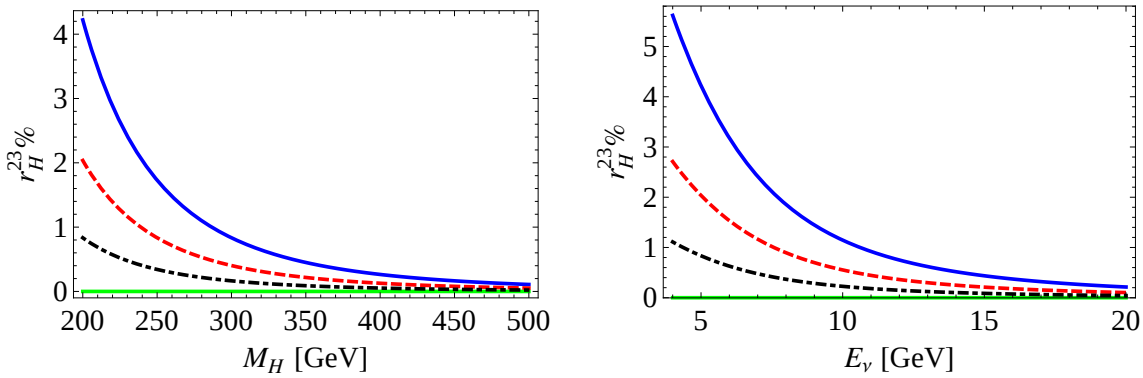

Figure 7.10. Resonance (H): The figures illustrate variation of $r_H^{23}\%$ with M_H (left) and E_ν (right). The green line corresponds to the SM prediction. The black (dotdashed), red (dashed), and blue (solid) lines correspond to $\tan\beta = 40, 50, 60$ at $E_\nu = 5$ GeV (left) and at $M_H = 200$ GeV (right).

7.5.3 Δ-Resonance production - W' model

We next consider modification to the Δ-RES production in $\nu_\tau + n \to \tau^- + \Delta^+$ and $\bar{\nu}_\tau + p \to \tau^+ + \Delta^0$ in models with a W' gauge boson. The lowest dimension effective

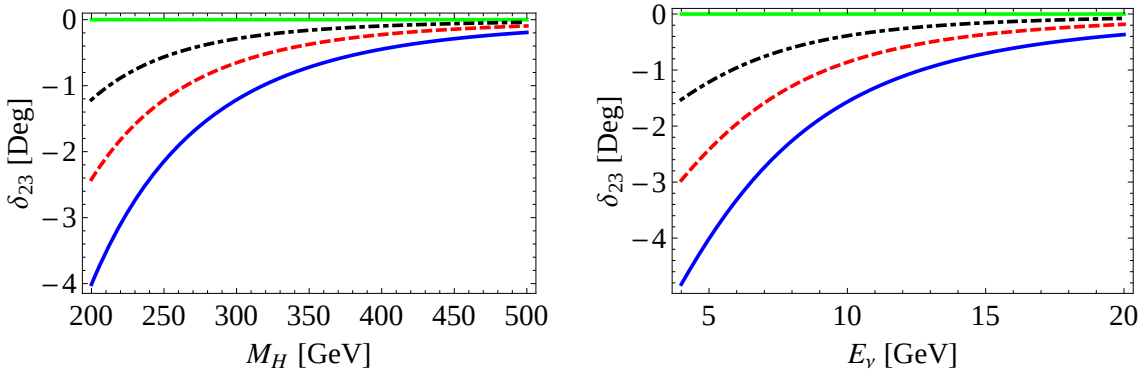

Figure 7.11. Resonance (H): The figures illustrate variation of δ_{23} with M_H (left) and E_ν (right). The green line corresponds to the SM prediction. The black (dotdashed), red (dashed), and blue (solid) lines correspond to $\tan\beta = 40, 50, 60$ at $E_\nu = 5$ GeV (left) and at $M_H = 200$ GeV (right). Here, we use the best-fit value $\theta_{23} = 42.8°$ [285].

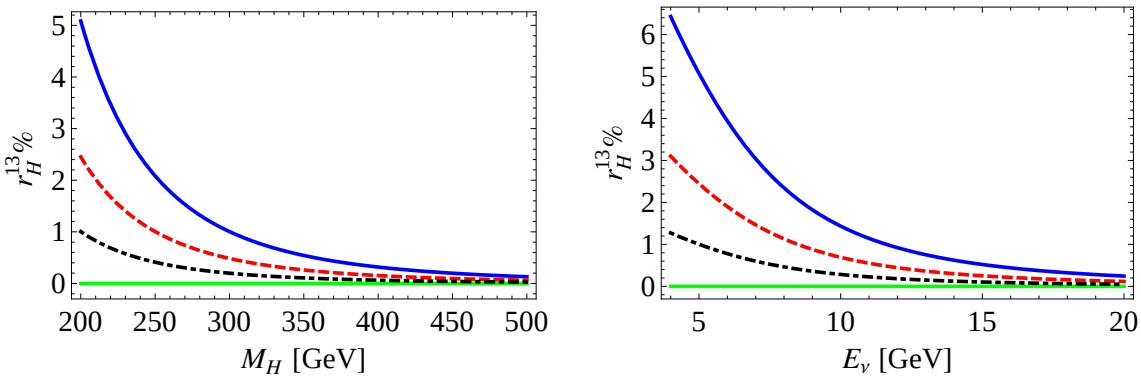

Figure 7.12. Resonance (H): The figures illustrate variation of $r_H^{13}\%$ with M_H (left) and E_ν (right). The green line corresponds to the SM prediction. The black (dotdashed), red (dashed), and blue (solid) lines correspond to $\tan\beta = 40, 50, 60$ at $E_\nu = 5$ GeV (left) and at $M_H = 200$ GeV (right).

Lagrangian of W' interactions to the SM fermions has the form

$$\mathcal{L} \;=\; \frac{g}{\sqrt{2}} V_{f'f}\, \bar{f}'\gamma^\mu (g_L^{f'f} P_L + g_R^{f'f} P_R) f W'_\mu + \;\; h.c., \tag{7.54}$$

where f' and f refer to the fermions and $g_{L,R}^{f'f}$ are the left and the right handed couplings of the W'. We will assume $g_{L,R}^{f'f}$ to be real. Constraints on the couplings in Eq. (7.54) come from the hadronic τ decay channels $\tau^- \to \pi^-\nu_\tau$ and $\tau^- \to \rho^-\nu_\tau$, which are consistent with the ones in Ref. [299]. From Eq. 7.54, the NSI parameters $\varepsilon_{\tau\tau}^{ud(L,R)}$ defined in Ref. [299] are given as $\varepsilon_{\tau\tau}^{ud(L,R)} \equiv g_L^{\tau\nu} g_{(L,R)}^{ud} (\frac{M_W}{M_{W'}})^2$.

The current J_μ for the process $\nu_\tau + n \to \tau^- + \Delta^+$ and $\bar{\nu}_\tau + p \to \tau^+ + \Delta^0$ in the W' model

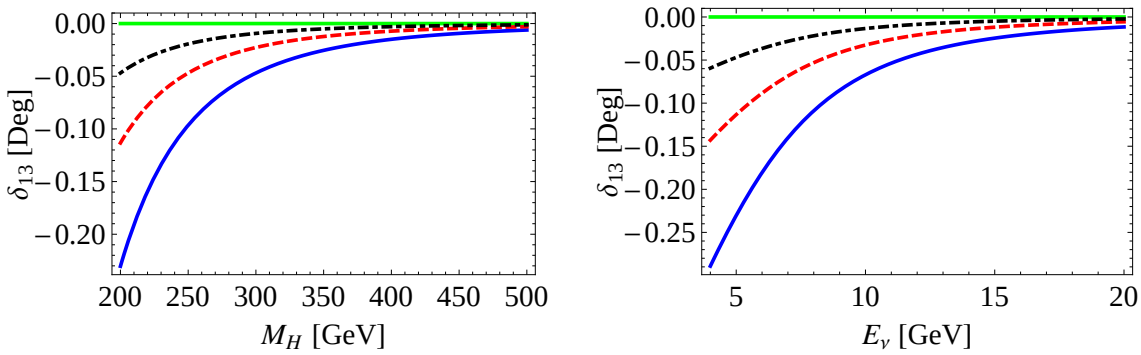

Figure 7.13. Resonance (H): The figures illustrate variation of δ_{13} with M_H (left) and E_ν (right). The green line corresponds to the SM prediction. The black (dotdashed), red (dashed), and blue (solid) lines correspond to $\tan\beta = 40, 50, 60$ at $E_\nu = 5$ GeV (left) and at $M_H = 200$ GeV (right). Here, we use the best-fit value $\theta_{13} = 9.1^\circ$ [47].

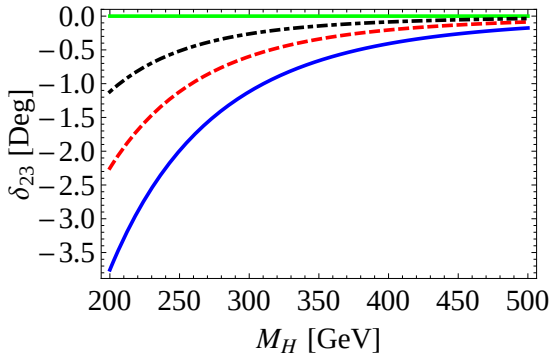

Figure 7.14. Resonance (H): The figures illustrate variation of δ_{23} with M_H. The green line corresponds to the SM prediction. The black (dotdashed), red (dashed), and blue (solid) lines correspond to $\tan\beta = 40, 50, 60$. Here, we use the best-fit value $\theta_{23} = 42.8^\circ$ [285]. We take into account the atmospheric neutrino flux for Kamioka where the Super-Kamiokande experiment locates [300].

is defined as

$$J_\mu = \langle \Delta^+(p')|\hat{J}_\mu|n(p)\rangle = \langle \Delta^0(p')|\hat{J}_\mu|p(p)\rangle = \bar{\psi}^\alpha_{\Delta^+}(p')\,(g_L^{ud}\Gamma_{\mu\alpha} + g_R^{ud}\Gamma'_{\mu\alpha})\,u_n(p), \tag{7.55}$$

where $\Gamma_{\mu\alpha}$ is the left-handed vertex, given in Ref. [272], and $\Gamma'_{\mu\alpha}$ is the right-handed vertex, with $(\gamma_5 \to -\gamma_5)$, for the W' gauge boson. The hadronic tensor in the W' model is now calculated from

$$\begin{aligned} W^{\rm RES}_{\mu\nu} &= \frac{\cos^2\theta_c}{4}\,{\rm Tr}\left[P^{\beta\alpha}(g_L^{ud}\Gamma_{\mu\alpha} + g_R^{ud}\Gamma'_{\mu\alpha})(\not{p} + M)(g_L^{ud}\bar{\Gamma}_{\nu\beta} + g_R^{ud}\bar{\Gamma}'_{\nu\beta})\right] \\ &\quad \frac{1}{\pi}\frac{W\Gamma(W)}{(W^2 - M_\Delta^2)^2 + W^2\Gamma^2(W)}. \end{aligned} \tag{7.56}$$

Using the constraints on the W' couplings, the ratios of the W' contributions to $\nu_\tau + n \to \tau^- + \Delta^+$ and $\bar{\nu}_\tau + p \to \tau^+ + \Delta^0$ relative to the SM cross sections $r^{23}_{W'} = \frac{\sigma_{W'}(\nu_\tau)}{\sigma_{SM}(\nu_\tau)}$ and $r^{13}_{W'} = \frac{\sigma_{W'}(\bar{\nu}_\tau)}{\sigma_{SM}(\bar{\nu}_\tau)}$, respectively, are shown in Figs. (7.15, 7.18). The $r^{23}_{W'}$ and $r^{13}_{W'}$ values are mostly positive which, in turn, leads to δ_{23} and δ_{13} being mostly negative. The variation of δ_{23} and δ_{13} with the W' mass and E_ν in the SM-like case, with only left-handed couplings, and for the case where both the LH and RH couplings are present are shown in Figs. (7.16, 7.17, 7.19). As a typical example, we find that $\delta_{23} \approx -14^\circ$ at $E_\nu = 4$ GeV, $M_{W'} = 200$ GeV, and $(g_L^{\tau\nu_\tau}, g_L^{ud}, g_R^{ud}) = (1.23, 0.84, 0.61)$. Because of the smallness of θ_{13}, the NP effect on the extraction of θ_{13} is small. Achieving large δ_{13} within the constraints given in previous section is difficult in this model. As an example, we find that $\delta_{13} \approx -2^\circ$ at $E_\nu = 4$ GeV, $M_{W'} = 200$ GeV, and $(g_L^{\tau\nu_\tau}, g_L^{ud}, g_R^{ud}) = (1.23, 0.84, 0.61)$. In Fig. 7.20, the results show small modification to the δ_{23} values when considering the atmospheric neutrino flux [300] - of the size of one degree.

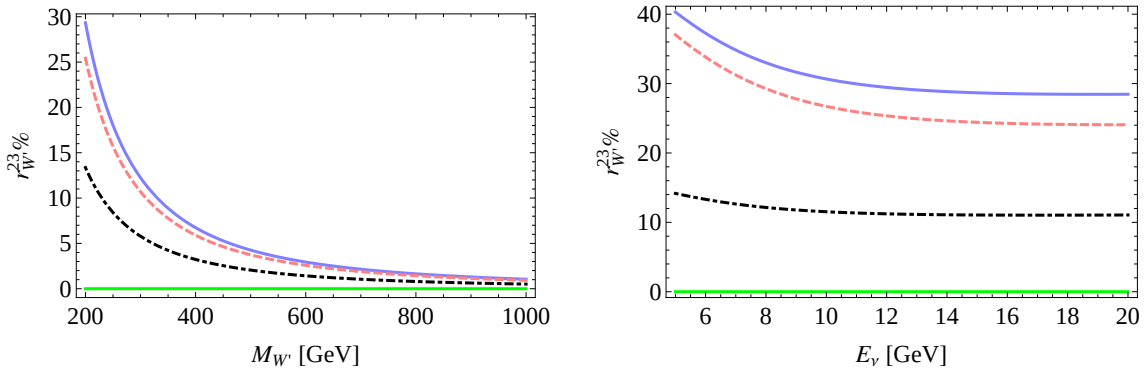

Figure 7.15. Resonance (W'): The left (right) panel figures illustrate the variation of $r^{23}_{W'}$% with the W' mass $M_{W'}$ (E_ν) when both left and right-handed W' couplings are present. The lines show predictions for some representative values of the W' couplings $(g_L^{\tau\nu_\tau}, g_L^{ud}, g_R^{ud})$. The green line (solid, lower) corresponds to the SM prediction. The blue line (solid, upper) in the left figure corresponds to (-0.94 , -1.13 , -0.85) at $E_\nu = 17$ GeV, and the blue line (solid, upper) in the right figure corresponds to (1.23 , 0.84 , 0.61) at $M_{W'} = 200$ GeV.

7.6 Deep inelastic scattering

In this section we will discuss the charged Higgs and W' effects to the Deep inelastic scattering.

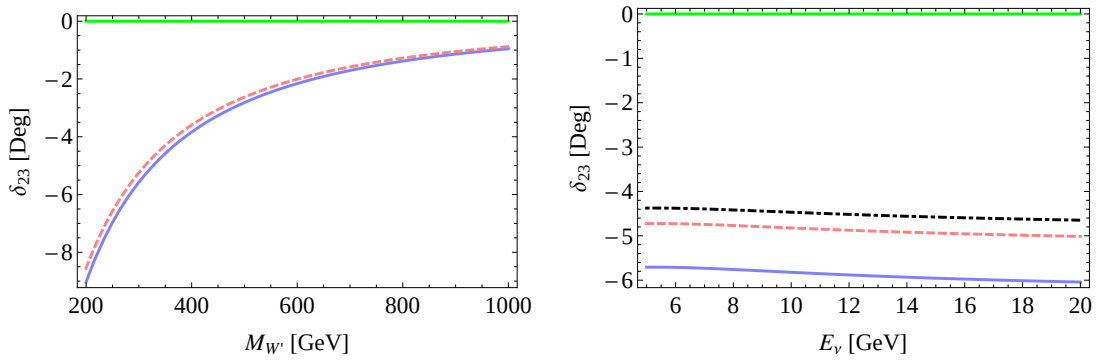

Figure 7.16. Resonance (W'): The left (right) panel figures illustrate the deviation δ_{23} with the W' mass $M_{W'}$ (E_ν) when only left-handed W' couplings are present. The lines show predictions for some representative values of the W' couplings $(g_L^{\tau\nu_\tau}, g_L^{ud})$. The green line (solid, upper) corresponds to the SM prediction. The blue line (solid, lower) in the left figure corresponds to (0.69, 0.89) at $E_\nu = 17$ GeV, and the blue line (solid, lower) in the right figure corresponds to (1.42, 0.22) at $M_{W'} = 200$ GeV. Here, we use the best-fit value $\theta_{23} = 42.8^\circ$ [285].

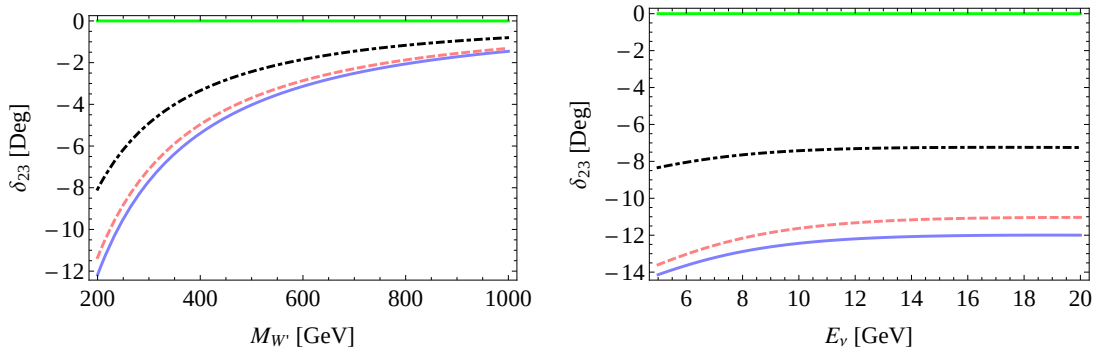

Figure 7.17. Resonance (W'): The left (right) panel figures illustrate the deviation δ_{23} with the W' mass $M_{W'}$ (E_ν) when both left and right-handed W' couplings are present. The lines show predictions for some representative values of the W' couplings $(g_L^{\tau\nu_\tau}, g_L^{ud}, g_R^{ud})$. The green line (solid, upper) corresponds to the SM prediction. The blue line (solid, lower) in the left figure corresponds to (-0.94 , -1.13 , -0.85) at $E_\nu = 17$ GeV, and the blue line (solid, lower) in the right figure corresponds to (1.23 , 0.84 , 0.61) at $M_{W'} = 200$ GeV. Here, we use the best-fit value $\theta_{23} = 42.8^\circ$ [285].

7.6.1 Deep inelastic scattering – SM

In this section, we present the standard model cross sections for the two deep inelastic scattering (DIS) processes which include ν_τ and $\bar{\nu}_\tau$,

$$\begin{aligned} \nu_\tau + N &\to \tau^- + X, \\ \bar{\nu}_\tau + N &\to \tau^+ + X. \end{aligned} \tag{7.57}$$

From Hagiwara model, see Ref. [272] for details, the differential cross section can be

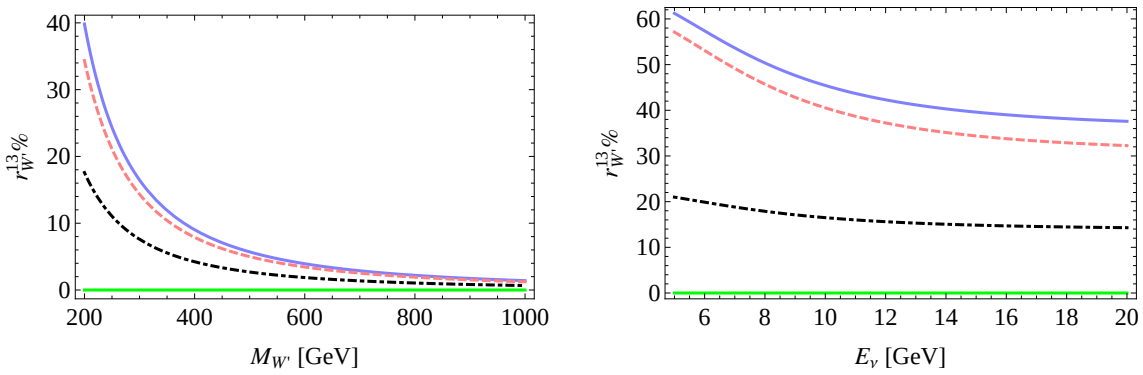

Figure 7.18. Resonance (W'): The left (right) panel figures illustrate the variation of $r^{13}_{W'}\%$ with the W' mass $M_{W'}$ (E_ν) when both left and right-handed W' couplings are present. The lines show predictions for some representative values of the W' couplings $(g_L^{\tau\nu_\tau}, g_L^{ud}, g_R^{ud})$. The green line (solid, lower) corresponds to the SM prediction. The blue line (solid, upper) in the left figure corresponds to (-0.94 , -1.13 , -0.85) at $E_\nu = 17$ GeV, and the blue line (solid, upper) in the right figure corresponds to (1.23 , 0.84 , 0.61) at $M_{W'} = 200$ GeV.

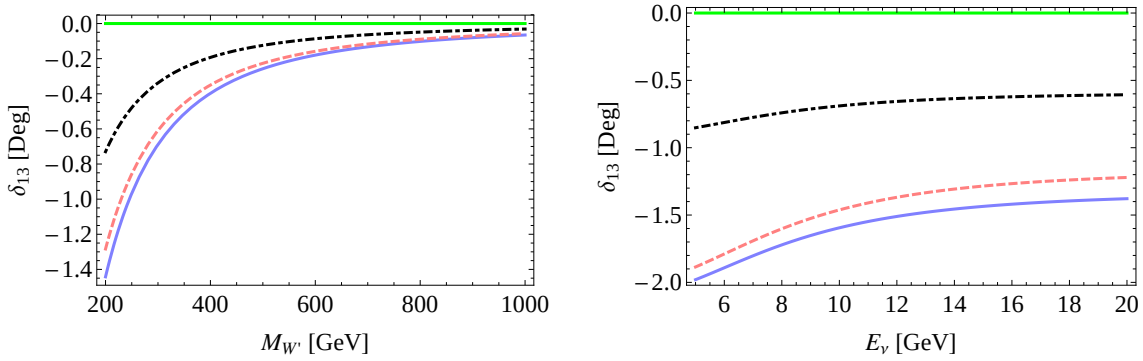

Figure 7.19. Resonance (W'): The left (right) panel figures illustrate the deviation δ_{13} with the W' mass $M_{W'}$ (E_ν) when both left and right-handed W' couplings are present. The lines show predictions for some representative values of the W' couplings $(g_L^{\tau\nu_\tau}, g_L^{ud}, g_R^{ud})$. The green line (solid, upper) corresponds to the SM prediction. The blue line (solid, lower) in the left figure corresponds to (-0.94 , -1.13 , -0.85) at $E_\nu = 17$ GeV, and the blue line (solid, lower) in the right figure corresponds to (1.23 , 0.84 , 0.61) at $M_{W'} = 200$ GeV. Here, we use the best-fit value $\theta_{13} = 9.1^\circ$ [47].

parametrized as follows, for $Q^2 \ll m_W^2$,

$$\frac{d^2\sigma^{\nu_\tau(\bar{\nu}_\tau)}}{dxdy} = \left(\frac{G_F^2 V_{qq'}^2}{2\pi}\right) y \left(A\,W_1 + \frac{1}{M^2} B\,W_2 \pm \frac{1}{M^2} C\,W_3 + \frac{1}{M^2} D\,W_5\right) \delta(\xi - x), \quad (7.58)$$

where $p_q^\mu = \xi p^\mu$ is the four-momentum of the scattering quark and ξ is its momentum

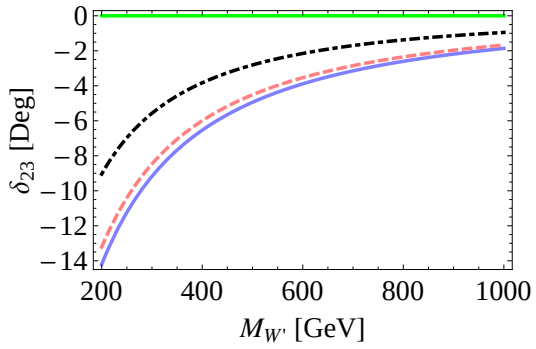

Figure 7.20. Resonance (W'): The figure illustrates the deviation δ_{23} with the W' mass $M_{W'}$ when both left and right-handed W' couplings are present. The lines show predictions for some representative values of the W' couplings $(g_L^{\tau\nu_\tau}, g_L^{ud}, g_R^{ud})$. The green line (solid, upper) corresponds to the SM prediction. The blue line (solid, lower) corresponds to (-0.94 , -1.13 , -0.85). Here, we use the best-fit value $\theta_{23} = 42.8^\circ$ [285]. We take into account the atmospheric neutrino flux for Kamioka where the Super-Kamiokande experiment locates [300].

fraction. The coefficients A,B,C,D are defined as

$$\begin{aligned} A &= y\left(yx + \frac{{m_l}^2}{2E_\nu M}\right), \\ B &= \left(1 - \frac{{m_l}^2}{4{E_\nu}^2}\right) - \left(1 + \frac{Mx}{2E_\nu}\right) y, \\ C &= 2y\left(x\left(1 - \frac{y}{2}\right) - \frac{{m_l}^2}{4E_\nu M}\right), \\ D &= \frac{{m_l}^2}{E_\nu M}, \end{aligned} \tag{7.59}$$

where x is the Bjorken variable and y is the inelasticity and they are related by

$$x = \frac{Q^2}{2E_\nu M y}. \tag{7.60}$$

The functions $W_{1,2,3,5}$ are given in Ref. [272].

7.6.2 Deep inelastic scattering − Charged Higgs Effect

The charged Higgs contributions to the matrix elements of the interactions $\nu_\tau + N \to \tau^- + X$ and $\bar{\nu}_\tau + N \to \tau^+ + X$ are given by

$$\begin{aligned} M_H^{\nu_\tau} &= \left(\frac{G_F V_{qq'}}{\sqrt{2}}\right) X_H \, g_S^{\nu_\tau \tau} \, [\bar{u}_\tau(k') \, (1+\gamma_5) u_{\nu_\tau}(k)] \, \left[\bar{u}_{q'}(p'_{q'})(g_S^{qq'} + g_P^{qq'}\gamma_5) \, u_q(p_q)\right], \\ M_H^{\bar{\nu}_\tau} &= \left(\frac{G_F V_{qq'}}{\sqrt{2}}\right) X_H \, g_S^{\nu_\tau \tau} \, [\bar{v}_{\nu_\tau}(k)(1-\gamma_5) v_\tau(k')] \, \left[\bar{u}_{q'}(p'_{q'})(g_S^{qq'} - g_P^{qq'}\gamma_5) \, u_q(p_q)\right], \end{aligned} \tag{7.61}$$

where $q, q' = (u_i, d_j)$ and the couplings $g_{S,P}^{qq'}$, $g_S^{\nu_\tau \tau}$ are defined in Eq. 7.46.

The differential cross section is given by

$$\begin{aligned} \frac{d^2\sigma^{\nu_\tau(\bar{\nu}_\tau)}}{dxdy} &= \left(\frac{G_F^2 V_{qq'}^2}{2\pi}\right) X_H^2 \, (g_S^{v_l l})^2 \, y \, L_{\mu\nu}^{\nu_\tau(\bar{\nu}_\tau)} \, W^{\mu\nu} \, \delta(\xi - x) \\ &= \left(\frac{G_F^2 V_{qq'}^2 E_\nu \, M}{\pi}\right) X_H^2 \, (g_S^{v_l l})^2 \, \left[y\left(yx + \frac{{m_l}^2}{2E_\nu M}\right)\right] \\ &\quad \frac{1}{4} \, \left[(g_S^{qq'})^2 + (g_P^{qq'})^2\right] \, F_1 \, \delta(\xi - x), \end{aligned} \tag{7.62}$$

where $X_H = M_W^2/M_H^2$ and the definitions of the 2HDM coupling constants are given in Eqs. 7.46. There is no interference term of the SM and NP amplitudes. Thus, with the constraints on the NP parameters $(M_H, \, \tan\beta)$, the charged Higgs contributions relative to the SM $r_H^{23} = \sigma_H(\nu_\tau)/\sigma_{SM}(\nu_\tau)$ and $r_H^{13} = \sigma_H(\bar{\nu}_\tau)/\sigma_{SM}(\bar{\nu}_\tau)$ are small within the kinematical interval $W_{cut} < W < \sqrt{s} - m_\tau$ GeV with $W_{cut} = 1.4$ GeV. Thus, the deviations δ_{23} and δ_{13} of the mixing angles are negligibly small.

7.6.3 Deep inelastic scattering - W' model

The matrix elements are

$$\begin{aligned} M_{W'}^{\nu_\tau} &= \left(\frac{-iG_F V_{qq'} K_{W'}}{\sqrt{2}}\right) \, [\bar{u}_\tau(k')\gamma^\mu(1-\gamma_5)u_{\nu_\tau}(k)] \, \left[\bar{u}_{q'}(p'_{q'}) \, \gamma_\mu \, (\gamma_{W'}^\rho - \gamma_{W'}^\kappa\gamma_5) \, u_q(p_q)\right], \\ M_{W'}^{\bar{\nu}_\tau} &= \left(\frac{-iG_F V_{qq'} K_{W'}}{\sqrt{2}}\right) \, [\bar{v}_{\nu_\tau}(k)\gamma^\mu(1-\gamma_5)v_\tau(k')] \, \left[\bar{u}_{q'}(p'_{q'}) \, \gamma_\mu \, (\gamma_{W'}^\rho - \gamma_{W'}^\kappa\gamma_5) \, u_q(p_q)\right], \end{aligned} \tag{7.63}$$

where the definitions are

$$\begin{aligned}
\gamma^{\rho}_{W'} &= X_{W'} g_L^{\nu_\tau \tau}(g_L^{qq'} + g_R^{qq'}), \\
\gamma^{\kappa}_{W'} &= X_{W'} g_L^{\nu_\tau \tau}(g_L^{qq'} - g_R^{qq'}), \\
X_{W'} &= \left(\frac{m_W^2}{m_{W'}^2}\right), \\
K_{W'} &= \left(1 + \frac{Q^2}{m_{W'}^2}\right)^{-1}.
\end{aligned} \tag{7.64}$$

The total differential cross section has the same form as the SM one in Eq. (7.58), after setting $K_{W'}^2 \sim 1$,

$$\frac{d^2\sigma^{\nu_\tau(\bar{\nu}_\tau)}_{SM+W'}}{dxdy} = \left(\frac{G_F^2 V_{qq'}^2}{2\pi}\right)\, y\left(A'\, W_1 + \frac{1}{M^2} B'\, W_2 \pm \frac{1}{M^2} C'\, W_3 + \frac{1}{M^2} D'\, W_5\right)\delta(\xi - x), \tag{7.65}$$

where A',B',C', and D' are defined as:

$$\begin{aligned}
A' &= \frac{1}{2} A\left(|a'|^2 + |b'|^2\right), \\
B' &= \frac{1}{2} B\left(|a'|^2 + |b'|^2\right), \\
C' &= Re[a'b'^*]C, \\
D' &= \frac{1}{2} D\left(|a'|^2 + |b'|^2\right).
\end{aligned} \tag{7.66}$$

with

$$\begin{aligned}
a' &= 1 + \gamma^{\rho}_{W'}, \\
b' &= 1 + \gamma^{\kappa}_{W'}.
\end{aligned} \tag{7.67}$$

The ratios of the W' contributions to the SM cross sections $r^{23}_{W'}$ and $r^{13}_{W'}$ and the deviations δ_{23} and δ_{13} are shown within the allowed kinematical range $M + m_\pi < W < 1.4$ GeV in Figs. (7.22, 7.23, 7.24, 7.25). The $r^{23}_{W'}$ and $r^{13}_{W'}$ values are mostly positive which, in turn, leads to δ_{23} and δ_{13} being mostly negative, respectively. As some examples, we find that $\delta_{23} \approx -14^\circ$ and $\delta_{13} \approx -1.5^\circ$ at $E_\nu = 17$ GeV, $M_{W'} = 200$ GeV, and $(g_L^{\tau\nu_\tau}, g_L^{ud}, g_R^{ud}) = (-0.94, -1.13, -0.85)$. In Fig. 7.26, the results show a negligible change to the δ_{23} values when considering the atmospheric neutrino flux [300].

Finally, we note that one could detect the presence of NSI's by comparing the number of observed events to the number of expected events based on the SM. One can calculate the

number of events in the SM as $N_{\rm SM} \pm \Delta N_{\rm SM}$ where $\Delta N_{\rm SM}$ is the error in the SM estimation of the number of events. If the number of events estimated in the W' model $N_{\rm NSI}$ falls beyond the uncertainty of the SM measurement, then the impact of NSI is large enough to be detectable at neutrino oscillation experiments.
The rate of change of the observed electron and muon-neutrino scattering cross sections with respect to the neutrino energy become constant at high energies [302], i.e. $\sigma_{\nu_{e/\mu}}(E) = \left(d\sigma_{\nu_{e,\mu}}/dE\right)^{\rm const} E$. Because of the kinematic effects due to the τ-lepton mass, the ν_τ cross section can be parametrized as [268]

$$\sigma_{\nu_\tau}^{\rm SM} = \left(\frac{d\sigma_{\nu_\tau}}{dE}\right)^{\rm const} EK(E), \tag{7.68}$$

where $(d\sigma_{\nu_\tau}/dE)^{\rm const}$ is the energy-independent factor of the cross section, and K gives the part of the tau-neutrino cross section that depends on kinematic effects due to the τ-lepton mass. From the measured muon-neutrino cross section in the PDG [302], $\left(d\sigma_{\nu_\mu}/dE\right)^{\rm const} = (0.51 \pm 0.056) \times 10^{-38}$ cm^2/GeV. The average error (0.056×10^{-38} cm^2/GeV) of the cross-section includes the systematic, statistical, and normalization uncertainties and has been taken for neutrino energies above 30 GeV, where the DIS contribution is dominant. For instance, the measured muon-neutrino scattering cross section at MINOS experiment [303] provides an explicit value $\left(d\sigma_{\nu_\mu}/dE\right)^{\rm const} = (0.675 \pm 0.012 \pm 0.004 \pm 0.011) \times 10^{-38}$ cm^2/GeV with the uncertainty types statistical, systematic, and normalization resulting in the total uncertainty 0.018 for the energy range 30-50 GeV (the MINOS results are included in the average value). Since we consider the NP contributions in the tau sector only, we can take the energy-independent factor of the SM tau-neutrino cross section to be given as $(d\sigma_{\nu_\tau}/dE)^{\rm const} = \left(d\sigma_{\nu_\mu}/dE\right)^{\rm const}$ because of the SM universality of the weak interactions. The uncertainty of the number of ν_τ events calculated in the SM limit follow from the uncertainty of $(d\sigma_{\nu_\tau}/dE)^{\rm const}$.

The number of tau-neutrino events in the SM is found to be $N_{\rm SM} = 30.66 \pm 3.37$ using the PDG cross section value for the 22.5 kton fiducial volume of the Super-K detector [265] during the 2806 day running period. The atmospheric neutrino flux [301] has been taken for vertically upward going neutrinos ($\cos\theta = -1$) where θ is the zenith angle. The distance d traveled by atmospheric neutrinos can be calculated by [301]

$$d = \sqrt{(h^2 + 2R_e h) + (R_e \cos\theta)^2} - R_e \cos\theta, \tag{7.69}$$

where h is the neutrino production height and R_e is the radius of the earth - its surface is assumed to be spherical. In Ref. [301] there is a distribution for the atmospheric neutrino

flux at a zenith angle around ($\cos\theta = 1$). Since the distribution of the flux over the zenith angle is symmetric at high neutrino energy, see [273], the flux is the same at $\cos\theta = -1$ and 1. We choose to work with $\cos\theta = -1$ because the distance d will be maximum, through the diameter of the earth, which in turns enhances the transition probability We take $h = 4.5 \times 10^4$ m for the accumulated probability of 99% for the vertical production height [301] and we integrate over the neutrino energies from $30 - 100$ GeV.

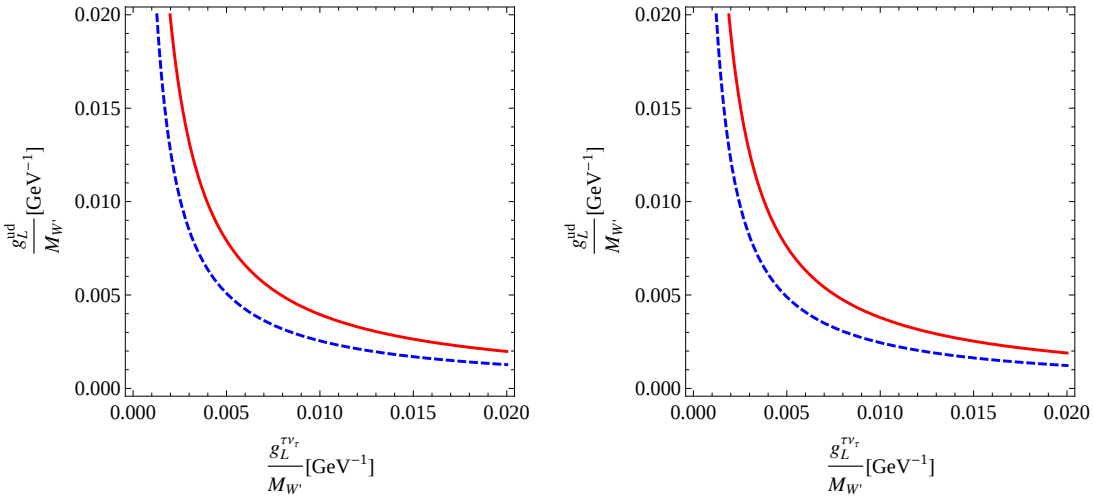

Figure 7.21. Contour plot for 3σ (blue dashed) and 5σ (red solid) for the number of events in the presence of NSI. The left panel is for $g_R^{ud} = 0$ and the right panel is for $g_R^{ud} = g_L^{ud}$.

Next we calculate the number of events in the W' model in the DIS energy region ignoring the QE and Δ-RES contributions. In order to cross-check our calculations we find the SM number of events to be $N_{SM} = 30.08$ by setting the couplings $(g_L^{\nu_\tau\tau}, g_L^{ud}, g_R^{ud}) = (0, 0, 0)$ which is very close to $N_{\rm SM}$ estimated above. In Fig. 7.21, we show the contour plot for the number of events in the presence of the NSI. We use the χ^2 measure to make the 3σ and 5σ plots where

$$\chi^2(M_{W'}, g_L^{\nu_\tau\tau}, g_L^{ud}, g_R^{ud}) = \frac{\left[N_{NSI}(M_{W'}, g_L^{\nu_\tau\tau}, g_L^{ud}, g_R^{ud}) - N_{SM}\right]^2}{\sigma^2}, \tag{7.70}$$

and $\sigma = 3.37$ is the standard deviation. We calculate the contour plots for $N_{NSI} = 40.75$ and $N_{NSI} = 47.48$ which are 3σ and 5σ, respectively, away from the SM prediction $N_{\rm SM} = 30.66 \pm 3.37$. In Fig. 7.21 left panel we assume non-zero value for the left handed coupling and a vanishing right handed coupling $g_R^{ud} = 0$, while in the right panel we assume $g_R^{ud} = g_L^{ud}$. In the DIS cross section, we find that the cross section is symmetric under the interchange of a' and b', see Eq. 7.66. This means that the contour plot for $g_R^{ud} = g_L^{ud}$ and $g_R^{ud} = -g_L^{ud}$ are the same.

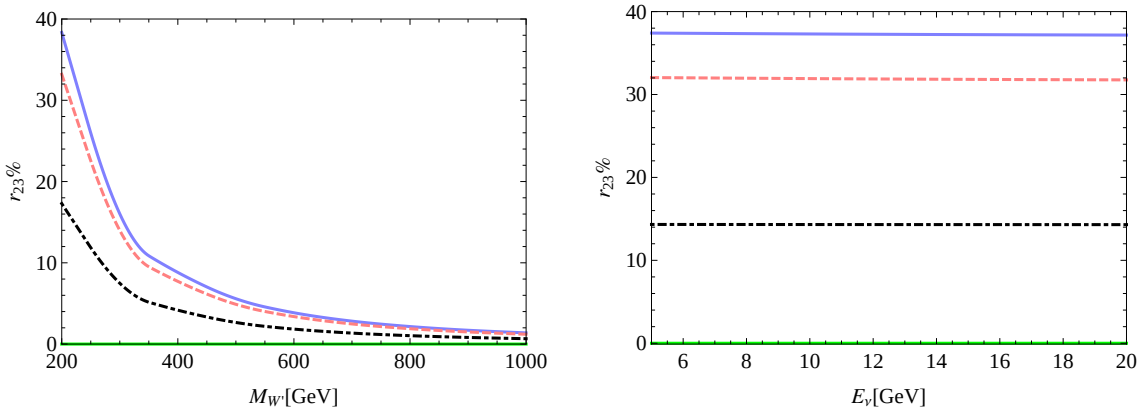

Figure 7.22. DIS (W'): The left (right) panel figures illustrate the variation of $r^{23}_{W'}$% with the W' mass $M_{W'}$ (E_ν) when both left and right-handed W' couplings are present. The lines show predictions for some representative values of the W' couplings $(g_L^{\tau\nu_\tau}, g_L^{ud}, g_R^{ud})$. The green line (solid, lower) corresponds to the SM prediction. The blue line (solid, upper) in the left figure corresponds to (-0.94 , -1.13 , -0.85) at $E_\nu = 17$ GeV, and the blue line (solid, upper) in the right figure corresponds to (1.23 , 0.84 , 0.61) at $M_{W'} = 200$ GeV.

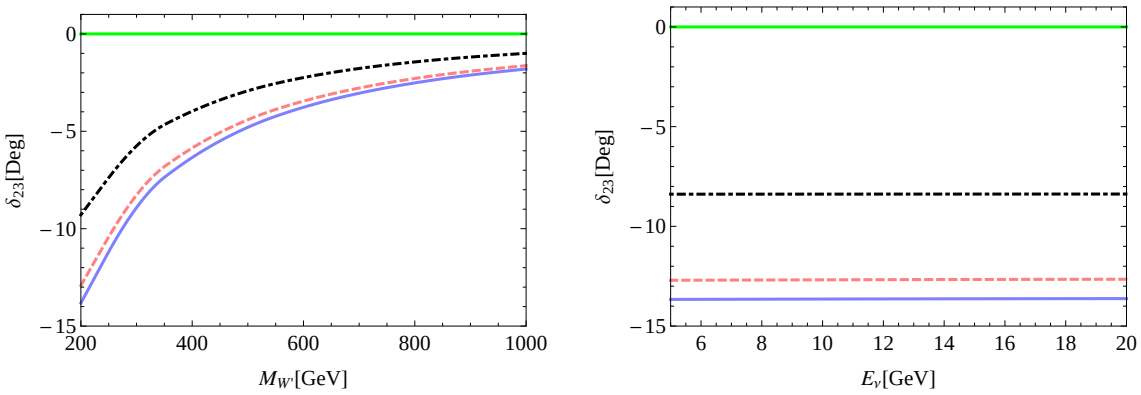

Figure 7.23. DIS (W'): The left (right) panel figures illustrate the deviation δ_{23} with the W' mass $M_{W'}$ (E_ν) when both left and right-handed W' couplings are present. The lines show predictions for some representative values of the W' couplings $(g_L^{\tau\nu_\tau}, g_L^{ud}, g_R^{ud})$. The green line (solid, upper) corresponds to the SM prediction. The blue line (solid, lower) in the left figure corresponds to (-0.94 , -1.13 , -0.85) at $E_\nu = 17$ GeV, and the blue line (solid, lower) in the right figure corresponds to (1.23 , 0.84 , 0.61) at $M_{W'} = 200$ GeV. Here, we use the best-fit value $\theta_{13} = 9.1^\circ$ [47].

7.7 Polarization of the produced $\tau^\pm$

In this section we study the effects of NP on the polarization of the produced τ. The starting point is to construct the spin-density matrix $\rho_{\lambda,\lambda'}$, where λ and λ' are the helicity of the τ lepton. The spin-density matrix $\rho_{\lambda,\lambda'}$ is related to the spin dependent differential cross section as

$$\frac{d\sigma_{\lambda,\lambda'}}{dE_l d\cos\theta} = |\rho_{\lambda\lambda'}|^2 \frac{d\sigma_{total}}{dE_l d\cos\theta}, \tag{7.71}$$

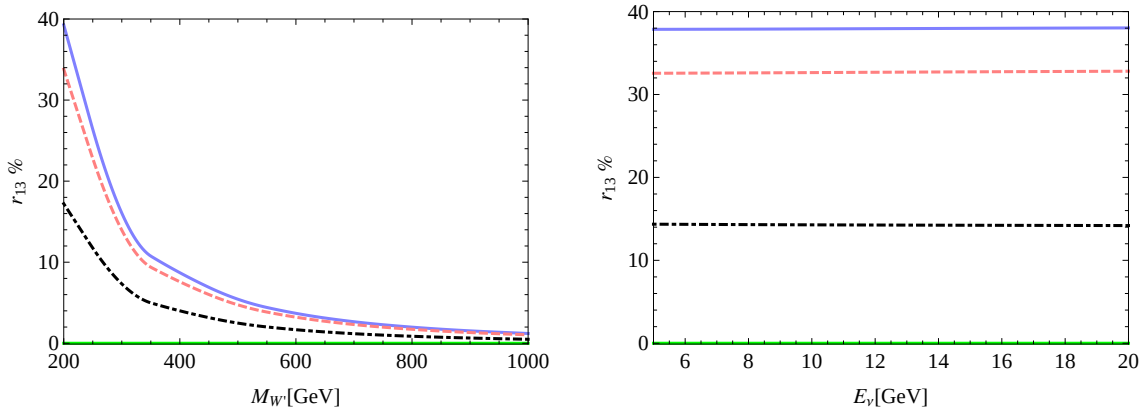

Figure 7.24. DIS (W'): The left (right) panel figures illustrate the variation of $r^{13}_{W'}$% with the W' mass $M_{W'}$ (E_ν) when both left and right-handed W' couplings are present. The lines show predictions for some representative values of the W' couplings $(g_L^{\tau\nu_\tau}, g_L^{ud}, g_R^{ud})$. The green line (solid, lower) corresponds to the SM prediction. The blue line (solid, upper) in the left figure corresponds to (-0.94 , -1.13 , -0.85) at $E_\nu = 17$ GeV, and the blue line (solid, upper) in the right figure corresponds to (1.23 , 0.84 , 0.61) at $M_{W'} = 200$ GeV.

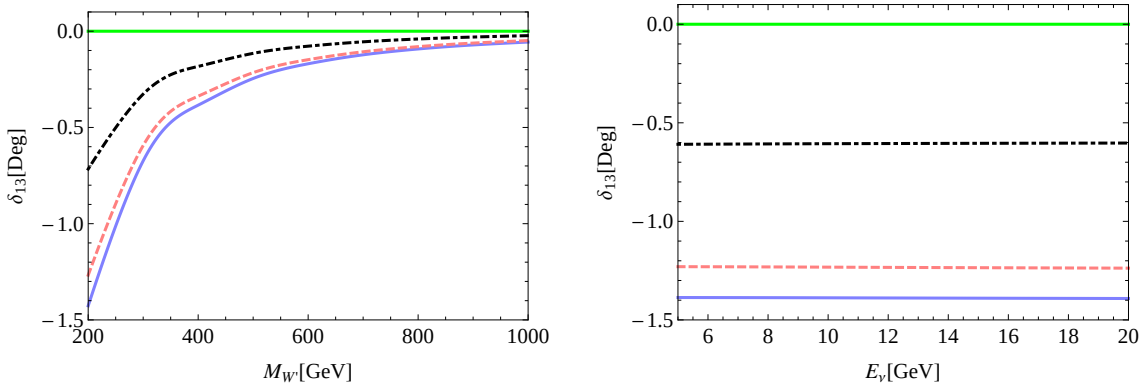

Figure 7.25. DIS (W'): The left (right) panel figures illustrate the deviation δ_{13} with the W' mass $M_{W'}$ (E_ν) when both left and right-handed W' couplings are present. The lines show predictions for some representative values of the W' couplings $(g_L^{\tau\nu_\tau}, g_L^{ud}, g_R^{ud})$. The green line (solid, upper) corresponds to the SM prediction. The blue line (solid, lower) in the left figure corresponds to (-0.94 , -1.13 , -0.85) at $E_\nu = 17$ GeV, and the blue line (solid, lower) in the right figure corresponds to (1.23 , 0.84 , 0.61) at $M_{W'} = 200$ GeV. Here, we use the best-fit value $\theta_{13} = 9.1^\circ$ [47].

where the total cross section $\sigma_{total} = \sigma_{\frac{1}{2}\frac{1}{2}} + \sigma_{-\frac{1}{2}-\frac{1}{2}}$. The spin-density matrix $\rho_{\lambda,\lambda'}$ is expressed in terms of the spin dependent matrix element $M_{\lambda,\lambda'} = L^{\mu\nu}_{\lambda,\lambda'} W_{\mu\nu}$ as

$$\rho_{\lambda,\lambda'} \;=\; \frac{\mathcal{M}_{\lambda,\lambda'}}{\sum_{\lambda=\pm\frac{1}{2}} \mathcal{M}_{\lambda,\lambda}} \,. \tag{7.72}$$

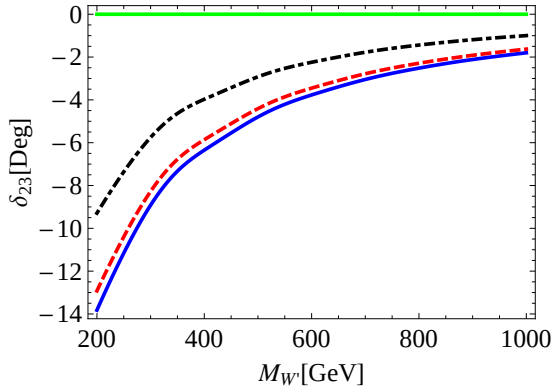

Figure 7.26. DIS (W'): The figure illustrates the deviation δ_{23} with the W' mass $M_{W'}$ when both left and right-handed W' couplings are present. The lines show predictions for some representative values of the W' couplings $(g_L^{\tau\nu_\tau}, g_L^{ud}, g_R^{ud})$. The green line (solid, upper) corresponds to the SM prediction. The blue line (solid, lower) corresponds to (-0.94 , -1.13 , -0.85). Here, we use the best-fit value $\theta_{23} = 42.8^\circ$ [285]. We take into account the atmospheric neutrino flux for Kamioka where the Super-Kamiokande experiment locates [300].

The most general form of the polarization density matrix ρ of a fermion is parametrized as

$$\rho \;=\; [\rho_{\lambda,\lambda'}] = \frac{1}{2}(I + \tau^a \cdot \vec{P}) = \frac{1}{2}\begin{pmatrix} 1+P_z & P_x - iP_y \\ P_x + iP_y & 1-P_z \end{pmatrix}, \tag{7.73}$$

where I is the 2×2 identity matrix and $\vec{P}$ is the polarization vector of the decaying spin-1/2 lepton.

To determine the components (P_x, P_y, P_z) of the polarization vector we choose the following kinematic variables. The four-momenta of incoming neutrino (k), target nucleon (p) and produced lepton (k') in the laboratory frame are

$$\begin{aligned} k^\mu &= (E_\nu, 0, 0, E_\nu)\,, \\ p^\mu &= (M, 0, 0, 0)\,, \\ k'^\mu &= (E_l, p_l \sin\theta\cos\phi, p_l \sin\theta \sin\phi, p_l \cos\theta)\,. \end{aligned} \tag{7.74}$$

We introduce three four-vectors s^a_μ , a = 1, 2, 3 such that the s^a and k'_l/m_l form an orthonormal set of four-vectors as defined in [304]: We choose the three spin four-vectors of

the lepton such that

$$\begin{aligned} s^a \cdot k' &= 0, \\ s^a \cdot s^b &= -\delta^{ab}, \\ s^a_\mu \cdot s^b_\nu &= -g_{\mu\nu} + \frac{k'_\mu k'_\nu}{m_l^2}, \end{aligned} \tag{7.75}$$

where

$$\begin{aligned} s^1_\mu &= (0, \cos\theta\cos\phi, \cos\theta\sin\phi, -\sin\theta)\,, \\ s^2_\mu &= (0, -\sin\phi, \cos\phi, 0)\,, \\ s^3_\mu &= (p_l/m_l, E_l/m_l \sin\theta\cos\phi, E_l/m_l \sin\theta\sin\phi, E_l/m_l\cos\theta)\,. \end{aligned} \tag{7.76}$$

Finally we define the degree of τ polarization P as

$$P = \sqrt{P_x^2 + P_y^2 + P_z^2}. \tag{7.77}$$

The SM results for the polarization components P_x, P_y, P_z can be found in Ref. [272] for the processes QE, Δ-RES and DIS. We calculated these components in the presence of the charged Higgs and W' contributions. We computed the degree of τ polarization P with respect to E_τ for 0 degree, 5 degrees and 10 degrees scattering angles with the incident neutrino energy at 10 GeV. In the polarization results we found the charged Higgs and W' model produce tiny deviations from the SM values.

7.8 Conclusion

In this work we calculated the effect of a charged Higgs and a W' contribution to $\nu_\tau + N \to \tau^- + X$ and $\bar{\nu}_\tau + N \to \tau^+ + X$ scattering. We constrained the parameters of both the models from $\tau^- \to \pi^-\nu_\tau$ and $\tau^- \to \rho^-\nu_\tau$ decays. Corrections to the SM contribution to $\nu_\tau + N \to \tau^- + X$ and $\bar{\nu}_\tau + N \to \tau^+ + X$ impact the extraction of the neutrino atmospheric mixing angles θ_{23} and θ_{13}, respectively. We found that the charged Higgs model can produce significant corrections to $\delta_{23,13}$ that measure the deviation of the actual $\theta_{23,13}$ from the $(\theta_{23,13})_{SM}$ angles which are extracted assuming the SM $\nu_\tau/\bar{\nu}_\tau$ scattering cross sections.

In quasielastic scattering, the W' model effect generates a large deviation δ_{23} but negligibly small δ_{13}. As θ_{13} is smaller than θ_{23} larger NP in $\bar{\nu}_\tau + p \to \tau^+ + n$ is required to produce effects in δ_{13} similar in size to δ_{23}. When a charged Higgs is involved, $\delta_{23,13}$ are negative. This is because there is no interference of the charged Higgs contribution with the SM contribu-

tion, for massless neutrinos, and so the cross sections for $\nu_\tau + n \to \tau^- + p$ and $\bar{\nu}_\tau + p \to \tau^+ + n$ are always larger than the SM cross sections. This means that experiments should measure $\theta_{23,13}$ larger than the present values in the presence of a charged Higgs contribution. In this case we also found that $\delta_{23,13}$ increase in magnitude with the neutrino energy. Hence, a possible sign of the charged Higgs effect would be a measurement of $\theta_{23,13}$ that shows an increase with increasing neutrino energy. For the W' model we calculated a significant contribution to δ_{23} which can be both positive and negative, but is mostly negative. The deviation δ_{23} was found to be independent of the neutrino energy for a left-handed W' but neutrino energy dependent when both left- and right-handed W' chiralities were present. A negligibly small deviation, δ_{13}, was found in the W' model because of the small value of θ_{13}.

In the case of Δ resonance production, the charged Higgs contribution was found to be proportional to q^2 which suppressed the NP effect within the allowed kinematical region. The values of the deviations δ_{23} and δ_{13} were negative as the interference term in the cross section vanishes in the limit of ignoring the neutrino mass and, in turn, the total cross section is always larger than the SM one. The values of δ_{23} and δ_{13} in the W' gauge boson contributions were found to be both positive and negative, but were mostly negative. The δ_{23} and δ_{13} values decreased in magnitude with increasing incident neutrino energy and the new state masses $(M_{W'}, M_H)$.

In the case of deep inelastic scattering, the charged Higgs contribution does not have interference with the SM cross section. With the constraints on the NP parameters, the NP effects were negligible and the deviations δ_{23} and δ_{13} were very small. The values of deviations were found to be mostly negative in the W' model. The δ_{23} and δ_{13} values increased in magnitude with increasing incident neutrino energy and decreased with increasing $M_{W'}$.

We took into account the flux of incoming atmospheric neutrinos from Kamioka, where the Super-Kamiokande experiment is located, in the calculations of δ_{23} when considering the charged Higgs and W' contributions. By integrating over the incoming neutrino energy we found that considering the neutrino flux did not change the δ_{23} results significantly. We showed the 3σ and 5σ deviation contour plots, using the χ^2 measure and the W' NSI model, for the number of events for neutrino energies above 30 GeV where the DIS contribution is dominant. Finally, we studied the NP effects on the degree of polarization of the produced τ and found that the deviation of the polarization results in the NP models from the SM values were negligibly small at different scattering angles.

We have presented in this work a first estimation of the charged Higgs and W' effects in the extraction of θ_{23} and θ_{13}. We hope more detailed calculations including nuclear as well as detector effects, will be done to find out whether these new physics effects can be

observed at present $\nu_\tau/\bar{\nu}_\tau$ appearance experiments and/or to motivate new experiments that can detect these effects.

OVERALL CONCLUSION

In this dissertation, we presented a study of the phenomenological implications of two-Higgs-doublet model on the properties of neutrino sector and heavy quark systems. We discussed neutrino mixing within the framework of two-Higgs-doublet model by introducing different flavor symmetries in the lepton sector with the leading order structures being bi-maximal and tri-bimaximal pattern. We found that a mixing model with 2-3 flavor symmetry can accommodate the sizable θ_{13} value. Moreover, we introduced a model with A_4 flavor symmetry where the smallness of the neutrino mass is not due to the seesaw mechanism, i.e. not inversely proportional to some large mass scale, at the level of a one-loop mechanism with dark matter in the loop consisting of singlet Majorana fermions. In the nonstandard neutrino interactions, new physics contributions to the tau-neutrino nucleon scattering were considered in this work. We discussed charged Higgs and W' effects to the three processes; quasi-elastic interaction, Δ resonance production and deep inelastic scattering in the neutrino-nucleon interactions $\nu_\tau + N \to \tau^- + X$ and $\bar{\nu}_\tau + N \to \tau^+ + X$. Considering these effects in the neutrino detection process at neutrino oscillation experiments modifies the measured atmospheric and reactor mixing angles θ_{23} and θ_{13}, respectively.

We studied the decay channel of the quarkonium $\eta_b \to \tau^+\tau^-$ which has an experimental upper limit of $\lesssim 8\%$ on its branching ratio. We evaluated the standard model branching ratio for this decay to be $\sim 4 \times 10^{-9}$. We showed that the contributions of models with a light pseudoscalar or a light axial vector state enhance the branching ratio up to the present experimental limit. In the top sector, the forward-backward asymmetry $A_{\rm FB}$ in the top quark pair production in the $t\bar{t}$ rest frame has been measured in the CDF and found to have a deviation from the next-to leading order SM prediction. Here, we accommodated the CDF measurement of the $A_{\rm FB}$ by introducing a $u \to t$ transition via a flavor-changing Z' which can explain the data. We considered the most general form of the tuZ' interaction, which includes vector-axial vector as well as tensor type couplings, and studied how these couplings

affect the top forward-backward asymmetry.

BIBLIOGRAPHY

Bibliography

[1] K. Abe *et al.* [T2K Collaboration], Phys. Rev. Lett. **107**, 041801 (2011) [arXiv:1106.2822 [hep-ex]]. 2, 9, 69

[2] L. Whitehead [MINOS Collaboration], "*Recent results from MINOS*", Joint Experimental-Theoretical Seminar (24 June 2011, Fermilab, USA). Websites: theory.fnal.gov/jetp, http://www-numi.fnal.gov/pr-plots/ 2, 9

[3] *P. Adamson et al.* [MINOS Collaboration], "*Improved search for muon-neutrino to electron-neutrino oscillations in MINOS*," arXiv:1108.0015 [hep-ex]. 2

[4] L. Wolfenstein, Phys. Rev. D 17, 2369 (1978); L. Wolfenstein, Phys. Rev. D 20, 2634 (1979); S. P. Mikheev and A. Y. Smirnov, Sov. J. Nucl. Phys. 42, 913 (1985) [Yad. Fiz. 42, 1441 (1985)]; S. P. Mikheev and A. Y. Smirnov, Nuovo Cim. C 9, 17 (1986). V. D. Barger, K. Whisnant, S. Pakvasa and R. J. N. Phillips, Phys. Rev. D 22, 2718 (1980). 2

[5] F. Englert and R. Brout, *Phys. Rev. Lett.* **13**, 321 (1964). 3

[6] P. W. Higgs, *Phys. Rev. Lett.* **13**, 508 (1964).

[7] G. S. Guralnik, C. R. Hagen and T. W. B. Kibble, *Phys. Rev. Lett.* **13**, 585 (1964). 3

3

[8] John F. Gunion, Howard E. Haber, Gordon Kane, and Sally Dawson. Book title "The Higgs Hunter's Guide". ISBN: 0-7382-0305-X. 5

[9] [CMS Collaboration], CMS-PAS-HIG-12-020. 6

[10] [ATLAS Collaboration], ATLAS-CONF-2012-093. 6

[11] S. Chang, R. Dermisek, J. F. Gunion and N. Weiner, Ann. Rev. Nucl. Part. Sci. **58**, 75 (2008) [arXiv:0801.4554 [hep-ph]]. 6, 34

[12] B. Aubert *et al.* [BABAR Collaboration], Phys. Rev. Lett. **101**, 071801 (2008) [Erratum-ibid. **102**, 029901 (2009)], hep-ex/0807.1086v4. 7, 35

[13] B. Aubert *et al.* [BABAR Collaboration], hep-ex/0903.1124. 7, 35, 40

[14] S.W. Herb et al., Phys. Rev. Lett. **39**, 252 (1977); W.R. Innes et al., Phys. Rev. Lett. **39**, 1240 (1977) [Erratum-ibid. **39**, 1640(E) (1977)]. 7

[15] A. H. Mahmood *et al.* [CLEO Collaboration], hep-ex/0207057, M. Artuso *et al.* [CLEO Collaboration], Phys. Rev. Lett. **94**, 032001 (2005), hep-ex/0411068. 7

[16] A. Heister *et al.* [ALEPH Collaboration], Phys. Lett. B **530**, 56 (2002), hep-ex/0202011, M. Levtchenko [L3 Collaboration], Nucl. Phys. Proc. Suppl. **126**, 260 (2004). A. Sokolov, Nucl. Phys. Proc. Suppl. **126**, 266 (2004). J. Abdallah [DELPHI Collaboration], Phys. Lett. B **634**, 340 (2006), hep-ex/0601042. N. Brambilla *et al.* [Quarkonium Working Group], arXiv:hep-ph/0412158. 7, 34

[17] F. Maltoni and A. D. Polosa, Phys. Rev. D **70**, 054014 (2004) [arXiv:hep-ph/0405082]. 7, 34

[18] T. W. Chiu, T. H. Hsieh, C. H. Huang and K. Ogawa [TWQCD Collaboration], Phys. Lett. B **651**, 171 (2007) [arXiv:0705.2797 [hep-lat]], A. Gray, I. Allison, C. T. H. Davies, E. Dalgic, G. P. Lepage, J. Shigemitsu and M. Wingate, Phys. Rev. D **72**, 094507 (2005) [arXiv:hep-lat/0507013], T. Burch and C. Ehmann, Nucl. Phys. A **797**, 33 (2007) [arXiv:hep-lat/0701001]. 7

[19] A. Penin, arXiv:0905.4296v1 [hep-ph]. 7

[20] B. A. Kniehl, A. A. Penin, A. Pineda, V. A. Smirnov and M. Steinhauser, Phys. Rev. Lett. **92**, 242001 (2004) [Erratum-ibid. **104**, 199901 (2010)] [arXiv:hep-ph/0312086]. 7

[21] B. Aubert *et al.* [BABAR Collaboration], Phys. Rev. Lett. **103**, 181801 (2009) [arXiv:0906.2219 [hep-ex]]. 7, 33

[22] T. Aaltonen *et al.* [CDF Collaboration], arXiv:1101.0034 [hep-ex]. xi, 8, 52

[23] J. H. Kuhn and G. Rodrigo, *Phys.Rev.Lett.* **81** (1998) 49, [hep-ph/9802268]. 8

[24] J. H. Kuhn and G. Rodrigo, *Phys.Rev.* **D59** (1999) 054017, [hep-ph/9807420]. 8

[25] M. Bowen, S. Ellis, and D. Rainwater, *Phys.Rev.* **D73** (2006) 014008, [hep-ph/0509267]. 8

[26] L. G. Almeida, G. F. Sterman, and W. Vogelsang, *Phys.Rev.* **D78** (2008) 014008, [arXiv:0805.1885 [hep-ph]]. 8

[27] D0 Collaboration, V. Abazov *et. al.*, *Phys.Rev.Lett.* **100** (2008) 142002, [arXiv:0712.0851 [hep-ex]]. 8

[28] T. Aaltonen *et al.* [CDF Collaboration], Conf. Note 9913 (2009); 8

[29] U. Langenfeld, S. Moch, and P. Uwer , Phys. Rev. D. **80**, 054009 (2009). [arXiv:0906.5273[hep-ph]].

[30] M. Cacciari *et al.* , JHEP **09**, 127 (2008). [arXiv:0804.2800[hep-ph]]. 8

8

[31] N. Kidonakis and R. Vogt , Phys. Rev. D. **78**, 074005 (2008). [arXiv:0805.3844 [hep-ph]]. 8

[32] V. Ahrens, A. Ferroglia, M. Neubert, B. D. Pecjak and L. Li , JHEP **09**, 097 (2010). [arXiv:1003.5827[hep-ph]]. 8

[33] L. Sehgal and M. Wanninger, **B200** (1988) 211. J. Bagger, C. Schmidt, and S. King, *Phys.Rev.* **D37** (1988) 1188. P. Ferrario and G. Rodrigo, *Phys.Rev.* **D80** (2009) 051701,[arXiv:0906.5541[hep-ph]]. P. H. Frampton, J. Shu, and K. Wang, *Phys. Lett.* **B683** (2010) 294, [arXiv:0911.2955 [hep-ph]]. R. Chivukula, E. H. Simmons, and C.-P. Yuan, *Phys.Rev.* **D82** (2010) 094009, [arXiv:1007.0260 [hep-ph]]. A. Djouadi, G. Moreau, F. Richard, and R. K. Singh, *Phys.Rev.* **D82** (2010) 071702, [arXiv:0906.0604 [hep-ph]]. M. Bauer, F. Goertz, U. Haisch, T. Pfoh, and S. Westhoff, *JHEP* **1011** (2010) 039, [arXiv:1008.0742 [hep-ph]]. E. Alvarez, L. Da Rold, and A. Szynkman, arXiv:1011.6557 [hep-ph]. C.-H. Chen, G. Cvetic, and C. Kim, *Phys.Lett.* **B694** (2011) 393, [arXiv:1009.4165 [hep-ph]]. C. Delaunay, O. Gedalia, S. J. Lee, G. Perez, E. Ponton, arXiv:1101.2902 [hep-ph]. Y. Bai, J. L. Hewett, J. Kaplan, T. G. Rizzo, JHEP **1103** (2011) 003, [arXiv:1101.5203 [hep-ph]]. A. R. Zerwekh, arXiv:1103.0956 [hep-ph]. E. R. Barreto, Y. A. Coutinho, J. S. Borges, arXiv:1103.1266 [hep-ph]. A. Djouadi, G. Moreau, F. Richard, arXiv:1105.3158 [hep-ph]. R. Barcelo, A. Carmona, M. Masip, J. Santiago, arXiv:1105.3333 [hep-ph] S. Westhoff, arXiv:1105.4624[hep-ph]. U. Haisch, S. Westhoff, arXiv:1106.0529[hep-ph]. E. Gabrielli, M. Raidal, arXiv:1106.4553 [hep-ph]. 8

[34] S. Jung, H. Murayama, A. Pierce, and J. D. Wells, *Phys. Rev.* **D81** (2010) 015004, [arXiv:0907.4112 [hep-ph]]. K. Cheung, W.-Y. Keung, and T.-C. Yuan, *Phys.Lett.*

B682 (2009) 287, [arXiv:0908.2589 [hep-ph]]. J. Shu, T. M. P. Tait, and K. Wang, *Phys. Rev.* **D81** (2010) 034012, [arXiv:0911.3237 [hep-ph]]. I. Dorsner, S. Fajfer, J. F. Kamenik, and N. Kosnik, *Phys.Rev.* **D81** (2010) 055009, [arXiv:0912.0972 [hep-ph]]. A. Arhrib, R. Benbrik, and C.-H. Chen, *Phys. Rev.* **D82** (2010) 034034, [arXiv:0911.4875 [hep-ph]]. V. Barger, W.-Y. Keung, and C.-T. Yu, *Phys. Rev.* **D81** (2010) 113009, [arXiv:1002.1048 [hep-ph]]. S. K. Gupta, G. Valencia, Phys. Rev. **D82**, 035017 (2010). [arXiv:1005.4578 [hep-ph]]. B. Xiao, Y.-k. Wang, and S.-h. Zhu, *Phys.Rev.* **D82** (2010) 034026, [arXiv:1006.2510 [hep-ph]]. S. K. Gupta, arXiv:1011.4960 [hep-ph]. K. Cheung and T.-C. Yuan, arXiv:1101.1445 [hep-ph]. J. Cao, L. Wang, L. Wu, J. M. Yang, [arXiv:1101.4456 [hep-ph]. E. L. Berger, Q. -H. Cao, C. -R. Chen, C. S. Li, H. Zhang, arXiv:1101.5625 [hep-ph]. V. Barger, W. -Y. Keung, C. -T. Yu, arXiv:1102.0279 [hep-ph]. B. Grinstein, A. L. Kagan, M. Trott, J. Zupan, arXiv:1102.3374 [hep-ph]. K. M. Patel, P. Sharma, arXiv:1102.4736 [hep-ph]. S. Jung, A. Pierce, J. D. Wells, arXiv:1103.4835 [hep-ph]. M. R. Buckley, D. Hooper, J. .Kopp, E. .Neil, arXiv:1103.6035[hep-ph]. J. Shu, K. Wang, G. Zhu, arXiv:1104.0083 [hep-ph]. A. Rajaraman, Z. Surujon, T. M. P. Tait, arXiv:1104.0947 [hep-ph]. J. A. Aguilar-Saavedra, M. Perez-Victoria, arXiv:1104.1385 [hep-ph]. C. Degrande, J. M. Gerard, C. Grojean, F. Maltoni, G. Servant, arXiv:1104.1798 [hep-ph]. X. P. Wang,Y. K. Wang, B. Xiao, J. Xu, S. h. Zhu, arXiv:1104.1917 [hep-ph]. A. E. Nelson, T. Okui, T. S. Roy, arXiv:1104.2030 [hep-ph]. S. Jung, A. Pierce, J. D. Wells, arXiv:1104.3139 [hep-ph]. D. W. Jung, P. Ko, S. J. Lee, arXiv:1104.4443 [hep-ph]. K. S. Babu, M. Frank, S. K. Rai, arXiv:1104.4782 [hep-ph]. J. A. Aguilar-Saavedra, M. Perez-Victoria, arXiv:1105.4606 [hep-ph]. 8, 51

[35] K. Kodama et al. (DONUT), Phys. Lett. B504 (2001), 218, hep-ex/0012035 9

[36] Super-Kamiokande, Y. Fukuda et al., Evidence for oscillation of atmospheric neutrinos, Phys. Rev. Lett. 81 (1998), 1562, hep-ex/9807003. Super-Kamiokande, Y. Ashie et al., Evidence for an oscillatory signature in atmospheric neutrino oscillation, Phys. Rev. Lett. 93 (2004), 101801, hep-ex/0404034. 9

[37] Super-Kamiokande, J. P. Cravens et al., Solar neutrino measurements in Super-Kamiokande-II, Phys. Rev. D78 (2008), 032002, 0803.4312. B. T. Cleveland et al., Measurement of the solar electron neutrino flux with the Homestake chlorine detector, Astrophys. J. 496 (1998), 505. SAGE, J. N. Abdurashitov et al., Measurement of the solar neutrino capture rate by the Russian-American gallium solar neutrino experiment during one half of the 22-year cycle of solar activity, J. Exp. Theor. Phys. 95 (2002), 181, astro-ph/0204245. GALLEX, W. Hampel et al., GALLEX solar neutrino

observations: Results for GALLEX IV, Phys. Lett. B447 (1999), 127. GNO, M. Altmann et al., GNO solar neutrino observations: Results for GNO I, Phys. Lett. B490 (2000), 16, hep-ex/0006034. 9

[38] SNO, Q. R. Ahmad et al., Direct evidence for neutrino flavor transformation from neutral-current interactions in the Sudbury Neutrino Observatory, Phys. Rev. Lett. 89 (2002), 011301, nucl-ex/0204008. 9

[39] Super-Kamiokande, Y. Ashie et al., A measurement of atmospheric neutrino oscillation parameters by Super-Kamiokande I, Phys. Rev. D71 (2005), 112005, hep-ex/0501064. 9

[40] KamLAND, K. Eguchi et al., First results from KamLAND: Evidence for reactor anti-neutrino disappearance, Phys. Rev. Lett. 90 (2003), 021802, hep-ex/0212021. The KamLAND Collaboration, Precision measurement of neutrino oscillation parameters with KamLAND, (2008), arXiv:0801.4589 [hep-ex]. 9

[41] CHOOZ, M. Apollonio et al., Search for neutrino oscillations on a long baseline at the CHOOZ nuclear power station, Eur. Phys. J. C27 (2003), 331, hep-ex/0301017. 9

[42] K2K, M. H. Ahn et al., Indications of neutrino oscillation in a 250-km long- baseline experiment, Phys. Rev. Lett. 90 (2003), 041801, hep-ex/0212007. K2K,M. H. Ahn et al., Measurement of neutrino oscillation by the K2K experiment, Phys. Rev. D74 (2006), 072003, hep-ex/0606032. 9

[43] MINOS, D. G. Michael et al., Observation of muon neutrino disappearance with the MINOS detectors and the NuMI neutrino beam, Phys. Rev. Lett. 97 (2006), 191801, hep-ex/0607088. MINOS, P. Adamson et al., Measurement of neutrino oscillations with the MINOS detectors in the NuMI beam, Phys. Rev. Lett. 101 (2008), 131802, 0806.2237. 9

[44] Y. Abe *et al.* [DOUBLE-CHOOZ Collaboration], Phys. Rev. Lett. **108**, 131801 (2012) [arXiv:1112.6353 [hep-ex]]. 9

[45] F. P. An *et al.* [DAYA-BAY Collaboration], Phys. Rev. Lett. **108**, 171803 (2012) [arXiv:1203.1669 [hep-ex]]. 9

[46] J. K. Ahn *et al.* [RENO Collaboration], Phys. Rev. Lett. **108**, 191802 (2012) [arXiv:1204.0626 [hep-ex]]. 9

[47] D. V. Forero, M. Tortola and J. W. F. Valle, arXiv:1205.4018 [hep-ph]. xiii, xiv, xvi, xvii, 10, 83, 119, 128, 131, 137, 138

[48] D. Marzocca, S. T. Petcov, A. Romanino, M. Spinrath, [arXiv:1108.0614 [hep-ph]]. Y. H. Ahn, H. -Y. Cheng, S. Oh, [arXiv:1107.4549 [hep-ph]]. R. d. A. Toorop, F. Feruglio, C. Hagedorn, [arXiv:1107.3486 [hep-ph]]. P. S. Bhupal Dev, R. N. Mohapatra, M. Severson, [arXiv:1107.2378 [hep-ph]]. S. Dev, S. Gupta, R. R. Gautam, [arXiv:1107.1125 [hep-ph]]. D. Meloni, [arXiv:1107.0221 [hep-ph]]. N. Haba, R. Takahashi, Phys. Lett. **B702**, 388-393 (2011). [arXiv:1106.5926 [hep-ph]]. S. Zhou, [arXiv:1106.4808 [hep-ph]]. X. -G. He, A. Zee, [arXiv:1106.4359 [hep-ph]]. Y. -j. Zheng, B. -Q. Ma, [arXiv:1106.4040 [hep-ph]]. H. Ishimori, T. Kobayashi, [arXiv:1106.3604 [hep-ph]]. M. -C. Chen, K. T. Mahanthappa, A. Meroni, S. T. Petcov, [arXiv:1109.0731 [hep-ph]]. S. Davidson, M. Elmer, [arXiv:1108.0548 [hep-ph]]. J. Heeck, W. Rodejohann, Phys. Rev. **D84**, 075007 (2011). [arXiv:1107.5238 [hep-ph]]. S. Antusch, V. Maurer, [arXiv:1107.3728 [hep-ph]]. X. -G. He, S. K. Majee, [arXiv:1111.2293 [hep-ph]]. N. Haba, T. Horita, K. Kaneta, Y. Mimura, [arXiv:1110.2252 [hep-ph]]. A. Aranda, C. Bonilla, A. D. Rojas, [arXiv:1110.1182 [hep-ph]]. 10, 14, 56

[49] S. Kumar, [arXiv:1108.2137 [hep-ph]]. H. Fritzsch, Z. -z. Xing, S. Zhou, [arXiv:1108.4534 [hep-ph]]. S. Antusch, S. F. King, C. Luhn, M. Spinrath, [arXiv:1108.4278 [hep-ph]]. M. Huang, D. Liu, J. -C. Peng, S. D. Reitzner, W. -C. Tsai, [arXiv:1108.3906 [hep-ph]]. T. Araki, C. -Q. Geng, [arXiv:1108.3175 [hep-ph]]. Riazuddin, [arXiv:1108.1469 [hep-ph]]. T. Schwetz, M. Tortola, J. W. F. Valle, [arXiv:1108.1376 [hep-ph]]. S. -F. Ge, D. A. Dicus, W. W. Repko, [arXiv:1108.0964 [hep-ph]]. G. J. Mathews, T. Kajino, W. Aoki, W. Fujiya, [arXiv:1108.0725 [astro-ph.HE]]. S. F. King, C. Luhn, [arXiv:1107.5332 [hep-ph]]. M. -C. Chen, K. T. Mahanthappa, [arXiv:1107.3856 [hep-ph]]. W. Rodejohann, H. Zhang, S. Zhou, [arXiv:1107.3970 [hep-ph]]. X. Chu, M. Dhen, T. Hambye, [arXiv:1107.1589 [hep-ph]]. H. Zhang, S. Zhou, [arXiv:1107.1097 [hep-ph]]. W. Chao, Y. -j. Zheng, [arXiv:1107.0738 [hep-ph]]. S. Morisi, K. M. Patel, E. Peinado, [arXiv:1107.0696 [hep-ph]]. G. L. Fogli, E. Lisi, A. Marrone, A. Palazzo, A. M. Rotunno, [arXiv:1106.6028 [hep-ph]]. T. Araki, Phys. Rev. **D84**, 037301 (2011). [arXiv:1106.5211 [hep-ph]]. A. B. Balantekin, [arXiv:1106.5021 [hep-ph]]. S. F. King, [arXiv:1106.4239 [hep-ph]]. E. Ma, D. Wegman, Phys. Rev. Lett. **107**, 061803 (2011). [arXiv:1106.4269 [hep-ph]]. J. -M. Chen, B. Wang, X. -Q. Li, [arXiv:1106.3133 [hep-ph]]. Z. -z. Xing, [arXiv:1106.3244 [hep-ph]]. N. Qin, B. Q. Ma, Phys. Lett. **B702**, 143-149 (2011). [arXiv:1106.3284 [hep-ph]]. J. Barry, W. Rodejohann, H. Zhang, JHEP **1107**, 091 (2011). [arXiv:1105.3911 [hep-ph]]. Q. -H. Cao, S. Khalil, E. Ma,

H. Okada, [arXiv:1108.0570 [hep-ph]]. S. Antusch, P. Di Bari, D. A. Jones, S. F. King, [arXiv:1107.6002 [hep-ph]]. M. Blennow, E. Fernandez-Martinez, Phys. Lett. **B704**, 223 (2011). [arXiv:1107.3992 [hep-ph]]. A. Adulpravitchai, R. Takahashi, JHEP **1109**, 127 (2011). [arXiv:1107.3829 [hep-ph]]. S. Dev, S. Gupta, R. R. Gautam, L. Singh, [arXiv:1111.1300 [hep-ph]]. Y. -L. Zhou, [arXiv:1110.5023 [hep-ph]]. D. Meloni, [arXiv:1110.5210 [hep-ph]]. P. Coloma, E. Fernandez-Martinez, [arXiv:1110.4583 [hep-ph]]. G. -J. Ding, L. L. Everett, A. J. Stuart, [arXiv:1110.1688 [hep-ph]]. G. Bhattacharyya, H. Pas, D. Pidt, [arXiv:1109.6183 [hep-ph]]. C. Hartmann, [arXiv:1109.5143 [hep-ph]]. 10, 14

[50] V. M. Lobashev et al., Direct search for mass of neutrino and anomaly in the tritium beta-spectrum, Phys. Lett. B460 (1999), 227. C. Kraus et al., Final results from phase II of the Mainz neutrino mass search in tritium beta decay, Eur. Phys. J. C40 (2005), 447, hep-ex/0412056. 10

[51] G. L. Fogli et al., Observables sensitive to absolute neutrino masses (Addendum), Phys. Rev. D78 (2008), 033010, 0805.2517. 10

[52] H. V. Klapdor-Kleingrothaus et al., Latest results from the Heidelberg- Moscow double-beta- decay experiment, Eur. Phys. J. A12 (2001), 147, hep-ph/0103062. 10

[53] S. Davidson, C. Pena-Garay, N. Rius, and A. Santamaria, Present and future bounds on non-standard neutrino interactions, JHEP 03 (2003), 011, hep-ph/0302093. M. C. Gonzalez-Garcia and M. Maltoni, Phenomenology with massive neutrinos, Phys. Rept. 460 (2008), 1, 0704.1800. M. Maltoni, New interactions: past and future experiments, J. Phys. Conf. Ser. 136 (2008), 022024, 0810.3517. 10

[54] M. C. Gonzalez-Garcia and M. Maltoni, Status of oscillation plus decay of atmospheric and long-baseline neutrinos, Phys. Lett. B663 (2008), 405, 0802.3699. 10

[55] Y. Farzan, T. Schwetz, and A. Y. Smirnov, Reconciling results of LSND, Mini- BooNE and other experiments with soft decoherence, JHEP 07 (2008), 067, 0805.2098. 10

[56] M. Maltoni and T. Schwetz, Sterile neutrino oscillations after first MiniBooNE results, Phys. Rev. D76 (2007), 093005, 0705.0107. 10

[57] J. N. Bahcall, arXiv:physics/0406040; R. N. Mohapatra *et al.*, arXiv:hep-ph/0510213; R. N. Mohapatra and A. Y. Smirnov, Ann. Rev. Nucl. Part. Sci. **56** (2006) 569 [arXiv:hep-ph/0603118]; S. F. King, Rept. Prog. Phys. **67** (2004) 107 [arXiv:hep-ph/0310204]; G. Altarelli and F. Feruglio, New J. Phys. **6** (2004) 106 [arXiv:hep-ph/0405048]. 10

[58] Z. Maki, M. Nakagawa and S. Sakata, Prog. Theo. Phys. **28** (1962) 247; B. W. Lee, S. Pakvasa, R. E. Shrock and H. Sugawara, Phys. Rev. Lett. **38** (1977) 937 [Erratum-ibid. **38** (1977) 1230]. W.-M. Yao *et al.* [Particle Data Group Collaboration], 11

[59] A. Upadhyay and M. Batra, arXiv:1112.0445 [hep-ph]. 11, 112

[60] H. Fritzsch and Z. Z. Xing, Phys. Lett. B **372**, 265 (1996); Phys. Lett. B **440**, 313 (1998); Phys. Rev. D **61**,073016 (2000). 14

[61] Z. Z. Xing, arXiv:1106.3244[hep-ph]. 14

[62] F. Vissani, hep-ph/9708483; V.D. Barger, S.Pakvasa, T.J. Weiler, and K. Whisnant, Phys. Lett. **B437**, 107 (1998); A.J. Baltz, A.S. Goldhaber, and M. Goldhaber, Phys. Rev. Lett. **81**, 5730 (1998); I. Stancu and D.V. Ahluwalia, Phys. Lett. **B460**, 431 (1999); H. Georgi and S.L. Glashow, Phy. Rev. **D61**, 097301 (2000); N. Li and B.-Q. Ma, Phys. Lett. B **600**, 248 (2004) [arXiv:hep-ph/0408235]. 14

[63] V. Barger, S. Pakvasa, T. Weiler and K. Whisnant, Phys. Lett. B **437**, 107 (1998); N. Li and B. Q. Ma, Phys. Lett. B **600**, 248 (2004) [arXiv:hep-ph/0408235]. I. Stancu and D. V. Ahluwalia, Phys. Lett. B **460**, 431 (1999) [arXiv:hep-ph/9903408]. 14

[64] P.F. Harrison, D.H. Perkins, and W.G. Scott, Phys. Lett. **B458**, 79 (1999); Phys. Lett. **B530**, 167 (2002); Z.Z. Xing, Phys. Lett. **B533**, 85 (2002); P.F. Harrison and W.G. Scott, Phys. Lett. **B535**, 163 (2002); Phys. Lett. **B557**, 76 (2003); X.-G. He and A. Zee, Phys. Lett. **B560**, 87 (2003); See also L. Wolfenstein, Phys. Rev. **D18**, 958 (1978); Y. Yamanaka, H. Sugawara, and S. Pakvasa, Phys. Rev. **D25**, 1895 (1982); **D29**, 2135(E) (1984); N. Li and B.-Q. Ma, Phys. Rev. D **71**, 017302 (2005) [arXiv:hep-ph/0412126]. 14

[65] For a list of flavor symmetries and references see C. S. Lam, arXiv:0809.1185 [hep-ph]. 14

[66] For work related to TBM see also, for an incomplete list: P. H. Frampton, S. T. Petcov and W. Rodejohann, Nucl. Phys. B **687** (2004) 31 [arXiv:hep-ph/0401206]; A. Dighe, S. Goswami and W. Rodejohann, Phys. Rev. D **75** (2007) 073023 [arXiv:hep-ph/0612328]; F. Plentinger and W. Rodejohann, Phys. Lett. B **625** (2005) 264 [arXiv:hep-ph/0507143]; R. N. Mohapatra and W. Rodejohann, Phys. Rev. D **72** (2005) 053001 [arXiv:hep-ph/0507312]; K. A. Hochmuth, S. T. Petcov and W. Rodejohann, arXiv:0706.2975 [hep-ph]. G. Altarelli, F. Feruglio and Y. Lin, Nucl. Phys. B **775** (2007) 31 [arXiv:hep-ph/0610165]; G. Altarelli and F. Feruglio, Nucl. Phys. B **741**

(2006) 215 [arXiv:hep-ph/0512103]; G. Altarelli and F. Feruglio, Nucl. Phys. B **720** (2005) 64 [arXiv:hep-ph/0504165]; F. Feruglio, C. Hagedorn, Y. Lin and L. Merlo, Nucl. Phys. B **775** (2007) 120 [arXiv:hep-ph/0702194]. E. Ma, arXiv:0709.0507 [hep-ph]; E. Ma, arXiv:hep-ph/0701016; E. Ma, Mod. Phys. Lett. A **22** (2007) 101 [arXiv:hep-ph/0610342]; E. Ma, Mod. Phys. Lett. A **21** (2006) 2931 [arXiv:hep-ph/0607190]; E. Ma, Mod. Phys. Lett. A **21** (2006) 1917 [arXiv:hep-ph/0607056]; E. Ma, H. Sawanaka and M. Tanimoto, Phys. Lett. B **641** (2006) 301 [arXiv:hep-ph/0606103]; E. Ma, Phys. Rev. D **73** (2006) 057304; B. Adhikary, B. Brahmachari, A. Ghosal, E. Ma and M. K. Parida, Phys. Lett. B **638** (2006) 345 [arXiv:hep-ph/0603059]; E. Ma, Mod. Phys. Lett. A **20** (2005) 2601 [arXiv:hep-ph/0508099]; E. Ma, Phys. Rev. D **72** (2005) 037301 [arXiv:hep-ph/0505209]; S. L. Chen, M. Frigerio and E. Ma, Nucl. Phys. B **724** (2005) 423 [arXiv:hep-ph/0504181]; E. Ma, Phys. Rev. D **70** (2004) 031901 [arXiv:hep-ph/0404199]. I. de Medeiros Varzielas and G. G. Ross, Nucl. Phys. B **733** (2006) 31 [arXiv:hep-ph/0507176]; I. de Medeiros Varzielas, S. F. King and G. G. Ross, Phys. Lett. B **644** (2007) 153 [arXiv:hep-ph/0512313]; I. de Medeiros Varzielas, S. F. King and G. G. Ross, Phys. Lett. B **648** (2007) 201 [arXiv:hep-ph/0607045]; S. F. King and M. Malinsky, Phys. Lett. B **645** (2007) 351 [arXiv:hep-ph/0610250]; S. F. King and M. Malinsky, JHEP **0611** (2006) 071 [arXiv:hep-ph/0608021]; C. Luhn, S. Nasri and P. Ramond, Phys. Lett. B **652** (2007) 27 [arXiv:0706.2341 [hep-ph]]. P. F. Harrison and W. G. Scott, Phys. Lett. B **557** (2003) 76 [arXiv:hep-ph/0302025]; P. F. Harrison and W. G. Scott, Phys. Lett. B **535** (2002) 163 [arXiv:hep-ph/0203209]; R. N. Mohapatra, S. Nasri and H. B. Yu, Phys. Lett. B **639** (2006) 318 [arXiv:hep-ph/0605020]; R. N. Mohapatra and H. B. Yu, Phys. Lett. B **644** (2007) 346 [arXiv:hep-ph/0610023]; M. C. Chen and K. T. Mahanthappa, Phys. Lett. B **652** (2007) 34 [arXiv:0705.0714 [hep-ph]]; C. I. Low and R. R. Volkas, Phys. Rev. D **68** (2003) 033007 [arXiv:hep-ph/0305243]; X. G. He, Nucl. Phys. Proc. Suppl. **168** (2007) 350 [arXiv:hep-ph/0612080]; A. Aranda, arXiv:0707.3661 [hep-ph]. A. H. Chan, H. Fritzsch and Z. z. Xing, arXiv:0704.3153 [hep-ph]; Z. z. Xing, Phys. Lett. B **618** (2005) 141 [arXiv:hep-ph/0503200]; Z. z. Xing, H. Zhang and S. Zhou, Phys. Lett. B **641** (2006) 189 [arXiv:hep-ph/0607091]; S. K. Kang, Z. z. Xing and S. Zhou, Phys. Rev. D **73** (2006) 013001 [arXiv:hep-ph/0511157]; S. Luo and Z. z. Xing, Phys. Lett. B **632** (2006) 341 [arXiv:hep-ph/0509065]; M. Hirsch, E. Ma, J. C. Romao, J. W. F. Valle and A. Villanova del Moral, Phys. Rev. D **75** (2007) 053006 [arXiv:hep-ph/0606082]; N. N. Singh, M. Rajkhowa and A. Borah, arXiv:hep-ph/0603189; X. G. He and A. Zee, Phys. Lett. B **645** (2007) 427 [arXiv:hep-ph/0607163]; N. Haba, A. Watanabe and K. Yoshioka, Phys. Rev. Lett. **97** (2006) 041601 [arXiv:hep-ph/0603116]. S. Pakvasa, W. Rodejohann and

T. J. Weiler, arXiv:0711.0052 [hep-ph]. S. F. King, JHEP **0508** (2005) 105 [arXiv:hep-ph/0506297]; I. Masina, Phys. Lett. B **633** (2006) 134 [arXiv:hep-ph/0508031]; S. Antusch and S. F. King, Phys. Lett. B **631** (2005) 42 [arXiv:hep-ph/0508044]; S. Antusch, P. Huber, S. F. King and T. Schwetz, JHEP **0704** (2007) 060 [arXiv:hep-ph/0702286]. N. Li and B. Q. Ma, Phys. Rev. D **71** (2005) 017302 [arXiv:hep-ph/0412126]. 14

[67] W. Chao and Y. -j. Zheng, arXiv:1107.0738 [hep-ph]. 14

[68] Charged lepton contributions to neutrino mixings have been considered, e.g., in: P. H. Frampton, S. T. Petcov and W. Rodejohann, Nucl. Phys. B **687** (2004) 31, hep-ph/0401206; G. Altarelli, F. Feruglio and I. Masina, Nucl. Phys. B **689** (2004) 157, hep-ph/0402155; S. Antusch and S. F. King, Phys. Lett. B **591** (2004) 104, hep-ph/0403053; F. Feruglio, Nucl. Phys. Proc. Suppl. **143** (2005) 184 [Nucl. Phys. Proc. Suppl. **145** (2005) 225], hep-ph/0410131; R. N. Mohapatra and W. Rodejohann, hep-ph/0507312. S. Antusch and S. F. King, Phys. Lett. B **659** (2008) 640 [arXiv:0709.0666 [hep-ph]]. Y. Lin, Nucl. Phys. B **813**, 91 (2009) [arXiv:0804.2867 [hep-ph]]. K. S. Babu and S. Gabriel, arXiv:1006.0203 [hep-ph]. K. A. Hochmuth, S. T. Petcov and W. Rodejohann, Phys. Lett. B **654**, 177 (2007) [arXiv:0706.2975 [hep-ph]]. 14

[69] Some examples with A_4 flavor symmetry: E. Ma and G. Rajasekaran, Phys. Rev. D **64**, 113012 (2001) [arXiv:hep-ph/0106291]; K. S. Babu, E. Ma and J. W. F. Valle, Phys. Lett. B **552**, 207 (2003) [arXiv:hep-ph/0206292]; E. Ma, Phys. Rev. D **70**, 031901 (2004) [arXiv:hep-ph/0404199]; Phys. Rev. D **72**, 037301 (2005) [arXiv:hep-ph/0505209], Mod. Phys. Lett. A **20**, 2601 (2005) [arXiv:hep-ph/0508099]. arXiv:hep-ph/0409075; G. Altarelli and F. Feruglio, Nucl. Phys. B **720**, 64 (2005) [arXiv:hep-ph/0504165]; Nucl. Phys. B **741**, 215 (2006) [arXiv:hep-ph/0512103]; K. S. Babu and X. G. He, arXiv:hep-ph/0507217, A. Zee, Phys. Lett. B **630**, 58 (2005) [arXiv:hep-ph/0508278], 14

[70] D. E. Groom et al, The Review of Particle Physics, The European Physical Journal C15, 1 (2000); The Particle Data Group, http://pdg.lbl.gov/. 15

[71] Christian Weinheimer, Doct. Thesis, Mainz, Univ. (1993) 16

[72] M. Doi, T. Kotani and E. Takasugi, Prog. Theor. Phys. Suppl. 83 (1985) 1. 17

[73] J. Schechter and J. W. F. Valle, Phys. Rev. D **25**, 2951 (1982). 17

[74] C. Kraus *et al.*, Eur. Phys. J. C **40**, 447 (2005) [arXiv:hep-ex/0412056]. 17

[75] V. M. Lobashev *et al.*, Phys. Lett. B **460**, 227 (1999). 17

[76] A. Osipowicz *et al.* [KATRIN Collaboration], arXiv:hep-ex/0109033. 17

[77] H. V. Klapdor-Kleingrothaus *et al.*, Eur. Phys. J. A **12**, 147 (2001) [arXiv:hep-ph/0103062]. 17

[78] C. E. Aalseth *et al.* [IGEX Collaboration], Phys. Rev. C **59**, 2108 (1999); C. E. Aalseth *et al.* [IGEX Collaboration], Phys. Rev. D **65**, 092007 (2002) [arXiv:hep-ex/0202026]. 17

[79] C. Arnaboldi *et al.* [CUORICINO Collaboration], Phys. Rev. C **78**, 035502 (2008) [arXiv:0802.3439 [hep-ex]]. 17

[80] C. Arnaboldi *et al.* [CUORE Collaboration], Nucl. Instrum. Meth. A **518**, 775 (2004) [arXiv:hep-ex/0212053]; E. Fiorini, Phys. Rept. **307**, 309 (1998); R. Ardito *et al.*, arXiv:hep-ex/0501010. 17

[81] S. Schonert *et al.* [GERDA Collaboration], Nucl. Phys. Proc. Suppl. **145**, 242 (2005); I. Abt *et al.*, arXiv:hep-ex/0404039. 17

[82] C. E. Aalseth *et al.* [Majorana Collaboration], Phys. Atom. Nucl. **67**, 2002 (2004) [Yad. Fiz. **67**, 2025 (2004)] [arXiv:hep-ex/0405008]; F. T. . Avignone [Majorana Collaboration], J. Phys. Conf. Ser. **120**, 052059 (2008) [arXiv:0711.4808 [nucl-ex]]. 17

[83] D. N. Spergel *et al.* [WMAP Collaboration], Astrophys. J. Suppl. **170**, 377 (2007) [arXiv:astro-ph/0603449]; E. Komatsu *et al.* [WMAP Collaboration], arXiv:0803.0547 [astro-ph]. 18

[84] U. Seljak *et al.* [SDSS Collaboration], Phys. Rev. D **71**, 103515 (2005) [arXiv:astro-ph/0407372]; M. Tegmark *et al.* [SDSS Collaboration], Phys. Rev. D **74**, 123507 (2006) [arXiv:astro-ph/0608632]. 18

[85] P. Minkowski, $\mu \to e\gamma$ at a Rate of One Out of 1-Billion Muon Decays?, Phys. Lett. B67 (1977) 421. T. Yanagida in Workshop on Unified Theories, KEK Report 79-18, p. 95, 1979. M. Gell-Mann, P. Ramond, and R. Slansky, Supergravity, p. 315. Amsterdam: North Holland, 1979. S. L. Glashow, 1979 Cargese Summer Institute on Quarks and Leptons, p. 687. New York: Plenum, 1980. R. Barbieri, D. V. Nanopoulos, G. Morchio, and F. Strocchi, Neutrino Masses in Grand Unified Theories, Phys. Lett. B90 (1980) 91. R. N. Mohapatra and G. Senjanovic, Neutrino Masses and Mixings in Gauge Models with Spontaneous Parity Violation, Phys. Rev. D23 (1981) 165. 18

[86] W. Konetschny and W. Kummer, Phys. Lett. B **70**, 433 (1977); T. P. Cheng and L. F. Li, Phys. Rev. D **22**, 2860 (1980); J. Schechter and J. W. F. Valle, Phys. Rev. D **22**, 2227 (1980); G. Lazarides, Q. Shafi and C. Wetterich, Nucl. Phys. B **181**, 287 (1981); R. N. Mohapatra and G. Senjanovic, Phys. Rev. D **23**, 165 (1981). 19

[87] M. Magg and C. Wetterich, *Neutrino mass problem and gauge hierarchy*, *Phys. Lett.* **B94** (1980) 61. G. Lazarides, Q. Shafi, and C. Wetterich, *Proton Lifetime and Fermion Masses in an SO(10) Model*, *Nucl. Phys.* **B181** (1981) 287. R. N. Mohapatra and G. Senjanovic, *Neutrino Masses and Mixings in Gauge Models with Spontaneous Parity Violation*, *Phys. Rev.* **D23** (1981) 165. 20

[88] R. Foot, H. Lew, X. G. He and G. C. Joshi, Z. Phys. C **44**, 441 (1989). 20

[89] A. Zee, Phys. Lett. B **93**, 389 (1980) [Erratum-ibid. B **95**, 461 (1980)]. 21

[90] K. S. Babu, Phys. Lett. B **203**, 132 (1988). A. Zee, Nucl. Phys. B **264**, 99 (1986). 21

[91] R. N. Mohapatra, Phys. Rev. Lett. 56, 561 (1986). R. N. Mohapatra and J. W. F. Valle, Phys. Rev. D34, 1642 (1986); M. C. Gonzalez- Garcia and J. W. F. Valle, Phys. Lett. B216, 360 (1989). 22

[92] C. D. Carone and H. Murayama, Phys. Lett. B392, 403 (1997). M.-C. Chen, K. T. Mahanthappa, Phys. Rev. D75, 015001 (2007). M.-C. Chen, A. de Gouvea and B. A. Dobrescu, Phys. Rev. D75, 055009 (2007). 23

[93] B. Pontecorvo, Sov. Phys. JETP **6** (1957) 429 [Zh. Eksp. Teor. Fiz. **33** (1957) 549]. Z. Maki, M. Nakagawa and S. Sakata, Prog. Theor. Phys. **28** (1962) 870. 23

[94] R. Barbieri, L.J. Hall, S. Raby, and A. Romanino, Nucl.Phys. B493 (1997) 3; M.-C. Chen and K.T. Mahanthappa, hep-ph/0009059; A. Aranda, C.D. Carone, and R.F. Lebed, Phys. Lett. B474 (2000) 170; Phys. Rev. D62 (2000) 016009; G. Perez, JHEP 0012 (2000) 027; P.H. Frampton and A. Rasin, Phys. Lett. B478 (2000) 424; R. Dermisek and S. Raby, Phys. Rev. D62 (2000) 015007. 24

[95] G. Altarelli and F. Feruglio, Nucl. Phys. B **741**, 215 (2006) [arXiv:hep-ph/0512103]. 26

[96] L. Wolfenstein, Phys. Rev.D17, 2369, 1978. 28

[97] S. P. Mikheyev and A. Y. Smirnov, Sov. J. Nucl. Phys. 42, 913, 1985. 28

[98] E. Roulet, Phys. Rev. D **44**, 935 (1991). 28

[99] G. Brooijmans, hep-ph/9808498. 28

[100] M. M. Guzzo, A. Masiero and S. T. Petcov, Phys. Lett. B **260**, 154 (1991). 28

[101] M. M. Guzzo, H. Nunokawa, P. C. de Holanda and O. L. G. Peres, Phys. Rev. D **64**, 097301 (2001) [hep-ph/0012089]. 28

[102] M. Guzzo, P. C. de Holanda, M. Maltoni, H. Nunokawa, M. A. Tortola and J. W. F. Valle, Nucl. Phys. B **629**, 479 (2002) [hep-ph/0112310]. 28

[103] A. Friedland and C. Lunardini, Phys. Rev. D **74**, 033012 (2006) [hep-ph/0606101]. 28

[104] A. Esteban-Pretel, J. W. F. Valle and P. Huber, Phys. Lett. B **668**, 197 (2008) [arXiv:0803.1790 [hep-ph]]. 28

[105] M. Blennow, D. Meloni, T. Ohlsson, F. Terranova and M. Westerberg, Eur. Phys. J. C **56**, 529 (2008) [arXiv:0804.2744 [hep-ph]]. 28

[106] N. C. Ribeiro, H. Minakata, H. Nunokawa, S. Uchinami and R. Zukanovich-Funchal, JHEP **0712**, 002 (2007) [arXiv:0709.1980 [hep-ph]]. 28

[107] A. Bandyopadhyay *et al.* [ISS Physics Working Group Collaboration], Rept. Prog. Phys. **72**, 106201 (2009) [arXiv:0710.4947 [hep-ph]]. 28

[108] N. C. Ribeiro, H. Nunokawa, T. Kajita, S. Nakayama, P. Ko and H. Minakata, Phys. Rev. D **77**, 073007 (2008) [arXiv:0712.4314 [hep-ph]]. 28

[109] J. Kopp, T. Ota and W. Winter, Phys. Rev. D **78**, 053007 (2008) [arXiv:0804.2261 [hep-ph]]. 28

[110] M. Malinsky, T. Ohlsson and H. Zhang, Phys. Rev. D **79**, 011301 (2009) [arXiv:0811.3346 [hep-ph]]. 28

[111] A. M. Gago, H. Minakata, H. Nunokawa, S. Uchinami and R. Zukanovich Funchal, JHEP **1001**, 049 (2010) [arXiv:0904.3360 [hep-ph]]. 28

[112] A. Palazzo and J. W. F. Valle, Phys. Rev. D **80**, 091301 (2009) [arXiv:0909.1535 [hep-ph]]. A. Palazzo, Phys. Rev. D **83**, 101701 (2011) [arXiv:1101.3875 [hep-ph]]. 28

[113] L. Wolfenstein, Phys. Rev. D **17**, 2369 (1978). 28

[114] J. W. F. Valle, Phys. Lett. B **199** (1987) 432. 28

[115] M. M. Guzzo, A. Masiero and S. T. Petcov, Phys. Lett. B **260**, 154 (1991). 28

[116] E. Roulet, Phys. Rev. D **44**, 935 (1991). 28

[117] Y. Grossman, Phys. Lett. B **359**, 141 (1995) [arXiv:hep-ph/9507344]. 28

[118] Z. Berezhiani and A. Rossi, Phys. Lett. B **535**, 207 (2002) [arXiv:hep-ph/0111137]. 28

[119] S. Davidson, C. Pena-Garay, N. Rius and A. Santamaria, JHEP **0303**, 011 (2003) [arXiv:hep-ph/0302093]. 28

[120] J. Abdallah *et al.* [DELPHI Collaboration], Eur. Phys. J. C **38**, 395 (2005) [arXiv:hep-ex/0406019]. 28

[121] Y. Grossman, Phys. Lett. B **359**, 141 (1995) [hep-ph/9507344]. 28

[122] S. Bergmann, M. M. Guzzo, P. C. de Holanda, P. I. Krastev and H. Nunokawa, Phys. Rev. D **62**, 073001 (2000) [hep-ph/0004049]. 28

[123] Z. Berezhiani, R. S. Raghavan and A. Rossi, Nucl. Phys. B **638**, 62 (2002) [hep-ph/0111138]. 28

[124] A. Friedland, C. Lunardini and C. Pena-Garay, Phys. Lett. B **594**, 347 (2004) [hep-ph/0402266]. 28

[125] O. G. Miranda, M. A. Tortola and J. W. F. Valle, JHEP **0610**, 008 (2006) [hep-ph/0406280]. 28

[126] M. C. Gonzalez-Garcia, M. M. Guzzo, P. I. Krastev, H. Nunokawa, O. L. G. Peres, V. Pleitez, J. W. F. Valle and R. Zukanovich Funchal, Phys. Rev. Lett. **82**, 3202 (1999) [hep-ph/9809531]. 28

[127] S. Bergmann, Y. Grossman and D. M. Pierce, Phys. Rev. D **61**, 053005 (2000) [hep-ph/9909390]. 28

[128] N. Fornengo, M. Maltoni, R. Tomas and J. W. F. Valle, Phys. Rev. D **65**, 013010 (2002) [hep-ph/0108043]. 28

[129] M. C. Gonzalez-Garcia and M. Maltoni, Phys. Rev. D **70**, 033010 (2004) [hep-ph/0404085]. 28

[130] A. Friedland, C. Lunardini and M. Maltoni, Phys. Rev. D **70**, 111301 (2004) [hep-ph/0408264]. 28

[131] A. Friedland and C. Lunardini, Phys. Rev. D **72**, 053009 (2005) [hep-ph/0506143]. 28

[132] S. Bergmann and Y. Grossman, Phys. Rev. D **59**, 093005 (1999) [hep-ph/9809524]. 28

[133] T. Ota, J. Sato and N. -a. Yamashita, Phys. Rev. D **65**, 093015 (2002) [hep-ph/0112329]. 28

[134] T. Ota and J. Sato, Phys. Lett. B **545**, 367 (2002) [hep-ph/0202145]. 28

[135] M. Honda, N. Okamura and T. Takeuchi, hep-ph/0603268. 28

[136] N. Kitazawa, H. Sugiyama and O. Yasuda, hep-ph/0606013. 28

[137] M. Blennow, T. Ohlsson and J. Skrotzki, Phys. Lett. B **660**, 522 (2008) [hep-ph/0702059 [HEP-PH]]. 28

[138] M. C. Gonzalez-Garcia, Y. Grossman, A. Gusso and Y. Nir, Phys. Rev. D **64**, 096006 (2001) [hep-ph/0105159]. 28, 31

[139] P. Huber and J. W. F. Valle, Phys. Lett. B **523**, 151 (2001) [hep-ph/0108193]. 28

[140] A. M. Gago, M. M. Guzzo, H. Nunokawa, W. J. C. Teves and R. Zukanovich Funchal, Phys. Rev. D **64**, 073003 (2001) [hep-ph/0105196]. 28

[141] P. Huber, T. Schwetz and J. W. F. Valle, Phys. Rev. D **66**, 013006 (2002) [hep-ph/0202048]. 28

[142] M. Campanelli and A. Romanino, Phys. Rev. D **66**, 113001 (2002) [hep-ph/0207350]. 28

[143] M. Blennow, T. Ohlsson and W. Winter, Eur. Phys. J. C **49**, 1023 (2007) [hep-ph/0508175]. 28

[144] A. Bueno, M. Campanelli, M. Laveder, J. Rico and A. Rubbia, JHEP **0106**, 032 (2001) [hep-ph/0010308]. 28

[145] J. Kopp, M. Lindner and T. Ota, Phys. Rev. D **76**, 013001 (2007) [hep-ph/0702269 [HEP-PH]]. 28

[146] R. Adhikari, S. K. Agarwalla and A. Raychaudhuri, Phys. Lett. B **642**, 111 (2006) [hep-ph/0608034]. 28

[147] G. L. Fogli, E. Lisi, A. Mirizzi and D. Montanino, Phys. Rev. D **66**, 013009 (2002) [hep-ph/0202269]. 28

[148] H. Duan, G. M. Fuller, J. Carlson and Y. -Z. Qian, Phys. Rev. Lett. **97**, 241101 (2006) [astro-ph/0608050]. 28

[149] A. Esteban-Pretel, R. Tomas and J. W. F. Valle, Phys. Rev. D **76**, 053001 (2007) [arXiv:0704.0032 [hep-ph]]. 28

[150] G. Mangano, G. Miele, S. Pastor, T. Pinto, O. Pisanti and P. D. Serpico, Nucl. Phys. B **756**, 100 (2006) [hep-ph/0607267]. 28

[151] Z. Berezhiani and A. Rossi, Phys. Lett. B **535**, 207 (2002) [hep-ph/0111137]. 28

[152] J. Barranco, O. G. Miranda, C. A. Moura and J. W. F. Valle, Phys. Rev. D **73**, 113001 (2006) [hep-ph/0512195]. 28

[153] J. Barranco, O. G. Miranda and T. I. Rashba, JHEP **0512**, 021 (2005) [hep-ph/0508299]. 28

[154] J. Barranco, O. G. Miranda and T. I. Rashba, Phys. Rev. D **76**, 073008 (2007) [hep-ph/0702175]. 28

[155] Y. Grossman, H. E. Haber and Y. Nir, Phys. Lett. B **357**, 630 (1995) [hep-ph/9507213]. 31

[156] J. Kopp, M. Lindner, T. Ota and J. Sato, Phys. Rev. D **77**, 013007 (2008) [arXiv:0708.0152 [hep-ph]]. 31

[157] Z. -z. Xing, Int. J. Mod. Phys. A **23**, 4255 (2008) [arXiv:0810.1421 [hep-ph]]. 31

[158] S. Antusch, C. Biggio, E. Fernandez-Martinez, M. B. Gavela and J. Lopez-Pavon, JHEP **0610**, 084 (2006) [hep-ph/0607020]. 31, 32

[159] E. Fernandez-Martinez, M. B. Gavela, J. Lopez-Pavon and O. Yasuda, Phys. Lett. B **649**, 427 (2007) [hep-ph/0703098]. 31

[160] S. Goswami and T. Ota, Phys. Rev. D **78**, 033012 (2008) [arXiv:0802.1434 [hep-ph]]. 31

[161] Z. -z. Xing and S. Zhou, Phys. Lett. B **666**, 166 (2008) [arXiv:0804.3512 [hep-ph]]. 31

[162] S. Luo, Phys. Rev. D **78**, 016006 (2008) [arXiv:0804.4897 [hep-ph]]. 31

[163] G. Altarelli and D. Meloni, Nucl. Phys. B **809**, 158 (2009) [arXiv:0809.1041 [hep-ph]]. 31

[164] P. Langacker and D. London, Phys. Rev. D38,907 1988 32

[165] R. Dermisek and J. F. Gunion, arXiv:1002.1971 [hep-ph]. 34, 35

[166] E. Braaten, S. Fleming and A. K. Leibovich, Phys. Rev. D **63**, 094006 (2001) [arXiv:hep-ph/0008091]. 34

[167] See T. Armstrong *et al.* [Fermilab E760 Collaboration], Phys. Rev. D **54**, 7067 (1996) and references therein. 34, 35

[168] C. Amsler et al. (Particle Data Group), Physics Letters B667, 1 (2008) and 2009 partial update for the 2010 edition. 35, 40, 117, 118, 119, 120, 200

[169] R. Dermisek and J. F. Gunion, Phys. Rev. Lett. **95**, 041801 (2005) [arXiv:hep-ph/0502105]; R. Dermisek and J. F. Gunion, Phys. Rev. D **73**, 111701 (2006) [arXiv:hep-ph/0510322]; R. Dermisek and J. F. Gunion, Phys. Rev. D **75**, 075019 (2007) [arXiv:hep-ph/0611142]; R. Dermisek and J. F. Gunion, Phys. Rev. D **76**, 095006 (2007) [arXiv:0705.4387 [hep-ph]]; S. Chang, P. J. Fox and N. Weiner, JHEP **0608**, 068 (2006) [arXiv:hep-ph/0511250]. 35

[170] P. Fayet, Nucl. Phys. B **90** (1975) 104; Phys. Lett. B **64** (1976) 159; Phys. Lett. B **69** (1977) 489 and Phys. Lett. B **84** (1979) 416; H.P. Nilles, M. Srednicki and D. Wyler, Phys. Lett. B **120** (1983) 346; J.M. Frere, D.R. Jones and S. Raby, Nucl. Phys. B **222** (1983) 11; J.P. Derendinger and C.A. Savoy, Nucl. Phys. B **237** (1984) 307; A.I. Veselov, M.I. Vysotsky and K.A. Ter-Martirosian, Sov. Phys. JETP **63** (1986) 489; J.R. Ellis, J.F. Gunion, H.E. Haber, L. Roszkowski and F. Zwirner, Phys. Rev. D **39** (1989) 844; M. Drees, Int. J. Mod. Phys. A **4** (1989) 3635; J.E. Kim and H.P. Nilles, Phys. Lett. B **138** (1984) 150. B. A. Dobrescu, G. Landsberg and K. T. Matchev, Phys. Rev. D **63** (2001) 075003 [arXiv:hep-ph/0005308];
B. A. Dobrescu and K. T. Matchev, JHEP **0009** (2000) 031 [arXiv:hep-ph/0008192]. 35, 163

[171] J. F. Gunion, arXiv:0808.2509 [hep-ph]. 35

[172] F. Domingo, U. Ellwanger, E. Fullana, C. Hugonie and M. A. Sanchis-Lozano, JHEP **0901**, 061 (2009) [arXiv:0810.4736 [hep-ph]]. 35

[173] See for e.g F. Domingo, U. Ellwanger and M. A. Sanchis-Lozano, Phys. Rev. Lett. **103**, 111802 (2009) and references therein. [arXiv:0907.0348 [hep-ph]]. 36, 41

[174] See for e.g. Ref. 2 and 3 in [170]. 36

[175] P. Fayet, Phys. Lett. B **95**, 285 (1980); Nucl. Phys. B **187**, 184 (1981). 36

[176] C. Bouchiat and P. Fayet, Phys. Lett. B **608**, 87 (2005) [arXiv:hep-ph/0410260]. 36, 38, 39, 40, 41

[177] P. Fayet, Phys. Rev. D **75**, 115017 (2007) [arXiv:hep-ph/0702176]. 36, 38, 39, 40, 41

[178] P. Fayet, Phys. Rev. D **74**, 054034 (2006) [arXiv:hep-ph/0607318]. 36, 38, 39, 40, 41

[179] P. Fayet, "U(1)A symmetry in two-doublet models, U bosons or light pseudoscalars, and psi and Upsilon decays," arXiv:0812.3980 [hep-ph]. 36

[180] See for e.g. D. P. Finkbeiner and N. Weiner, *Exciting Dark Matter and the INTEGRAL/SPI 511 keV signal*, *Phys. Rev.* **D76** (2007) 083519: M. Pospelov, A. Ritz, and M. B. Voloshin, *Secluded WIMP Dark Matter*, *Phys. Lett.* **B662** (2008) 53; K. M. Zurek, *Multi-Component Dark Matter*, *Phys. Rev.* **D79** (2009) 115002; D. E. Morrissey, D. Poland, and K. M. Zurek, *Abelian Hidden Sectors at a GeV*, *JHEP* **07** (2009) 050; C. Cheung, J. T. Ruderman, L.-T. Wang, and I. Yavin, *Kinetic Mixing as the Origin of Light Dark Scales*, *Phys. Rev.* **D80** (2009) 035008, N. Arkani-Hamed, D. P. Finkbeiner, T. R. Slatyer, and N. Weiner, *A Theory of Dark Matter*, *Phys. Rev.* **D79** (2009) 015014; Y. Cui, D. E. Morrissey, D. Poland, and L. Randall, *Candidates for Inelastic Dark Matter*, *JHEP* **05** (2009) 076; A. Katz and R. Sundrum, *Breaking the Dark Force*, *JHEP* **06** (2009) 003. 36

[181] X. G. He, J. Tandean and G. Valencia, Phys. Rev. Lett. **98**, 081802 (2007) [arXiv:hep-ph/0610362]. 36

[182] V. V. Braguta, V. G. Kartvelishvili, Phys. Rev. D **81**,014012 (2010), hep-ph/0907.2772. 37

[183] Yu Jia and Wen-Long Sang, arXiv:hep-ph/0906.4782v3. 37

[184] S.D. Drell, Nuovo Cimento, **11**, 693 (1959); S. Berman and D. Geffen, Nuovo Cim. **18**, 1192 (1960); D. A. Geffen and B. l. Young, Phys. Rev. Lett. **15**, 316 (1965). 37

[185] See for example R. D. Diaz, hep-ph/0212237 and references there in. 38

[186] D. S. Hwang and G. H. Kim, Z. Phys. C **76**, 107 (1997) [arXiv:hep-ph/9703364]. 40

[187] H. W. Ke, X. Q. Li and X. Liu, arXiv:1002.1187 [hep-ph]. 40

[188] M. I. Gresham, I. W. Kim and K. M. Zurek, arXiv:1103.3501 [hep-ph]. 43, 54

[189] See for e.g. S. Baek, A. Datta, P. Hamel, O. F. Hernandez and D. London, Phys. Rev. D **72**, 094008 (2005) [arXiv:hep-ph/0508149]. S. Baek, P. Hamel, D. London, A. Datta and D. A. Suprun, Phys. Rev. D **71**, 057502 (2005) [arXiv:hep-ph/0412086]; A. Datta, Phys. Rev. D **66**, 071702 (2002) [arXiv:hep-ph/0208016]; A. Datta, X. G. He and S. Pakvasa, Phys. Lett. B **419**, 369 (1998) [arXiv:hep-ph/9707259]. 43

[190] T. Han, R. D. Peccei and X. Zhang, Nucl. Phys. B **454**, 527 (1995), [arXiv:hep-ph/9506461]; T. Han, K. Whisnant, B. L. Young and X. Zhang, Phys. Rev. D **55**, 7241 (1997), [arXiv:hep-ph/9603247]. T. Han, K. Whisnant, B. L. Young and X. Zhang, Phys. Lett. B **385**, 311 (1996), [arXiv:hep-ph/9606231]; 43

[191] P. J. Fox, J. Liu, D. Tucker-Smith and N. Weiner, arXiv:1104.4127 [hep-ph]. 44

[192] A. Datta and D. London, Int. J. Mod. Phys. A **19**, 2505 (2004), [arXiv:hep-ph/0303159]. A. Datta, M. Duraisamy and D. London, arXiv:1103.2442 [hep-ph]. 44

[193] A. Datta and X. Zhang, Phys. Rev. D **55**, 2530 (1997), [arXiv:hep-ph/9611247]. 45

[194] A. Lenz *et al.* , Phys. Rev. D. **83**, 036004 (2011), [arXiv:1008.1593 [hep-ph]]. 45, 47

[195] A. Abulencia *et al.* [CDF Collaboration], Phys. Rev. Lett. **97**, 242003 (2006), [arXiv:hep-ex/0609040]. 45

[196] V. M. Abazov *et al.* [D0 Collaboration], Phys. Rev. Lett. **101**, 241801 (2008), [arXiv:0802.2255 [hep-ex]]. 45

[197] D. Asner *et al.* [The Heavy Flavor Averaging Group] , arXiv:1010.1589 [hep-ex]. 45

[198] A. Datta and M. Duraisamy, Phys. Rev. D **81**, 074008 (2010), [arXiv:0912.4785 [hep-ph]]. 45

[199] C. H. Chen, Sandy S. C. Law and Run-Hui Li, arXiv:1104.1497 [hep-ph]. 49

[200] H. L. Lai *et al.* [CTEQ Collaboration], Eur. Phys. J. **C12**,375-392 (2000), [hep-ph/9903282]. 51

[201] A. D. Martin, W. J. Stirling, R. S. Thorne, G. Watt, Eur. Phys. J. **C63**,189-285 (2009), [arXiv:0901.0002 [hep-ph]]. 51

[202] Q. H. Cao, D. McKeen, J. L. Rosner, G. Shaughnessy and C. E. M. Wagne, Phys. Rev. D. **81**,114004 (2010), [arXiv:1003.3461 [hep-ph]]. 51

[203] T. Aaltonen *et al.* [CDF Collaboration], Phys. Rev. Lett. **102**, 222003 (2009). [arXiv: 0903.2850[hep-ex]]. xi, 51, 52

[204] D. -W. Jung, P. Ko, J. S. Lee, *Longitudinal top polarization as a probe of a possible origin of forward-backward asymmetry of the top quark at the Tevatron,* [arXiv:1011.5976 [hep-ph]]; D. Choudhury, R. M. Godbole, S. D. Rindani, and P. Saha, *Top polarization, forward-backward asymmetry and new physics*, 53

[205] P. H. Frampton, S. T. Petcov and W. Rodejohann, Nucl. Phys. B **687** (2004) 31, hep-ph/0401206; G. Altarelli, F. Feruglio and I. Masina, Nucl. Phys. B **689** (2004) 157, hep-ph/0402155; S. Antusch and S. F. King, Phys. Lett. B **591** (2004) 104, hep-ph/0403053; F. Feruglio, Nucl. Phys. Proc. Suppl. **143** (2005) 184 [Nucl. Phys. Proc. Suppl. **145** (2005) 225], hep-ph/0410131; R. N. Mohapatra and W. Rodejohann, hep-ph/0507312. S. Antusch and S. F. King, Phys. Lett. B **659** (2008) 640 [arXiv:0709.0666 [hep-ph]]. 56

[206] A. Datta, Phys. Rev. D **78**, 095004 (2008) [arXiv:0807.0795 [hep-ph]]; A. Datta, Phys. Rev. **D74**, 014022 (2006). [hep-ph/0605039]; A. Datta, P. J. O'Donnell, Phys. Rev. **D72**, 113002 (2005). [hep-ph/0508314]; A. S. Joshipura, B. P. Kodrani, Phys. Rev. **D82**, 115013 (2010). [arXiv:1004.3637 [hep-ph]]. 56, 59

[207] S. Baek, A. Datta, P. Hamel, O. F. Hernandez and D. London, Phys. Rev. D **72**, 094008 (2005) [arXiv:hep-ph/0508149]. S. Baek, P. Hamel, D. London, A. Datta and D. A. Suprun, Phys. Rev. D **71**, 057502 (2005) [arXiv:hep-ph/0412086]; A. Datta, M. Imbeault, D. London, V. Page, N. Sinha, R. Sinha, Phys. Rev. **D71**, 096002 (2005). [hep-ph/0406192]; A. Datta, D. London, Phys. Lett. **B595**, 453-460 (2004). [hep-ph/0404130]. A. Datta, Phys. Rev. D **66**, 071702 (2002) [arXiv:hep-ph/0208016]; A. Datta, X. G. He and S. Pakvasa, Phys. Lett. B **419**, 369 (1998) [arXiv:hep-ph/9707259]. 56

[208] C. I. Low and R. R. Volkas, Phys. Rev. D68 (2003) 033007, `hep-ph/0305243`; 56

[209] S. Andreas, O. Lebedev, S. Ramos-Sanchez *et al.*, JHEP **1008**, 003 (2010). [arXiv:1005.3978 [hep-ph]]. A. Rashed, M. Duraisamy, A. Datta, Phys. Rev. **D82**, 054031 (2010). [arXiv:1004.5419 [hep-ph]]. R. Dermisek, J. F. Gunion, Phys. Rev. **D81**, 055001 (2010). [arXiv:0911.2460 [hep-ph]]. 57

[210] W. Grimus, L. Lavoura, Phys. Lett. **B572**, 189-195 (2003). [hep-ph/0305046]. W. Grimus, L. Lavoura, J. Phys. G **G30**, 73-82 (2004). [hep-ph/0309050]. W. Grimus,

A. S. Joshipura, S. Kaneko, L. Lavoura, M. Tanimoto, JHEP **0407**, 078 (2004). [hep-ph/0407112]. W. Grimus, S. Kaneko, L. Lavoura, H. Sawanaka, M. Tanimoto, JHEP **0601**, 110 (2006). [hep-ph/0510326]. 57

[211] T. Fukuyama and H. Nishiura, hep-ph/9702253; in Proceedings of the International Workshop on Masses and Mixings of Quarks and Leptons, Shizuoka, Japan, 1997, edited by Y. Koide (World Scientific, Singapore, 1998), p. 252; R.N. Mohapatra and S. Nussinov, Phys. Rev. **D60**, 013002 (1999); E. Ma and M. Raidal, Phys. Rev. Lett. **87**, 011802 (2001); C. S. Lam, hep-ph/0104116; T. Kitabayashi and M. Yasue, Phys.Rev. **D67** 015006 (2003); Y. Koide, Phys.Rev. **D69**, 093001 (2004); R. N. Mohapatra, SLAC Summer Inst. lecture; http://www-conf.slac.stanford.edu/ssi/2004; hep-ph/0408187; JHEP, **0410**, 027 (2004); W. Grimus, A. S.Joshipura, S. Kaneko, L. Lavoura, H. Sawanaka, M. Tanimoto, hep-ph/0408123; A. Ghosal, Mod. Phys. Lett. A **19**, 2579 (2004). 58

[212] M. Gell-Mann, P. Ramond, and R. Slansky, in *Supergravity, Proceedings of the Workshop, Stony Brook, New York, 1979*, eds. F. van Nieuwenhuizen and D. Freedman (North Holland, Amsterdam, 1979); T. Yanagida, in *Proceedings of the Workshop on Unified Theories and Baryon Number in the Universe*, Tsukuba, Japan, 1979, eds. O. Sawada and A. Sugamoto (KEK report no. 79, Tsukuba, 1979); } R.N. Mohapatra and G. Senjanović, Phys. Rev. Lett. 44 (1980) 912. 65

[213] J. Barry and W. Rodejohann, Nucl. Phys. B **842**, 33 (2011) [arXiv:1007.5217 [hep-ph]]. 66, 75

[214] T. Schwetz, M. A. Tortola and J. W. F. Valle, New J. Phys. **10**, 113011 (2010) [arXiv:0808.2016v3 [hep-ph]]. 69

[215] S. F. King, Phys. Lett. B **659**, 244 (2008) [arXiv:0710.0530 [hep-ph]]. 69, 83

[216] R. N. Mohapatra and A. Y. Smirnov, Ann. Rev. Nucl. Part. Sci. **56**, 569 (2006) [arXiv:hep-ph/0603118]. 75, 85

[217] M. -C. Chen, J. Huang, [arXiv:1105.3188 [hep-ph]]. 75

[218] Y. -L. Wu, Phys. Rev. **D60**, 073010 (1999), [hep-ph/9810491], J. -Y. Liu, Y. Tang, Y. -L. Wu, [arXiv:1108.5012 [hep-ph]]. 77

[219] M. Sher and C. Triola, Phys. Rev. D **83**, 117702 (2011) [arXiv:1105.4844 [hep-ph]]. F. Chen, J. M. Cline and A. R. Frey, Phys. Rev. D **80**, 083516 (2009) [arXiv:0907.4746 [hep-ph]]. X. -G. He, J. Tandean and G. Valencia, Phys. Rev. D **74**, 115015 (2006)

[hep-ph/0610274]. D. L. Anderson, C. D. Carone and M. Sher, Phys. Rev. D **67**, 115013 (2003) [hep-ph/0303215]. J. McDonald, Phys. Rev. Lett. **88**, 091304 (2002) [hep-ph/0106249]. A. Rashed, M. Duraisamy and A. Datta, Phys. Rev. D **82**, 054031 (2010) [arXiv:1004.5419 [hep-ph]]. S. M. Davidson and H. E. Logan, Phys. Rev. D **82**, 115031 (2010) [arXiv:1009.4413 [hep-ph]]. 85

[220] A. Rashed and A. Datta, Phys. Rev. D **85**, 035019 (2012) [arXiv:1109.2320 [hep-ph]]. N. Haba, T. Horita, K. Kaneta and Y. Mimura, arXiv:1110.2252 [hep-ph]. A. Ibarra, E. Molinaro and S. T. Petcov, JHEP **1009**, 108 (2010) [arXiv:1007.2378 [hep-ph]]. W. Chao, Phys. Rev. D **82**, 016008 (2010) [arXiv:1003.1468 [hep-ph]]. Z. -z. Xing and S. Zhou, Phys. Lett. B **679**, 249 (2009) [arXiv:0906.1757 [hep-ph]]. W. Loinaz, N. Okamura, S. Rayyan, T. Takeuchi and L. C. R. Wijewardhana, Phys. Rev. D **68**, 073001 (2003) [hep-ph/0304004]. J. C. Montero, C. A. de S.Pires and V. Pleitez, Phys. Lett. B **502**, 167 (2001) [hep-ph/0011296]. E. Ma, Phys. Rev. Lett. **86**, 2502 (2001) [hep-ph/0011121]. C. D. Carone and H. Murayama, Phys. Lett. B **392**, 403 (1997) [hep-ph/9610383]. M. -C. Chen and J. Huang, Mod. Phys. Lett. A **26**, 1147 (2011) [arXiv:1105.3188 [hep-ph]]. 85

[221] E. Ma, Phys. Rev. **D73**, 077301 (2006). 92, 95, 102, 103, 104, 107

[222] N. G. Deshpande and E. Ma, Phys. Rev. **D18**, 2574 (1978). 92, 103

[223] E. Ma and G. Rajasekaran, Phys. Rev. **D64**, 113012 (2001). 92, 93, 104

[224] E. Ma, Mod. Phys. Lett. **A17**, 2361 (2002). 92, 104

[225] K. S. Babu, E. Ma, and J. W. F. Valle, Phys. Lett. **B552**, 207 (2003). 92, 104

[226] E. Ma, Phys. Rev. **D70**, 031901 (2004). 92, 93, 94

[227] Daya Bay Collaboration: F. P. An *et al.*, Phys. Rev. Lett. **108**, 171803 (2012) [arXiv:.1669 [hep-ex]]. 93

[228] RENO Collaboration: J. K. Ahn *et al.*, Phys. Rev. Lett. **108**, 191802 (2012) [arXiv:1204.0626 [hep-ex]]. 93

[229] H. Ishimori and E. Ma, arXiv:1205.0075 [hep-ph]. 93, 94, 97, 98

[230] E. Ma, Phys. Rev. **D82**, 037301 (2010). 94

[231] Q.-H. Cao, S. Khalil, E. Ma, and H. Okada, Phys. Rev. Lett. **106**, 131801 (2011). 94

[232] Q.-H. Cao, A. Damanik, E. Ma, and D. Wegman, Phys. Rev. **D83**, 093012 (2011). 94

[233] E. Ma and D. Wegman, Phys. Rev. Lett. **107**, 061803 (2011). 94

[234] Particle Data Group: K. Nakamura *et al.*, J. Phys. G: Nucl. Part. Phys. **37**, 075021 (2010). 95

[235] S. Weinberg, Phys. Rev. Lett. **43**, 1566 (1979). 102

[236] E. Ma, Phys. Rev. Lett. **81**, 1171 (1998). 102

[237] F. Bonnet, M. Hirsch, T. Ota, and W. Winter, JHEP **1207**, 153 (2012). 102

[238] E. Ma, Phys. Lett. **B717**, 235 (2012). 102, 104, 107

[239] T. Yanagida, in *Proc. of the Workshop on Unified Theories and Baryon Number in the Universe* (KEK, Tsukuba, 1979), edited by O. Sawada and A. Sugamoto, p. 95; M. Gell-Mann, P. Ramond, and R. Slansky, in *Supergravity*, edited by P. van Nieuwenhuizen and D. Z. Freedman (North-Holland, Amsterdam, 1979), p. 315; R. N. Mohapatra and G. Senjanovic, Phys. Rev. Lett. **44**, 912 (1980); P. Minkowski, Phys. Lett. **67B**, 421 (1977). 103

[240] R. Barbieri, L. J. Hall, and V. S. Rychkov, Phys. Rev. **D74**, 015007 (2006). 103

[241] L. Lopez Honorez, E. Nezri, J. F. Oliver, and M. H. G. Tytgat, JCAP **0702**, 028 (2007). 103

[242] D. Aristizabal Sierra *et al.*, Phys. Rev. **D79**, 013011 (2009). 104

[243] G. B. Gelmini, E. Osoba, and S. Palomares-Ruiz, Phys. Rev. **D81**, 063529 (2010). 104

[244] E. Ma, A. Natale, and A. Rashed, Int. J. Mod. Phys. **A27**, 1250134 (2012). 207 (2003). 104

[245] E. Ma and M. Raidal, Phys. Rev. Lett. **87**, 011802 (2001); Erratum: *ibid.* **87**, 159901(E) (2001). 105

[246] H. J. de Vega and N. G. Sanchez, arXiv:1109.3187 [astro-ph.CO]. 105, 107

[247] H. J. de Vega, M. C. Falvella, and N. G. Sanchez, arXiv:1203.3562 [astro-ph.CO]. 105, 107

[248] For a recent review, see for example K. N. Abazajian *et al.*, arXiv:1204.5379 [hep-ph]. 105

[249] C. R. Watson, Z. Li, and N. K. Polley, JCAP **1203**, 018 (2012). 105, 107

[250] M. Viel, G. D. Becker, J. S. Bolton, M. G. Haehnelt, M. Rauch, and W. L. W. Sargent, Phys. Rev. Lett. **100**, 041304 (2008). 105

[251] E. Ma, Phys. Rev. **D85**, 091701(R) (2012). 105

[252] F. Bezrukov, H. Hettmansperger, and M. Lindner, Phys. Rev. **D81**, 085032 (2010). 105

[253] F. Bezrukov, A. Kartavstsev, and M. Lindner, arXiv:1204.5477 [hep-ph]. 105

[254] M. Nemevsek, G. Senjanovic, and Y. Zhang, JCAP **1207**, 006 (2012). 105

[255] A. Pierce and J. Thaler, JHEP **0708**, 026 (2007). 106

[256] E. Dolle, X. Miao, S. Su, and B. Thomas, Phys. Rev. **D81**, 035003 (2010). 106

[257] ATLAS Collaboration, G. Aad *et al.*, Phys. Lett. **B716**, 1 (2012). 106

[258] CMS Collaboration, S. Chatrchyan *et al.*, Phys. Lett. **B716**, 30 (2012). 106

[259] P. Posch, Phys. Lett. **B696**, 447 (2011). 106

[260] A. Arhrib, R. Benbrik, and N. Gaur, Phys. Rev. **D85**, 095021 (2012). 106

[261] J. Chang, K. Cheung, P.-Y. Tseng, and T.-C. Yuan, Int. J. Mod. Phys. **A27**, 1230030 (2012). 106

[262] B. Swiezewska and M. Krawczyk, arXiv:1212.4100 [hep-ph]. 106

[263] CMS Collaboration, Physics Analysis Summary: CMS PAS SMP-12-013. 106

[264] E. Ma, Phys. Lett. **B659**, 885 (2008). 106

[265] K. Abe *et al.* [Super-Kamiokande Collaboration], arXiv:1206.0328 [hep-ex]. 108, 109, 135

[266] K. Abe *et al.* [Super-Kamiokande Collaboration], Phys. Rev. Lett. **97**, 171801 (2006) [hep-ex/0607059]. 108, 109

[267] N. Agafonova et al [OPERA Collaboration], arXiv:1107.2594 [hep-ex]. B. Wonsak [OPERA Collaboration], J. Phys. Conf. Ser. **335**, 012051 (2011). 108, 109

[268] K. Kodama *et al.* [DONuT Collaboration], Phys. Rev. D **78**, 052002 (2008) [arXiv:0711.0728 [hep-ex]]. 108, 135

[269] Y. Abe *et al.* [DOUBLE-CHOOZ Collaboration], Phys. Rev. Lett. **108**, 131801 (2012) [arXiv:1112.6353 [hep-ex]]. 109

[270] F. P. An *et al.* [DAYA-BAY Collaboration], Phys. Rev. Lett. **108**, 171803 (2012) [arXiv:1203.1669 [hep-ex]]. 109

[271] J. K. Ahn *et al.* [RENO Collaboration], Phys. Rev. Lett. **108**, 191802 (2012) [arXiv:1204.0626 [hep-ex]]. 109

[272] K. Hagiwara, K. Mawatari and H. Yokoya, Nucl. Phys. B **668**, 364 (2003) [Erratum-ibid. B **701**, 405 (2004)] [hep-ph/0305324]. 109, 113, 115, 124, 128, 130, 132, 140

[273] J. Conrad, A. de Gouvea, S. Shalgar and J. Spitz, Phys. Rev. D **82**, 093012 (2010) [arXiv:1008.2984 [hep-ph]]. 109, 136

[274] A. Rashed et.al. in preparation.

[275] K. Ikado *et al.*, Phys. Rev. Lett. **97**, 251802 (2006) [arXiv:hep-ex/0604018]. 109

[276] J. P. Lees *et al.* [BaBar Collaboration], Phys. Rev. Lett. **109**, 101802 (2012) [arXiv:1205.5442 [hep-ex]]. 109

[277] A. Datta, M. Duraisamy and D. Ghosh, Phys. Rev. D **86**, 034027 (2012) [arXiv:1206.3760 [hep-ph]]. 109

[278] M. C. Gonzalez-Garcia, Y. Grossman, A. Gusso and Y. Nir, Phys. Rev. D **64**, 096006 (2001) [hep-ph/0105159]. 109

[279] D. Delepine, V. G. Macias, S. Khalil and G. Lopez Castro, Phys. Rev. D **79**, 093003 (2009) [arXiv:0901.1460 [hep-ph]]. 109

[280] C. Biggio, M. Blennow and E. Fernandez-Martinez, JHEP **0908**, 090 (2009) [arXiv:0907.0097 [hep-ph]]. 109, 117, 118, 120

[281] U. Nierste, S. Trine and S. Westhoff, Phys. Rev. D **78**, 015006 (2008) [arXiv:0801.4938 [hep-ph]]. X. -G. He and G. Valencia, arXiv:1211.0348 [hep-ph]. 109

[282] K. Kiers, K. Little, A. Datta, D. London, M. Nagashima and A. Szynkman, Phys. Rev. D **78**, 113008 (2008) [arXiv:0808.1707 [hep-ph]]; A. Datta, K. Kiers, D. London, P. J. O'Donnell and A. Szynkman, Phys. Rev. D **75**, 074007 (2007) [Erratum-ibid. D **76**, 079902 (2007)] [hep-ph/0610162]. 109, 118

[283] D. Meloni and M. Martini, arXiv:1203.3335 [hep-ph]. 110

[284] T. Teshima and T. Sakai, Analysis of atmospheric neutrino oscillations in three flavor neutrinos, Phys. Rev. D 62, 113010 (2000) [hep-ph/0003038]. 110

[285] M. C. Gonzalez-Garcia, M. Maltoni and J. Salvado, JHEP **1004**, 056 (2010) [arXiv:1001.4524 [hep-ph]]. xiii, xiv, xv, xvi, xvii, 111, 119, 122, 123, 127, 128, 130, 132, 139

[286] A. Donini, D. Meloni and P. Migliozzi, Nucl. Phys. B **646**, 321 (2002) [hep-ph/0206034]. 112

[287] P. Huber, M. Lindner, M. Rolinec and W. Winter, Phys. Rev. D **74**, 073003 (2006) [hep-ph/0606119]. 112

[288] E. A. Paschos and J. Y. Yu, Phys. Rev. D**65**(2002)033002. 113

[289] D. Rein and L. M. Sehgal, Ann. Phys. **133**(1981)79. 113

[290] E. A. Paschos, L. Pasquali and J. Y. Yu, Nucl. Phys. B**588**(2000)263. 113

[291] C. H. Llewellyn Smith, Phys. Rept. 3, 261 (1972). S. K. Singh and E. Oset, Phys. Rev. C48, 1246 (1993). A. Strumia and F. Vissani, Phys. Lett. B **564**, 42 (2003) [astro-ph/0302055]. T. Gorringe and H. W. Fearing, Rev. Mod. Phys. **76**, 31 (2003) [nucl-th/0206039]. 114, 115, 200

[292] C. H. Llewellyn Smith, Phys. Rept. **3**, 261 (1972). 115

[293] A. Strumia and F. Vissani, Phys. Lett. B **564**, 42 (2003) [astro-ph/0302055]. 115

[294] O. Deschamps, S. Descotes-Genon, S. Monteil, V. Niess, S. T'Jampens and V. Tisserand, Phys. Rev. D **82**, 073012 (2010) [arXiv:0907.5135 [hep-ph]]. 116

[295] See, e.g., R. A. Diaz, hep-ph/0212237, O. Deschamps, S. Descotes-Genon, S. Monteil, V. Niess, S. T'Jampens and V. Tisserand, Phys. Rev. D **82**, 073012 (2010) [arXiv:0907.5135 [hep-ph]], G. C. Branco, P. M. Ferreira, L. Lavoura, M. N. Rebelo, M. Sher and J. P. Silva, arXiv:1106.0034 [hep-ph]. 117, 124

[296] M. Davier, A. Hocker and Z. Zhang, Rev. Mod. Phys. **78**, 1043 (2006) [hep-ph/0507078]. 117

[297] B. C. Barish, In *Stanford 1989, Proceedings, Study of tau, charm and J/psi physics* 113-126 and Caltech Pasadena - CALT-68-1580 (89,rec.Oct.) 14 p 117, 120

[298] Z. G. Wang and S. L. Wan, Phys. Rev. C **76**, 025207 (2007) [hep-ph/0607135]. 120

[299] C. Biggio, M. Blennow and E. Fernandez-Martinez, JHEP **0908**, 090 (2009) [arXiv:0907.0097 [hep-ph]]. 124, 127

[300] M. Honda, T. Kajita, K. Kasahara and S. Midorikawa, Phys. Rev. D **83**, 123001 (2011) [arXiv:1102.2688 [astro-ph.HE]]. xiv, xvi, xvii, 126, 128, 129, 132, 134, 139

[301] M. Honda, T. Kajita, K. Kasahara and S. Midorikawa, Phys. Rev. D **70**, 043008 (2004) [astro-ph/0404457]. 126, 135, 136

[302] W.M. Yao et al. (Particle Data Group), J. Phys. G 33, 1 (2006). 135

[303] P. Adamson *et al.* [MINOS Collaboration], Phys. Rev. D **81**, 072002 (2010) [arXiv:0910.2201 [hep-ex]]. 135

[304] H. E. Haber, In *Stanford 1993, Spin structure in high energy processes* 231-272 [hep-ph/9405376]. 139

[305] A. A. Aguilar-Arevalo et al. [MiniBooNE Collaboration], Phys. Rev. D 81 (2010) 092005. 200

[306] T. Gorringe and H. W. Fearing, Rev. Mod. Phys. **76**, 31 (2003) [nucl-th/0206039]. 200

[307] K. S. Kuzmin, V. V. Lyubushkin and V. A. Naumov, Eur. Phys. J. C **54**, 517 (2008) [arXiv:0712.4384 [hep-ph]]. 201

LIST OF APPENDICES

APPENDIX A: MAJORANA FIELD

CHAPTER 8

Majorana Field

8.1 Weyl spinor

In physics, a Majorana fermion is a fermion which is its own anti-particle. This definition refers to the Majorana condition $\psi = \psi^c$ where ψ^c is the charge conjugate field. No Majorana fermions are known in nature as elementary particles. The neutrino might be a Majorana fermion or it might be a Dirac fermion. If it is a Majorana fermion, then neutrinoless double beta decay is possible; experiments are underway to search for this. The hypothetical neutralino of supersymmetric models is a Majorana fermion. The charge conjugation transformation is defined as

$$\psi^c = C\bar{\psi}^T, \tag{8.1}$$

where C is the charge conjugation operator.

There are different kinds of matrix representations for the charge conjugation operator. The one we will use in here is

$$C = -i\gamma_2\gamma_0. \tag{8.2}$$

In this representation, the C matrix is independent of the basis. In the following we will use the Weyl (Chiral) basis to take a closer look at C.

$$\begin{aligned} C &= -i\gamma_2\gamma_0 \\ &= -i\begin{pmatrix} 0 & \sigma_2 \\ -\sigma_2 & 0 \end{pmatrix}\begin{pmatrix} 0 & 1 \\ 1 & 0 \end{pmatrix} \\ &= \begin{pmatrix} 0 & -1 & 0 & 0 \\ 1 & 0 & 0 & 0 \\ 0 & 0 & 0 & 1 \\ 0 & 0 & -1 & 0 \end{pmatrix}. \end{aligned} \tag{8.3}$$

There are some basic properties of the C matrix

$$\begin{aligned} C^\dagger &= C^T = C^{-1} = -C, \\ C^{-1}\gamma_\mu C &= -\gamma^T, \\ C^{-1}\gamma_5 C &= \gamma_5 = \gamma_5^T. \end{aligned} \tag{8.4}$$

Under Lorentz transformation, the field function is transformed as follows

$$\psi'^c = S(\Lambda)\psi^c, \tag{8.5}$$

where $S(\Lambda)$ is the Lorentz transformation matrix. Now, we want to find the explicit form of the Lorentz operator. Pure 'boost' Lorentz transformations are those connecting two inertial frames, moving with relative speed v. Pure Lorentz transformations can be parameterized as follows

$$\begin{pmatrix} x^{0\prime} \\ x^{1\prime} \\ x^{2\prime} \\ x^{3\prime} \end{pmatrix} = \begin{pmatrix} \cosh\phi & \sinh\phi & 0 & 0 \\ \sinh\phi & \cosh\phi & 0 & 0 \\ 0 & 0 & 1 & 0 \\ 0 & 0 & 0 & 1 \end{pmatrix} \begin{pmatrix} x^0 \\ x^1 \\ x^2 \\ x^3 \end{pmatrix}, \tag{8.6}$$

where the variable $\phi = v/c$ with $\gamma = \cosh\phi$ and $\gamma\beta = \sinh\phi$. Let us call the above matrix the boost matrix B. The generator K_x of this boost transformation along the x axis is defined by

$$K_x = \frac{1}{i}\frac{\partial B}{\partial \phi}\bigg|_{\phi_0} = -i \begin{pmatrix} 0 & 1 & 0 & 0 \\ 1 & 0 & 0 & 0 \\ 0 & 0 & 0 & 0 \\ 0 & 0 & 0 & 0 \end{pmatrix}. \tag{8.7}$$

Similarly, the other boost generators are

$$K_y = -i \begin{pmatrix} 0 & 0 & 1 & 0 \\ 0 & 0 & 0 & 0 \\ 1 & 0 & 0 & 0 \\ 0 & 0 & 0 & 0 \end{pmatrix}, \quad K_z = -i \begin{pmatrix} 0 & 0 & 0 & 1 \\ 0 & 0 & 0 & 0 \\ 0 & 0 & 0 & 0 \\ 1 & 0 & 0 & 0 \end{pmatrix}. \tag{8.8}$$

In this 4×4 matrix notation, the rotation generators may be written

$$J_x = -i \begin{pmatrix} 0 & 0 & 0 & 0 \\ 0 & 0 & 0 & 0 \\ 0 & 0 & 0 & 1 \\ 0 & 0 & -1 & 0 \end{pmatrix}, \quad J_y = -i \begin{pmatrix} 0 & 0 & 0 & 0 \\ 0 & 0 & 0 & -1 \\ 0 & 0 & 0 & 0 \\ 0 & 1 & 0 & 0 \end{pmatrix}, \quad J_z = -i \begin{pmatrix} 0 & 0 & 0 & 0 \\ 0 & 0 & 1 & 0 \\ 0 & -1 & 0 & 0 \\ 0 & 0 & 0 & 0 \end{pmatrix}. \quad (8.9)$$

The most general Lorentz transformation is composed of boosts in three directions, and rotations about three axes, and the six generators are those above. Their commutation relations may be calculated explicitly, and we find

$$\begin{aligned} [K_x, K_y] &= -iJ_z \text{ and cyclic perms,} \\ [J_x, K_x] &= 0 \text{ etc.,} \\ [J_x, K_y] &= iK_z \text{ and cyclic perms.} \end{aligned} \quad (8.10)$$

It is clear that pure Lorentz transformations do not form a group since the generators K and do not form a closed algebra under commutation. The above commutation relations are satisfied by

$$\mathbf{K} = \pm i\frac{\boldsymbol{\sigma}}{2}, \quad (8.11)$$

where $\boldsymbol{\sigma}$ are Pauli matrices. There should be two types of spinors, corresponding to the two possible signs of $\mathbf{K}$. Let us define the generators

$$\begin{aligned} \mathbf{A} &= \frac{1}{2}(\mathbf{J} + i\mathbf{K}), \\ \mathbf{B} &= \frac{1}{2}(\mathbf{J} - i\mathbf{K}), \end{aligned} \quad (8.12)$$

where their commutation relations can be written as

$$\begin{aligned} [A_x, A_y] &= iA_z \text{ and cyclic perms,} \\ [B_x, B_y] &= iB_z \text{ and cyclic perms,} \\ [A_i, B_j] &= 0 \quad (i, j = x, y, z). \end{aligned} \quad (8.13)$$

This shows that $\mathbf{A}$ and $\mathbf{B}$ each generate a group $SU(2)$, and the two groups commute. The Lorentz group is then essentially $SU(2) \bigotimes SU(2)$, and states transforming in a well-defined way will be labelled by two angular momenta (j, j'), the first one corresponding to $\mathbf{A}$, and

the second to $\mathbf{B}$. As special cases, one or other will correspond to spin zero:

$$\begin{aligned}(j,0) &\rightarrow \mathbf{J}^{(j)} = i\mathbf{K}^{(j)} \quad (\mathbf{B}=0),\\ (0,j) &\rightarrow \mathbf{J}^{(j)} = -i\mathbf{K}^{(j)} \quad (\mathbf{A}=0).\end{aligned} \tag{8.14}$$

We may now define two types of spinors:

$$\text{Type I: } (\frac{1}{2},0): \quad \mathbf{J}^{(1/2)} = \sigma/2, \quad \mathbf{K}^{(1/2)} = -i\boldsymbol{\sigma}/2. \tag{8.15}$$

We denote the spinor χ. If $(\boldsymbol{\theta},\boldsymbol{\phi})$ are the parameters of a rotation and pure Lorentz transformation, χ transforms as

$$\begin{aligned}\chi &\rightarrow exp(i\mathbf{J}\cdot\boldsymbol{\theta} + i\mathbf{K}\cdot\boldsymbol{\phi})\chi\\ &= exp(i\frac{\boldsymbol{\sigma}}{2}\cdot\boldsymbol{\theta} + \frac{\boldsymbol{\sigma}}{2}\cdot\boldsymbol{\phi})\chi\\ &= exp(i\frac{\boldsymbol{\sigma}}{2}\cdot(\boldsymbol{\theta} - i\boldsymbol{\phi}))\chi \equiv M\chi.\end{aligned} \tag{8.16}$$

Similarly

$$\begin{aligned}&\text{Type II}: \quad (0,\frac{1}{2}): \quad \mathbf{J}^{(1/2)} = \boldsymbol{\sigma}/2, \quad \mathbf{K}^{(1/2)} = i\boldsymbol{\sigma}/2,\\ &\bar{\eta} \rightarrow exp(i\frac{\boldsymbol{\sigma}}{2}\cdot(\boldsymbol{\theta} + i\boldsymbol{\phi}))\bar{\eta} \equiv N\bar{\eta}.\end{aligned} \tag{8.17}$$

Let us introduce the parity operation, under which the velocity in the Lorentz boost changes sign: $\mathbf{v} \rightarrow -\mathbf{v}$. Hence, the generators $\mathbf{K}$ change sign, $\mathbf{K} \rightarrow -\mathbf{K}$, like the components of a vector, whereas $\mathbf{J}$ does not change sign, $\mathbf{J} \rightarrow +\mathbf{J}$, behaving like an axial vector or pseudovector, which indeed is how angular momentum transforms under parity. It follows that the $(j,0)$ and $(0,j)$ representations become interchanged,

$$(j,0) \leftrightarrow (0,j), \quad \text{under parity} \tag{8.18}$$

and hence

$$\chi \leftrightarrow \bar{\eta}. \tag{8.19}$$

If we consider parity, then, it is no longer sufficient to consider the 2-spinors χ and $\bar{\eta}$ separate, but the 4-spinor

$$\psi = \begin{pmatrix}\chi\\ \bar{\eta}\end{pmatrix}, \tag{8.20}$$

where $(\chi,\bar{\eta})$ are the left and right handed components of the field ψ. Under Lorentz trans-

formations ψ transforms as follows:

$$\begin{pmatrix} \chi \\ \bar{\eta} \end{pmatrix} \rightarrow \begin{pmatrix} e^{i\frac{\boldsymbol{\sigma}}{2}\cdot(\boldsymbol{\theta}-i\boldsymbol{\phi})} & 0 \\ 0 & e^{i\frac{\boldsymbol{\sigma}}{2}\cdot(\boldsymbol{\theta}+i\boldsymbol{\phi})} \end{pmatrix} \begin{pmatrix} \chi \\ \bar{\eta} \end{pmatrix}. \tag{8.21}$$

8.2 Majorana spinor

The Lorentz transformation may be written as

$$\psi^{c'} = S(\Lambda)\psi^{c}, \tag{8.22}$$

where the transformation matrix is given by

$$S(\Lambda) = \begin{pmatrix} e^{i\frac{\boldsymbol{\sigma}}{2}\cdot(\boldsymbol{\theta}-i\boldsymbol{\phi})} & 0 \\ 0 & e^{i\frac{\boldsymbol{\sigma}}{2}\cdot(\boldsymbol{\theta}+i\boldsymbol{\phi})} \end{pmatrix}. \tag{8.23}$$

From the above equation

$$S \equiv e^{i\frac{\boldsymbol{\sigma}}{2}(\boldsymbol{\theta}-i\boldsymbol{\phi})}, \tag{8.24}$$

$$S^{-1} \equiv e^{-i\frac{\boldsymbol{\sigma}}{2}(\boldsymbol{\theta}-i\boldsymbol{\phi})}, \tag{8.25}$$

$$S^{-1\dagger} \equiv e^{i\frac{\boldsymbol{\sigma}}{2}(\boldsymbol{\theta}+i\boldsymbol{\phi})}, \tag{8.26}$$

$$S(\Lambda) = \begin{pmatrix} S & 0 \\ 0 & S^{-1\dagger} \end{pmatrix}. \tag{8.27}$$

Thus, under Lorentz transformations

$$\chi \rightarrow S\chi, \quad \bar{\eta} \rightarrow S^{-1\dagger}\bar{\eta} \tag{8.28}$$

We want to construct Lorentz invariant terms out of the spinors $\chi,\ \bar{\eta}$

χ-Field

Under Lorentz transformation

$$\begin{aligned} \chi &\rightarrow \chi' \equiv S\chi, \\ (i\sigma^{(2)}\chi) &\rightarrow (i\sigma^{(2)}\chi') \equiv (i\sigma^{(2)}S\chi). \end{aligned} \tag{8.29}$$

Since

$$\sigma^{(2)}\boldsymbol{\sigma}^T\sigma^{(2)} = -\boldsymbol{\sigma}. \tag{8.30}$$

Thus,

$$\begin{aligned}\sigma^{(2)}S\sigma^{(2)} &= \sigma^{(2)}e^{\frac{i}{2}\boldsymbol{\sigma}(\boldsymbol{\theta}-i\boldsymbol{\phi})}\sigma^{(2)} \\ &= e^{-\frac{i}{2}\boldsymbol{\sigma}^T(\boldsymbol{\theta}-i\boldsymbol{\phi})} \\ &= S^{-1T},\end{aligned} \tag{8.31}$$

or

$$\sigma^{(2)}S^*\sigma^{(2)} = S^{-1\dagger}. \tag{8.32}$$

We see that S^* and $S^{-1\dagger}$ are equivalent representations of the Lorentz group. Under Lorentz transformation

$$\begin{aligned}(i\sigma^{(2)}\chi) &\rightarrow i\sigma^{(2)}\chi' \\ &= i\sigma^{(2)}S\chi \\ &= S^{-1T}(i\sigma^{(2)}\chi),\end{aligned} \tag{8.33}$$

hence

$$(i\sigma^{(2)}\chi)^T \rightarrow (i\sigma^{(2)}\chi)^T S^{-1}, \tag{8.34}$$

which together with Eq. 8.29 implies that

$$(i\sigma^{(2)}\chi)^T\chi \text{ is Lorentz invariant.} \tag{8.35}$$

Now let us give explicit indicies to the spinor χ. We put

$$\chi \equiv \chi_\alpha = \begin{pmatrix}\chi_1 \\ \chi_2\end{pmatrix}. \tag{8.36}$$

We further put

$$\begin{pmatrix}\chi^1 \\ \chi^2\end{pmatrix} \equiv \chi^\alpha = (i\sigma^{(2)}\chi) = \begin{pmatrix}0 & 1 \\ -1 & 0\end{pmatrix}\begin{pmatrix}\chi_1 \\ \chi_2\end{pmatrix} = \begin{pmatrix}\chi_2 \\ -\chi_1\end{pmatrix}, \tag{8.37}$$

which leads to

$$\chi^{\alpha T}\chi_\alpha \text{ is Lorentz invariant.} \tag{8.38}$$

$\bar{\eta}$- ***Field***

Under Lorentz transformation

$$\bar{\eta} \;\; \rightarrow \;\; \bar{\eta}' \equiv S^{-1\dagger}\bar{\eta}, \tag{8.39}$$

then

$$\begin{aligned} (-i\sigma^{(2)}\bar{\eta}) \;\; &\rightarrow \;\; (-i\sigma^{(2)}\bar{\eta}') \\ &= \;\; -i\sigma^{(2)}S^{-1\dagger}\bar{\eta} \\ &= \;\; S^{*}(-i\sigma^{(2)}\bar{\eta}), \end{aligned} \tag{8.40}$$

or

$$(-i\sigma^{(2)}\bar{\eta})^{T} \;\; \rightarrow \;\; (-i\sigma^{(2)}\bar{\eta})^{T}S^{\dagger}. \tag{8.41}$$

Here we have used the relation 8.32. Thus

$$(-i\sigma^{(2)}\bar{\eta})^{T}\bar{\eta} \;\text{ is Lorentz invariant.} \tag{8.42}$$

Now let us give explicit indicies to the spinor χ. We put

$$\bar{\eta} \equiv \bar{\eta}^{\dot{\alpha}} = \begin{pmatrix} \bar{\eta}^{\dot{1}} \\ \bar{\eta}^{\dot{2}} \end{pmatrix}. \tag{8.43}$$

We further put

$$\begin{pmatrix} \bar{\eta}_{\dot{1}} \\ \bar{\eta}_{\dot{2}} \end{pmatrix} \equiv \bar{\eta}_{\dot{\alpha}} = (-i\sigma^{(2)}\bar{\eta}) = \begin{pmatrix} 0 & -1 \\ 1 & 0 \end{pmatrix}\begin{pmatrix} \bar{\eta}^{\dot{1}} \\ \bar{\eta}^{\dot{2}} \end{pmatrix} = \begin{pmatrix} -\bar{\eta}^{\dot{2}} \\ \bar{\eta}^{\dot{1}} \end{pmatrix}, \tag{8.44}$$

which leads to

$$\bar{\eta}_{\dot{\alpha}}^{T}\bar{\eta}^{\dot{\alpha}} \;\text{ is Lorentz invariant.} \tag{8.45}$$

Now, we have four types of Weyl spinors:

$$\chi_{\alpha},\; \chi^{\alpha},\; \bar{\chi}_{\dot{\alpha}},\; \bar{\chi}^{\dot{\alpha}}, \tag{8.46}$$

where we simply rename the spinors

$$\bar{\chi}_{\dot{\alpha}} \equiv \bar{\eta}_{\dot{\alpha}}, \text{ and } \bar{\chi}^{\dot{\alpha}} \equiv \bar{\eta}^{\dot{\alpha}}. \tag{8.47}$$

It is common to refer to these types as dotted and undotted spinors. The relationship between them is not hard to deduce. From Eqs. (8.28, 8.33, 8.40) we have the following transformation property for the spinors under a Lorentz transformation

$$\begin{aligned} \chi_\alpha \to \chi'_\alpha &= S_\alpha^\beta \chi_\beta \\ \chi^\alpha \to \chi'^\alpha &= (S^{-1T})_\beta^\alpha \chi^\beta. \end{aligned} \tag{8.48}$$

and

$$\begin{aligned} \bar{\chi}^{\dot{\alpha}} \to \bar{\chi}'^{\dot{\alpha}} &= (S^{-1\dagger})_{\dot{\beta}}^{\dot{\alpha}} \bar{\chi}^{\dot{\beta}} \\ \bar{\chi}_{\dot{\alpha}} \to \bar{\chi}'_{\dot{\alpha}} &= S_{\dot{\alpha}}^{*\dot{\delta}} \bar{\chi}'_{\dot{\delta}}. \end{aligned} \tag{8.49}$$

Comparing Eqs. (8.48, 8.49), we are justified in identifying dotted spinors with the complex conjugate of undeotted ones:

$$\bar{\chi}_{\dot{\alpha}} = (\chi_\alpha)^*, \bar{\chi}^{\dot{\alpha}} = (\chi^\alpha)^*. \tag{8.50}$$

8.3 Majorana condition

Putting in spinor indices we have from Eqs. (8.20, 8.47), using Eq. 8.50,

$$\psi = \begin{pmatrix} \chi_\alpha \\ \bar{\eta}^{\dot{\alpha}} \end{pmatrix} \Rightarrow \psi^\dagger = (\bar{\chi}_{\dot{\alpha}} \;\; \eta^\alpha) \Rightarrow \bar{\psi} = \psi^\dagger \gamma^0 = (\eta^\alpha \;\; \bar{\chi}_{\dot{\alpha}}) \Rightarrow \bar{\psi}^T = \begin{pmatrix} \eta^\alpha \\ \bar{\chi}_{\dot{\alpha}} \end{pmatrix}. \tag{8.51}$$

Hence, using Eq. 8.3

$$\psi^c = C\bar{\psi}^T = \eta_c \begin{pmatrix} -\sigma^{(2)}\eta^\alpha \\ \sigma^{(2)}\bar{\chi}_{\dot{\alpha}} \end{pmatrix} = \begin{pmatrix} \eta_\alpha \\ \bar{\chi}^{\dot{\alpha}} \end{pmatrix}, \tag{8.52}$$

where we have chosen $\eta_c = i$. Then the Majorana condition $\psi = \psi^c$ leads to

$$\eta = \chi, \tag{8.53}$$

hence

$$\begin{aligned}\psi = \psi^c &= \begin{pmatrix} \chi_\alpha \\ \bar{\chi}^{\dot{\alpha}} \end{pmatrix} \\ &= \begin{pmatrix} \chi_\alpha \\ (\chi^\alpha)^* \end{pmatrix} \end{aligned} \tag{8.54}$$

8.4 Majorana Lagrangian

The Dirac Lagrangian of fermions is given by

$$\mathcal{L} = \frac{1}{2} i \bar{\psi} \gamma^\mu \partial_\mu \psi - \frac{1}{2} m \bar{\psi} \psi + h.c. \tag{8.55}$$

The complex conjugate field

$$\psi^c = C \bar{\psi}^T \Rightarrow \bar{\psi}^T = C^{-1} \psi^c \Rightarrow \bar{\psi} = \psi^{cT} (C^{-1})^T. \tag{8.56}$$

Using the Majorana condition

$$\bar{\psi} = \psi^T (C^{-1})^T, \tag{8.57}$$

then

$$\bar{\psi} = -\psi^T C^{-1}. \tag{8.58}$$

Thus, the mass term is given by

$$\begin{aligned}\frac{1}{2} m \bar{\psi} \psi &= \frac{1}{2} m \left(-\psi^T C^{-1} \right) \psi \\ &= -\frac{1}{2} m \psi^T C^{-1} \psi. \end{aligned} \tag{8.59}$$

The kinetic term is given by

$$\begin{aligned}\frac{1}{2} i \bar{\psi} \gamma^\mu \partial_\mu \psi &= \frac{1}{2} i \left(-\psi^T C^{-1} \right) \gamma^\mu \partial_\mu \psi \\ &= -\frac{1}{2} i \psi^T C^{-1} \gamma^\mu \partial_\mu \psi. \end{aligned} \tag{8.60}$$

Using Eqs. (8.59, 8.60), the Majorana Lagrangian is written as

$$\begin{aligned}\mathcal{L} &= -\frac{1}{2}i\psi^T C^{-1}\gamma^\mu\partial_\mu\psi + \frac{1}{2}m\psi^T C^{-1}\psi + h.c. \\ &= -\frac{1}{2}i\left(\psi_L^T C^{-1}\gamma^\mu\partial_\mu\psi_L + \psi_R^T C^{-1}\gamma^\mu\partial_\mu\psi_R\right) \\ &+ \frac{1}{2}m\left(\psi_L^T C^{-1}\psi_L + \psi_R^T C^{-1}\psi_R\right) + h.c. \end{aligned} \tag{8.61}$$

The above Lagrangian shows that the Majorana mass term can be composed from either left- or right-handed components. We want to check the hermitian conjugate term in the Lagrangian. For example, we will check the hermitian conjugate of $\psi_R^T C^{-1}\psi_R$

$$\begin{aligned}\left(\psi_R^T C^{-1}\psi_R\right)^\dagger &= \psi_R^\dagger (C^{-1})^\dagger (\psi_R^T)^\dagger \\ &= (\psi_R^*)^T(-C)^\dagger\psi_R^* \\ &= -(\psi_R^*)^T C^T\psi_R^*. \end{aligned} \tag{8.62}$$

Using the Majorana condition

$$\begin{aligned}\psi &= C\bar{\psi}^T \\ &= C(\psi^\dagger\gamma_0)^T \\ &= C\gamma_0\psi^*. \end{aligned} \tag{8.63}$$

Substitute in the above equation

$$\begin{aligned}-(\psi_R^*)^T C^T\psi_R^* &= -(\gamma_0 C^{-1}\psi_R)^T C^T(\gamma_0 C^{-1}\psi_R) \\ &= -\psi_R^T(C^{-1})^T\gamma_0 C^T(\gamma_0 C^{-1}\psi_R) \\ &= \psi_R^T C^{-1}\gamma_0 C^{-1}\gamma_0 C^{-1}\psi_R \\ &= -\psi_R^T C\gamma_0 C^{-1}\gamma_0 C^{-1}\psi_R \\ &= \psi_R^T\gamma_0\gamma_0 C^{-1}\psi_R \\ &= \psi_R^T C^{-1}\psi_R. \end{aligned} \tag{8.64}$$

That means the hermitian conjugate of the Lagrangian is similar to itself.

8.5 Canonical quantization of spinor fields

The general solution of the Dirac equation is:

$$\begin{aligned}
\psi(x) &= \sum_{s=\pm}\int \frac{d^3p}{(2\pi)^3 2\omega}\left[b_s(\mathbf{p})u_s(\mathbf{p})e^{ip\cdot x} + d_s^\dagger(\mathbf{p})v_s(\mathbf{p})e^{-ip\cdot x}\right], \\
\bar\psi(x) &= \sum_{s=\pm}\int \frac{d^3p}{(2\pi)^3 2\omega}\left[b_s^\dagger(\mathbf{p})\bar u_s(\mathbf{p})e^{-ip\cdot x} + d_s(\mathbf{p})\bar v_s(\mathbf{p})e^{ip\cdot x}\right], \\
C\bar\psi(x)^T &= \sum_{s=\pm}\int \frac{d^3p}{(2\pi)^3 2\omega}\left[b_s^\dagger(\mathbf{p})C\bar u_s^T(\mathbf{p})e^{-ip\cdot x} + d_s(\mathbf{p})C\bar v_s^T(\mathbf{p})e^{ip\cdot x}\right]. \qquad (8.65)
\end{aligned}$$

Let us assume that

$$\begin{aligned}
C\bar u_s^T(\mathbf{p}) &= v_s(\mathbf{p}), \\
C\bar v_s^T(\mathbf{p}) &= u_s(\mathbf{p}). \qquad (8.66)
\end{aligned}$$

Then

$$\psi^c = C\bar\psi(x)^T = \sum_{s=\pm}\int \frac{d^3p}{(2\pi)^3 2\omega}\left[b_s^\dagger(\mathbf{p})v_s(\mathbf{p})e^{-ip\cdot x} + d_s(\mathbf{p})u_s(\mathbf{p})e^{ip\cdot x}\right]. \qquad (8.67)$$

Using the Majorana condition, then

$$b_s(\mathbf{p}) = d_s(\mathbf{p}), \qquad (8.68)$$

thus

$$\psi = \psi^c = \sum_{s=\pm}\int \frac{d^3p}{(2\pi)^3 2\omega}\left[b_s(\mathbf{p})u_s(\mathbf{p})e^{ip\cdot x} + b_s^\dagger(\mathbf{p})v_s(\mathbf{p})e^{-ip\cdot x}\right]. \qquad (8.69)$$

Now, we want to prove Eqs. 8.66. The four-component spinors $u_s(\mathbf{p})$ and $v_s(\mathbf{p})$ obey the equations

$$\begin{aligned}
(\not p + m)u_s(\mathbf{p}) &= 0, \\
(-\not p + m)v_s(\mathbf{p}) &= 0. \qquad (8.70)
\end{aligned}$$

Each of these equations has two solutions with labels $s = \pm$. For $m \neq 0$, we can go to the rest frame, $\mathbf{p} = \mathbf{0}$. We will then distinguish the two solutions by the eigenvalue of the spin

matrix in z-direction $\boldsymbol{\sigma}^z$, or

$$\boldsymbol{\sigma}^{12} = \frac{i}{4}\left[\gamma^1, \gamma^2\right] = \frac{i}{2}\gamma^1\gamma^2 = \begin{pmatrix} \frac{1}{2}\sigma_3 & 0 \\ 0 & \frac{1}{2}\sigma_3 \end{pmatrix}. \tag{8.71}$$

Specifically, we will require

$$\begin{aligned} \boldsymbol{\sigma}^z u_\pm(\mathbf{0}) &= \pm\frac{1}{2}u_\pm(\mathbf{0}), \\ \boldsymbol{\sigma}^z v_\pm(\mathbf{0}) &= \mp\frac{1}{2}v_\pm(\mathbf{0}). \end{aligned} \tag{8.72}$$

The reason for the opposite sign for the v spinor is that this choice results in

$$\begin{aligned} \left[J_z, b^\dagger_\pm(\mathbf{0})\right] &= \pm\frac{1}{2}b^\dagger_\pm(\mathbf{0}), \\ \left[J_z, d^\dagger_\pm(\mathbf{0})\right] &= \pm\frac{1}{2}d^\dagger_\pm(\mathbf{0}), \end{aligned} \tag{8.73}$$

where J_z is the z component of the angular momentum operator. Eq. 8.73 implies that $b^\dagger_+(\mathbf{0})$ and $d^\dagger_+(\mathbf{0})$ each creates a particle with spin up along the z axis. Eqs. (8.70, 8.72) are then easy to solve. Choosing a specific normalization and phase for each of $u_\pm(\mathbf{0})$ and $v_\pm(\mathbf{0})$, we get

$$\begin{aligned} u_+(\mathbf{0}) &= \sqrt{m}\begin{pmatrix} 1 \\ 0 \\ 1 \\ 0 \end{pmatrix}, \quad u_-(\mathbf{0}) = \sqrt{m}\begin{pmatrix} 0 \\ 1 \\ 0 \\ 1 \end{pmatrix}, \\ v_+(\mathbf{0}) &= \sqrt{m}\begin{pmatrix} -1 \\ 0 \\ 1 \\ 0 \end{pmatrix}, \quad v_-(\mathbf{0}) = \sqrt{m}\begin{pmatrix} 0 \\ 1 \\ 0 \\ -1 \end{pmatrix}, \end{aligned} \tag{8.74}$$

and in the Weyl representation

$$\begin{aligned} \bar{u}_+(\mathbf{0}) &= \sqrt{m}\begin{pmatrix} 0 & 1 & 0 & 1 \end{pmatrix}, \quad \bar{u}_-(\mathbf{0}) = \sqrt{m}\begin{pmatrix} 1 & 0 & 1 & 0 \end{pmatrix}, \\ \bar{v}_+(\mathbf{0}) &= \sqrt{m}\begin{pmatrix} 0 & 1 & 0 & -1 \end{pmatrix}, \quad \bar{v}_-(\mathbf{0}) = \sqrt{m}\begin{pmatrix} -1 & 0 & 1 & 0 \end{pmatrix}. \end{aligned} \tag{8.75}$$

The charge conjugation operator is given by

$$\begin{aligned} C &= \eta_c \gamma_2 \gamma_0 \\ &= \begin{pmatrix} 0 & -1 & 0 & 0 \\ 1 & 0 & 0 & 0 \\ 0 & 0 & 0 & 1 \\ 0 & 0 & -1 & 0 \end{pmatrix}, \end{aligned} \tag{8.76}$$

where $\eta_c = i$. One can find that

$$C\bar{u}_+^T(\mathbf{0}) = \sqrt{m} \begin{pmatrix} 0 & -1 & 0 & 0 \\ 1 & 0 & 0 & 0 \\ 0 & 0 & 0 & 1 \\ 0 & 0 & -1 & 0 \end{pmatrix} \begin{pmatrix} 1 \\ 0 \\ 1 \\ 0 \end{pmatrix} = \sqrt{m} \begin{pmatrix} 0 \\ 1 \\ 0 \\ -1 \end{pmatrix} = v_+(\mathbf{0}). \tag{8.77}$$

Thus

$$\begin{aligned} C\bar{u}_+^T(\mathbf{0}) &= v_+(\mathbf{0}), \\ C\bar{u}_-^T(\mathbf{0}) &= v_-(\mathbf{0}), \\ C\bar{v}_+^T(\mathbf{0}) &= u_+(\mathbf{0}), \\ C\bar{v}_+^T(\mathbf{0}) &= u_-(\mathbf{0}), \end{aligned} \tag{8.78}$$

or, in a compact form

$$\begin{aligned} C\bar{u}_s^T(\mathbf{0}) &= v_s(\mathbf{0}), \\ C\bar{v}_s^T(\mathbf{0}) &= u_s(\mathbf{0}). \end{aligned} \tag{8.79}$$

Now, we want to boost the spinors using Lorentz transformation

$$S(\Lambda) = exp\left(\frac{i}{2}\lambda_{\mu\nu}\boldsymbol{\sigma}^{\mu\nu}\right), \tag{8.80}$$

where

$$\boldsymbol{\sigma}^{\mu\nu} = \frac{i}{4}[\gamma^\mu, \gamma^\nu]. \tag{8.81}$$

For boosting, $\lambda_{\mu\nu} \to \lambda_{i0} \equiv \mathbf{p}$ (momentum) and

$$\boldsymbol{\sigma}^{\mu\nu} \to \boldsymbol{\sigma}^{i0} = \frac{i}{4}[\gamma^i, \gamma^0] = \frac{i}{2}\gamma^i\gamma^0, \tag{8.82}$$

and

$$S(\Lambda) = exp\left(\frac{i}{2}\lambda_{i0}\boldsymbol{\sigma}^{i0}\right), \tag{8.83}$$

where

$$\{\gamma^{\mu}, \gamma^{\nu}\} = 2g^{\mu\nu}. \tag{8.84}$$

Using Eq. 8.4, one gets

$$C^{-1}\boldsymbol{\sigma}^{i0}C = -(\boldsymbol{\sigma}^{i0})^{T}. \tag{8.85}$$

Thus, we can write the spinors for some momentum $\mathbf{p}$ after Lorentz transformation as follows

$$\begin{aligned}
u_s(\mathbf{p}) &= exp\left(\frac{i}{2}\lambda_{i0}\boldsymbol{\sigma}^{i0}\right) u_s(\mathbf{0}), \\
v_s(\mathbf{p}) &= exp\left(\frac{i}{2}\lambda_{i0}\boldsymbol{\sigma}^{i0}\right) v_s(\mathbf{0}), \\
\bar{u}_s(\mathbf{p}) &= \bar{u}_s(\mathbf{0}) exp\left(-\frac{i}{2}\lambda_{i0}\boldsymbol{\sigma}^{i0}\right), \\
\bar{v}_s(\mathbf{p}) &= \bar{v}_s(\mathbf{0}) exp\left(-\frac{i}{2}\lambda_{i0}\boldsymbol{\sigma}^{i0}\right).
\end{aligned} \tag{8.86}$$

Let us assume that the required is true to prove Eq. 8.96. We suppose that

$$C\bar{u}_s^{T}(\mathbf{p}) = v_s(\mathbf{p}). \tag{8.87}$$

Then

$$\begin{aligned}
LHS &= C\left(\bar{u}_s(\mathbf{0}) exp\left(-\frac{i}{2}\lambda_{i0}\boldsymbol{\sigma}^{i0}\right)\right)^{T} \\
&= C exp\left(\frac{i}{2}\lambda_{i0}(C^{-1}\boldsymbol{\sigma}^{i0}C)\right)\bar{u}_s(\mathbf{0})^{T} \\
&= exp\left(\frac{i}{2}\lambda_{i0}\boldsymbol{\sigma}^{i0}\right) C\bar{u}_s(\mathbf{0})^{T}.
\end{aligned} \tag{8.88}$$

Substituting in Eq. 8.87 and using Eq. 8.86, one gets

$$C\bar{u}_s^{T}(\mathbf{0}) = v_s(\mathbf{0}). \tag{8.89}$$

Thus, we now have proved that

$$\begin{aligned}
C\bar{u}_s^{T}(\mathbf{p}) &= v_s(\mathbf{p}), \\
C\bar{v}_s^{T}(\mathbf{p}) &= u_s(\mathbf{p}).
\end{aligned} \tag{8.90}$$

8.6 Canonical anticommutation relations

The Canonical momentum is defined as, using Eq. 8.61,

$$\begin{aligned} \Pi_b(\mathbf{x},t) &= \frac{\partial \mathcal{L}}{\partial(\partial_0 \psi_b(\mathbf{x},t))} \\ &= i\psi_d^T (C\gamma^0)_{db}, \end{aligned} \tag{8.91}$$

where we used Eq. 8.61. We can calculate the anticommutation relation as follows

$$\begin{aligned} \{\psi_a(\mathbf{x},t), \Pi_b(\mathbf{y},t)\} &= i\delta_{ab}\delta^3(\mathbf{x}-\mathbf{y}), \\ \left\{\psi_a(\mathbf{x},t), i\psi_d^T(\mathbf{y},t)(C\gamma^0)_{db}\right\} &= i\delta_{ab}\delta^3(\mathbf{x}-\mathbf{y}), \\ \left\{\psi_a(\mathbf{x},t), \psi_d^T(\mathbf{y},t)C_{db}\right\}\gamma^0_{db} &= \delta_{ab}\delta^3(\mathbf{x}-\mathbf{y}). \end{aligned} \tag{8.92}$$

From the definition of the Majorana field, we have

$$\psi^T(\mathbf{x},t)C = \bar{\psi}(\mathbf{x},t). \tag{8.93}$$

Thus

$$\begin{aligned} \left\{\psi_a(\mathbf{x},t), \bar{\psi}_d(\mathbf{y},t)\right\}\gamma^0_{db} &= \delta_{ab}\delta^3(\mathbf{x}-\mathbf{y}), \\ \left\{\psi_a(\mathbf{x},t), \bar{\psi}_d(\mathbf{y},t)\right\} &= (\gamma^0)_{ad}\delta^3(\mathbf{x}-\mathbf{y}). \end{aligned} \tag{8.94}$$

Using Eq. 8.92, one gets the other anticommutation relation

$$\{\psi_a(\mathbf{x},t), \psi_d(\mathbf{y},t)\} = (\gamma^0 C)_{ad}\delta^3(\mathbf{x}-\mathbf{y}), \tag{8.95}$$

where γ^0 is symmetric and $\psi_d(\mathbf{y},t)$ is a matrix element.

Now, we want to find the anticommutation of the creation and annihilation operators

using the field function in Eq. 8.67

$$\begin{aligned}
\int d^3x e^{-ip\cdot x}\psi(x) &= \sum_{s=\pm}\int \frac{d^3p}{(2\pi)^3 2\omega}\Big[b_s(\mathbf{p})u_s(\mathbf{p})\int d^3x e^{(-i\mathbf{p}\cdot\mathbf{x}+i\omega t)}e^{(i\mathbf{p}\cdot\mathbf{x}-i\omega t)} \\
&+ b_s^\dagger(\mathbf{p})v_s(\mathbf{p})\int d^3x e^{(-i\mathbf{p}\cdot\mathbf{x}+i\omega t)}e^{(-i\mathbf{p}\cdot\mathbf{x}+i\omega t)}\Big] \\
&= \sum_{s=\pm}\int \frac{d^3p}{(2\pi)^3 2\omega}\left[b_s(\mathbf{p})u_s(\mathbf{p})(2\pi)^3\delta(\mathbf{p}-\mathbf{p})\right. \\
&+ \left. b_s^\dagger(\mathbf{p})v_s(\mathbf{p})(2\pi)^3\delta(\mathbf{p}+\mathbf{p})e^{2i\omega t}\right] \\
&= \frac{1}{2\omega}\sum_{s=\pm}\left[b_s(\mathbf{p})u_s(\mathbf{p}) + b_s^\dagger(-\mathbf{p})v_s(-\mathbf{p})e^{2i\omega t}\right]. \qquad (8.96)
\end{aligned}$$

Using the orthogonality conditions

$$\begin{aligned}
\bar{u}_s(\mathbf{p})\gamma^\mu u_{s'}(\mathbf{p}) &= 2p^\mu\delta_{ss'}, \\
\bar{v}_s(\mathbf{p})\gamma^\mu v_{s'}(\mathbf{p}) &= 2p^\mu\delta_{ss'}, \\
\bar{u}_s(\mathbf{p})\gamma^0 v_{s'}(-\mathbf{p}) &= 0, \\
\bar{v}_s(\mathbf{p})\gamma^0 u_{s'}(-\mathbf{p}) &= 0. \qquad (8.97)
\end{aligned}$$

Multiply Eq. 8.96 by $\bar{u}_{s'}(\mathbf{p})\gamma^0$, thus

$$\int d^3x e^{-ip\cdot x}\bar{u}_{s'}(\mathbf{p})\gamma^0\psi(x) = \frac{1}{2\omega}\sum_{s=\pm}\left[b_s(\mathbf{p})\bar{u}_{s'}(\mathbf{p})\gamma^0 u_s(\mathbf{p}) + b_s^\dagger(-\mathbf{p})\bar{u}_{s'}(\mathbf{p})\gamma^0 v_s(-\mathbf{p})e^{2i\omega t}\right]. \qquad (8.98)$$

Thus

$$b_s(\mathbf{p}) = \int d^3x e^{-ip\cdot x}\bar{u}_s(\mathbf{p})\gamma^0\psi(x). \qquad (8.99)$$

Taking the complex conjugate

$$b_s^\dagger(\mathbf{p}) = \int d^3x e^{ip\cdot x}\bar{\psi}(x)\gamma^0 u_s(\mathbf{p}), \qquad (8.100)$$

where

$$\begin{aligned}
\bar{\psi}(x) &= \psi^\dagger(x)\gamma^0, \\
\bar{u}_s^\dagger(\mathbf{p}) &= \gamma^0 u_s(\mathbf{p}). \qquad (8.101)
\end{aligned}$$

Now we are ready to calculate the anticommutation relations

$$\begin{aligned}
\left\{b_s(\mathbf{p}), b^\dagger_{s'}(\mathbf{p}')\right\} &= \int\int d^3x d^3y e^{(-ip\cdot x + ip'\cdot y)} \bar{u}_s(\mathbf{p})\gamma^0 \left\{\psi(x), \bar{\psi}(y)\right\} \gamma^0 u_{s'}(\mathbf{p}') \\
&= \int\int d^3x d^3y e^{(-ip\cdot x + ip'\cdot y)} \bar{u}_s(\mathbf{p})\gamma^0\gamma^0\delta^3(\mathbf{x}-\mathbf{y})\gamma^0 u_{s'}(\mathbf{p}') \\
&= \int d^3x e^{-i(p-p')\cdot x} \bar{u}_s(\mathbf{p})\gamma^0\gamma^0\gamma^0 u_{s'}(\mathbf{p}') \\
&= \int d^3x e^{-i(p-p')\cdot x} \bar{u}_s(\mathbf{p})\gamma^0 u_{s'}(\mathbf{p}') \\
&= (2\pi)^3\delta^3(\mathbf{p}-\mathbf{p}')\bar{u}_s(\mathbf{p})\gamma^0 u_{s'}(\mathbf{p}) \\
&= (2\pi)^3\delta^3(\mathbf{p}-\mathbf{p}')2\omega\delta_{ss'}, \qquad (8.102)
\end{aligned}$$

where we have used Eq. 8.94 and

$$\frac{1}{(2\pi)^3}\int d^3x e^{-i(p-p')x} = \delta(p-p'). \qquad (8.103)$$

We have assumed that $x_0 = y_0 \equiv t$ without losing the generality because the operators $b_s(\mathbf{p})$ and $b^\dagger_{s'}(\mathbf{p}')$ are time independent. Similarly, one can get

$$\begin{aligned}
\{b_s(\mathbf{p}), b_{s'}(\mathbf{p}')\} &= \int\int d^3x d^3y e^{(-ipx - ip'y)} \bar{u}_s(\mathbf{p})\gamma^0 \bar{u}_{s'}(\mathbf{p}')\gamma^0 \{\psi(x), \psi(y)\} \\
&= \int d^3x e^{-i(p+p')x} \bar{u}_s(\mathbf{p})\gamma^0 \bar{u}_{s'}(\mathbf{p}')\gamma^0 C\gamma^0 \\
&= \int d^3x e^{-i(p+p')x} \bar{u}_s(\mathbf{p})\gamma^0 \bar{u}_{s'}(\mathbf{p}')\gamma^0(-i\gamma^2\gamma^0)\gamma^0 \\
&= (2\pi)^3\delta^3(\mathbf{p}+\mathbf{p}')\bar{u}_s(\mathbf{p})\gamma^0 \bar{u}_{s'}(-\mathbf{p})C^T \\
&= (2\pi)^3\delta^3(\mathbf{p}+\mathbf{p}')\bar{u}_s(\mathbf{p})\gamma^0 v_{s'}(-\mathbf{p}), \\
&= 0 \qquad (8.104)
\end{aligned}$$

where $C = -i\gamma^2\gamma^0$ and we have used the orthogonality condition. Also we have used the Majorana condition.

APPENDIX B: FUNCTIONS IN SCATTERING AMPLITUDES

CHAPTER 9

Functions in Scattering Amplitudes

For the scattering amplitudes calculation in $t\bar{t}$ c.m. frame, we choose the relevant coordinates of particle momenta as

$$\begin{aligned} p_{q,\bar{q}} &= \frac{\hat{s}}{2}\,(1,0,0,\pm 1)\,, \\ p_{t,\bar{t}} &= \frac{\hat{s}}{2}\,(1,\pm\beta_t \sin\theta, 0, \pm\beta_t \cos\theta). \end{aligned} \tag{9.1}$$

.

With this choice and assume all the couplings in Eq. (3.3) to be real, we obtain the functions f_i in the scattering amplitude in Eq. (3.23) as

$$\begin{aligned} f_1 &= \frac{\hat{s}}{2}\Big[8\Big(2a^2+2b^2+ac-c^2+3bd+d^2\Big)\frac{m_t^2}{\hat{s}} + 2\Big(2a^2(1+c_\theta)^2 + 2b^2(1+c_\theta)^2 \\ &\quad + bd(-7+4c_\theta+6c_\theta^2-3\beta_t^2) - (c^2-d^2)(-1+3c_\theta^2-2\beta_t^2) + ac(-1+\beta_t^2)\Big) \\ &\quad - \Big((-1+c_\theta)(c^2-d^2)(-1+2c_\theta+c_\theta^2-2\beta_t^2)\hat{s}^2\Big)\frac{\hat{s}}{m_t^2}\Big]\,, \\ f_2 &= -\Big(\frac{m_t^2}{\hat{t}}\Big)\hat{s}(a^2+b^2)\Big[(-1+c_\theta)^2 + \frac{4m_t^2}{\hat{s}}\Big]. \end{aligned} \tag{9.2}$$

$$
\begin{aligned}
f_3 &= \frac{1}{16}\hat{s}^2\Big[32(a^4+b^4)\Big(3+2c_\theta+c_\theta^2+2\beta_t^2\Big)+\frac{1}{m_t^4}(c^4+d^4)\Big(32(9-2c_\theta+c_\theta^2)m_t^4 \\
&\quad +32(-5+3c_\theta+c_\theta^2+c_\theta^3)m_t^2\hat{s}+\hat{s}^2(5-2c_\theta^2+\beta_t^2-c_\theta(3+\beta_t^2))^2\Big)+128a^3c\Big(-2c_\theta+c_\theta^2+\beta_t^2\Big) \\
&\quad -\frac{1}{m_t^4}2c^2d^2\Big(-32(-5+3c_\theta+c_\theta^2+c_\theta^3)m_t^2\hat{s}+32m_t^4(-11+6c_\theta+c_\theta^2-4\beta_t^2) \\
&\quad -\hat{s}^2(5-2c_\theta^2+\beta_t^2-c_\theta(3+\beta_t^2))^2\Big)+\frac{16}{m_t^2}ac\Big(8b^2m_t^2(-2+2c_\theta+3c_\theta^2-3\beta_t^2) \\
&\quad +c^2(-1+c_\theta)(8(-3+c_\theta)m_t^2+\hat{s}(5+2c_\theta^2-3\beta_t^2-c_\theta(3+\beta_t^2)))-d^2(8m_t^2(-5+8c_\theta+c_\theta^2-4\beta_t^2) \\
&\quad -(-1+c_\theta)\hat{s}(5+2c_\theta^2-3\beta_t^2-c_\theta(3+\beta_t^2)))\Big)+\frac{16}{m_t^2}b^2\Big(c^2(2m_t^2(-11-2c_\theta+5c_\theta^2-8\beta_t^2) \\
&\quad -(-1+c_\theta)\hat{s}(5+3\beta_t^2+c_\theta(7+\beta_t^2)))-d^2(4m_t^2(7-2c_\theta+2c_\theta^2+\beta_t^2) \\
&\quad +(-1+c_\theta)\hat{s}(5+3\beta_t^2+c_\theta(7+\beta_t^2)))\Big)+\frac{16}{m_t^2}a^2\Big(4b^2m_t^2(1+6c_\theta+3c_\theta^2-2\beta_t^2) \\
&\quad -d^2(2m_t^2(3+18c_\theta+3c_\theta^2-8\beta_t^2)+(-1+c_\theta)\hat{s}(5+3\beta_t^2+c_\theta(7+\beta_t^2))) \\
&\quad +c^2(5\hat{s}+4m_t^2\beta_t^2+3\hat{s}\beta_t^2-2c_\theta(24m_t^2+\hat{s}(-1+\beta_t^2))+c_\theta^2(12m_t^2-\hat{s}(7+\beta_t^2)))\Big)\Big], \\
f_4 &= -\frac{1}{2}\Big(\frac{m_t^2}{\hat{t}}\Big)\hat{s}\Big[32(a^4+b^4+2a^3c+2ab^2c+a^2(2b^2+c^2)-b^2d^2)m_t^2+8(-3+2c_\theta+c_\theta^2) \\
&\quad (a^3c+ab^2c+a^2c^2-b^2d^2)\hat{s}+\frac{1}{m_t^2}(-1+c_\theta)^2(a^2c^2-b^2d^2)\hat{s}^2(5+2c_\theta+\beta_t^2)\Big], \\
f_5 &= \Big(\frac{m_t^2}{\hat{t}}\Big)^2\hat{s}^2(a^2+b^2)^2(-1+c_\theta)^2. \qquad (9.3)
\end{aligned}
$$

APPENDIX C: CHARGED LEPTON SECTOR

CHAPTER 10

Charged Lepton Sector

We analytically calculate the deviation of the leptonic mixing from the symmetric limit due to corrections from the charged lepton sector. We, here, are going to determine the sizes for the Yukawa matrix elements in Y^L in Eq. 4.44. We first consider the breaking of the 2-3 symmetry in the charged lepton sector via the introduction of a higher dimensional operator that generates the muon mass

$$O_1 = cy_2 \bar{D}_{\mu_L} \mu_R \phi_1 \frac{\phi_1 \phi_1^\dagger}{\Lambda^2}. \tag{10.1}$$

Thus, we consider the Yukawa matrix,

$$Y_{23}^L = \begin{pmatrix} l_e & 0 & 0 \\ 0 & \frac{1}{2} l_T (1 + 2\kappa_l) & \frac{1}{2} l_T \\ 0 & \frac{1}{2} l_T & \frac{1}{2} l_T \end{pmatrix}. \tag{10.2}$$

The structure above breaks the $2-3$ symmetry because of the correction to the 22 element. Note that we do not break the $2-3$ symmetry in the 23 element so that the Yukawa matrix remains symmetric. The matrix Y_{23}^L is now diagonalized by the unitary matrix, $U_l = W_{23}^l R_{23}^l$. Applying the relation $(Y_{23}^L)_{23} = (Y_{23}^L)_{33}$ in Eq. 10.2 to $Y_{23}^L = U_l Y_{diag}^L U_l^\dagger$ leads to

$$t_{23l} = \frac{1}{2} \left[z_\mu - 1 + \sqrt{z_\mu^2 - 6 z_\mu + 1} \right], \tag{10.3}$$

where $t_{23l} \equiv \tan \theta_{23l}$ and we have chosen the solution that leads to small angle θ_{23l} and to small flavor symmetry breaking. Keeping terms up to first order in z_μ we get

$$t_{23l} \approx -z_\mu. \tag{10.4}$$

We further obtain for κ_l and l_T in Eq. 10.2,

$$\begin{aligned} \kappa_l &= -\tan 2\theta_{23l} \approx 2z_\mu, \\ l_T &= (l_\tau - l_\mu)\cos 2\theta_{23l}. \end{aligned} \tag{10.5}$$

Comparing the above equation with Eq. 10.1, the size of the higher dimensional operator can be estimated as

$$\frac{cv_1^2}{2\Lambda^2} \approx 2z_\mu. \tag{10.6}$$

Since $v_1 \approx 250$ GeV therefore the scale of Λ is in the TeV range.

To obtain a realistic charged lepton matrix, we take into account the mixing involving the second and the third generations in the full Yukawa matrix

$$O_2 = y' \left(\bar{D}_{e_L}\mu_R - \bar{D}_{e_L}\tau_R + \bar{D}_{\mu_L}e_R - \bar{D}_{\tau_L}e_R\right)\phi_1 \frac{\phi_1\phi_1^\dagger}{\Lambda^2}. \tag{10.7}$$

Thus, the full mixing matrix will be give by

$$Y^L = \begin{pmatrix} l_{11} & l_{12} & -l_{12} \\ l_{12} & \frac{1}{2}l_T(1+2\kappa_l) & \frac{1}{2}l_T \\ -l_{12} & \frac{1}{2}l_T & \frac{1}{2}l_T \end{pmatrix}. \tag{10.8}$$

We will assume that the Yukawa matrix Y^L is now diagonalized by the unitary matrix U_l given by

$$U_l = W_{23}^l R_{23}^l R_{13}^l R_{12}^l. \tag{10.9}$$

From the Yukawa matrix (10.8), one can find the two relations

$$\begin{aligned} Y_{12} &= -Y_{13}, \\ Y_{22} &= \frac{1}{2}(Y_{23} + Y_{33})(1+2\kappa_l). \end{aligned} \tag{10.10}$$

Applying the above two relations to

$$Y^L = U_l Y^L_{diag} U_l^\dagger \tag{10.11}$$

using Eq. 10.9, one can obtain the solutions

$$\begin{aligned} s_{12l} &\approx \pm c_{23l}\sqrt{\frac{z_\mu - 2\kappa_l + (-3+3z_\mu-2\kappa_l)c_{23l}s_{23l} + 2z_\mu\kappa_l c_{23l}s_{23l}}{z_\mu - z_\mu^2(3+2\kappa_l)c_{23l}s_{23l}}}, \\ s_{13l} &\approx \pm\sqrt{z_\mu}c_{12l}s_{23l}\sqrt{\frac{z_\mu - 2\kappa_l + (-3+3z_\mu-2\kappa_l)c_{23l}s_{23l} + 2z_\mu\kappa_l c_{23l}s_{23l}}{1 - z_\mu(3+2\kappa_l)c_{23l}s_{23l}}}. \end{aligned} \quad (10.12)$$

By comparing Eqs. (10.8, 10.11), one can get the matrix element l_{12} after substituting Eqs. (10.4, 10.5, 10.12) up to the first order in z_μ

$$l_{12} \approx \sqrt{\frac{z_\mu}{2}}(l_e - l_\mu). \quad (10.13)$$

The leptonic mixing matrix is now given by

$$U_{PMNS} = U_\ell^\dagger U_\nu, \quad (10.14)$$

where $U_\ell = W_{23}^l R_{23}^l R_{13}^l R_{12}^l$ and $U_\nu = W_{12}^\nu$.

APPENDIX D: HADRONIC FORM FACTORS

CHAPTER 11

Hadronic form factors

The expressions for the vector and axial-vector hadronic currents in Eq. 11.9 are

$$\begin{aligned}
\langle p(p')|V_\mu|n(p)\rangle &= \bar{u}_p(p')\Big[\gamma_\mu F_1^V + \frac{i}{2M}\sigma_{\mu\nu}q^\nu F_2^V + \frac{q_\mu}{M}F_S\Big]u_n(p), \\
-\langle p(p')|A_\mu|n(p)\rangle &= \bar{u}_p(p')\Big[\gamma_\mu F_A + \frac{i}{2M}\sigma_{\mu\nu}q^\nu F_T + \frac{q_\mu}{M}F_P\Big]\gamma_5 u_n(p). \qquad (11.1)
\end{aligned}$$

Here $q = p' - p$ and the form factors F_i are functions of $t = q^2$. The parametrizations of the axial-vector and pseudoscalar form factors are [291]

$$\begin{aligned}
F_A(t) &= F_A(0)\Big(1 - \frac{t}{M_A^2}\Big)^{-2}, \\
F_P(t) &= \frac{2M^2 F_A(0)}{m_\pi^2 - t}\,, \qquad (11.2)
\end{aligned}$$

where $F_A(0) = -1.2695$ is the axial coupling [168], m_π is the charged pion mass, and $M_A = 1.35$ GeV is the axial-vector mass [305]. The expression for $F_P(t)$ can be shown to be true at low energy, where the predictions of chiral perturbation theory are valid [306]. We have assumed the relation to hold at high t also. Note that $F_A(0)$ is sometimes replaced by $F_A(t)$, which gives similar results for $F_P(t)$ at low t but very different results at high t.

The Dirac and Pauli form factors $F_{1,2}^V$ are

$$F_1^V(t) = \frac{G_E(t) - x_t G_M(t)}{1 - x_t},\ F_2^V(t) = \frac{G_M(t) - G_E(t)}{1 - x_t}\,, \qquad (11.3)$$

where $x_t = t/4M^2$ and

$$G_M = G_M^p - G_M^n,\ G_E = G_E^p - G_E^n\,. \qquad (11.4)$$

Here $G_E^{p,n}$ and $G_M^{p,n}$ are the electric and magnetic form factors of the proton and neutron,

respectively. The simplest parametrizations of these form factors are given by the dipole approximation

$$G_E^p \approx G_D,\ G_E^n \approx 0,\ G_M^p \approx \mu_p G_D,\ G_M^n \approx \mu_n G_D\,, \tag{11.5}$$

where $G_D = (1 - t/M_V^2)^{-2}$, $M_V = 0.843$ GeV is the vector mass, and $\mu_p(\mu_n)$ is the anomalous magnetic moment of the proton (neutron) [307].

In the presence of the charged Higgs, applying the equation of motion to the hadronic matrix elements for the scalar and pseudoscalar currents for the process $\nu_\tau + n \to \tau^- + p$ gives

$$\langle p(p')|\bar{u}(g_S^{u_i d_j} - g_P^{u_i d_j}\gamma_5)d|n(p)\rangle = V_{ud}\,\bar{p}(p_4)\left(g_S^{u_i d_j} G_S + g_P^{u_i d_j} G_P \gamma_5\right) n(p_2), \tag{11.6}$$

or

$$\begin{aligned} \langle p(p')|\bar{u}d|n(p)\rangle &= \bar{p}(p_4) G_S n(p_2), \\ -\langle p(p'))|\bar{u}\gamma_5 d|n(p)\rangle &= \bar{p}(p_4) G_P \gamma_5 n(p_2)\,, \end{aligned} \tag{11.7}$$

where

$$\begin{aligned} G_S(t) &= r_N F_1^V(t), \ \text{ with } \ r_N = \frac{M_n - M_p}{(m_d - m_u)} \sim \mathcal{O}(1), \\ G_P(t) &= \frac{M[F_A(t) + 2x_t F_P(t)]}{\bar{m}_q}, \end{aligned} \tag{11.8}$$

with $\bar{m}_q = (m_u + m_d)/2$. In the W' model, the current has both $V \pm A$ structures. One has to calculate the matrix element,

$$\langle p(p')|J_\mu^+|n(p)\rangle = V_{ud}\,\langle p(p')|\bar{u}\left(g_L^{ud}\gamma_\mu(1-\gamma_5) + g_R^{ud}\gamma_\mu(1+\gamma_5)\right) d|n(p)\rangle. \tag{11.9}$$

Kinematic details

The Mandelstam variables in terms of E_ν and the lepton energy E_l are

$$\begin{aligned} s &= M^2 + 2ME_\nu,\ t = 2M(E_l - E_\nu), \\ s - u &= 4ME_\nu + t - m_l^2. \end{aligned} \tag{11.10}$$

Then t and E_l lie in the intervals

$$m_l^2 - 2E_\nu^{\rm cm}\left(E_l^{\rm cm} + p_l^{\rm cm}\right) \leq t \leq m_l^2 - 2E_\nu^{\rm cm}\left(E_l^{\rm cm} - p_l^{\rm cm}\right), \tag{11.11}$$

$$E_\nu + \frac{m_l^2 - 2E_\nu^{\rm cm}(E_l^{\rm cm} + p_l^{\rm cm})}{2M} \leq E_l \leq E_\nu + \frac{m_l^2 - 2E_\nu^{\rm cm}(E_l^{\rm cm} - p_l^{\rm cm})}{2M}, \tag{11.12}$$

where the energy and momentum of the lepton and the neutrino in the center of mass (cm) system are

$$\begin{aligned} E_\nu^{cm} &= \frac{(s - M^2)}{2\sqrt{s}}, \;\; p_l^{\rm cm} = \sqrt{(E_l^{cm})^2 - m_l^2}, \\ E_l^{cm} &= \frac{(s - M^2 + m_l^2)}{2\sqrt{s}}. \end{aligned} \tag{11.13}$$

The threshold neutrino energy to create the charged lepton partner is given by

$$E_{\nu_l}^{\rm th} = \frac{(m_l + M_p)^2 - M_n^2}{2M_n}, \tag{11.14}$$

where $m_l,\; M_p,\; M_n$ are the masses of the charged lepton, proton, and neutron, respectively. In our case, the threshold energy of the tau neutrino is $E_{\nu_\tau}^{\rm th} = 3.45$ GeV.

The differential cross section in the laboratory frame is given by

$$\frac{d\sigma_{tot}(\nu_l)}{dt} = \frac{|\bar{\mathcal{M}}|^2}{64\pi E_\nu^2 M^2}. \tag{11.15}$$

The expressions for the coefficients f_{SM} $(f = A, B, C)$ in the SM differential cross section [see Eq.(7.20)] are

$$\begin{aligned} A_{SM} &= 4(x_t - x_l)\Big[(F_1^V)^2(1 + x_l + x_t) + (F_A)^2(-1 + x_l + x_t) + (F_2^V)^2(x_l + x_t^2 + x_t) \\ &\quad + 4F_P^2 x_l x_t + 2F_1^V F_2^V(x_l + 2x_t) + 4F_A F_P x_l\Big], \\ B_{SM} &= 4x_t F_A(F_1^V + F_2^V), \\ C_{SM} &= \frac{(F_1^V)^2 + F_A^2 - x_t(F_2^V)^2}{4}, \end{aligned} \tag{11.16}$$

where $x_l = m_l^2/4M^2$.

The expressions for the quantities $A_H^{I,P}$ and B_H^I in the differential cross section in Eq. (7.33)

are

$$
\begin{aligned}
A_H^I &= 2\sqrt{x_l}(x_t - x_l) g_P^{ud} (g_S^{l\nu_l} - g_P^{l\nu_l}) G_P (F_A + 2F_P x_t)\,, \\
B_H^I &= \frac{1}{2}\sqrt{x_l} g_S^{ud} (g_S^{l\nu_l} - g_P^{l\nu_l}) G_S (F_1^V + F_2^V x_t)\,, \\
A_H^P &= 2(x_t - x_l)(|g_S^{l\nu_l}|^2 + |g_P^{l\nu_l}|^2)(|g_P^{ud}|^2 G_P^2 x_t + |g_S^{ud}|^2 G_S^2 (x_t - 1))\,. \qquad (11.17)
\end{aligned}
$$

For the 2HDM II model couplings, $g_{S,P}$ are given in Eq. (7.46). Note that the interference terms A_H^I and B_H^I vanish in this model.

The expressions for the quantities f' ($f = A, B, C$) in the differential cross section in Eq. (7.41) are

$$
\begin{aligned}
A' &= 4(x_t - x_l)\Big[(1 + r_{W'}^{\rho})^2 \Big((F_1^V)^2 (1 + x_l + x_t) + 2F_1^V F_2^V (x_l + 2x_t) + (F_2^V)^2 (x_l + x_t^2 + x_t) \Big) \\
&\quad + (1 + r_{W'}^{\pi})^2 \Big((F_A)^2 (-1 + x_l + x_t) + 4F_A F_P x_l + 4F_P^2 x_l x_t \Big) \Big]\,, \\
B' &= 4Re[(1 + r_{W'}^{\rho})(1 + r_{W'}^{\pi *})] x_t F_A (F_1^V + F_2^V)\,, \\
C' &= \frac{1}{4}\Big[(1 + r_{W'}^{\rho})^2 ((F_1^V)^2 - x_t (F_2^V)^2) + (1 + r_{W'}^{\pi})^2 F_A^2 \Big]\,. \qquad (11.18)
\end{aligned}
$$

In the absence of W' contributions, the f''s reduce to the respective SM results in Eq. 11.16.

VITA

List of Publications

The content of this dissertation is mainly based on the following papers:

1. Ahmed Rashed, Murugeswaran Duraisamy, and Alakabha Datta; "Probing light pseudoscalar, axial vector states through $\eta_b \to \tau^+\tau^-$"; **Phys.Rev.D82, 054031 (2010), arXiv:1004.5419 [hep-ph]**.

2. Murugeswaran Duraisamy, Ahmed Rashed, Alakabha Datta; "The top forward backward asymmetry with general Z' couplings."; **Phys.Rev.D84, 054018 (2011), arXiv: 1106.5982 [hep-ph]**.

3. Ahmed Rashed, Alakabha Datta; "The charged lepton mass matrix and non-zero θ_{13} with TeV scale new physics."; **Phys.Rev.D85, 035019 (2012)**, **arXiv:1109.2320 [hep-ph]**.

4. Ahmed Rashed; "Deviation from tri-bimaximal mixing and large reactor mixing angle."; **Nucl.Phys.B874:679-697,2013, arXiv:1111.3072 [hep-ph]**

5. Ahmed Rashed, Murugeswaran Duraisam, and Alakabha Dattay; "Nonstandard interactions of tau neutrino via charged Higgs and W' contribution"; **Phys. Rev. D 87, 013002 (2013) [arXiv:1204.2023 [hep-ph]].**

6. Ernest Ma, Alexander Natale, and Ahmed Rashed; "Scotogenic A_4 Neutrino Model for Nonzero θ_{13} and Large δ_{CP}"; **Int.J.Mod.Phys. A27 (2012) 1250134**. **arXiv:1206. 1570v1 [hep-ph]**.

7. Subhaditya Bhattacharya, Ernest Ma, Alexander Natale, and Ahmed Rashed; "Radiative Scaling Neutrino Mass with A_4 Symmetry"; **Phys. Rev. D 87, 097301 (2013), arXiv:1302.6266 [hep-ph]**.

8. Ahmed Rashed, Preet Sharma, and Alakabha Datta, "Tau neutrino as a probe of non-standard interactions"; **Nucl. Phys. B 877, 662 (2013), arXiv: 1303.4332 [hep-ph]**.

9. Ahmed Rashed and Alakabha Datta, "Non-standard interaction effects in determination of neutrino mass hierarchy at HyerpK"; **Under preperation**.

10. Ahmed Rashed, Shanmuka Shivashankara, and Alakabha Datta, "Probing CP violation in the top-pair production"; **Under preperation**.

Conference proceedings

1. Ahmed Rashed, "Tau neutrino as a probe of nonstandard interactions via charged Higgs and W' contribution". Proceeding of DPF 2013 Meeting at UC Santa Cruz, Santa Cruz, California, USA, 14-17 August 2013. **Mod. Phys. Lett. A, Vol. 29, No.7:1450040, 2014.**

2. Subhaditya Bhattacharya (UC Riverside), Ernest Ma (UC Riverside), Alexander Natale (UC Riverside), and Ahmed Rashed, "Radiative Scaling Neutrino Mass with A_4 Symmetry and Warm Dark Matter". Proceeding of Phenomenology 2013 Symposium at Pittsburgh University, Pennsylvania, USA, 6-8 May 2013.

3. Ahmed Rashed, "Corrections to the tau neutrino mixing from charged Higgs and W' contribution to ν_τ-nucleon scattering". Proceeding of Phenomenology 2012 Symposium: LHC Lights the Way to New Physics (PHENO 2012) at Pittsburgh University, Pennsylvania, USA, 7-9 May 2012.

4. Ahmed Rashed and Alakabha Datta, "The Charged Lepton Mass Matrix and Non-zero θ_{13} with TeV Scale New Physics". Proceeding of APS April Meeting 2012 at Atlanta, Georgia, USA, 31 Mar - 3 Apr 2012. **Mod. Phys. Lett. A 28, 1330030 (2013)**.

5. Ahmed Rashed, Murugeswaran Duraisamy, and Alakabha Datta, "Study of the $\eta_b \to \tau^+\tau^-$ decay as a probe for light pseudoscalar, axial vector states". PHENO 2011 Symposium at Madison, Wisconsin , USA, 9-11 May 2011.

6. J. L. Hewett, H. Weerts, R. Brock, J. N. Butler, B. C. K. Casey, J. Collar, A. de Govea and R. Essig *et al.*, "Fundamental Physics at the Intensity Frontier". Proceeding of Fundamental Physics at the Intensity Frontier Workshop at Rockville, MD, USA, November 30-December 2, 2011. arXiv:1205.2671 [hep-ex].

Education

1. Ph.D. (May 2014), particle phenomenology, University of Mississippi, USA.

2. M.A. (Dec 2011), University of Mississippi, USA.

3. Diploma (2008), Mathematical Science and Theoretical Physics, African Institute for Mathematical Science (AIMS), South Africa.

4. M.SC. (2006), Theoretical Physics, Ain Shams University, Egypt.

5. B.SC. (2000), Physics, Ain Shams University, Egypt.

Appointments

1. Instructor at the Northwest Mississippi Community College, fall 2013.

2. Teaching/Reaserch assistant and graduate student at the University of Mississippi, USA, Jan 2009-May 2014.

3. Assistant lecturer at Ain Shams University, Egypt, July 2000-July 2007.

Honors and Awards

1. American Physical Society DPF Travel Award, 2014.

2. American Physical Society DPF Travel Award, 2013.

3. Graduate Student Achievement Award, University of Mississippi, 2013.

4. Dissertation Fellowship Award, University of Mississippi, 2012.

5. Scientific Publications Award, Misr El-Kheir Foundation, Egypt, 2012.

6. Tutorial Performance Award for Outstanding Pedagogy in Presentation, the international neutrino summer school 2012, Virginia Tech and Fermilab, 2012.

7. Summer Research Assistantship, University of Mississippi, (2011 and 2012).

8. Graduate Student Council Research Grant 2011-2012, University of Mississippi, 2011.

9. American Physical Society FGSA Travel Award, 2011.

10. Zdravko Stipcevic Honors Fellowship, University of Mississippi, 2010-till graduation.

11. Ph.D. scholarship from the University of Mississippi, January 2009-present.

12. Diploma scholarship from the African Institute for Mathematical Science (AIMS), 2008.

Memberships

1. Sigma Pi Sigma **Honor** Society ($\Sigma\Pi\Sigma$).

2. American Physical Society (APS).

3. Mississippi Academy of Sciences (MAS).

4. Society of Physics Students (SPS).

Talks/Presentations

1. "American Physical Society (APS) April Meeting", Savannah, GA, USA, April 5 - 8, 2014.

2. "Meeting of the American Physical Society(APS) Division of Particles and Fields(DPF)", University of California Santa Cruz, USA, August 13-17, 2013.

3. "The 2013 Phenomenology Symposium", University of Pittsburgh, USA, May 6-8, 2013.

4. "American Physical Society (APS) April Meeting", Denver, CO, USA, April 13 - 16, 2013.

5. "The 2012 Phenomenology Symposium", University of Pittsburgh, USA, May 7-9, 2012.

6. "American Physical Society (APS) April Meeting", Atlanta, GA, USA, March 31 - April 3, 2012.

7. "The Mississippi Academy of Sciences Annual Meeting", University of Southern Mississippi, USA, February 23-24, 2012.

8. The physics department colloquium, University of Mississippi, USA, October, 2011.

9. Theoretical Advanced Study Institute in Elementary Particle Physics (TASI) School "The Dark Secrets of the Terascale", University of Colorado, Boulder, Colorado, USA, June 6-July 1, 2011.

10. "The Coordinated Theoretical-Experimental Project on QCD (CTEQ) School", University of Wisconsin- Madison, Wisconsin, USA, July 10-20, 2011.

11. "The 2011 Phenomenology Symposium", University of Wisconsin-Madison, Wisconsin, USA, May 9-11, 2011.

12. "The Mississippi Academy of Sciences Annual Meeting", University of Southern Mississippi, USA, February 17-18, 2011.

13. A poster at the XXXVIII SLAC Summer Institute (SSI) 2010, "Neutrinos Natures Mysterious Messengers.", SLAC, USA, August 2-13, 2010.

Travel Awards

1. "Canadian-American-Mexican Graduate Student Physics Conference (CAM2013)", University of Waterloo, Waterloo, Ontario, Canada, August 15-18, 2013, **(USD 1130).**

2. "Meeting of the American Physical Society(APS) Division of Particles and Fields(DPF)", University of California Santa Cruz, USA, August 13-17, 2013, **(USD 470).**

3. "The 2013 Phenomenology Symposium", University of Pittsburgh, USA, May 6-8, 2013, **(USD 300).**

4. "Behind Neutrino Mass - Workshop on theoretical aspects of the neutrino mass and mixing", ICTP in Trieste, Italy, September 17-21, 2012, **(Full coverage).**

5. "The 4th International Summer School on Neutrino Physics (INSS2012)", Virginia Tech's Center for Neutrino Physics in Blacksburg, Virginia, USA, July 10-21, 2012, **(USD 800).**

6. "Fundamental Physics at the Intensity Frontier Workshop", Rockville, MD, Nov.30-Dec.2, 2011, **(Full Coverage = USD 580).**

7. "The Coordinated Theoretical-Experimental Project on QCD (CTEQ) School", University of Wisconsin- Madison, Wisconsin, USA, July 10-20, 2011, **(USD 300).**

8. TASI School "The Dark Secrets of the Terascale", University of Colorado, Boulder, Colorado, USA, June 6-July 1, 2011, **(USD 1500).**

9. XXXVIII SLAC Summer Institute (SSI) 2010, "Neutrinos Natures Mysterious Messengers.", SLAC, USA, August 2-13, 2010, **(Registration fee waiving, USD 235).**

10. "International Conference on Neutrino Physics in the LHC Era", Luxor, Egypt, Nov. 15-19, 2009, **(USD 1000, lodging).**

11. "Introductory School on Gauge Theory/Gravity Correspondence", ICTP, May 19-30 2008, **(Full coverage).**